UNIVERSITY OF SOUTHAMPTON

NMR of Liquid Crystals

Michael Ian Charles Furby

A thesis submitted in partial fulfilment

of the requirements for the degree of

Doctor of Philosophy

at the University of Southampton

Department of Chemistry

April 1998

UNIVERSITY OF SOUTHAMPTON

ABSTRACT

FACULTY OF SCIENCE

CHEMISTRY

Doctor of Philosophy

NMR of Liquid Crystals

Michael Ian Charles Furby

The analysis of NMR spectra of molecules in the liquid crystal phase gives rise to information that can be used to determine molecular structure and internal flexibility. The information extracted, the dipolar couplings, are directly related to the separation between atomic pairs averaged over the entire motion of the molecules in the liquid crystal phase. The dipolar couplings are modelled using the Additive Potential model, which yields the order parameters and the potential barriers for rotation within flexible molecules. Traditionally, due to the complexity of these spectra, studies have been restricted to small molecules dissolved in liquid crystal solvents, often with simplified spin systems from chemical substitution. The analysis of phenyl benzoate is an example of this type of work and is presented here. In order to advance beyond these limitations, the possibilities of Variable Angle Sample Spinning combined with ^{13}C-{^{1}H} NMR spectroscopy are explored. Early work concentrates on the analysis of fluorobenzene and 2,2'-difluorobiphenyl dissolved in nematic liquid crystal solvents. VASS has proved to be a powerful tool which has allowed the analysis of NMR spectra to be simplified and has demonstrated that spectra taken near the magic angle can be used to determine the absolute signs of the scalar couplings simply. Different decoupling schemes are also investigated and compared to further optimise the procedure being developed. Finally, the NMR spectra of the liquid crystals I35 and I52 in the liquid crystal phase were successfully analysed combining all the preceding techniques, and the internal motion of the molecules successfully modelled.

Acknowledgements

I would like to thank the following people for their support throughout the duration of this research. Professor Jim Emsley, for his continued input, help and ideas and for giving me the opportunity to engage in this most challenging experience, from which I have gained so much and now have much to look forward to, especially considering my position before I came to Southampton. All the members of the liquid crystal group at the University of Southampton, whose names are too numerous to mention or even remember. I must give special thanks to those with whom I worked closely on the various projects contained within this thesis. Dr. Pina De Luca, who guided me through the early stages and was heavily involved in the work presented in chapter 2. Dr. Lizzy Foord, whose computer program was used as a prototype and further developed for use throughout this thesis. Dr. Mark Edgar, who never lacked enthusiasm and was also involved to a great extent with the work presented in chapters 4 and 5. Elisabetta Ciampi, whose persistence with the analysis of difficult spectra provided much of the excellent data in Chapter 6. And also, Dr. Giovanni La Penna and Dr. Philippe Lesot who were members of our research group. I would also like to thank the EPSRC for providing me with the funding, and the BLCS for accepting my presentation for the annual conference.

There are many people outside of the liquid crystal group who have played a significant part in my life during my time in Southampton. These include all those with whom I have shared accommodation with, and the members of the University Triathlon Club. Especially I must thank Eli for her encouragement and inspiration and of course my family who have supported me throughout.

Table of Contents

Appendices

Chapter 1

NMR of Liquid Crystals

1.1 Introduction

The analysis of the Nuclear Magnetic Resonance (NMR) spectra of molecules in a liquid crystal phase is well documented [1]. The first such example was that by Saupe and Englert [2]. They published the proton (^{1}H) NMR spectrum of benzene dissolved in a nematic liquid crystal. The spectrum consisted of 72 transitions, compared to a single transition in the isotropic liquid, the extra lines are because the dipolar interaction between a pair of protons, D_{ij}, is not averaged to zero, as it is in an isotropic sample. Since then, many other similar liquid crystal NMR experiments have been conducted, covering a wide range of molecules from simple rigid molecules such as fluorobenzene [3, 4][chapter3] to much more complex, flexible molecules such as phenyl benzoate [5][chapter 2], 2,2'-difluorobiphenyl [6, 7] [chapter 4, chapter5] and liquid crystals themselves [8][chapter 6]. The partially averaged D_{ij} are directly related to molecular structure. They are averages over all motion which is fast compared to their magnitude. The motion producing the averaging is of the whole molecule relative to the magnetic field, and internal motion such as bond rotations. Therefore it is possible in principle to determine conformational distributions of molecules in the liquid crystalline phase. There are many examples of such studies on relatively simple molecules [9, 10, 11]. In theory it appears possible to subject many other molecules to such conformational analysis, however, in practice it soon becomes impossible to analyse their proton spectra. In the case of the large molecules which form liquid crystals, the proton spectrum is so complex it appears as a broad unresolved line and is difficult to distinguish from the baseline. The solute spectrum is superimposed on this and through spectral manipulation can be enhanced. It is also possible to study the solvent molecules by NMR, but now the most useful techniques have been deuterium [12] and carbon-13 [13]. We will describe how ^{13}C-{^{1}H} spectra may be used when the molecules contain one or more ^{19}F atoms. Before discussing the experiments we will briefly discuss some properties of liquid crystals, followed by the effects of the magnetic field in the NMR experiment on molecular alignment. The contributions to the NMR spectrum will then be discussed and methods of spectral simplification described. Finally in this chapter we will see how the experimental

data is used to obtain molecular structures and to gain an insight into the flexibility of the molecules

1.2 Orientational Ordering of Liquid Crystals

In order to understand how the NMR experiment allows us to extract information otherwise unobtainable from solutions in the isotropic phase, we first discuss some properties of liquid crystal phases themselves and their behaviour within the magnetic field.

Liquid Crystal describes a phase that molecules can form in certain conditions that lies structurally somewhere between the liquid and solid phases, a bridge between these two very different phases. In the liquid crystal phase, the molecules are free flowing, and they are constantly undergoing rotational and translational motion, however, individual molecules are affected by their neighbours to such a degree that they are forced to align to form some sort of order, depending on the class of liquid crystal phase formed.

There are two classes of liquid crystals, the lyotropics form phases in solution, and are especially important in the detergents industry and in biology, and the thermotropics which form phases under certain conditions of temperature and pressure, and are prominent in the polymers and display device industries. Thermotropics can be further subdivided on the basis of the shape of the molecule, where calamitics are rod-like and discotics are disc-like, the size of the molecules, where monomers have low molar mass and polymer have high

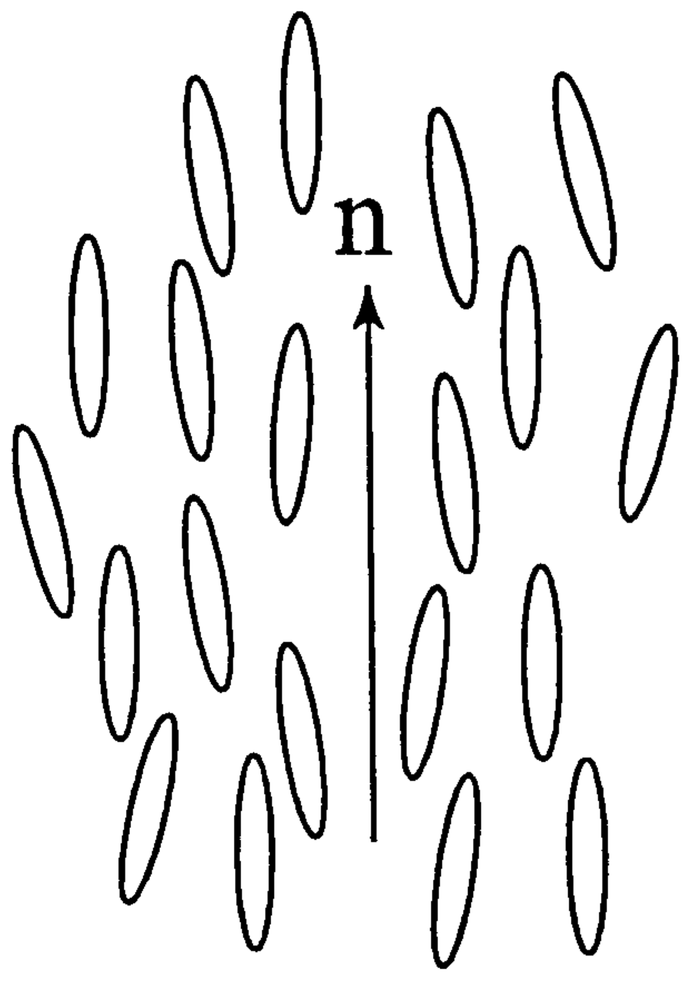

Figure 1 Schematic of the nematic liquid crystal phase. Net alignment of the molecules is given by the director, **n**.

molar mass and on chirality where molecules have a chiral centre. A more important division is between the nematic phases, in which molecules have only orientational order and smectics which also have spatial order. The work described in this thesis has been concerned only with the nematic calamitic phase.

1.3 The Liquid Crystal Director

The nematic phase exhibits long range orientational order, whilst maintaining its liquid like properties i.e. low viscosity. Molecules that form calamitic nematic phases are often approximated to be rigid and of uniaxial symmetry. We can see that the molecules are anisotropic in nature and have a preferred direction of orientation, as shown in figure 1, known as the director, **n**.

In an unconstrained environment the directors are randomly oriented with respect to a fixed direction in space. There is therefore microscopic orientational order of the liquid crystal molecules but macroscopic disorder of the directors.

Macroscopic alignment of the directors may be induced by the presence of an external constraint such as an electric or magnetic field, or confinement between glass plates. In the case of NMR we are particularly interested in the effect of the magnetic field.

The application of a magnetic field induces a torque on the molecules due to the dependence of the magnetic free energy on the director orientation. For a single, rigid, cylindrically symmetric molecule at fixed orientation θ_i, with respect to the magnetic field, B_0, the magnetic free energy (F_i) is given as

$$F_i = -\frac{1}{2}\Delta\chi_B B_0^2 \qquad (1)$$

where

$$\Delta\chi_B = \Delta\chi^{mol}\left(\frac{3\cos^2\theta_i - 1}{2}\right) \qquad (2)$$

to give

$$F_i = -\frac{1}{2}\Delta\chi^{mol} B_0^2 \left(\frac{3\cos^2\theta_i - 1}{2}\right) \quad (3)$$

$\Delta\chi_B$ is equal to the difference in the magnetic susceptibilities perpendicular and parallel to the magnetic field and when $\Delta\chi^{mol}$ is > 0, the minimum free energy occurs when $\theta_i = 0°$ and molecules will prefer to orientate themselves parallel to B_0, however, when $\Delta\chi^{mol} < 0$, the minimum occurs when $\theta_i = 90°$, and molecules will prefer a perpendicular orientation to B_0.

In the isotropic phase, molecular collisions cause a randomising effect which is larger than the orientational effect of B_0, however, in the liquid crystal phase, the magnetic field can be regarded as acting on the directors, n_i, and the free energy becomes

$$F(\alpha_i) = -\frac{1}{3}\Delta\chi^{mol}\overline{P_2}B_0^2\left(\frac{3\cos^2\alpha_i - 1}{2}\right) \quad (4)$$

where α_i is the angle between n_i and B_0 and $\overline{P_2}$ is the average of the Legendre polynomial, $P_2 = (3\cos^2\beta - 1)/2$, where β is the angle between the molecular symmetry axis and the director. The energy $F(\alpha_i)$ is a minimum at $\alpha = 0°$ with $\Delta\chi^{mol}$ positive and $\alpha = 90°$ with $\Delta\chi^{mol}$ negative. It can now be seen that when $\Delta\chi^{mol}$ is positive the director aligns with B_0, and when $\Delta\chi^{mol}$ is negative the director aligns perpendicular to B_0, and virtually complete director alignment is obtained.

We know that molecular motion in the liquid crystal phase is rapid but not random. At any point in time a molecule has a preferred orientation which can be described in relation to the director, **n**. In the simplest case of a cylindrically symmetric molecule in a uniaxial phase the probability that a molecule is at an angle between $\cos\beta$ and $\cos\beta + d\cos\beta$ (figure 2) is given by the singlet orientation distribution function, $f(\beta)$.

$f(\beta)$ can be used to characterise the orientational order of the molecules, however, this is difficult to measure, and is usually unknown. We can expand $f(\beta)$ as a sum of the Legendre polynomials, $P_L(\cos\beta)$:

$$f(\beta) = \sum_{L\ even} f_L P_L(\cos\beta) \quad (5)$$

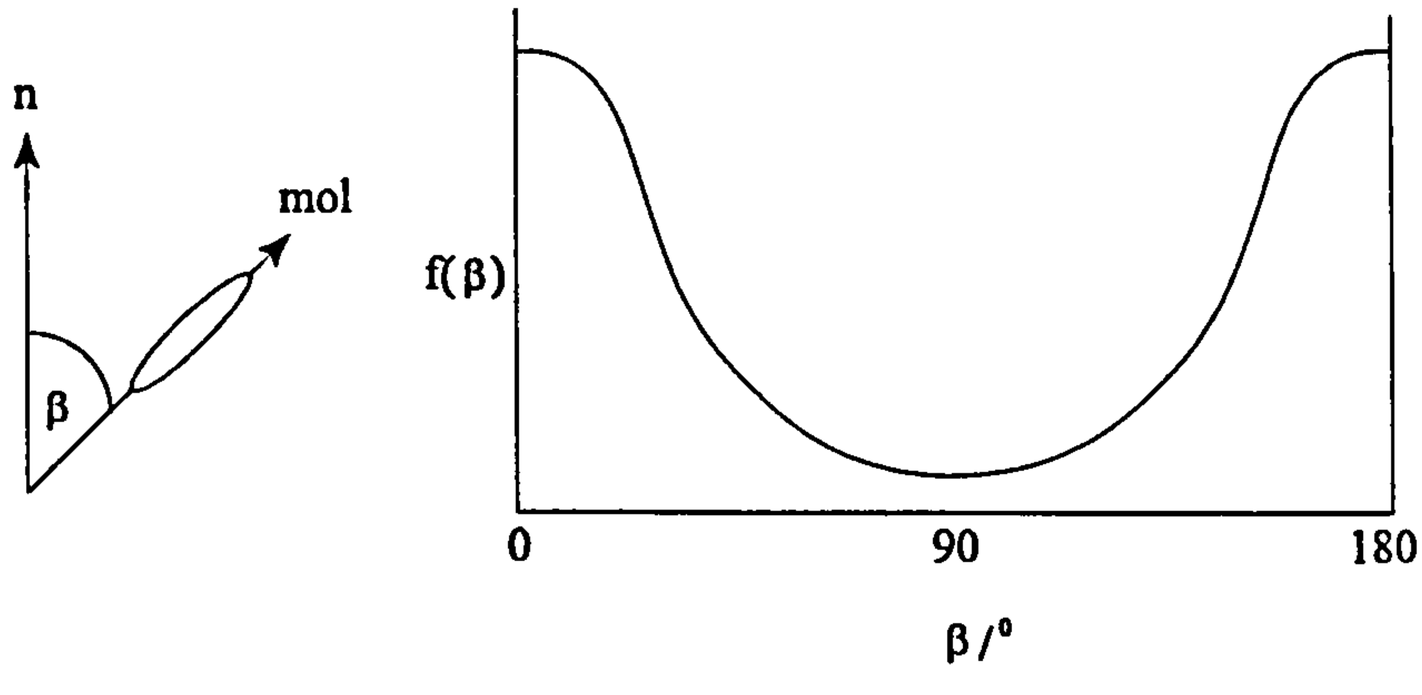

Figure 2 The probability f(β) that a molecule adopts an angle between cosβ and cosβ+dcosβ to the director, **n**.

f_L are the expansion coefficients, where L is even to reflect the mesophase symmetry about the plane orthogonal to n. The f_L are given by

$$f_L = \overline{P_L} \frac{(2L+1)}{2} \tag{6}$$

so that the singlet orientation distribution function is

$$f(\beta) = \sum_{L\ even} \frac{2L+1}{2} \overline{P_L} P_L(\cos\beta) \tag{7}$$

where $\overline{P_L}$ are the averaged values of P_L over all cosβ and are known as the order parameters. To completely characterise f(β), we need to measure an infinite set of order parameters

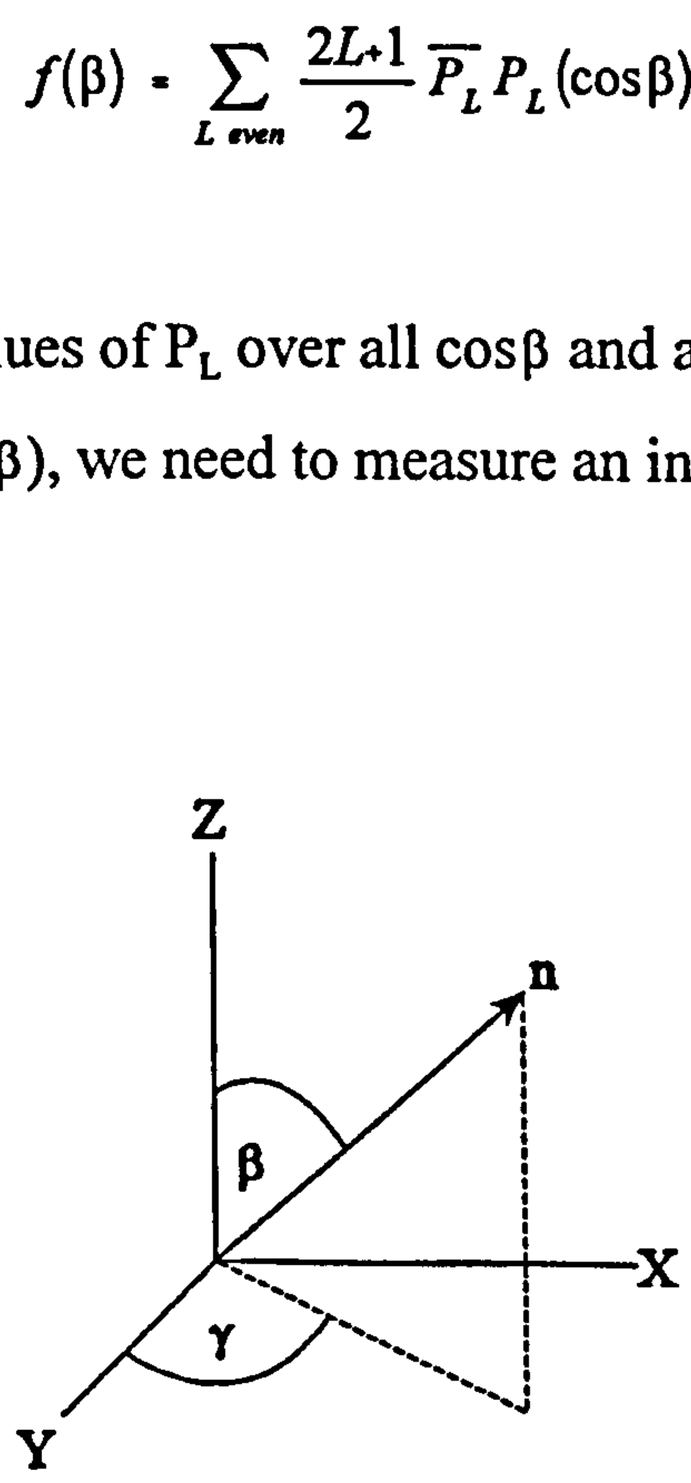

Figure 3 Euler angles defining orientation of the director in axes fixed in a biaxial molecule.

where all of $\overline{P_L}$ are finite, however, only $\overline{P_2}$ is easily obtained experimentally, hence we only obtain a partial description of the ordering.

To describe the orientation of rigid biaxial molecules in a uniaxial mesophase two angles, β and γ are required (figure 3). The singlet orientation function is now an unknown function of two angles, f(β,γ), and must therefore be expanded as a series of orthogonal functions of β and γ, known as modified spherical harmonics

$$f(\beta,\gamma) = \sum_{L,m}^{\infty} F_{L,m} C_{L,m}(\beta,\gamma) \qquad (8)$$

where L is even and m takes values of +L to -L. Equation 8 can be expanded to

$$f(\beta,\gamma) = \sum_{L,m}^{\infty} \frac{2L+1}{4\pi} \overline{C}_{*L,m} C_{L,m}(\beta,\gamma) \qquad (9)$$

for L is even $\overline{C}_{*L,m} = \overline{C}_{L,m}$. Again, an infinite number of order parameters are required to completely characterise f(β,γ), however, only the second rank ones (L=2) are measurable with NMR. There are five independent second rank order parameters, $\overline{C}_{*2,2}$, $\overline{C}_{*2,1}$, $\overline{C}_{*2,0}$, $\overline{C}_{*2,-1}$ and $\overline{C}_{*2,-2}$.

The $\overline{C}_{*2,m}$ are related to $S_{\alpha\beta}$, the Saupe order matrix elements which are defined as

$$S_{\alpha\beta} = \left\langle \left(3\cos\theta_\alpha \cos\theta_\beta - \delta_{\alpha\beta}\right) / 2 \right\rangle \qquad (10)$$

where $\delta_{\alpha\beta}$ is the Kronecker delta and is equal to 1 if α=β and equal to 0 otherwise and α and β are Cartesian axes. Using X, Y and Z fixed in a molecule. the Saupe order parameters for a molecule are S_{ZZ}, S_{XX}-S_{YY}, S_{XY}, S_{XZ} and S_{YZ}. In the principal axis system, defined according to the structure of the molecule in such a way that the order matrix is diagonalised removing the off diagonal elements, this is reduced to S_{ZZ} and S_{XX}-S_{YY}, while for a uniaxial molecule this can be further reduced to S_{ZZ} only.

1.4 NMR of Liquid Crystals

Nuclear Magnetic Resonance (NMR) spectroscopy is based upon the measurement of absorption of electromagnetic radiation in the radio frequency range. Nuclei are required to develop energy states for absorption to occur. Exposure to a magnetic field leads to a splitting in energy levels of nuclei with properties of spin. Not all nuclei have properties of spin and cannot therefore be observed in NMR, a property that is used to our advantage (see chapters 3-6, ^{13}C NMR). Nuclear spins act like small bar magnets, in that they align with the magnetic field. The nuclei absorb the radiation, which results in the spinning axis tipping over away from the magnetic field direction. The nuclear spin relaxes back to the equilibrium position over time, whilst emitting a radio frequency that is received by the spectrometer. The signal, known as the free induction decay (fid), is measured as a function of time. Although it is possible to analyse this signal, it becomes very complex, very quickly with the occurrence of inequivalent nuclei contributing their distinctive patterns to the decay signal. Fourier transformation of the fid converts the data into the frequency domain, and transitions appear corresponding to the frequency of radiation emitted by each type of nucleus during relaxation, to give the NMR spectrum, in which it is possible to extract the information about inter nuclear interactions.

The frequency and intensity of the lines in the NMR spectrum are given by the nuclear spin Hamiltonian, $\mathcal{H}$, when used in the time independent Schrödinger equation

$$\mathcal{H}\psi_n = E\psi_n \tag{11}$$

where E_n are the eigenvalues and ψ_n are the corresponding eigenfunctions. The form of the Hamiltonian is

$$\mathcal{H} = \mathcal{H}_Z + \mathcal{H}_J + \mathcal{H}_D + \mathcal{H}_Q \tag{12}$$

which in the isotropic phase is simplified to

$$\mathcal{H} = \mathcal{H}_Z + \mathcal{H}_J \tag{13}$$

Here, the Hamiltonian will be described using the spin operator, I_{Zi}, where Z is the direction of B_0, and the ladder operators, $I_{\pm i}$, given by

$$I_+ = I_X + iI_Y$$
$$and \qquad (14)$$
$$I_- = I_X - iI_Y$$

1.4.1 The Zeeman Hamiltonian $\mathcal{H}_Z$

$$\mathcal{H}_Z = -\frac{B_0}{2\pi}\sum_i \gamma_i I_{Zi}\left(1 - \sigma_{ZZi}\right) \qquad (15)$$

Note that $\mathcal{H}$ has been divided by h, Planck's constant, to give units of Hertz. The component along B_0 of the partially averaged total shielding tensor at the ith site, σ_{ZZi}, can be divided into a contribution, σ_i^{iso}, which is non-zero in all phases, and σ_{ZZi}^{aniso}, which vanishes in an isotropic phase:

$$\sigma_{ZZi} = \sigma_i^{iso} + \sigma_{ZZi}^{aniso} \qquad (16)$$

The anisotropic term is related to $\sigma_{\alpha\beta}$, where α and β are axes fixed in the molecule, by

$$\begin{aligned}\sigma_{ZZi}^{aniso} &= \frac{2}{3}S_{aa}\left[\sigma_{aai} - \frac{1}{2}\left(\sigma_{bbi} + \sigma_{cci}\right)\right] \\ &+ \frac{1}{3}\left(S_{bb} - S_{cc}\right)\left(\sigma_{bbi} - \sigma_{cci}\right) \\ &+ \frac{4}{3}S_{ab}\,\sigma_{abi} + \frac{4}{3}S_{ac}\,\sigma_{aci} + \frac{4}{3}S_{bc}\,\sigma_{bci}\end{aligned} \qquad (17)$$

Choosing the molecular axes a, b and c to be either the principal axes for the order matrix, S, or for the shielding tensor, σ, simplifies the equation since all the terms involving $S_{\alpha\beta}$ with $\alpha \neq \beta$ vanish.

1.4.2 The Spin-Spin Hamiltonian $\mathcal{H}_J$

$$\mathcal{H}_J = \sum_{i<j} \left\{ J_{ij}^{iso} \left[I_{Zi} I_{Zj} + \frac{1}{2} \left(I_{+i} I_{-j} + I_{-i} I_{+j} \right) \right] + J_{ZZij}^{aniso} \left[I_{Zi} I_{Zj} - \frac{1}{4} \left(I_{+i} I_{-j} + I_{-i} I_{+j} \right) \right] \right\} \quad (18)$$

J_{ij}^{iso} is the scalar spin-spin coupling constant, and J_{ZZij}^{aniso} is the component along B_0 of the anisotropic part of the spin-spin interaction.

1.4.3 The Dipolar Hamiltonian $\mathcal{H}_D$

$$\mathcal{H}_D = \sum_{i<j} 2D_{ij} \left[I_{Zi} I_{Zj} - \frac{1}{4} \left(I_{+i} I_{-j} + I_{-i} I_{+j} \right) \right] \quad (19)$$

D_{ij} is the component along B_0 of the dipolar interaction tensor. It is an entirely anisotropic interaction occurring between two nuclei i and j with spin, and unlike the scalar coupling occurs through space. It can be seen that the operators in equation 19 are identical in form to the anisotropic component of equation 18, J_{ZZij}^{aniso} and so the two are spectroscopically indistinguishable and must be taken into consideration when measuring the magnitudes of the dipolar couplings.

The manifestation of these interactions is not unique to the liquid crystal phase. The complexity of solids stems from intermolecular as well as intramolecular interactions. The viscosity of the liquid crystal phase is comparable, in the nematic phase at least, to that of isotropic liquids and molecules undergo rapid rotational and translational motion in the bulk medium. This results in the averaging of the intermolecular interactions to zero. The low viscosities and fast relaxation rates also result in higher resolution of individual resonances.

The averaged dipolar coupling between a pair of nuclei, i and j, is given by

$$D_{ij} = -\left(\frac{\gamma_i \gamma_j h}{4\pi^2} \right) \left\langle \frac{3\cos^2\theta_{ij} - 1}{2r_{ij}^3} \right\rangle \quad (20)$$

where γ is the gyromagnetic ratio of a nucleus and h is Planck's constant. For r_{ij} fixed, the

angular term only is averaged over all orientations of r_{ij} with respect to the magnetic field and as such is termed the order parameter, S_{ij}, for the ij axis. For axes X, Y and Z fixed in a rigid molecule, the dipolar couplings are given as

$$D_{ij} = -\frac{\gamma_i \gamma_j h}{8\pi^2 r_{ij}^3}\left[S_{ZZ}\left(3\cos^2\theta_{ijz} - 1\right)\right. \\ + \left(S_{XX} - S_{YY}\right)\left(\cos^2\theta_{ijX} - \cos^2\theta_{ijY}\right) \\ + 4S_{XY}\cos\theta_{ijX}\cos\theta_{ijY} \\ + 4S_{XZ}\cos\theta_{ijX}\cos\theta_{ijZ} \\ \left. + 4S_{YZ}\cos\theta_{ijY}\cos\theta_{ijZ}\right] \qquad (21)$$

In a flexible molecule, the dipolar couplings are also averaged over all internal motions

$$D_{ij} = \int D_{ij}(\beta,\gamma,\phi)\, P_{LC}(\beta,\gamma,\phi)\sin\beta\, d\beta d\gamma d\phi \qquad (22)$$

where β and γ are the Euler angles describing the orientation of r_{ij} with respect to B_0, and ϕ is the conformation described by a set of internal angles. $P_{LC}(\beta,\gamma,\phi)$ is the probability of any particular conformer ϕ at an orientation β, γ to B_0, which is the singlet orientation distribution function for the molecules, $f(\beta,\gamma)$, in the conformation ϕ. $D_{ij}(\beta,\gamma,\phi)$ is known for any fixed molecular geometry, however, $P_{LC}(\beta,\gamma,\phi)$ is unknown and must be modelled. The method used for modelling P_{LC}, in order to calculate values of the D_{ij}, is discussed later.

1.4.4 The Quadrupolar Hamiltonian $\mathcal{H}_Q$

The nuclear electric quadrupole-electric field gradient interaction occurs with nuclei which possess a spin greater than ½. The charge distribution in such nuclei is not spherical and has an electric quadrupole moment that interacts with any electric field gradient at the nucleus.

$$\mathcal{H}_Q = \sum_i \left[q_{ZZi} / \left(4I_i(2I_i-1)\right) \left(3I_{Zi}^2 - I_i(I_i+1)\right)\right] \qquad (23)$$

q_{ZZi} is the component of the quadrupolar tensor along B_0. Quadrupolar interactions also provide information on the orientation of the molecule in the liquid crystal phase, and can be used to determine the order parameters for a molecule, as the tensor q_i is purely

anisotropic. The components in the molecular frame, $q_{\alpha\beta i}$, are related to q_{ZZi} by

$$q_{ZZi} = q_{aai}\left[S_{aa} + \frac{1}{3}\eta_i\left(S_{bb} - S_{cc}\right)\right] \tag{24}$$

where $|q_{aai}| > |q_{bbi}| > |q_{cci}|$ and

$$\eta_i = \frac{\left(q_{bbi} - q_{cci}\right)}{q_{aai}} \tag{25}$$

The axes a, b and c are principal axes for q_i. The splitting from each inequivalent nucleus with $I \geq 1$ in the molecule gives rise to a doublet in the NMR spectrum with a splitting of $\Delta\nu = 3q_{ZZi}/2$. However, the effect of η_i is small and can usually be ignored and then the splitting is

$$\Delta\nu = 3/2\, q_{aa} S_{aa} \tag{26}$$

In the case of a liquid crystal, we usually observe the quadrupole interaction of deuterons attached to carbons and in this case the axis a is along the C-D bond, so that

$$\Delta\nu_i = \frac{3}{2}\, q_{CDi}\, S_{CDi} \tag{27}$$

The order parameter, S_{CD}, for the C-D bond is

$$S_{CDi} = \left\langle \frac{\left(3\cos^2\theta_{CDi} - 1\right)}{2} \right\rangle \tag{28}$$

where θ_{CDi} is the angle between the ith C-D bond and B_0, and $\langle\rangle$ is an average over all the molecules. The order parameter S_{CDi} is equal to zero in the isotropic phase, as all orientations within the solvent are possible. In this case the splitting disappears from the spectrum. The S_{CDi} are related to order parameters S_{XX}, S_{YY}, S_{ZZ}, S_{XY}, S_{XZ} and S_{YZ} which are defined with respect to the director.

$$
\begin{aligned}
S_{CDi} &= S_{ZZ}\left(3\cos^2\theta_{CDiZ} - 1\right)/2 \\
&+ \left(S_{XX} - S_{YY}\right)\left(\cos^2\theta_{CDiX} - \cos^2\theta_{CDiY}\right)/2 \\
&+ 2S_{XY}\cos\theta_{CDiX}\cos\theta_{CDiY} \\
&+ 2S_{XZ}\cos\theta_{CDiX}\cos\theta_{CDiZ} \\
&+ 2S_{YZ}\cos\theta_{CDiY}\cos\theta_{CDiZ}
\end{aligned}
\tag{29}
$$

1.5 Analysis of Liquid Crystal NMR Spectra

The additions to the Hamiltonian in the liquid crystal phase from the partially averaged anisotropic interactions have a dramatic effect on NMR spectra. These spectra may consist of many hundreds of lines compared to their respective spectra in isotropic solution. As the size of the spin system studied increases, the spectra become even more complex with the growth in the number of internuclear interactions producing further splittings in the spectra. In the case of liquid crystals themselves, ^{1}H NMR spectra consist of so many transitions that in fact the spectra appear as broad humps spanning tens of kilohertz. The spectra of molecules dissolved in liquid crystals are, however, superimposed over the top of the liquid crystal spectra and are distinguishable from the liquid crystal background, and are therefore analysable.

It was said by Jacques Courtieu in a review article

"Our drawers are full of spectra that we have never been able to analyse, and the situation is probably the same in many specialised laboratories around the world" [14].

The purpose of this work was not to analyse those spectra which had defeated Jacques, but to develop the technique to obtain new, better and more friendly spectra to analyse. There are methods that can be used in order to reduce the complexity of the problem, ranging from complex chemistry to different types of NMR experiments.

In cases of nuclei with spin = ½, such as ^{1}H, we only observe contributions from the dipolar coupling to the nuclear spin Hamiltonian. It is these dipolar couplings that we aim to extract from the liquid crystal NMR spectra of liquid crystals or molecules dissolved in the liquid crystal phase, so that we can determine structural information. A problem exists in that the anisotropic part of the scalar coupling constant, J_{ij}^{aniso}, is not separable from the dipolar

coupling constant, D_{ij}, and in fact it is a total interaction, T_{ij}, that is measured from the NMR spectrum

$$T_{ij} = 2D_{ij} + J_{ij}^{aniso} \quad (30)$$

We cannot therefore determine molecular structures unless J_{ij}^{aniso} is known, however, in many cases this is much smaller than D_{ij} and can therefore be safely ignored.

In order to analyse these spectra we must use computer simulation and iteration programs as it is only possible to analyse very small spin systems analytically. Such programs calculate NMR spectra from a set of trial parameters, provided by the user, which are varied through iteration until a good agreement is found between the calculated and experimental spectra.

The ^{1}H NMR spectra were analysed using a program, ARCANA [15], running on a Silicon Graphics Indy platform. ARCANA is based on LAOCOON [16], which uses the Castellano - Bothner-By iterative method of refining the spectral parameters. ARCANA uses symmetry to factorise the Hamiltonian matrix which gives a reduction in the computer memory required, and a reduction in the computation time.

The method of obtaining starting parameters is an important part in the successful and speedy analysis of complex spectra. ARCANA requires a set of chemical shifts, scalar and dipolar couplings as starting parameters. The chemical shifts for protons are not affected greatly by the anisotropic term and so those for the isotropic phase can be used as starting values. The same is true for the scalar couplings, whose values can be assumed to be those in similar compounds, if an isotropic spectrum is not available, or is itself very difficult to analyse. Dipolar couplings can be calculated from the order parameters and the molecular geometry. Geometry can be either assumed or may have already been determined. The order parameters can be obtained either through analysis of the anisotropy of the chemical shifts of the carbon atoms in ^{13}C NMR, or more simply through the measurement of quadrupolar splitting in the ^{2}H NMR spectra of perdeuterated isotopomers. This method works very well for rigid fragments, but for flexible molecules the splittings are averaged over all motion, and it is not so easy to determine the conformation of molecule through the use of the quadrupole interaction. Again assumptions must be made and the D_{ij} calculated from a small set of probable minimum energy structures.

Very often, the ^1H NMR spectra of the fully protonated isotopomers are so complex that even with these starting parameters it is not possible to relate the calculated and experimental spectra. We must therefore seek methods of simplifying such spectra to enable us to succeed in the final analysis. Three methods are commonly used for such purposes, partial deuteration, scaling of the anisotropic interactions and multiple quantum NMR. The first two methods are explored within this thesis, however, multiple quantum was not a method of choice here and will not be discussed further.

Partial deuteration of molecules can be used to reduce the number of protons within a molecule. This actually increases the complexity of the proton spectrum, but the ^1H-^2H interactions can be removed by spin decoupling. However, there is a price to pay. The deuteration is often difficult to perform and then to achieve with a reasonable yield. The compounds are also expensive. However, through this method it becomes possible to analyse spectra that would have otherwise defeated us. The result of the analysis of the ^1H-$\{^2H\}$ spectra of the partially deuterated samples is the collection of refined dipolar couplings to be used as the starting set in the analysis of the more complex spectra ^1H spectra.

Scaling of the anisotropic interactions to such an extent that the dipolar couplings are in the same order of magnitude as the scalar couplings, makes the spectrum easier to analyse, in that the spectrum is similar to that in the isotropic phase. Spinning samples at or near the magic angle in the NMR experiment, achieves scaling of the dipolar couplings without changing the sample conditions.

1.6 Variable Angle Sample Spinning

Spinning a liquid crystal about an axis D, tilted from B_0 by an angle, η, at an angular velocity, ω, greater than a critical spinning speed, ω_c, (figure 4) the director, **n**, does not have time to realign to the direction of the magnetic field, but will orient such that over one cycle the potential energy is a minimum. For nematics with $\Delta\chi > 0$ when $\eta < \theta_m$ the potential energy is a minimum at $\gamma=0°$ and the director will align along D; when $\eta = \theta_m$ the potential energy is independent of γ which means that the director has no preferred orientation and the distribution is isotropic; when $\eta > \theta_m$ the potential energy is a minimum for $\gamma=90°$ and the director is distributed in the plane perpendicular to D. For liquid crystals

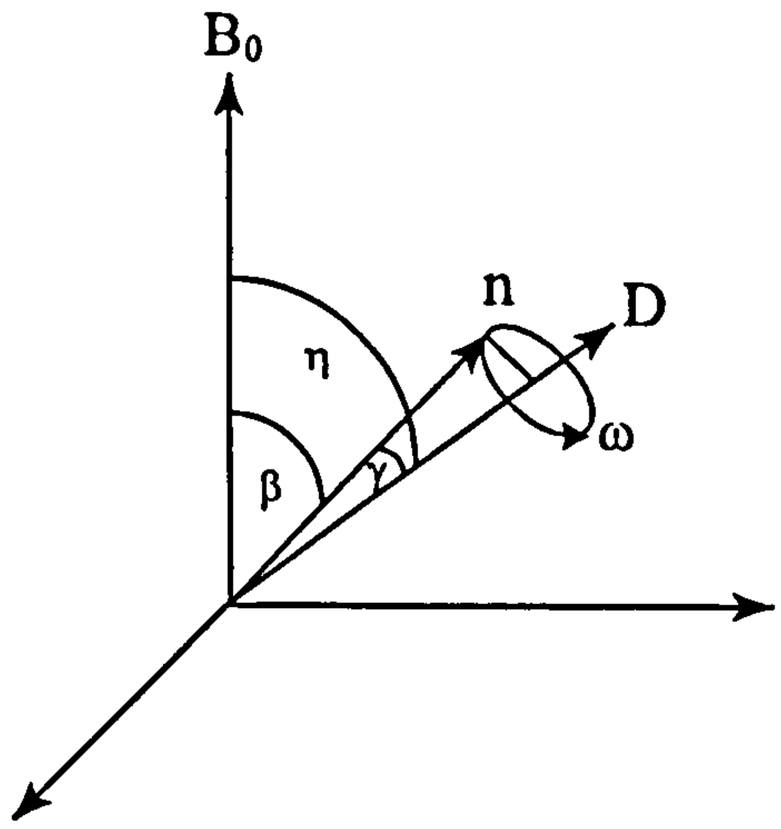

Figure 4 The position of the director, **n**, with respect to the spinning axis, D.

with $\Delta\chi < 0$ the situation is reversed. When the director is at an angle β to B_0 all anisotropic interactions are changed by $(3\cos^2\beta - 1)/2$, known as the reduction factor, R.

Here we discuss the application of VASS to solutes dissolved in liquid crystal solvents. It is the reduction of the dipolar interactions that is important in the application to enable the simplification of complex NMR spectra. In chapter 3 we show how the ^1H-^1H dipolar couplings are reduced in a sample of fluorobenzene dissolved in the liquid crystal ZLI-1167, however, it is the simplification of ^{13}C-{^1H} NMR spectra that is found to be most useful, and is described in chapters 3 and 4.

The goal of the experiment is to reduce the anisotropic interactions, in particular the D_{ij} in a complex liquid crystal NMR spectrum in a controlled way. It is possible to see how the spectrum changes as the spinning axis is varied through a range of angles to B_0. When $\eta = \theta_m$, the spectrum is dominated by the isotropic scalar couplings, J_{ij} and chemical shifts, δ_i, and is equivalent to the NMR spectrum of the solute in an isotropic solution and as such is relatively easy to assign. Once the spectrum at θ_m is assigned, we may observe the growth in magnitude of the anisotropic interactions and see the effect they have on the liquid crystal spectrum.

The resonance frequency of a carbon, δ_i, which for liquid crystalline samples is usually measured relative to the transmitter frequency, depends on δ_i^{iso}, the value for an isotropic

sample, and δ_i^{aniso}, the anisotropic contribution (see equation (16)) by

$$\delta^{exp} = \delta^{iso} + \frac{1}{2}(3\cos^2\eta - 1)\delta^{aniso} \quad (31)$$

The value of δ is zero when β is < 54.7° for $\Delta\chi$ positive, and when β > 54.7° for $\Delta\chi$ negative. In these cases plotting $(\delta_i - \delta_i^{iso})$ against R gives δ_i^{aniso}.

This application, is ideal for the analysis of ^{13}C-{^1H} NMR spectra, in which the spectra consist of multiplets arising from single ^{13}C atoms. The natural low abundance of ^{13}C ensures that no ^{13}C-^{13}C couplings interfere with the spectrum, and we only observe single ^{13}C atoms coupling with other nuclei with nuclear spins greater than zero. In liquid crystals without other nuclei with spins greater than zero, the liquid crystal spectrum is simply a single peak for each non equivalent carbon where the position is the result of the effect of chemical shift anisotropy on the ^{13}C atoms. For our experiments we are interested in observing dipolar couplings, which will occur if another nucleus spin greater than zero is present. It is convenient that many liquid crystals contain a small number of fluorine atoms. The ^{19}F isotope is 100% naturally abundant and has a spin of 1/2. The liquid crystal spectrum of a liquid crystal containing one ^{19}F atom would then consist of doublets arising from the ^{13}C-^{19}F dipolar coupling. VASS NMR spectra would then show the effect of the growth in magnitude of the D_{ij}^{CF}.

1.7 Conformational Analysis of Flexible Molecules

Molecules which are flexible can be regarded as consisting of several rigid sub-units, or fragments. The dipolar and quadrupolar couplings obtained from analysis of the NMR spectra of flexible molecules dissolved in the LC phase are the averaged couplings over all internal motions, as well as the motion of the molecule within the solvent. Therefore it is possible to investigate the internal motions of the molecules using the partially averaged dipolar and quadrupolar couplings. For rigid molecules we need only one set of order parameters to describe the orientation of the molecule within the solvent. However, for flexible molecules, we need a set of order parameters for each rigid fragment, as the D_{ij}'s depend on the internal motions of these fragments.

Equation 22, shows the relationship between the dipolar couplings and the singlet orientational distribution function. The dipolar couplings depend not only on the orientation of the liquid crystal molecules but also on the internal conformation. The probability that a liquid crystal is in any particular conformation regardless of its orientation with respect to the director is

$$P_{LC}(\phi) = \int P_{LC}(\beta,\gamma,\phi)\sin\beta\, d\beta\, d\gamma \tag{32}$$

which describes the conformation distribution of molecules in the liquid crystal phase. Writing D_{ij} as

$$D_{ij} = \int P_{LC}(\phi)\, D_{ij}(\phi)\, d\phi \tag{33}$$

where $D_{ij}(\phi)$ can be determined from equation 21 for each conformer, which is treated like one rigid unit and has a set of related order parameters gives

$$\begin{aligned} D_{ij}(\phi) = & -\frac{\gamma_i\,\gamma_j\,h}{8\pi^2\, r_{ij}^3}\Big[S_{ZZ}(\phi)\left(3\cos^2\theta_{ijZ} - 1\right) \\ & + \left(S_{XX}(\phi) - S_{YY}(\phi)\right)\left(\cos^2\theta_{ijX} - \cos^2\theta_{ijY}\right) \\ & + 4S_{XY}(\phi)\,\cos\theta_{ijX}\cos\theta_{ijY} \\ & + 4S_{XZ}(\phi)\,\cos\theta_{ijX}\cos\theta_{ijZ} \\ & + 4S_{YZ}(\phi)\,\cos\theta_{ijY}\cos\theta_{ijZ}\Big] \end{aligned} \tag{34}$$

Similarly, the doublet splitting from the quadrupolar interaction, given in equation 27, is conformationally dependant.

In order to calculate an averaged dipolar coupling it is necessary to be able to model the conformational dependence of the order parameters, and the $P_{LC}(\phi)$.

1.8 The Additive Potential Method

The energy of interactions for flexible molecules are dependant on their orientation and conformation [16]. The singlet orientation function is given by

$$P_{LC}(\beta,\gamma,\phi) = Z^{-1} \exp\left\{\frac{-U(\beta,\gamma,\phi)}{RT}\right\} \tag{35}$$

where $U(\beta,\gamma,\phi)$ is the mean potential of the molecule in conformation ϕ and orientation (β,γ) and Z is the normalisation function

$$Z = \int \exp\left\{\frac{-U(\beta,\gamma,\phi)}{RT}\right\} \sin\beta \, d\beta \, d\gamma \, d\phi \tag{36}$$

The mean potential can be written as the sum of the internal energy $U_{int}(\phi)$, dependant only on conformation, and $U_{ext}(\beta,\gamma,\phi)$, dependant on both orientation and conformation.

$$U(\beta,\gamma,\phi) = U_{int}(\phi) + U_{ext}(\beta,\gamma,\phi) \tag{37}$$

The external energy $U_{ext}(\beta,\gamma,\phi)$, the potential of mean torque for rigid conformation ϕ, is expanded in terms of modified spherical harmonics to give

$$U_{ext}(\beta,\gamma,\phi) = -\epsilon_{2,0}(\phi) C_{2,0}(\beta,\gamma) - 2\epsilon_{2,2}(\phi) C_{2,2}(\beta,\gamma) \tag{38}$$

In the AP method, the conformation dependence of the interaction coefficient $\epsilon_{2,m}(\phi)$ is approximated as a sum of terms, $\epsilon_{2,p}(j)$, from each of j rigid fragments.

$$\epsilon_{2,m}(\phi) = \sum_{j} \sum_{p} \epsilon_{2,p}(j) D_{p,m}^{2}(\Omega_{j\phi}) \tag{39}$$

$D_{p,m}^{2}(\Omega_{j\phi})$ is the second rank Wigner rotation matrix, which describes the orientation of the jth fragment in the molecular reference frame for the conformation ϕ.

The probability of a conformation, $P_{LC}(\phi)$, depends upon the energy of the conformation and the potential for rotation within the molecule

$$P_{LC}(\phi) = Z^{-1} \exp[-V(\phi)/RT] \int \exp[-U_{ext}(\beta,\gamma,\phi)/RT] \sin\beta \, d\beta \, d\gamma \tag{40}$$

where for a continuous distribution, $V(\phi)$ can be expressed as a cosine series which is

provided as part of the assumption of the general shape of the potential barrier for rotation

$$V(\phi) = \sum_n V_n \cos(n\phi) \tag{41}$$

and Z is the normalisation function

$$Z = \int \exp[-V(\phi)/RT]\, d\phi \int \exp[-U_{ext}(\beta,\gamma,\phi)/RT] \sin\beta\, d\beta\, d\gamma\, d\phi \tag{42}$$

The AP method also allows the calculation of $P_{iso}(\phi)$, the probability distribution in the isotropic phase, thus

$$P_{ISO}(\phi) = Q^{-1} \exp[-V(\phi)/RT] \tag{43}$$

where Q is

$$Q = \int \exp[-V(\phi)/RT]\, d\phi \tag{44}$$

1.9 The Rotational Isomeric State Model

The RIS model, often referred to as the jump model, is the simplest as it approximates the conformational distribution of molecules to the set of minimum energy conformations. The molecules are assumed to jump between these conformations. This model is also particularly useful in cases of many degrees of freedom with respect to flexibility. With these molecules, such as liquid crystals, the number of possible conformations that would need to be explored using a continuous distribution method would be too great. This is shown to good effect in chapter 6, the Analysis of liquid crystals I35 and I52.

1.10 References

[1] M.Longeri and G.Celebre in "Encyclopedia of NMR" p.2774 (D. M. Grant and R. K. Harris, Eds.), Wiley, Chichester (1996)

[2] A.Saupe and G.Englert, *Phys.Rev.*, **11**, 462, (1963)

[3] L.C.Snyder, *J.Chem.Phys.*, **43**, 4041, (1965)

[4] J.Jokisaari, J.Kuonanoja, A.Pulkkinen, T.Vaananen, *Mol. Phys.*, **44**, 197, (1981)

[5] J.W.Emsley, M.I.C.Furby, G.De Luca, *Liq.Cryst,*. **21**, 877, (1996)

[6] M.Edgar, J.W.Emsley and M.I.C.Furby, *J.Mag.Res,*. **128**, 105, (1997)

[7] G.De Luca, M.Edgar, S.Edgar, J.W.Emsley, M.I.C.Furby, M.Webster, *Liq.Cryst.* **24**, 569, (1998).

[8] E.Ciampi, M.I.C.Furby, L.Brennan, J.W.Emsley, A.Lesage, L.Emsley, *in preparation.*

[9] G.Celebre, M.Longeri, J.W.Emsley, *J.Chem.Soc.Faraday Trans. 2.*, **84**, 1041, (1988)

[10] G.Celebre, G.De Luca, M.Longeri, D.Catalano, M.Lumetti, J.W.Emsley, *Mol.Phys.*, **85**, 221, (1995)

[11] E.K.Foord, J.Cole, M.J.Crawford, J.W.Emsley, G.Celebre, M.Longeri, J.C.Lindon, *Liq.Cryst.*, **18**, 615, (1995)

[12] J.W.Emsley, G.De Luca, G.Celebre, M.Longeri, *Liq.Cryst.*, **20**, 569, (1996)

[13] B.M.Fung, *J.Mag.Res.*, **55**, 475, (1983)

[14] J.Courtieu, J.P.Bayle, B.M.Fung, *Prog.NMR.Spectrosc.*, **26**, 141, (1994)

[15] G.Celebre, G.De Luca, M.Longeri, E.Sicilia, *J.Chem.Inf.Comp,Sci.*, **34**, 539, (1994)

[16] S.Castellano, A.A.Bothner-By, *J.Chem.Phys.*, **41**, 3863 (1964)

[17] J.W.Emsley, G.R.Luckhurst, C.P.Stockley, *Proc.Roy.Soc.London.*, **A381**, 117 (1982)

Chapter 2

The Conformation of Phenyl Benzoate when Dissolved in a Nematic Liquid Crystal Solvent

2.1 Introduction

Phenyl Benzoate, whose structure is shown in figure 1, is an example of a simple fragment that commonly occurs in both monomeric and polymeric liquid crystals. The popularity of the ester linkage and the importance of the phenyl benzoate fragment is clear. It should then

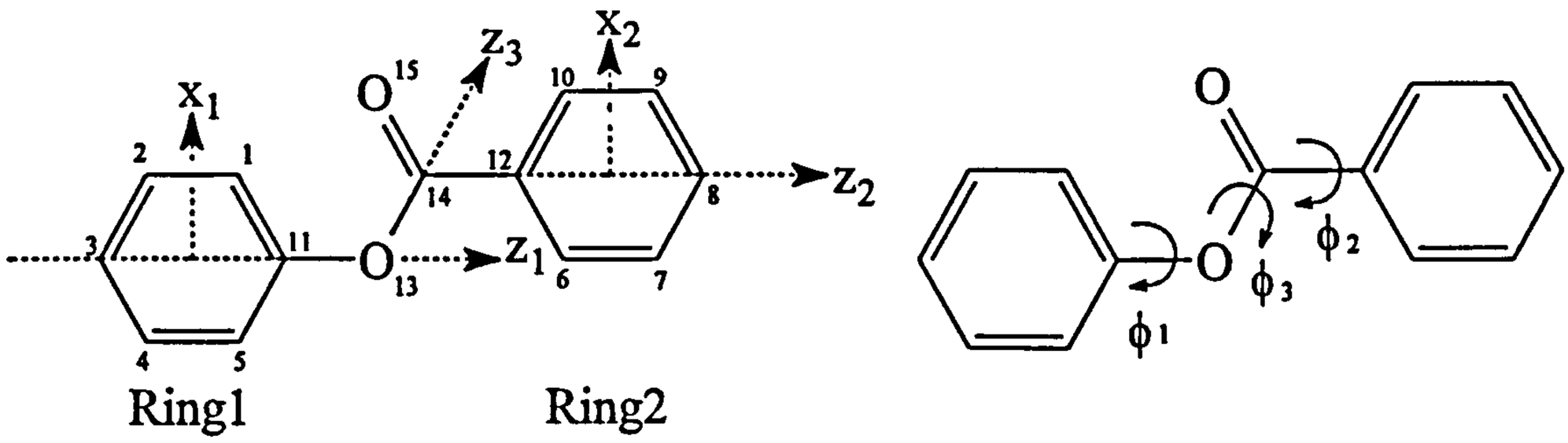

Figure 1 The structure of phenyl benzoate showing the atomic and axes labels.

be of great interest to study the conformational behaviour of this fragment in the liquid crystal phase. The reason we choose phenyl benzoate as opposed to other common liquid crystal fragments is that it extends our techniques of spectral and conformation analysis successfully used in the past to a more complex situation. Structural studies have been performed on mesogens and the mesogenic fragments such as biphenyl [1], chloroethylbenzene [2] and phenyl acetate [3]. The structural study of phenyl benzoate introduces new difficulties as the two rings are not equivalent. This complicates the anisotropic ^{1}H NMR spectrum for this ten spin system compared to the ten spin system of biphenyl whose two rings are equivalent. We are helped by the presence of symmetry within the two rings about their respective rotation axes, rotation about Z_1, for example, interchanges pairs of protons and creates a symmetry in the nuclear spin Hamiltonian. From the analysis of the anisotropic ^{1}H NMR spectrum of biphenyl it is possible to obtain twelve independent spin-spin, dipolar, couplings. From the same type of spectrum for phenyl benzoate we can obtain twenty one independent D_{ij}. A fragment of this degree of complexity

has not in the past been successfully analysed. With regard to the conformational analysis, we have the possibility of three axes of rotation within the molecule, this brings in a substantial time factor in the analysis when we consider all possible conformers, as in theory the number of conformers increases by the power of the number of rotors. The structure in the solid phase has been determined through X-ray diffraction [4]. This showed that ring 2 is rotated about Z_2 by ϕ_2=9.8°, and ring 1 is rotated about Z_1 by ϕ_1=65.1° both relative to the planar OCO group determining the resulting dihedral angle between the two rings to be 55.3°. Phenyl benzoate has also been the subject of a molecular orbital calculation on a single isolated molecule. This determined the minimum energy structure to be ϕ_1=46.4°, ϕ_2=0.2° and ϕ_3=0° which is comparable to the X-ray structure. The difference in twist angles determined, can be easily explained, as the barrier for rotation about the Z_1 axis is said to be very low, and that the difference in energy between ϕ_1=65.1° and ϕ_1=46.4° is of the order of RT [5]. Also the lowest energy structure in the crystal form often has slight geometry differences to those of free molecules due to the packing forces involved. Rotation about Z_3 if it occurs will result in severe steric hinderance as ϕ_3 approaches 180°. A survey of crystal structures of esters [6] found none of type 2 (ϕ_3=180°), with most structures being of type 1 approximate to ϕ_3=0°. This does not rule out the possibility of rotational freedom about Z_3 in fluid phases, however, we would not expect a great deviation from ϕ_3=0° for the minimum energy structure of phenyl benzoate in any phase. Here we are interested in determining the rotation potentials of phenyl benzoate in the nematic liquid crystal phase at approximately room temperature. As described in chapter 1, the proton NMR spectrum of such a sample can be analysed in order to extract the dipolar couplings, D_{ij}, which are directly related to the molecular structure and are averaged over all internal motions and the motion of the molecules within the sample.

We have already discussed the improvement in our ability to analyse more complex NMR spectra due to increase computer power and speed, in chapter 1. With these facilities it is now possible to attempt the analysis of this ten spin system within a reasonable time frame.

2.2 Experimental

2.2.1 NMR Spectroscopy of Phenyl Benzoate in the Nematic Liquid Crystal Phase

The 200 MHz ^{1}H NMR spectrum of phenyl benzoate as a 10% w/w solution in the nematic mixture ZLI 1132 (Merck Ltd.) is shown in figure 2. The spectrum consists of hundreds of transitions which need to be properly assigned in order to obtain the correct parameters. This can be contrasted to the proton NMR spectrum of phenyl benzoate in isotropic solution, shown in figure 3, which although itself is a difficult spectrum to analyse is no where near as complex as the spectrum of phenyl benzoate in the LC phase as the anisotropic interactions which dominate LC spectra are averaged to zero. It is practically impossible to start from scratch with the analysis of the liquid crystal spectrum, so we proceeded in stages by first analysing the deuterium decoupled proton spectra of samples of the four isotopomers **3**, **4**, **5** and **6**, shown in figure 4, dissolved at the approximate same concentration in ZLI 1132. For each isotopomer we recorded both ^{1}H-{^{2}H} and ^{2}H NMR spectra which are shown in figure 5.

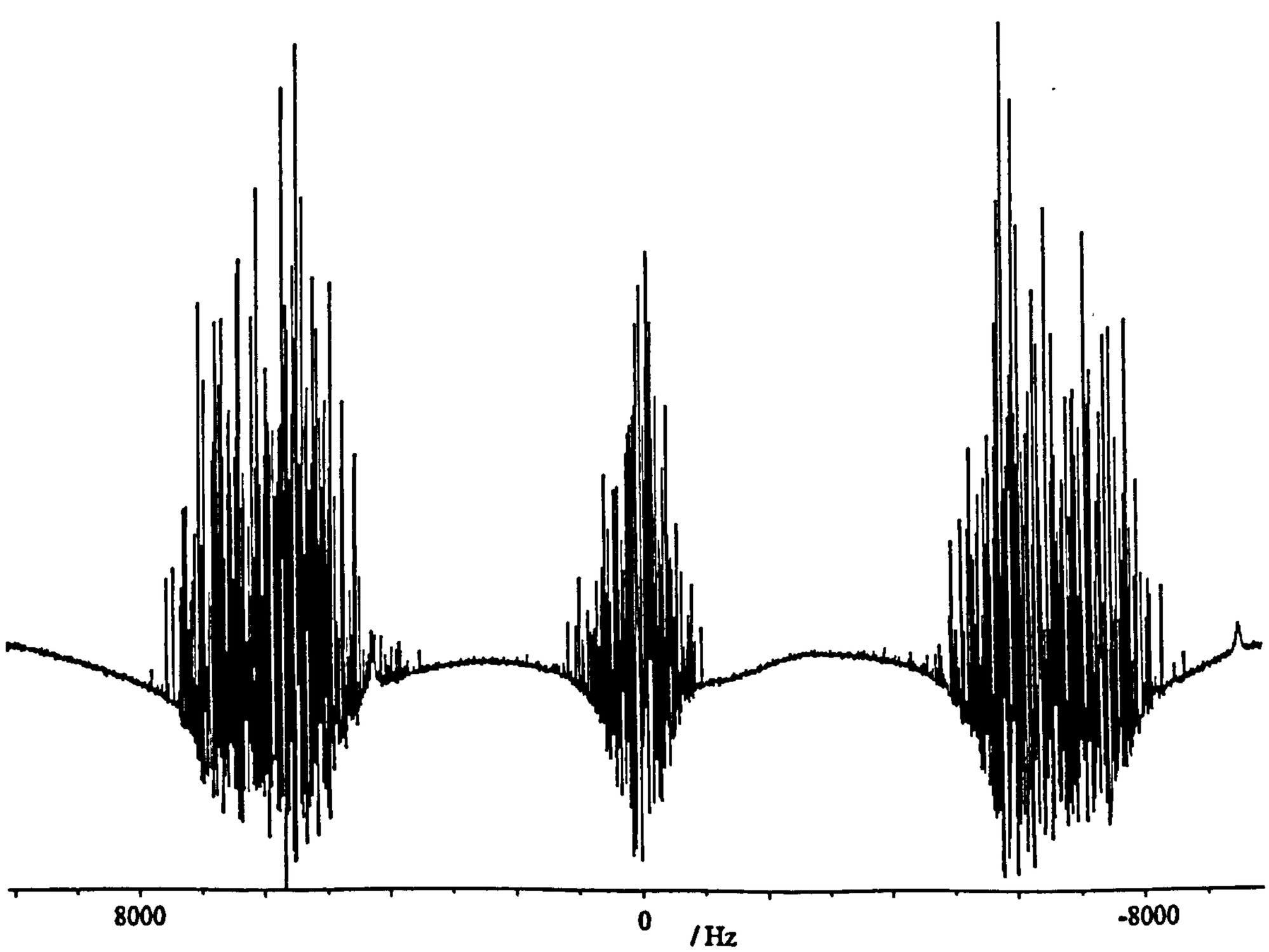

Figure 2 The 200 MHz proton spectrum of a sample of phenyl benzoate approximately 10% w/w dissolved in ZLI 1132 at 300K.

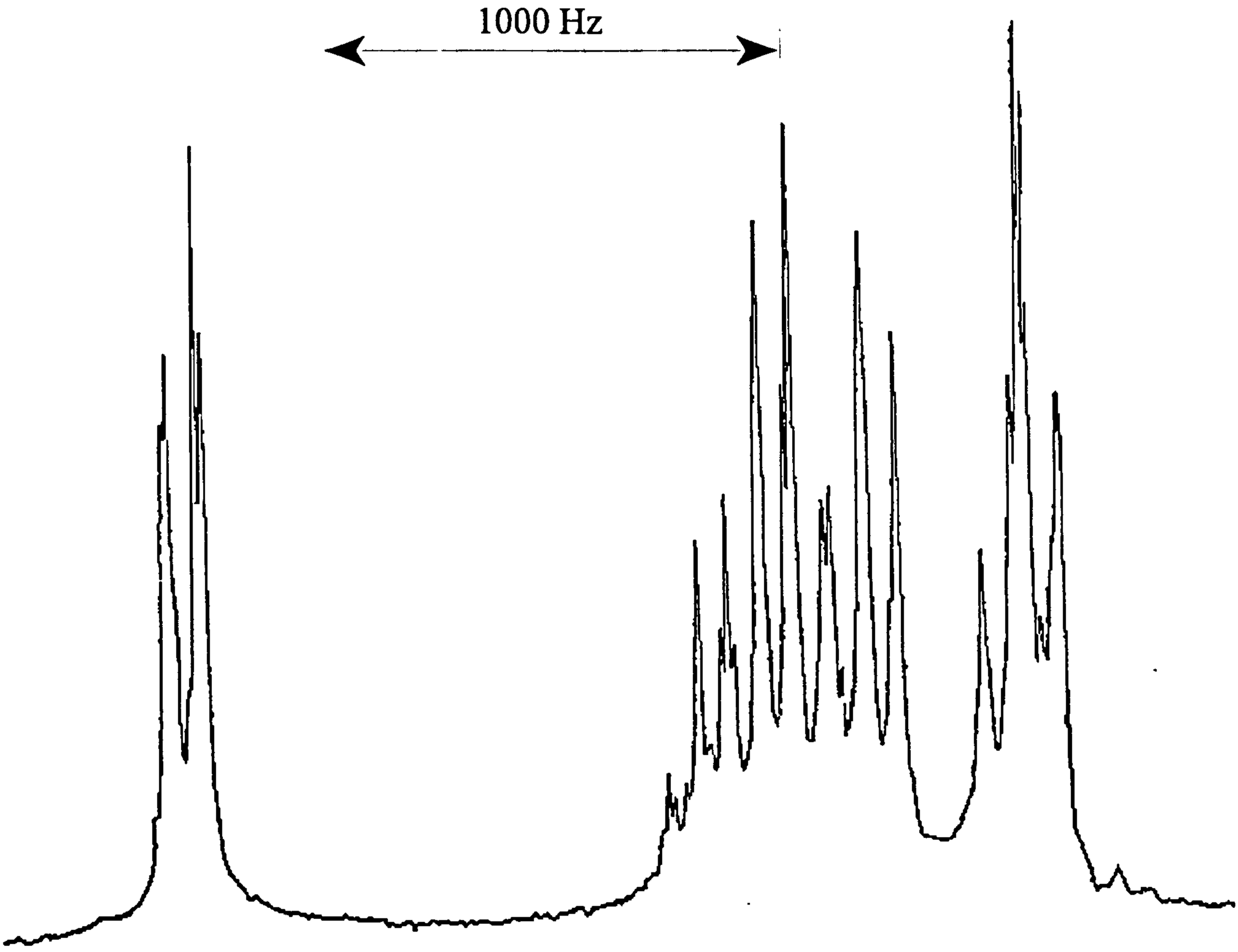

Figure 3 200MHz ^{1}H NMR spectrum of phenyl benzoate dissolved in chloroform.

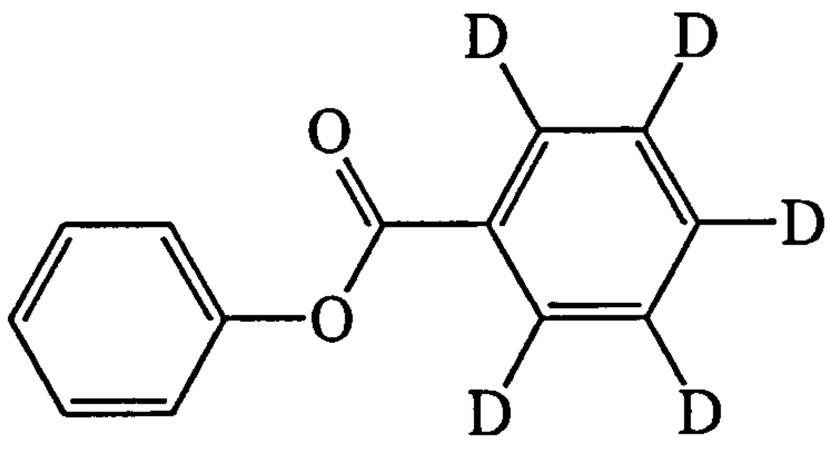

3

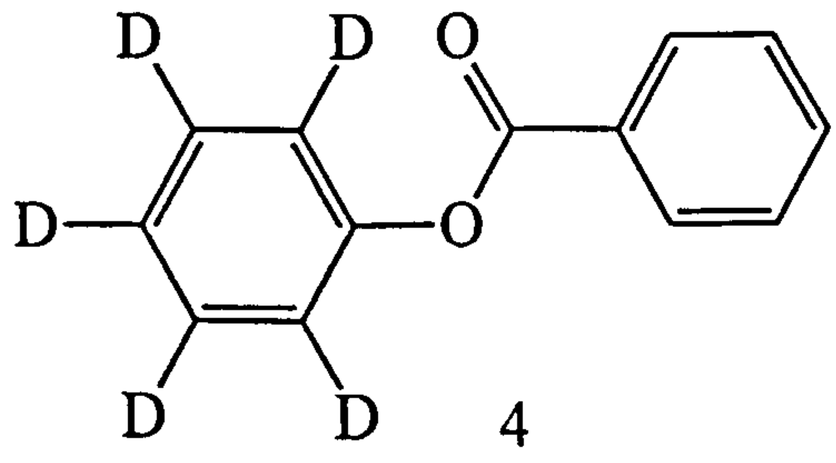

4

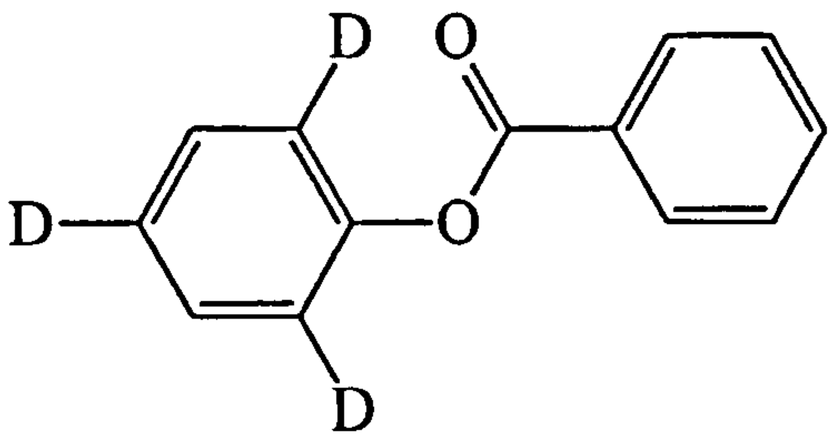

5

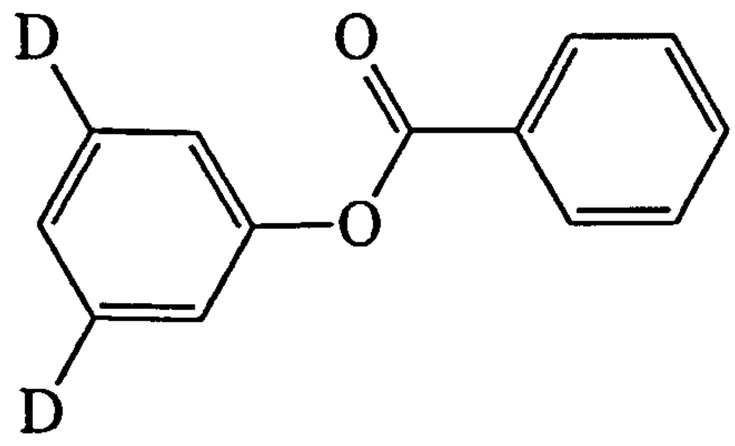

6

Figure 4 Partially deuterated phenyl benzoate isotopomers

Compound	^{2}H NMR spectra	^{1}H-{^{2}H} NMRspectra
3	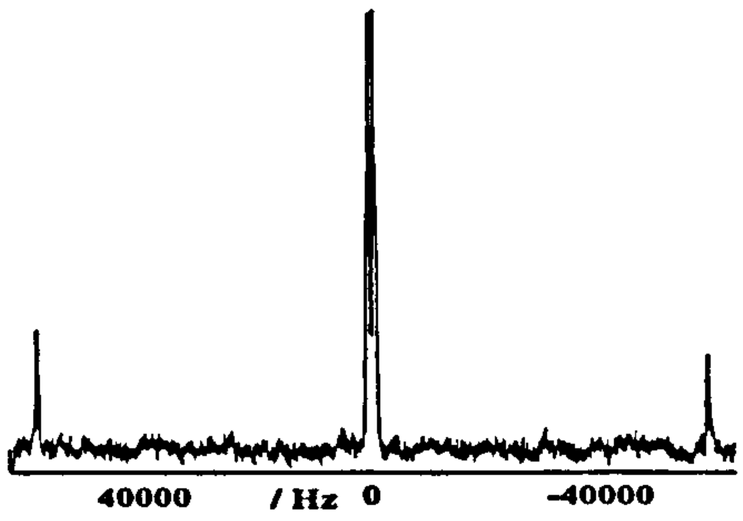	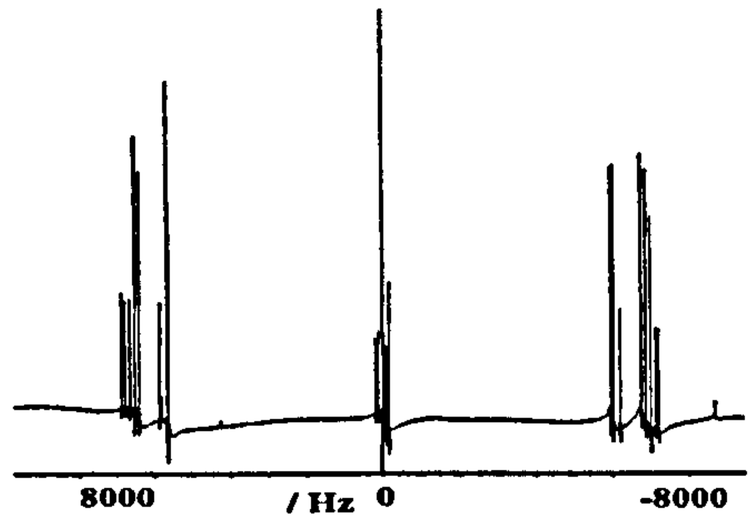
4	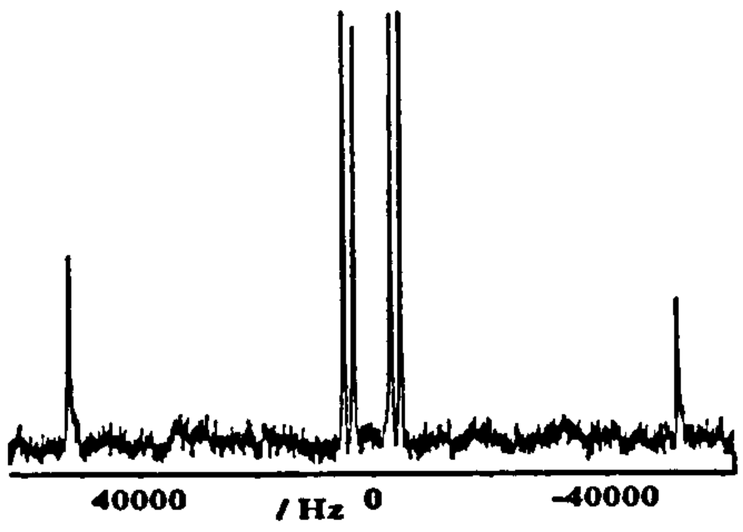	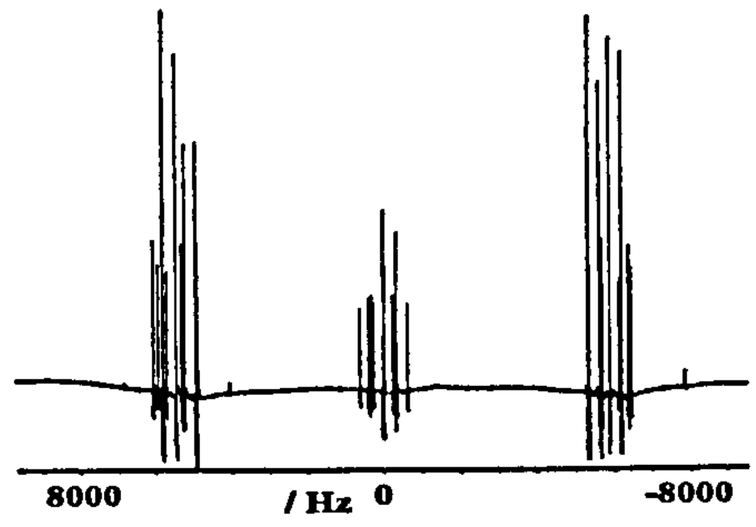
5	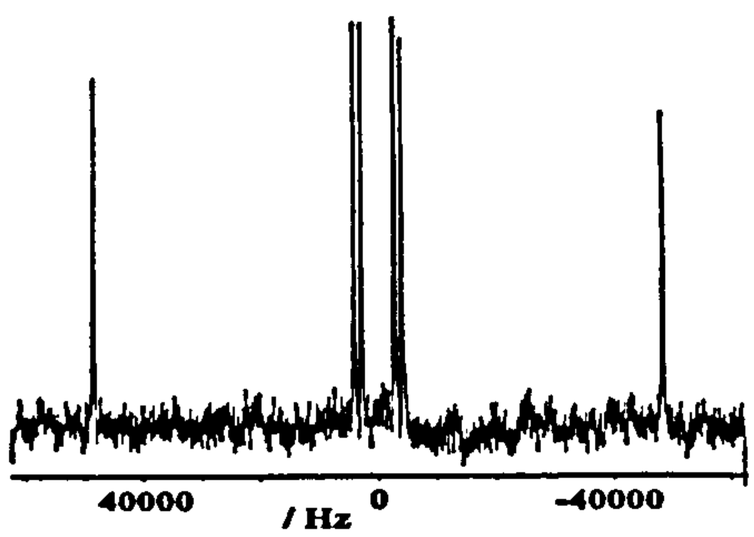	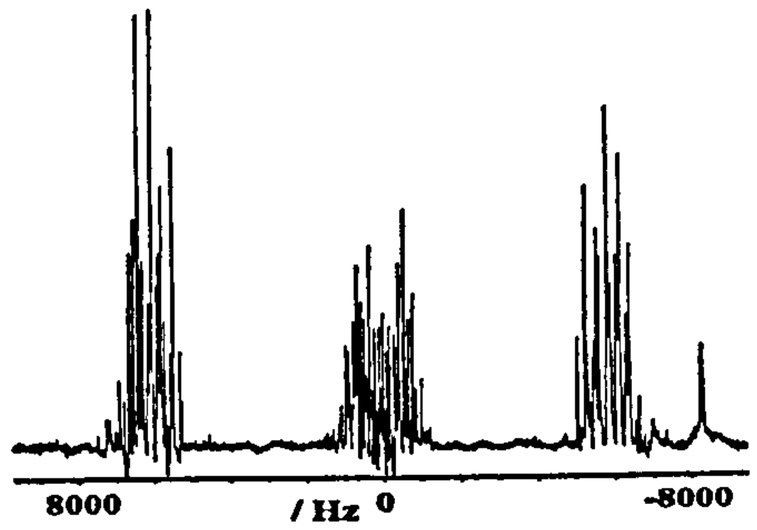
6	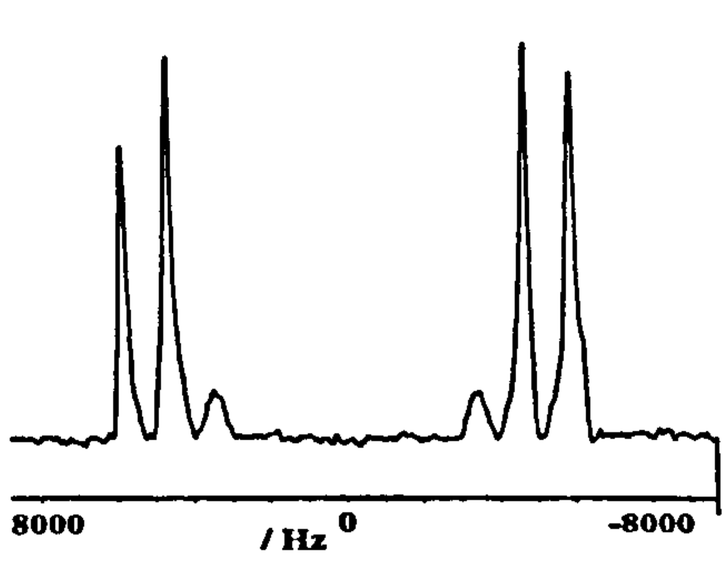	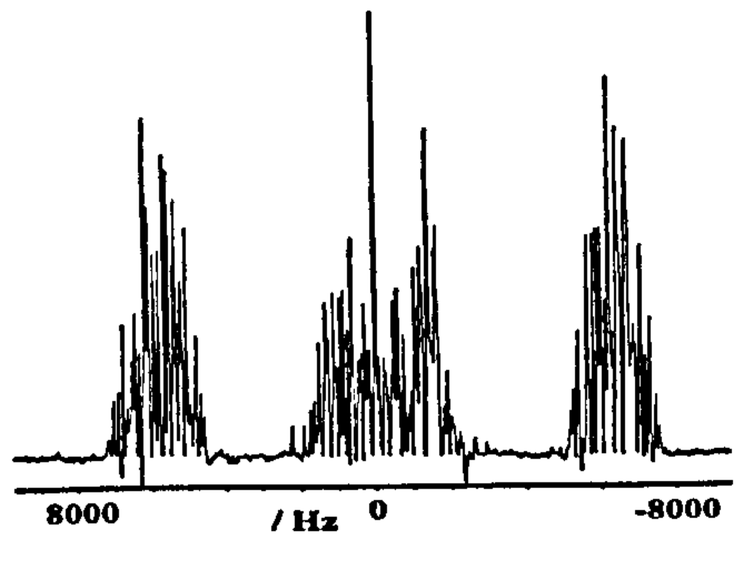

Figure 5. 30.7 MHz ^{2}H and 200 MHz ^{1}H-{^{2}H} NMR spectra of samples of partially deuterated phenyl benzoate approximately 10% w/w dissolved in the nematic solvent ZLI 1132 at 300K

2.2.2 Synthesis of Phenyl Benzoates

The four isotopomers were synthesised from the appropriate deuteriated materials by the following procedure as described by Vogel [7].

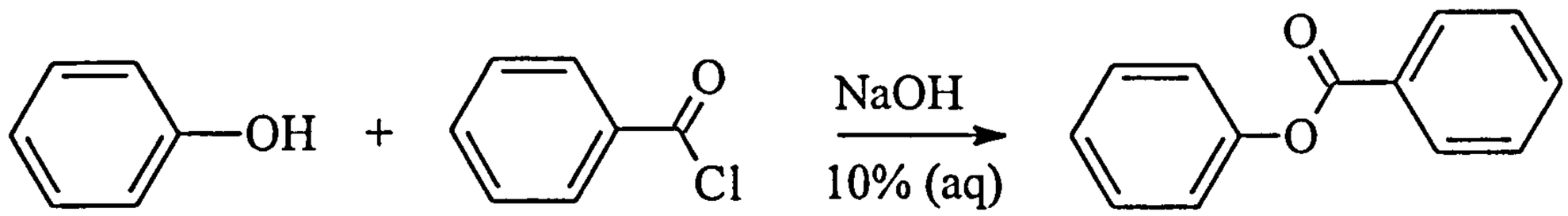

Phenol Benzoyl Chloride Phenyl Benzoate

Phenol (0.95g, 0.0101M) in 10% NaOH solution (15ml) were stirred together in a RB flask fitted with a condenser. Benzoyl chloride (1.42g, 0.0101M) was added and the mixture was stirred and allowed to cool for 30 minutes. After this time the solid product formed was filtered off under suction and washed with water. The solid product was recrystallised using rectified spirit, and filtered. The colourless crystals produced were dried and weighed. The mass of the product formed was 1.18g (0.0051 mol), corresponding to a yield of 50%. Thin Layer Chromatography (TLC) showed the product to be free of impurities and the melting point of the solid was found to be 71°C (cf. 69°C [8]).

The isotopomers **3-6** were synthesised by the same procedure, but using deuterated starting materials.

2.2.3 Synthesis of Fully Deuterated Benzoyl Chloride

Thionyl Chloride (2.5g, 0.0210M) was added dropwise to deuterated benzoic acid (1g, 0.0079M) (Aldrich) in a 3 way flask, in a water bath at 70° C, fitted with a separating funnel and a condenser. The water bath was removed and the mixture stirred for 2 hours under reflux. The excess thionyl chloride was then distilled off, followed by the deuterated benzoyl chloride, both under a reduced pressure to yield the product.

2.2.4 Synthesis of 2,4,6-d_3-phenol

20% DCl/D_2O (8ml) solution was added to phenol (2.01g, 0.0214M) in a RB flask and

heated under reflux for 48 hours at 150° C, whilst stirring. The deuterated phenol was extracted with diethyl ether. The product was dried overnight with $CaCO_3$, and filtered. The solvent was extracted using a rotary evaporator to leave an oily product, which can be used without further purification in the synthesis of compound 5.

2.2.5 Synthesis of 2,4-d_2-phenol

The reaction was similar to the synthesis of 2,4,6-d_3-phenol. However, the reaction was carried out over 72 hours, using 20% HCl/H_2O (8ml) and fully deuterated phenol (2g, 0.0202m), and used in the synthesis of compound 6.

2.3 Results and Discussion

2.3.1 Analysis of the NMR spectra from the Partially Deuterated Isotopmers

Deuterium Spectra

The analysis of the ^2H NMR spectra of **3** and **4**, in figure 6, yield the local order parameters for each benzene ring, which are in turn used to calculate D_{ij} values for those rings assuming a geometry as starting points for the analysis of the corresponding ^1H-{^2H} NMR spectra. The spectra were assigned as follows. Both the spectra of **3** and **4** give rise to three doublets from the three inequivalent deuterons in each ring. The doublet splittings are related to the order parameters through equation 1.

$$\Delta\nu_i = \frac{3}{2} q^i_{CD} S^i_{CD} \qquad (1)$$

where

$$S^i_{CD} = S_{ZZ}(3\cos^2\theta_{CDZ} - 1)/2 + (S_{XX} - S_{YY})(\cos^2\theta_{CDX} - \cos^2\theta_{CDY})/2 \qquad (2)$$

The order parameters are then related to the D_{ij} through equation 3.

$$D_{ij} = -(K_{ij}/r_{ij}^3)[S_{ZZ}(3\cos^2\theta_{ijZ} - 1) + (S_{XX} - S_{YY})(\cos^2\theta_{ijX} - \cos^2\theta_{ijY})] \quad (3)$$

In our reference frame, figure 6, the C-D3 bond lies along the Z axis and only contributes to the S_{ZZ} order parameter. The outer doublets in the ^2H spectra of **3** and **4** are assigned from their relative intensities to the C-D3 deuterons.

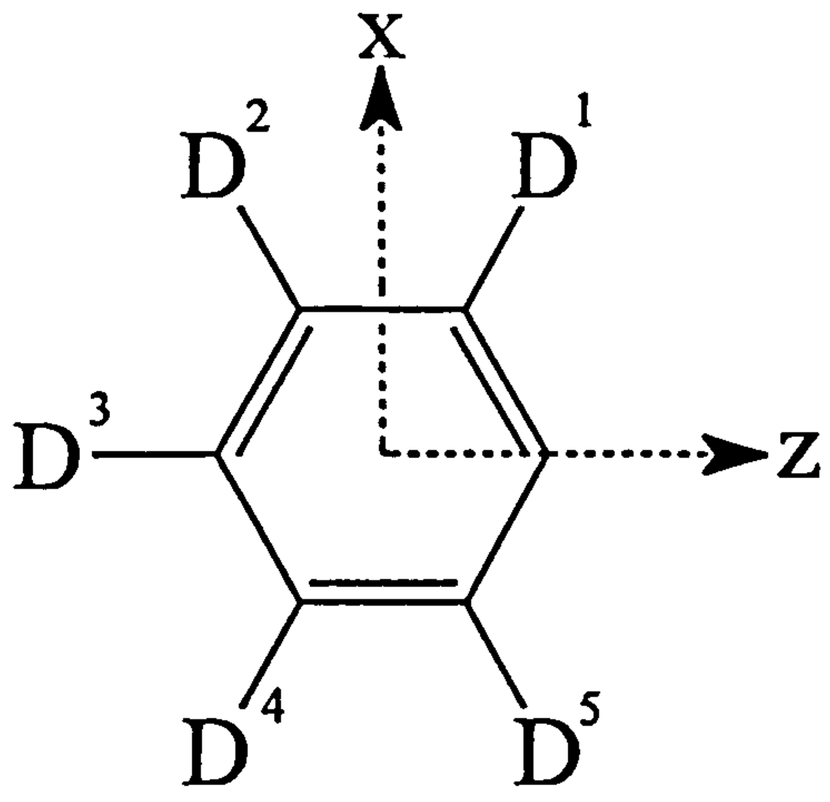

Figure 6 Reference frame for deuterated rings

The C-D1,2 bonds lie in the XZ plane so both depend on S_{ZZ} and S_{XX}-S_{YY} which can be calculated from the corresponding quadrupole splittings. The inner doublets are from D1(≡D5) and D2(≡D4), but cannot be assigned. In order to calculate the order parameters, the ring was assigned a regular hexagonal geometry, and $q_{CD}^1 = q_{CD}^2$ and the average splitting, $\frac{1}{2}(\Delta\nu_1 + \Delta\nu_2)$ used. The contribution to S_{ZZ} is already known from $\Delta\nu_3$, then S_{XX}-S_{YY} can be calculated.

2.3.2 *Proton Spectra*

In order to be able to analyse the very complex ^1H spectrum in figure 2, we first need to analyse simpler systems, and build up to the final analysis of the most complicated system. To begin the analysis of the proton spectra we require the calculated D_{HH} obtained through the analysis of the deuterium spectra and equation (3). To complete the analysis correctly, we need to consider the J_{HH}. Although we have not determined these in phenyl benzoate, they should be very similar to those determined in other substituted benzenes ($^3J_{HH} \sim 8$Hz,

$^4J_{HH} \sim 2Hz$, $^5J_{HH} \sim 0Hz$) [9]. The values of the J_{HH} are small compared to the D_{HH}, in a highly ordered system such as we are dealing with, and any effect on the final results due to small errors in the values of the J_{HH} are negligible. The substitution of deuterium for protons in the isotopomers of phenyl benzoate, removes the D_{HH} that were associated with those substituted protons. As a result the spectra are much simplified, and are easier to analyse. From the ^1H-{^2H} NMR five spin spectra of **3** and **4** we obtain six independent D_{HH}, we obtain ten independent D_{HH} from the seven spin system in **5**, fourteen from the eight spin system in **6** and twenty one from the ten spin system. Analysis of **5** and **6** also gives the values of some of the inter ring couplings.

The results of the analyses are given in tables 1 - 4 and were used as starting parameters in the analysis of the ten spin ^1H NMR spectrum in figure 3, the final results of which are reported in table 5.

2.3.3 Structure of Each Phenyl Ring

The dipolar couplings between protons within a rigid group, such as each of the phenyl rings, are given by equation (3). The rotational motion about the Z_1 and Z_2 axes imparts a 2-fold permutation symmetry to the nuclear spin Hamiltonian. Explaining more simply, without motion about these axes, the protons in each ring are all inequivalent and the spin system becomes an ABCDE. Motion about Z_1 averages, the chemical shifts of H-1 and H-5, and H-2 and H-4 (protons mirrored about the axis of rotation) and the spin system becomes AA'BB'C. The same applies for motion about Z_3. The molecular symmetry is also effectively C_{2v} for each phenyl fragment, so that the terms in equation (3) with $S_{\alpha\beta}$, $\alpha \neq \beta$, i.e. the off diagonal elements are averaged to zero, if we assume that no geometry change occurs during rotation, and we are left with 2 independent order parameters S_{XX}-S_{YY} and S_{ZZ} for each ring.

The relative positions of the protons, and the $S_{\alpha\beta}(n)$ were obtained by comparing observed and calculated values of D_{ij} and minimising the error function

$$R = \sum_{i<j} \Delta D_{ij}^2 \qquad (4)$$

Table 1 - Chemical shifts, δ_i, scalar couplings J_{ij}, and dipolar couplings, D_{ij}, obtained from the analysis of the 30.7 MHz ^2H and the 200 MHz ^1H NMR Spectrum, of 10% w/w phenyl benzoate isotopomer **3** dissolved in the nematic solvent ZLI 1132.

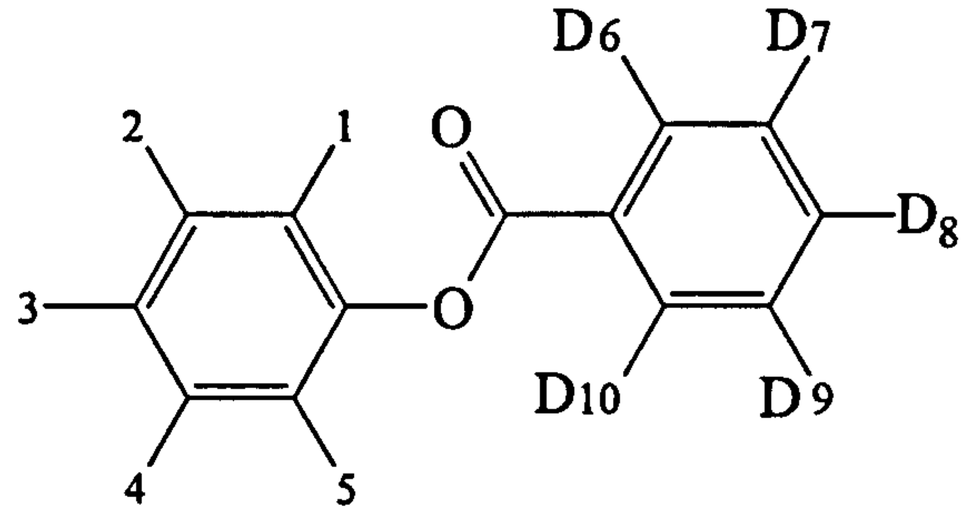

Doublet splittings from ^2H spectrum:

$\Delta\nu_8$	= 104428 ±50 Hz
$\Delta\nu_{6/7}$	= 9781 ±50 Hz
$\Delta\nu_{7/6}$	= 6302 ±150 Hz
$(\Delta\nu_6 + \Delta\nu_7) / 2$	= ± 8042 Hz

Calculated order parameters:

S_{ZZ}	= 0.376
S_{YY}	= -0.212 (or -0.289)
S_{XX}	= -0.164 (or -0.087)

Final results from analysis of ^1H spectrum

i,j	J_{ij} /Hz	D_{ij} /Hz (±1)
1,2	8.0	-4222
1,3	2.0	-534
1,4	0.0	42
1,5	2.0	370
2,3	8.0	374
2,4	2.0	370

i	δ_i /Hz (±1)
1	-177
2	-189
3	7

RMS deviation of transition frequencies = 3Hz

Table 2 - Chemical shifts, δ_i, scalar couplings J_{ij}, and dipolar couplings, D_{ij}, obtained from the analysis of the 30.7 MHz ^2H and the 200 MHz ^1H NMR Spectrum, of 10% w/w phenyl benzoate isotopomer **4** dissolved in the nematic solvent ZLI 1132.

Doublet Splittings from ^2H spectrum:

$\Delta\nu_3$	= 107760 ±50 Hz
$\Delta\nu_{1/2}$	= 2304 ±50 Hz
$\Delta\nu_{2/1}$	= 1358 ±50 Hz
$(\Delta\nu_1 + \Delta\nu_2)/2$	= ± 1831 Hz

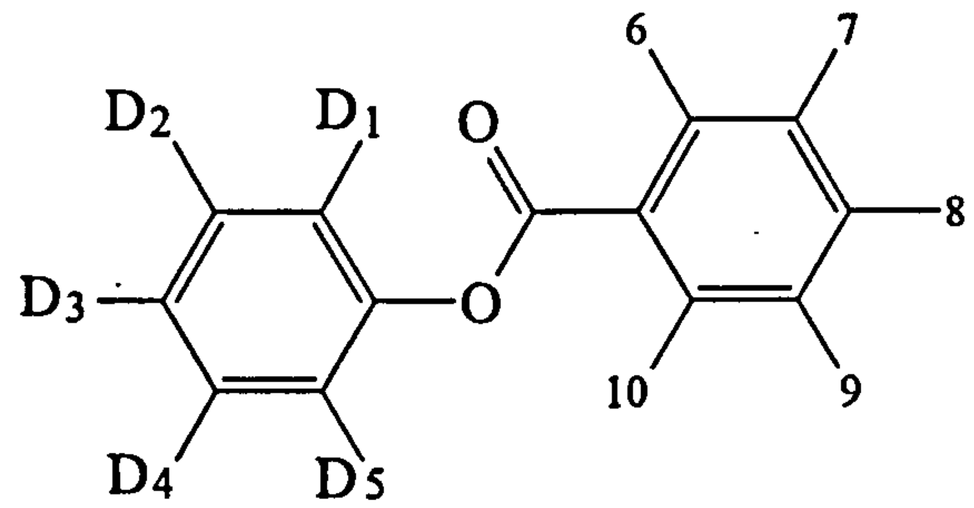

Calculated order parameters:

S_{ZZ}	= 0.388
S_{YY}	= -0.248 (or -0.269)
S_{XX}	= -0.140 (or -0.119)

Final results from analysis of ^1H spectrum

i,j	J_{ij} /Hz	D_{ij} /Hz (±1)
6,7	8.0	-3772
6,8	2.0	-483
6,9	0.0	12
6,10	2.0	272
7,8	8.0	121
7,9	2.0	272

i	δ_i /Hz (±1)
6	-170
7	-260
8	0

RMS deviation of transition frequencies = 3Hz

Table 3 - Chemical shifts, δ_i, scalar couplings J_{ij}, and dipolar couplings, D_{ij}, obtained from the analysis of the 30.7 MHz ^2H and the 200 MHz ^1H NMR Spectrum, of 10% w/w phenyl benzoate isotopomer **5** dissolved in the nematic solvent ZLI 1132.

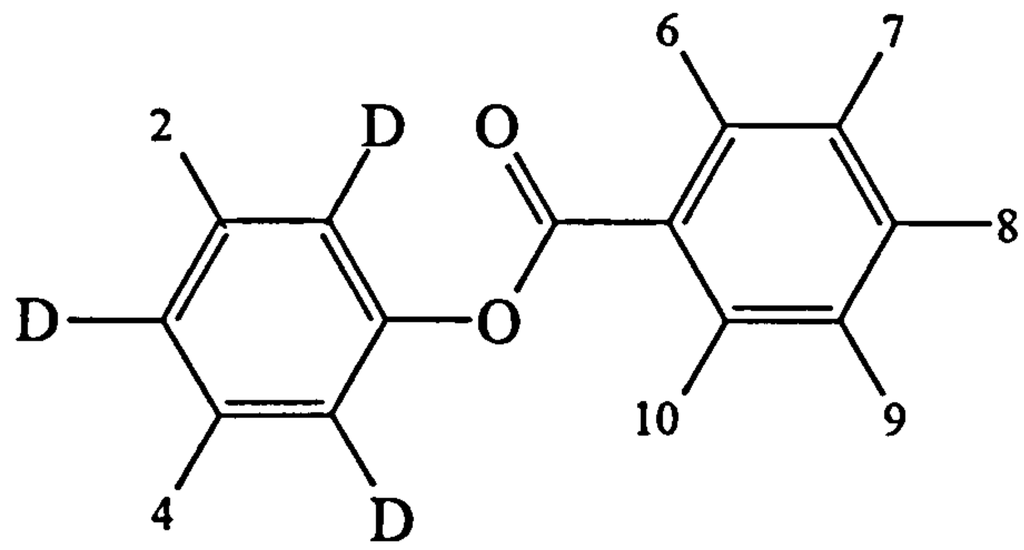

Final results from analysis of ^1H spectrum

i,j	J_{ij} /Hz	D_{ij} /Hz (±1)
6,7	8.0	-3935
6,8	2.0	-495
6,9	0.0	16
6,10	2.0	289
2,6	0.0	-155
7,8	8.0	128
7,9	2.0	277
2,7	0.0	-76
2,8	0.0	-58
2,4	2.0	35

i	δ_i /Hz (±1)
6	161
7	81
8	352
2	64

RMS deviation of transition frequencies = 4Hz

Table 4 - Chemical shifts, δ_i, scalar couplings J_{ij}, and dipolar couplings, D_{ij}, obtained from the analysis of the 30.7 MHz ^2H and the 200 MHz ^1H NMR Spectrum, of 10% w/w phenyl benzoate isotopomer **6** dissolved in the nematic solvent ZLI 1132.

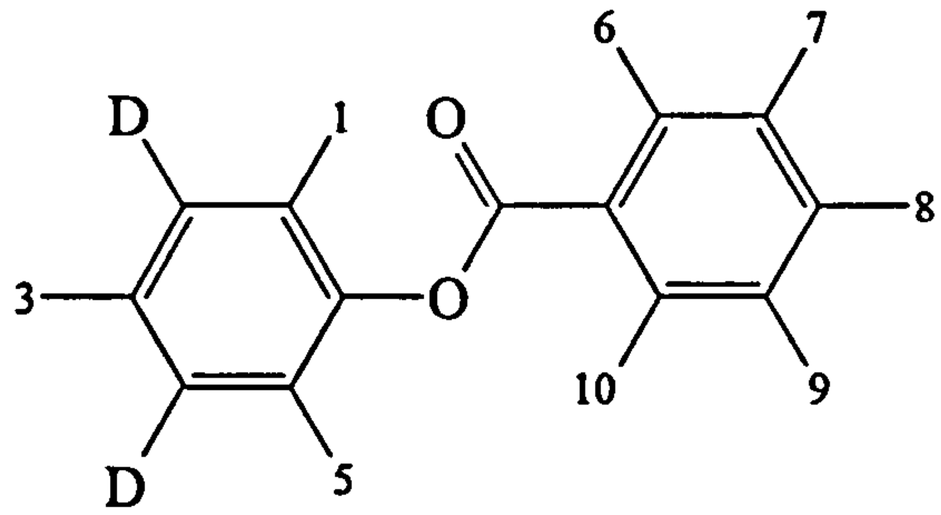

Final results from analysis of ^1H spectrum

i,j	J_{ij} /Hz	D_{ij} /Hz (±1)
6,7	8.0	-3978
6,8	2.0	-498
6,9	0.0	19
6,10	2.0	293
1,6	0.0	-369
3,6	0.0	-131
7,8	8.0	140
7,9	2.0	293
1,7	0.0	-156
3,7	0.0	-63
1,8	0.0	-128
3,8	0.0	-51
1,5	2.0	365
1,3	2.0	-527

i	δ_i /Hz (±1)
6	123
7	30
8	301
1	10
3	200

RMS deviation of transition frequencies = 8Hz

Table 5 - Chemical shifts, δ_i, scalar couplings J_{ij}, and dipolar couplings, D_{ij}, obtained from the analysis of the 200 MHz proton NMR Spectrum, of 10% w/w phenyl benzoate dissolved in the nematic solvent ZLI 1132.

ij	J_{ij} / Hz *	D_{ij} /Hz
12	8.0	-3918.3 ± 0.1
13	2.0	-499.6 ± 0.2
14	0.5	13.9 ± 0.1
15	2.0	285.1 ± 0.1
16	0.0	-373.9 ± 0.1
17	0.0	-155.1 ± 0.1
18	0.0	-126.0 ± 0.1
23	6.0	138.9 ± 0.2
24	2.0	285.1 ± 0.1
26	0.0	-156.4 ± 0.1
27	0.0	-73.2 ± 0.1
28	0.0	-60.1 ± 0.1
36	0.0	-126.5 ± 0.1
37	0.0	-59.5 ± 0.1
38	0.0	-48.2 ± 0.1
67	8.0	-4167.3 ± 0.1
68	2.0	-518.3 ± 0.2
69	0.5	42.7 ± 0.1
610	2.0	364.3 ± 0.1
78	6.0	363.3 ± 0.2
79	2.0	364.3 ± 0.1

i	δ_i / Hz
1	0.0 ± 0.2
2	-155.0 ± 0.2
3	330.6 ± 0.1
6	-167.3 ± 0.1
7	-176.6 ± 0.2
8	-162.0 ± 0.1

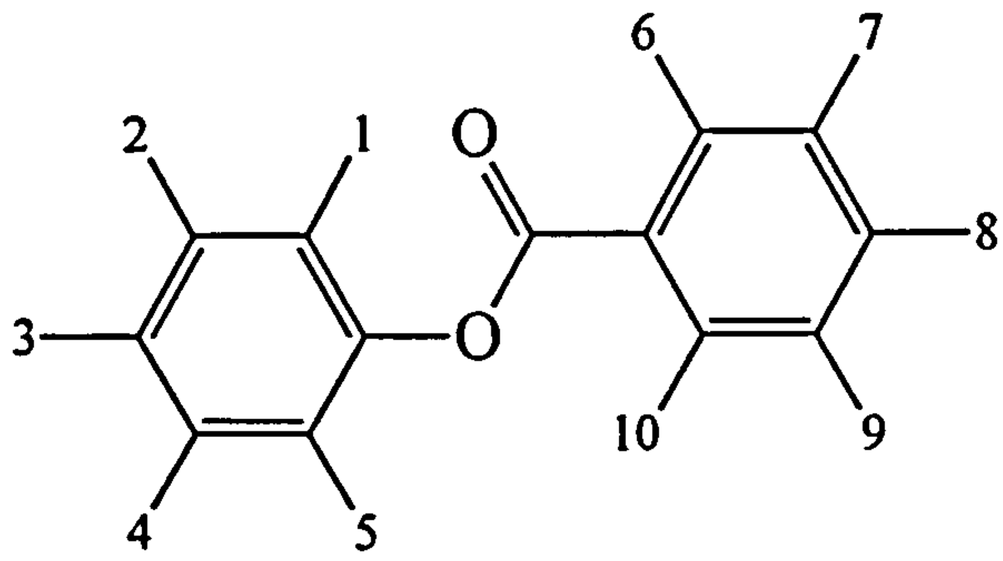

* Fixed at values assumed by comparison with similar compounds

with

$$\Delta D_{ij} = \left[D_{ij}(observed) - D_{ij}(calculated) \right] \quad (5)$$

The X-ray geometry was initially assumed as a good starting point for the relative positions of the ester linkage fragment C(11)-O(13)-C(14)-C(12). The rings in the solid state are distorted from regular hexagonal symmetry by small amounts, but in the solution where the rings are also distorted, the motion about Z_1 and Z_2 averages these distortions between the mirrored pairs of protons and the rings becomes symmetric about the axes of rotation. To begin with the two phenyl rings were assumed to have hexagonal symmetry with r_{CC} = 1.4Å and r_{CH} = 1.09Å. For ring 1, for example, the proton coordinates X_1(=-X_5), Z_2(=Z_4), and Z_3 were varied together with $S_{ZZ}(1)$ and $S_{XX}(1) - S_{YY}(1)$ to minimise R. A similar procedure was adopted for ring 2. The results are shown in table 6.

Table 6 - Local order parameters $S_{\alpha\beta}(1)$ and $S_{\alpha\beta}(2)$ for the phenyl rings of phenyl benzoate dissolved in the nematic solvent ZLI 1132, together with the relative coordinates (Å) of the protons.

Ring 1		Ring 2	
$S_{XX}(1) - S_{YY}(1)$	0.0597	$S_{XX}(2) - S_{YY}(2)$	0.1300
$S_{ZZ}(1)$	0.5490	$S_{ZZ}(2)$	0.5142
X_1=-X_5	2.1636	X_6=-X_{10}	2.1689
Y_1=Y_5	0.0000	Y_6=Y_{10}	0.0000
Z_1=Z_5	1.2450	Z_6=Z_{10}	1.2450
X_2=-X_4	2.1564	X_7=-X_9	2.1564
Y_2=Y_4	0.0000	Y_7=Y_9	0.0000
Z_2=Z_4	-1.2652	Z_7=Z_9	-1.2620
X_3	0.0000	X_8	0.0000
Y_3	0.0000	Y_8	0.0000
Z_3	-2.5084	Z_8	-2.4966

2.3.4 Conformational analysis

The intra-ring dipolar couplings cannot be calculated with eqn(3) since in principle the order parameters for the whole molecule vary with the angles ϕ_1, ϕ_2 and ϕ_3. This dependence will be modelled using the Additive Potential (AP) method [10].

The molecular fragments used to construct $\epsilon_{2,m}(\{\phi_k\})$ in this model are shown in figure 7.

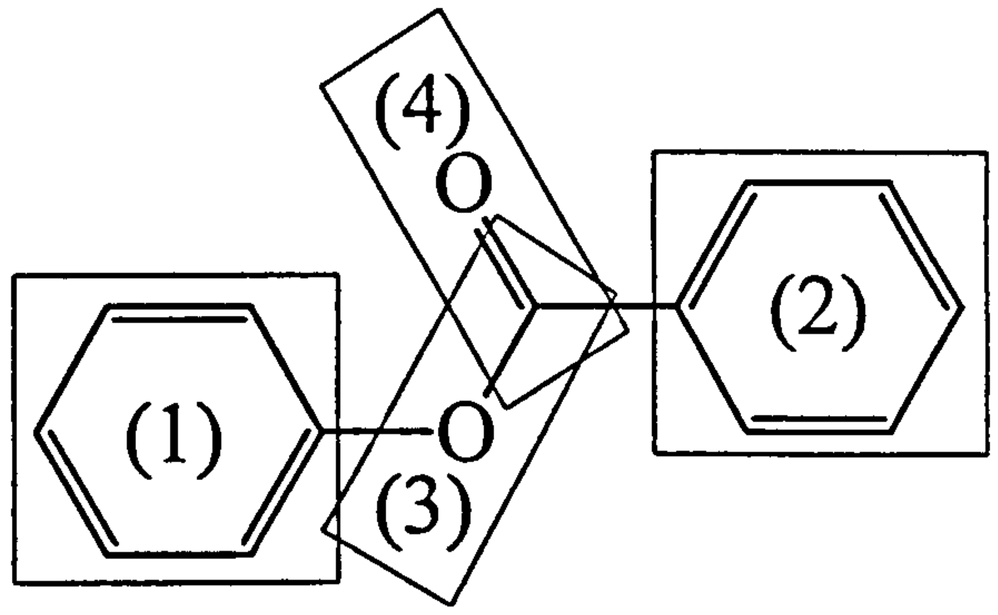

Figure 7 Fragment definition for phenyl benzoate

Symmetry requires $\epsilon_{2,0}(1)$ and $\epsilon_{2,2}(1)$ to be non-zero, but it is assumed that fragments 3 and 4 are axially symmetric, so that the only non-zero elements for these are $\epsilon_{2,0}(3)$ and $\epsilon_{2,0}(4)$.

Ring 2 also requires $\epsilon_{2,0}(2)$ and $\epsilon_{2,2}(2)$, but in practice it was found that the data cannot distinguish $\epsilon_{2,0}(1)$ from $\epsilon_{2,0}(2)$ and $\epsilon_{2,2}(1)$ from $\epsilon_{2,2}(2)$ and so these pairs of interaction coefficients were kept equal. This has an advantage that the number of variables is reduced, which although two degrees of freedom are lost the fit to the data is more constrained to find a reasonable minimum.

2.3.5 The two rotor model

An attempt was made to fit the D_{ij} to the case with no motion about ϕ_3.We choose this model as we have no evidence, in the literature, for any appreciable motion about Z_3. The rotation about ϕ_1 and ϕ_2 have repeat periods of 90° and the simplest potential is, therefore, $V_2\cos2\phi + V_4\cos4\phi$. The internal conformationally dependent energy $U_{int}(\{\phi_k\})$ therefore becomes :

$$U_{int}(\{\phi_k\}) = V_{21}\cos2\phi_1 + V_{41}\cos4\phi_1 + V_{22}\cos2\phi_2 + V_{42}\cos4\phi_2 \qquad (6)$$

Varying the V_{2k}, V_{4k} and the $\epsilon_{2,m}(j)$ values gave the differences ΔD_{ij} shown in table 7. The

Table 7 - The values of $\Delta D_{ij} = D_{ij}$(calculated) - D_{ij}(observed) obtained by the AP method with a 2- or 3-rotor model for the internal rotations.

ij	ΔD_{ij} / Hz	
	2 Rotor Model	3 Rotor Model
12	-1.9	-0.2
13	-0.3	-0.0
14	-0.1	-0.0
15	-0.2	-0.0
16	-2.2	0.0
17	5.7	-5.7
18	15.0	1.7
23	-1.1	-0.1
24	-0.2	-0.0
26	12.2	4.8
27	6.2	-0.1
28	7.9	1.9
36	13.2	3.1
37	6.3	0.6
38	6.3	1.3
67	1.1	0.3
68	0.0	0.0
69	-0.2	-0.0
610	-0.5	-0.0
78	-1.8	-0.2
79	-0.5	-0.0

agreement between calculated and observed couplings is unacceptable, and in particular, the calculated value of D_{38} is too large. But D_{38} is virtually independent of the motions about Z_1 and Z_2 as both H-3 and H-8 lie on the axes of rotation Z_1 and Z_2 and so its value could be reduced only by bringing the two rings closer together. However, reasonable changes in the bond lengths and angles fail to reduce D_{38} sufficiently to give an acceptable value of R. This indicates that there is an additional motion required to average D_{38}, and the most reasonable candidate is motion about Z_3.

2.3.6 Evidence for average non-parallel alignment of Z_1 and Z_2 from quadrupolar splittings.

A deuterium spectrum of a mixture of **3** and **4** in ZLI 1132 in a ratio of 2:1 was recorded and is shown in figure 8 and the quadrupolar splittings, $\Delta\nu_i$, are given in table 8. The quadrupolar splittings are related to S_{CD}^i, the orientational order of the C - D^i bond by equation 1. The values of the quadrupolar coupling constants, q_{CD}^i can be reasonably assumed to be identical and hence the differences in the splitting arises because $S_{CD}^3 \neq S_{CD}^8$. The ratio $\Delta\nu_3 : \Delta\nu_8 \propto S_{CD}^3 : S_{CD}^8$ is 1.0 : 0.8965. If ring 1 is kept fixed, Z_2 has the same

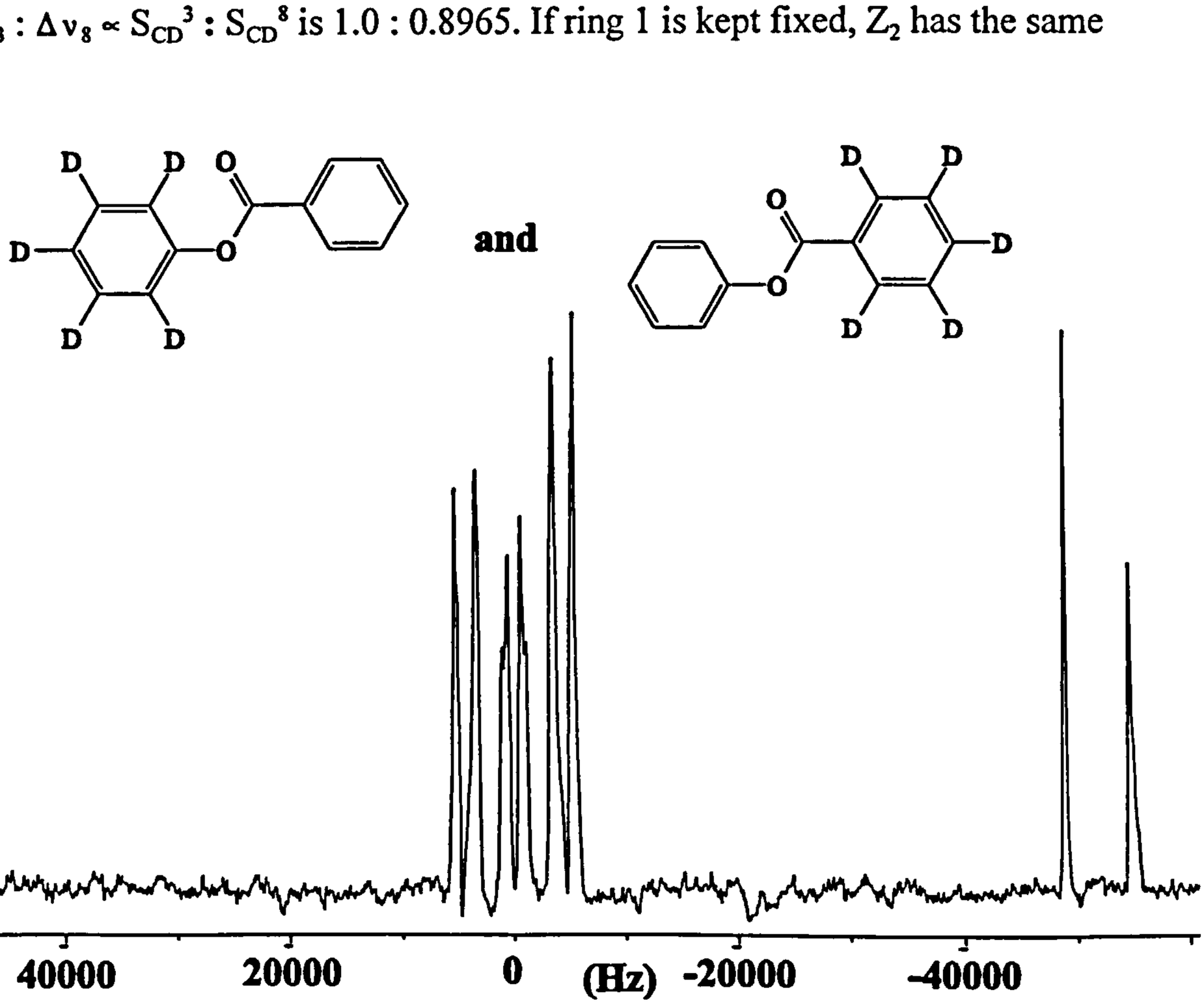

Figure 8 30.7 MHz deuterium spectrum of a mixture of compounds 3 and 4 in the approximate ratio 2:1 dissolved in the nematic solvent ZLI 1132 at 300K.

Table 8 - The magnitude of the quadrupolar splittings, $|\Delta\nu_i|$, from the mixture of compounds **3** and **4** in ZLI 1132

i	$\lvert\Delta\nu_i\rvert$ / Hz
1 or 2	6 716 ± 150
2 or 1	10 218 ± 36
3	109 889 ± 56
6 or 7	1 150 ± 21
7 or 6	2 108 ± 33
8	98 516 ± 41

orientation in the X_1, Y_1, Z_1 frame in all conformations. Thus, we can express $\Delta\nu_8$ as

$$\Delta\nu_8 = \tfrac{3}{4} q_{CD}\left[S_{ZZ}(1)(3\cos^2\phi_{CD8Z} - 1) + (S_{XX}(1) - S_{YY}(1))(\cos^2\phi_{CD8X} - \cos^2\phi_{CD8Y})\right] \quad (7)$$

$$\Delta\nu_3 = \tfrac{3}{2} q_{CD}\left[S_{ZZ}(1)\right] \quad (8)$$

where ϕ is the angle between Z_1 and Z_2, and θ_{CD8X} and θ_{CD8Y} are the angles between the C-D8 bond and X_1 and Y_1. If the two axes Z_1 and Z_2 are near parallel to one another then the $S_{XX}(1)$-$S_{YY}(1)$ term in equation (7) becomes small compared to the $S_{ZZ}(1)$ term. If this is indeed the case, as we think it is here then

$$\frac{\Delta\nu_8}{\Delta\nu_3} = \frac{3\cos^2\theta_{CD8} - 1}{2} \quad (9)$$

This gives ϕ as 15.23°. This compares to the X-ray geometry which shows that the difference in the two axes Z_1 and Z_2 is only 7.8°. Reasonable changes in the planar geometry of the O-C-O group cannot cope with an angle between Z_1 and Z_2 of the magnitude determined in this experiment if we constrict the two axes to the X_1Z_1 plane. Combining the evidence from the value of D_{38} with that from the $\Delta\nu_i$ suggests that the average separation and orientation of the two rings has to be changed in a way additional to that produced by motion only about Z_1 and Z_2.

2.3.7 The three rotor model

The model was adapted to include rotation about Z_3. Symmetry is such that rotation about this axis will be subject to a potential which has a repeat period of 180°, the simplest description being $V_1\cos\phi$. $U_{int}(\{\phi_k\})$ becomes :

$$U_{int}(\{\phi_k\}) = V_{21}\cos 2\phi_1 + V_{41}\cos 4\phi_1 + V_{22}\cos 2\phi_2 + V_{42}\cos 4\phi_2 + V_{31}\cos\phi_3 \qquad (10)$$

Varying all the V_{nk}, and $\epsilon_{2,0}(1) = \epsilon_{2,0}(2)$, $\epsilon_{2,2}(1) = \epsilon_{2,2}(2)$, $\epsilon_{2,0}(3)$ and $\epsilon_{2,0}(4)$ reduced the sum of squares error to 252 Hz with acceptably small ΔD_{ij} values for all the couplings, shown in table 7, and gave the parameters shown in table 9. The very large values for V_{22} and V_{42} are not reliable estimates of the potential function for rotation about Z_2 since they give probabilities $P_{LC}(\phi_2)$ everywhere effectively zero except for the positions $\phi_2 = 0°$or 180°, which correspond to the ring 2 and the C = O bond being coplanar. This is in agreement with the crystal structure of phenyl benzoate, and with the structure of acetophenone [11]. The distribution $P_{LC}(\phi_1,\phi_2,\phi_3)$ can be simplified to $P_{LC}(\phi_1, 0°,\phi_3)$, which is shown in fig. 6. The model also predicts the conformation in the isotropic phase (P_{ISO}), which is not orientationally dependent. In this case the results of P_{LC} compared to P_{ISO} are identical to within less than 1%.

Table 9 Potential Terms, $V_{k,n}$ ($kJmol^{-1}$) for rotations about Z_1, Z_2 and Z_3 , and values of the fragment interaction parameters, $\epsilon_{2,0}(j)$ and $\epsilon_{2,2}(j)$ ($kJmol^{-1}$).

Fragment, j	$\epsilon_{2,0}(j)$	$\epsilon_{2,2}(j)$
1 = 2	2.98 ± 0.03	2.77 ± 0.13
3	-0.85 ± 0.14	
4	-0.047 ± 0.04	

bond, k	V_1	V_2	V_4
1		1.9 ±0.5	2.9 ± 0.5
2		-84	-186
3	-16.3 ± 1.5		

2.4 Conclusion

The probability distribution obtained for phenyl benzoate in the liquid crystal phase is consistent with the structure determined for a crystalline sample in that the minimum energy form has $\phi_1 = 50°$, $\phi_2 = 0°$, and $\phi_3 = 0°$. However, in the liquid crystalline, and isotropic phase, of the solution in ZLI 1132 the conformations are distributed over a wide range of values of all three angles. The distribution in ϕ_3 is large, as shown in figure 9, and extends to ±50° from the O-C-O plane. It is interesting to speculate on whether there will be such a

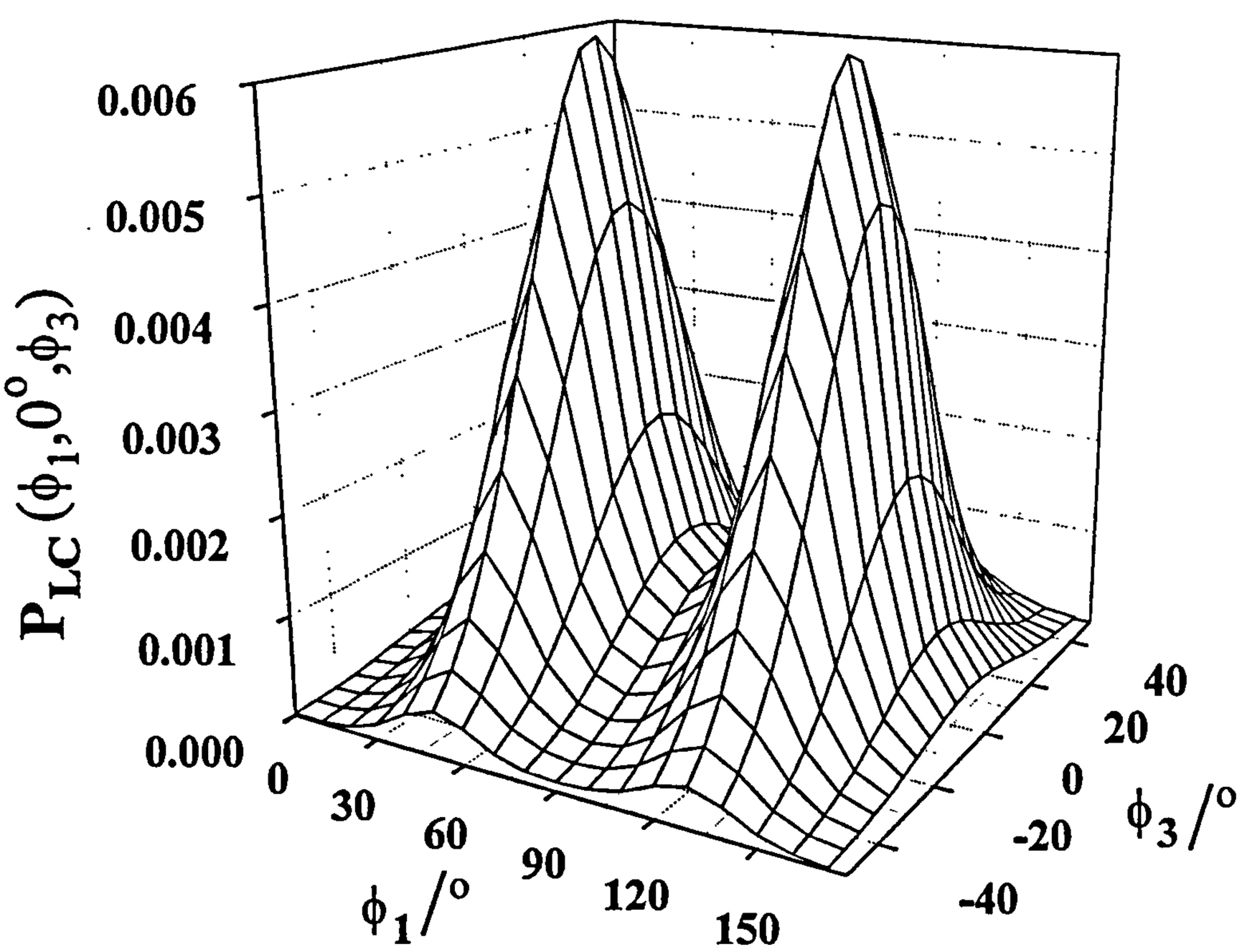

Figure 9 Probability distribution $P_{LC}(\phi_1,\phi_3)$ relative to a fixed ring 2 (ϕ_2=0°) of phenyl benzoate dissolved in the nematic solvent ZLI 1132 at 300K.

wide distribution of conformers with $\phi_3 \neq 0°$ in mesogenic molecules of the same type. The presence of bulky substituents X and Y, shown in figure 10, particularly in polymers in which the ester is part of the backbone, may quench the motion about Z_3, but this may not be the case in low molar mass compounds, or when the ester group is part of the side chain in a polymer. To investigate this possibility by the NMR method will be difficult in that the

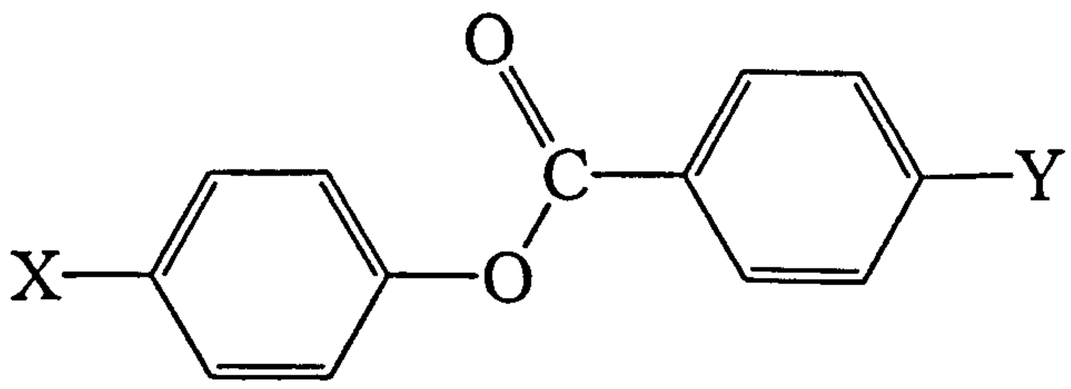

Figure 10 Substituent positions on phenyl benzoate as seen in many liquid crystals

presence of X and Y, shown in figure 11, removes from the data set the valuable coupling D_{38}, whose magnitude was important in revealing the necessity for motion about Z_3.

2.5 References

[1] G.Celebre, G.De Luca, M.Longeri, D.Catalano, C.A.Veracini, J.W.Emsley, *J.Chem.Soc.Faraday Trans.*, **87**, 2623, (1991)

[2] G.Celebre, G.De Luca, M.Longeri, D.Catalano, M.Lumetti, J.W.Emsley, Mol.Phys., **85**,221, (1995)

[3] E.K.Foord, J.Cole, M.J.Crawford, J.W.Emsley, G.Celebre, M.Longeri, J.C.Lindon, *Liq.Cryst.* **18**, 615, (1995)

[4] J.M.Adams and S.E.Morsi, *Acta.Cryst.* **B32**, 1345 (1976)

[5] J.Bicerano and H.A.Clark, *Macromolecules*, **21**, 585 (1988)

[6] W.B.Schweizer and J.D.Dunitz, *Helv.Chim.Acta*, **65**, 1547 (1982)

[7] A.I Vogel and B.S. Furniss, "Vogel's Textbook of Practical Organic Chemistry", 5th edition (Longman Scientific and Tecnical, London).

[8] Aldrich Catalogue Handbook of Fine Chemicals. (1994 - 1995)

[9] J.W.Emsley, L.Phillips, V.Wray, "Fluorine Coupling Constants" Pergamon Press 1977

[10] J.W.Emsley in "Encyclopedia of NMR" eds. D.M.Grant and R.K.Harris, John Wiley & Sons Ltd. (Chichester), 1996, p. 2781

[11] Y. Tanimoto, H. Kobayashi, S. Nagakura and Y. Saito, *Acta.Cryst.*, **B29**, 1822 (1973)

Chapter 3

Fluorobenzene.

A Simple Example of Using Variable Angle Sample Spinning.

3.1 Introduction

As described in chapter 1, Variable Angle Sample Spinning (VASS) NMR allows the variation of the angle that an aligned sample makes with the magnetic field direction, B_0. In liquid crystalline solutions, the director aligns to the sample spinning axis rather than to B_0 when the threshold spinning rate is exceeded. The effect of spinning at an angle to B_0 is the reduction, R, of the anisotropic interactions in the NMR spectrum, given by equation 1. When R = 0, at the magic angle (54.7°), all anisotropic interactions are scaled down to zero and the spectrum becomes equivalent to that in isotropic solution but with spinning side bands.

$$R = \left(\frac{3\cos^2\theta - 1}{2} \right) \qquad (1)$$

Fluorobenzene, whose structure is shown in figure 1, dissolved in a liquid crystal solvent, ZLI 1167, was initially chosen as a test sample for the VASS technique. Using this sample we attempted to obtain well resolved spectra through optimisation of the conditions for a range of angles to B_0 and to see the quality of information that could be obtained. There has

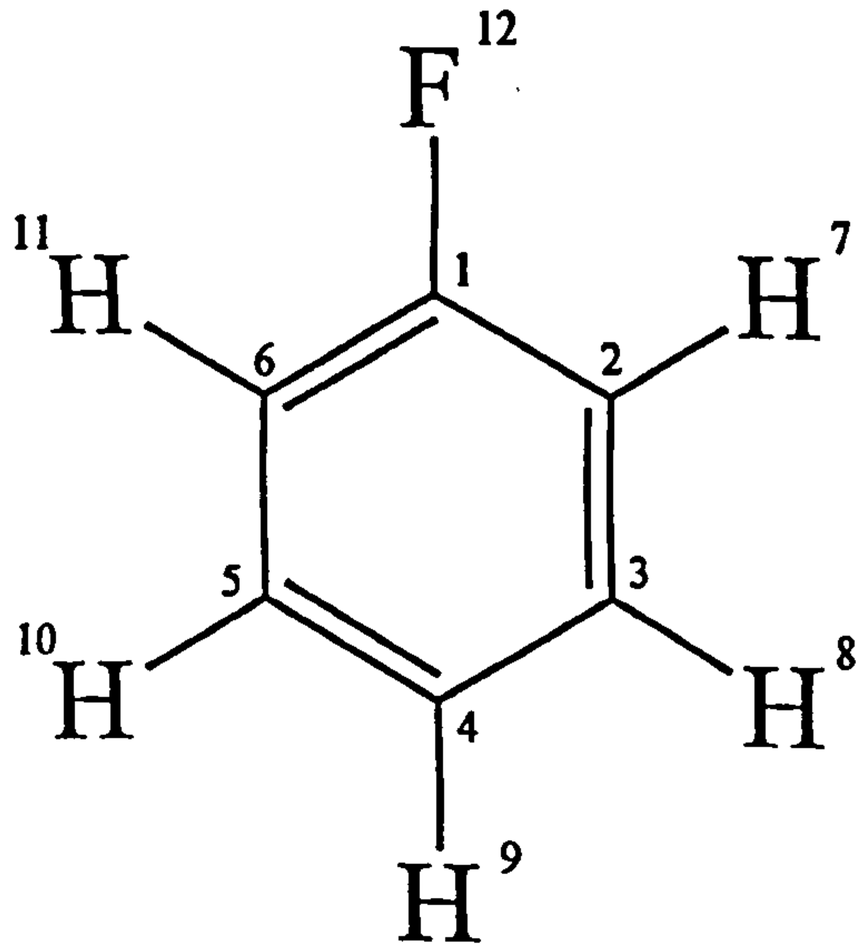

Figure 1 The structure of fluorobenzene

been a great deal of work already on the analysis of fluorobenzene in isotropic and liquid crystalline solutions of which some aspects of these studies will be discussed shortly. The information obtained from these studies provides us with the answers we expect to obtain from the VASS experiments with which we may make comparisons to our results. The data we expect to obtain from VASS NMR includes, the absolute values of the J_{ij} and D_{ij}, from which we can obtain order parameters and the molecular structure. We can also obtain the anisotropy in the chemical shifts, δ_i^{aniso}, which may be used to aid spectral assignment.

As mentioned, it is possible to obtain the absolute values of the J_{ij} from VASS experiments. In 1977, Emsley *et al.* [1] published a compilation of fluorine coupling constants based upon over a thousand separate references. While the magnitudes of these couplings are easily measured from NMR spectra, the determination of signs is sometimes more difficult. Relative signs of the couplings may be obtained from the spectrum for strongly coupled spin systems, for example F-F, H-H but not when the coupling is weak, i.e. H-F, C-H and C-F. There are experimental methods for obtaining the relative signs, i.e. spin tickling [2], however, these are difficult experiments to perform. The absolute signs of the couplings may be obtained from the spectra in liquid crystalline samples if a comparison can be made between J_{ij} and D_{ij}. If the order parameters, S_{ij}, of a molecule are known, the D_{ij} may be calculated and the J_{ij} determined.

The determination of the absolute signs of carbon-fluorine coupling constants, J_{CF}, is of particular interest to us. The signs of the couplings used by many researchers are based upon findings by Tiers [3], who determined that the $^1J_{CF}$ and $^2J_{CF}$ are of opposite sign in ClFC=CFCl and Cl_2FC-$CFCl_2$. There have been several attempts to calculate $^1J_{CF}$ for the fluoromethanes, these are reported by Emsley *et al.* [4] from which the authors show how difficult it is to calculate the coupling constants. However, all calculations do agree that this coupling, $^1J_{CF}$, has a large negative value. Longer range couplings are usually assumed to be positive, but there are only a very few examples of the determination of these signs.

Determination of the absolute signs of the couplings has been shown through the spinning of liquid crystalline samples in the magnetic field. In 1974, Emsley and Lindon [5] separated the isotropic from the anisotropic interactions in the ^{19}F NMR spectrum of trifluoroacetic acid dissolved in the nematic liquid crystal Merck Phase V by using slow sample rotation. Here it was shown that if the sample was spun at a particular speed, Ω,

below a critical spinning speed, Ω_C, the forces due to B_0 and the sample viscosity are in a balance and the director, n, is at a constant angle, θ, to B_0, as given in equation 2. The

$$\sin 2\theta = \frac{\Omega}{\Omega_C} \qquad (2)$$

anisotropic interactions are therefore reduced by R, given in equation 1. R can then be calculated at any rotation speed below Ω_C, allowing the separate values of J_{CF} and D_{CF} to be determined. The same experimental technique was employed again by Emsley and Lindon [6], in 1974, and the ^{19}F NMR spectrum of *cis*-difluoroethylene dissolved in a nematic phase. Through assumption of the molecular geometry it was shown that it is possible to determine the magnitudes and the relative signs of all the coupling constants. Courtieu [7], in 1982, extended this theory to VASS and recorded a set of ^{19}F spectra of CF_2=CFBr in the nematic phase. They noted that two sets of the three splittings passed through zero as the angle was changed and concluded that in these cases, J_{ij} was of opposite sign to D_{ij}, however, for the third splitting it was concluded that J_{ij} and D_{ij} were of the same sign. Courtieu also mentions that in order to determine the absolute signs of the couplings it is necessary to know the orientation of the molecules. There is no reason to believe that this technique cannot be applied to the determination of J_{CF} in more complicated aromatic molecules. We chose to study fluorobenzene as a preliminary step in the applications of VASS to more complicated aromatic molecules, for example, the liquid crystals I35 and I52 (chapter 6).

In 1971, Weigert and Roberts [8] analysed the ^{13}C NMR spectrum of fluorobenzene in isotropic solution, from which the values of J_{CF} were determined. However, Weigert and Roberts assumed the absolute values of J_{CF}, choosing $^1J_{CF}$ as negative whilst the signs of the other $^nJ_{CF}$, where n=2,3 and 4, were chosen to be positive. In 1977, Wray *et al.* [9] reported the complete analysis of fluorobenzenes in isotropic solution and obtained a full set of J_{ij} in which the signs of $^1J_{CH}$ and $^1J_{CF}$ were assumed to be positive and negative respectively. These results were later confirmed by Chertkov [10], however, the J_{CF} determined by Weigert and Roberts were used as starting parameters which would have biased the final results.

In 1965, Snyder [11] presented the analysis of fluorobenzene in the nematic phase of p,p'-di-

n-hexyloxyazoxybenzene, in which the values of D_{HH} and D_{HF} were reported to be of opposite sign to J_{HH} and J_{HF}. Long *et al* [12] analysed the NMR spectrum of fluorobenzene in a nematic potassium laurate mesophase and reported that the D_{HH} and D_{HF} are of the same sign as the J_{HH} and J_{HF}. The contradiction in these results may be easily explained by the liquid crystal solvents used in the respective experiments having opposite anisotropies in their magnetic susceptibilities. Jokisaari *et al.* [13] demonstrated this difference through the analysis of the NMR spectra of fluorobenzene in both the nematic liquid crystal solvents ZLI 1132, which has anisotropy in the magnetic susceptibility, $\Delta\chi$, positive, and ZLI 1167, which has $\Delta\chi$ negative. In ZLI 1132 the D_{HH} and D_{HF} are of opposite sign to the corresponding J_{ij}, while in ZLI 1167 the D_{HH} and D_{HF} are of the same sign as the corresponding J_{ij}. This study obtained the coupling constants from the ^{13}C satellites in the ^{1}H and ^{19}F spectra. This gives the couplings with high precision, but it cannot be used for more complex molecules. The ^{13}C-{^{1}H} VASS experiment to be described here obtains the couplings to a lower precision, but the method has a much wider range of application. The experiments on fluorobenzene allow us to assess how accurate the method is for determining the D_{ij}^{CF}, and also how accurately the structure can be determined from these values. J_{CF} and D_{CF} were also obtained in both solvents, considering the usual assumption of the absolute signs of J_{CF}. The absolute experimental proof of the signs of the J_{CF} in aromatic systems has not been previously published, however, through the technique of Variable Angle Sample Spinning (VASS) it will be simply shown here that $^{1}J_{CF}$ is of opposite sign to the $^{n}J_{CF}$ in fluorobenzene and that all previously made assumptions for the signs of the couplings have been correctly made.

In liquid crystalline solutions we may also need to consider the anisotropy of the chemical shift, δ_i^{aniso}. VASS NMR provides easy access to the determination of this quantity through simple observation of the changing centres of the multiplets corresponding to δ_i with θ.

3.2 Experimental

A sample of fluorobenzene (Fluorochem Ltd.) was prepared for the VASS experiment, using 10% by weight solution dissolved in the nematic liquid crystalline solvent ZLI 1167. ZLI 1167 is chosen as it contains no aromatic carbons which may interfere with the spectrum from fluorobenzene. The sample was contained in a glass bottle sealed by epoxy

resin which fits into a Zirconium rotor of 7mm o.d. for use in a VASS probe type MAS200 SB BL7 (figure 2). The spinning rate used has to be above the threshold at which the directors align along the spinning axis, and not to the magnetic field. In this case we chose to spin at 1000 Hz.

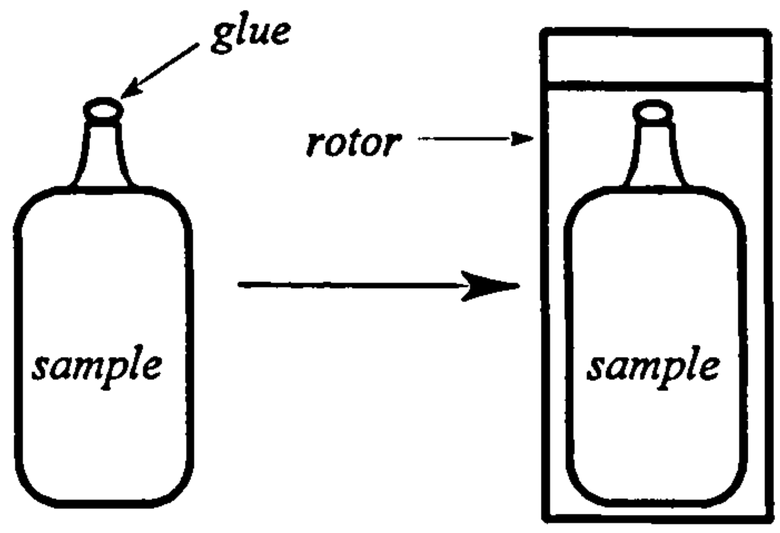

Figure 2 Sample containment for liquid VASS NMR.

A range of ^1H spectra were recorded between $54.7° < \theta < 90°$, on a Bruker MSL200 NMR spectrometer at 300K, and used to calibrate the ^1H decoupling pulse and to optimise the magnet homogeneity. In fact, the VASS technique has not been previously used to record ^1H spectra. This seems to have been because it was thought that the background spectrum of the liquid crystal, which also reduced in width as θ approaches 54.7°, would obscure the spectrum of the solute. A corresponding range of ^{13}C-{^1H} VASS NMR spectra were recorded at the same angles as the ^1H spectra Proton decoupling was achieved using WALTZ-16 [14] pulse sequence with a 90° proton pulse of 5.75μs.

3.3 Results and Discussion

3.3.1 ^1H NMR of fluorobenzene

The ^1H VASS NMR spectra of fluorobenzene, an ABB'CC'X spin system, are shown in figure 3. The spectrum at θ=90°, was analysed using the J_{HH} and J_{HF} reported by Wray [9] and the corresponding D_{ij} from Jokisaari [13] in ZLI 1167 as starting parameters and a calculated spectrum obtained. The calculated spectrum was assigned to the experimental spectrum and the D_{ij} and δ_i varied, using an iterative parameter fitting program, ARCANA [15], based on LAOCOON [16], until a good agreement was found between the experimental and the calculated spectra. The analysis was also attempted using opposite signs for the starting D_{ij}, however, a good agreement between the experimental and

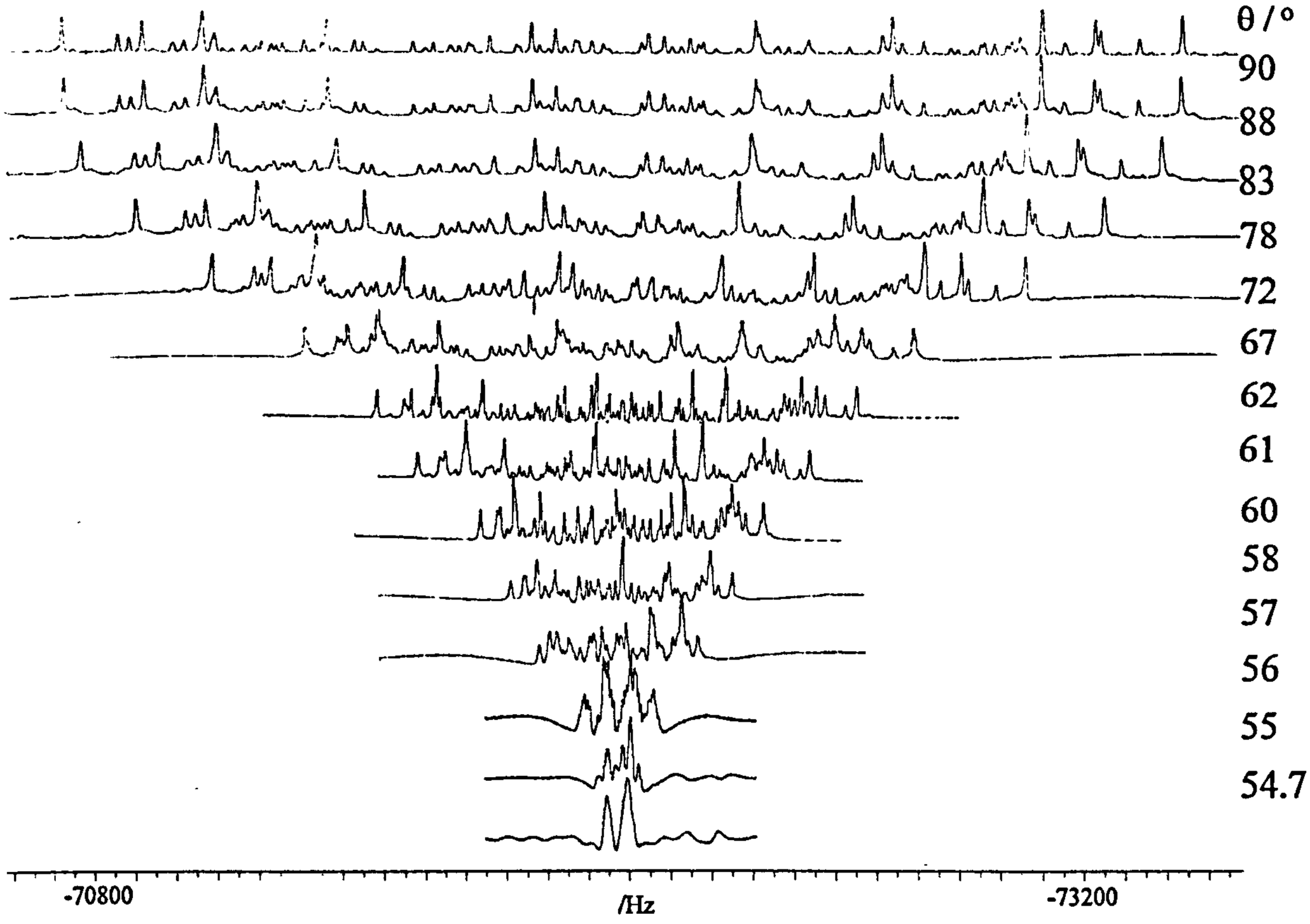

Figure 3 200 MHz ^{1}H VASS NMR spectra of fluorobenzene dissolved in ZLI 1167 at 300K.

calculated spectra could not be found, in this case. The final set of D_{HH}, D_{HF} and δ_H are given in table 1.

It has also been possible to analyse spectra at various angles to B_0. In these cases, the J_{ij} remain fixed and the D_{ij} are scaled by the reduction factor, R. The procedure of line assignment and iteration on the parameters was repeated and the spectra successfully analysed in the range $61° < \theta < 90°$. The results are also reported in table 1.

3.3.2 ^{13}C NMR of Fluorobenzene

The ^{13}C-{^{1}H} VASS NMR spectra of fluorobenzene are given in figure 4. Fluorobenzene is an example of an AX spin system, which give rise to simple spectra consisting of doublets, where the splitting, $\Delta\nu = 2D_{CF} + J_{CF}$. There are in fact four inequivalent carbon atoms in the molecule giving rise to four doublets, centred about the carbon chemical shift, δ_X. The spectrum at θ=90° can be analysed and a set of D_{CF} obtained, through the following procedure.

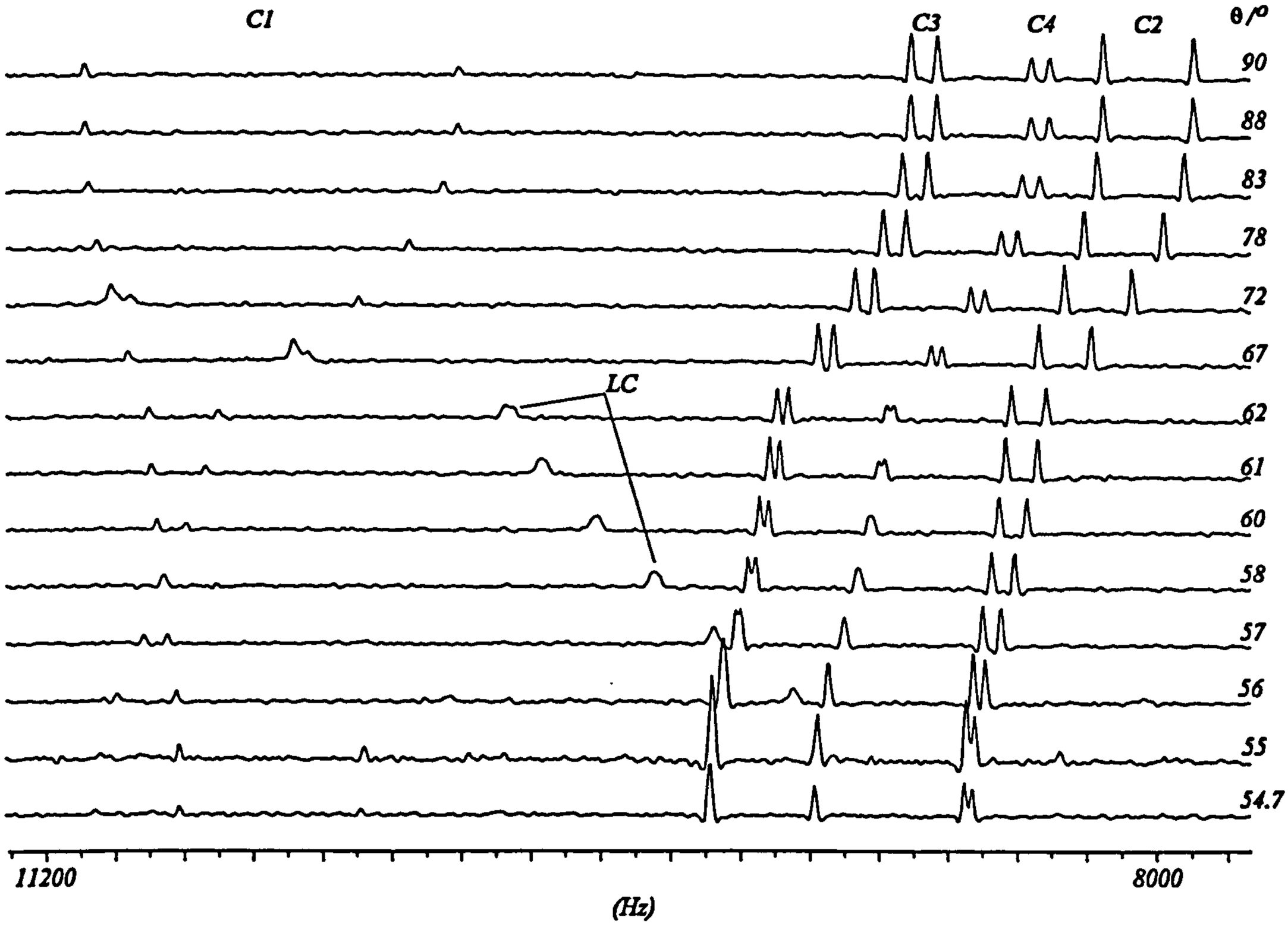

Figure 4 50.3 MHz ^{13}C-{^{1}H} VASS NMR spectra of a sample of fluorobenzene dissolved in the nematic solvent ZLI 1167. Most of the peaks from the solvent are at high field and are not shown. The angle, θ, between the spinning axis and B_0 is shown against each spectrum.

A trial set of D^{CF} were calculated from the order parameters, S_{ij}, calculated from the ^{1}H data and an assumed geometry. The geometry chosen is that determined by Jokisaari [13], in ZLI 1167 including vibrational corrections. The liquid crystal spectrum may now be analysed using known J_{CF} and the set of calculated D_{CF}, as starting parameters, in order to obtain the experimental D_{CF}. Firstly the spectrum at θ=54.7° (the magic angle) is assigned according to the assignment of the transitions in isotropic solution, given by Weigert and Roberts [8]. As θ is changed in range $54.7° < \theta < 90°$ so the positions of the transitions change due to the increasing magnitude of the anisotropic interactions. Each transition is followed and the spectrum at θ=90° assigned. The final parameters are given in table 2. Given that there may be more than one correct assignment, we can make a correct analysis in that we know the magnitude and signs of the D_{CF} and we have evidence for the signs of the J_{CF} in the above spectra. The way the splittings evolve gives the relative signs of J_{CF} and D_{CF} as the splittings are equal to the total coupling, $T_{CF} = 2D_{CF} + J_{CF}$. Clearly $D_{1,12}^{CF}$ is opposite in sign to $J_{1,12}^{CF}$, because the splitting decreases as θ increases away from 54.7° until it collapses to a singlet where $|D_{CF}| = -0.5\ |J_{CF}|$ As θ approaches 90° the splitting reemerges and steadily grows. For

Table 1 Chemical Shifts, δ_i, and dipolar couplings from ^{1}H VASS NMR spectra of fluorobenzene dissolved in ZLI 1167 at 300K.

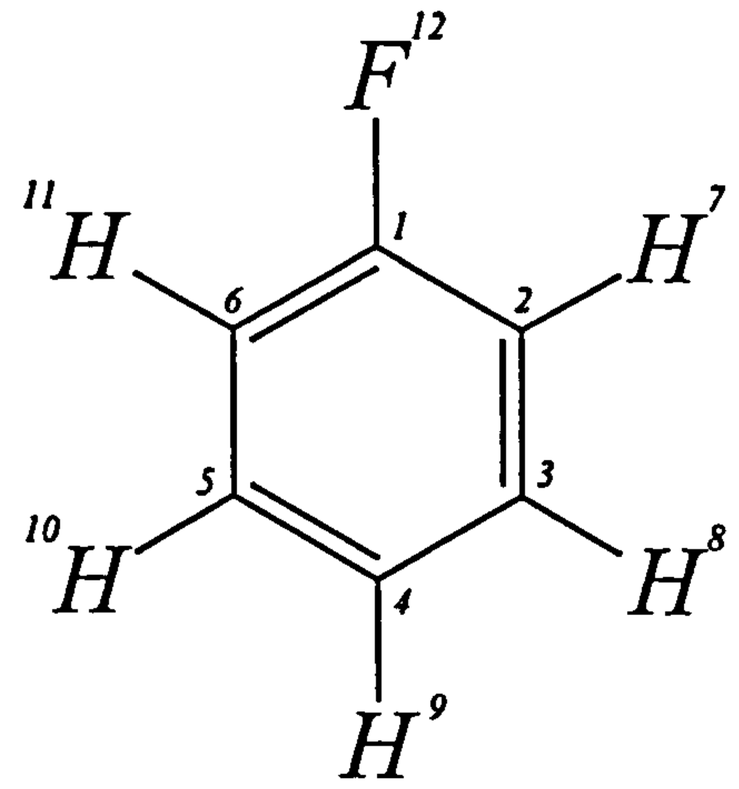

i	δ_i /ppm		
	90°	78°	61°
7	0.00 ± 0.01	0.02 ± 0.01	0.10 ± 0.01
8	0.31 ± 0.01	0.33 ± 0.01	0.39 ± 0.01
9	0.07 ± 0.01	0.09 ± 0.01	0.18 ± 0.01

i j	J_{ij} / Hz [9]	D_{ij} / Hz		
		90°	78°	61°
7 8	8.4	454.4 ± 0.1	392.2 ± 0.1	157.6 ± 0.1
7 9	1.1	82.2 ± 0.1	70.8 ± 0.2	28.6 ± 0.1
7 10	0.0	44.8 ± 0.1	38.5 ± 0.1	15.7 ± 0.1
7 11	2.8	61.8 ± 0.1	53.4 ± 0.1	21.5 ± 0.1
7 12	9.2	303.4 ± 0.2	261.7 ± 0.2	105.7 ± 0.1
8 9	7.5	349.6 ± 0.1	301.8 ± 0.2	122.0 ± 0.1
8 10	1.8	60.8 ± 0.2	52.5 ± 0.2	21.2 ± 0.1
8 12	5.8	68.4 ± 0.1	59.2 ± 0.2	23.8 ± 0.1
9 12	0.3	48.2 ± 0.2	41.9 ± 0.2	16.3 ± 0.2

the other three ^{13}C and ^{19}F pairs the D_{ij}^{CF} and J_{ij}^{CF} are of the same sign and we observe consistent growth in the magnitude of the splittings with θ. As with the ^{1}H VASS spectra it is possible to analyse the spectra at various angles to B_0.

Table 2 Chemical Shifts, δ_i, and dipolar couplings from ^{13}C VASS NMR spectra of fluorobenzene dissolved in ZLI 1167 at 300K.

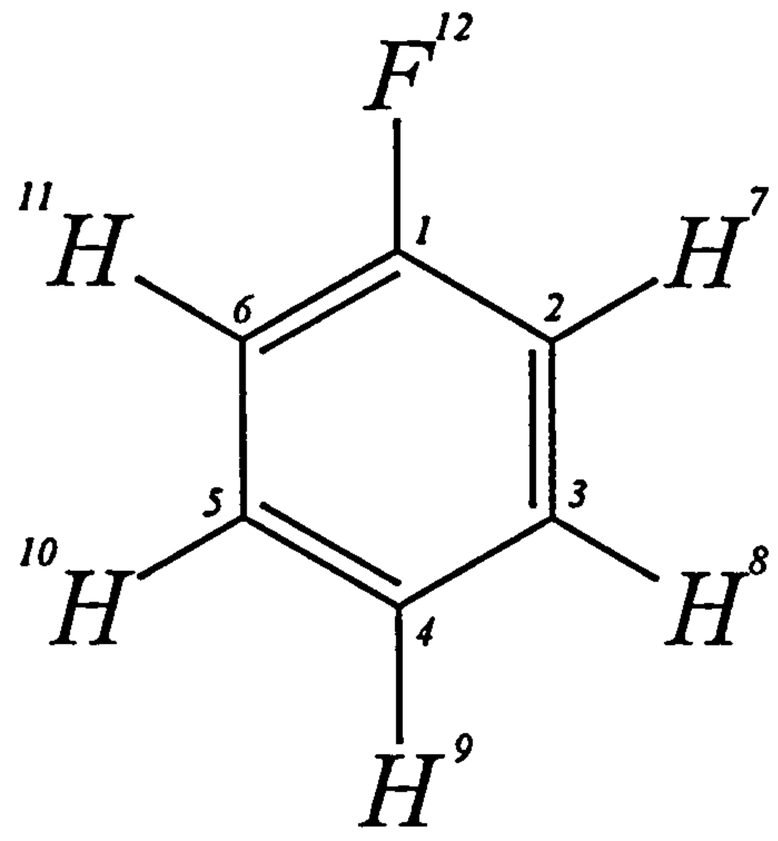

i	δ_i / ppm
1	50.204 ± 0.01
2	0.0 ± 0.01
3	12.752 ± 0.01
4	6.115 ± 0.01

i j	J_{ij} / Hz [13]	D_{ij} / Hz
1 12	-245.8	667.4 ± 1.0
2 12	20.8	117.8 ± 1.0
3 12	7.61	33.5 ± 1.0
4 12	3.18 [9]	25.0 ± 1.0

3.3.3 Chemical Shift Anisotropy

We may determine the anisotropy in the chemical shift, δ_A^{aniso}, of the fluorobenzene ^{13}C nuclei through analysis of the changing chemical shifts in the individual VASS spectra.

For the ^{13}C-{^{1}H} VASS NMR spectra it is possible to follow each individual carbon doublet in the spectrum as it shifts with changing θ, hence allowing the determination of the changing chemical shift, of A in each AX spin system, where the ^{13}C is denoted as the A part. Although this information is not very useful to us as a quantity on its own, it may be

used to locate the position of the doublet in any of the VASS spectra. In this case, it is not necessary as the doublets are clearly seen throughout and never overlap. The spectrum at $\theta=90°$ is easily assigned, however, in more complicated spin systems there may be some overlap leading to the apparent disappearance of some multiplets. δ_A^{aniso} may be used to understand where the 'missing' transitions are located in order that these complicated spectra may be assigned.

The chemical shift in a liquid crystalline sample can be expressed as the contribution of δ_i^0, the isotropic value which is orientation independent, and δ_i^{aniso}, the anisotropic part which is orientation dependent, thus,

$$\delta_i = \delta_i^0 + \delta_i^{aniso} \tag{3}$$

where

$$\delta_i^{aniso} = \frac{1}{3}(S_{XX} - S_{YY})(\sigma_{XX} - \sigma_{YY}) + \frac{2}{3}S_{ZZ}\left(\sigma_{ZZ} - \frac{1}{2}(\sigma_{XX} + \sigma_{YY})\right) \tag{4}$$

The XYZ axes are the principal axes for the order matrix, but not for the σ [17]. The order parameters are known in this case, but the shielding tensor components are not.

For our purposes the anisotropy of the chemical shifts are reported for completeness of results only. In the VASS experiment the anisotropic part of the chemical shift depends on the angle between the director and B_0, thus

$$\delta_i = \delta_i^0 + \delta_i^{aniso}\left(\frac{3\cos^2\theta - 1}{2}\right) \tag{5}$$

A plot of δ_i against $(3\cos^2 - 1)/2$ should be linear with a slope of δ_i^{aniso}. Figure 5 shows that equation 3 is obeyed and yields the values of δ_i^{aniso} shown in table 4.

Table 3 Chemical Shift Anisotropy of ^{13}C and ^{1}H of fluorobenzene dissolved in ZLI 1167 at 300K

i	δ_i^{aniso} / ppm
1	14.67 ± 0.25
2	19.51 ± 0.38
3	23.38 ± 0.44
4	24.73 ± 0.49
7	0.30 ± 0.01
8	0.25 ± 0.01
9	0.30 ± 0.02

A similar procedure should be possible for the determination of the anisotropy of the chemical shifts of the protons, from analysis of the ^{1}H VASS NMR spectra. The anisotropy in the chemical shifts of the protons are shown in figure 6 and the values reported in table 3.

3.3.4 Determination of Molecular structure

The elements $S_{\alpha\beta}$ with $\alpha \neq \beta$ in equation (21) of chapter 1 are zero for a molecule like fluorobenzene with C_{2v} symmetry. Thus

$$D_{ij} = k_{ij}\left[S_{ZZ}\left(3\cos^2\theta_{ijz} - 1\right) + \left(S_{XX} - S_{YY}\right)\left(\cos^2\theta_{ijX} - \cos^2\theta_{ijY}\right)\right] \qquad (6)$$

From the relationship given in equation (6), we know that the D_{ij} are directly related to molecular structure, where k_{ij} is constant and depends on the magnetic properties of the nuclei i and j, r_{ij} is the internuclear distance and the XYZ axes are shown in Table 3. We wish to investigate how accurately the structure can be determined when using a simplified model which can be applied to more complex molecules. Thus, we will also neglect the contribution from J_{aniso}^{CF} (see equation 30 chapter 2). Jokisaari [13], calculated the geometry of fluorobenzene in both ZLI 1167 and ZLI 1132, using vibrationally corrected D_{ij}. The structure and order parameters determined in ZLI 1167 were used as a starting

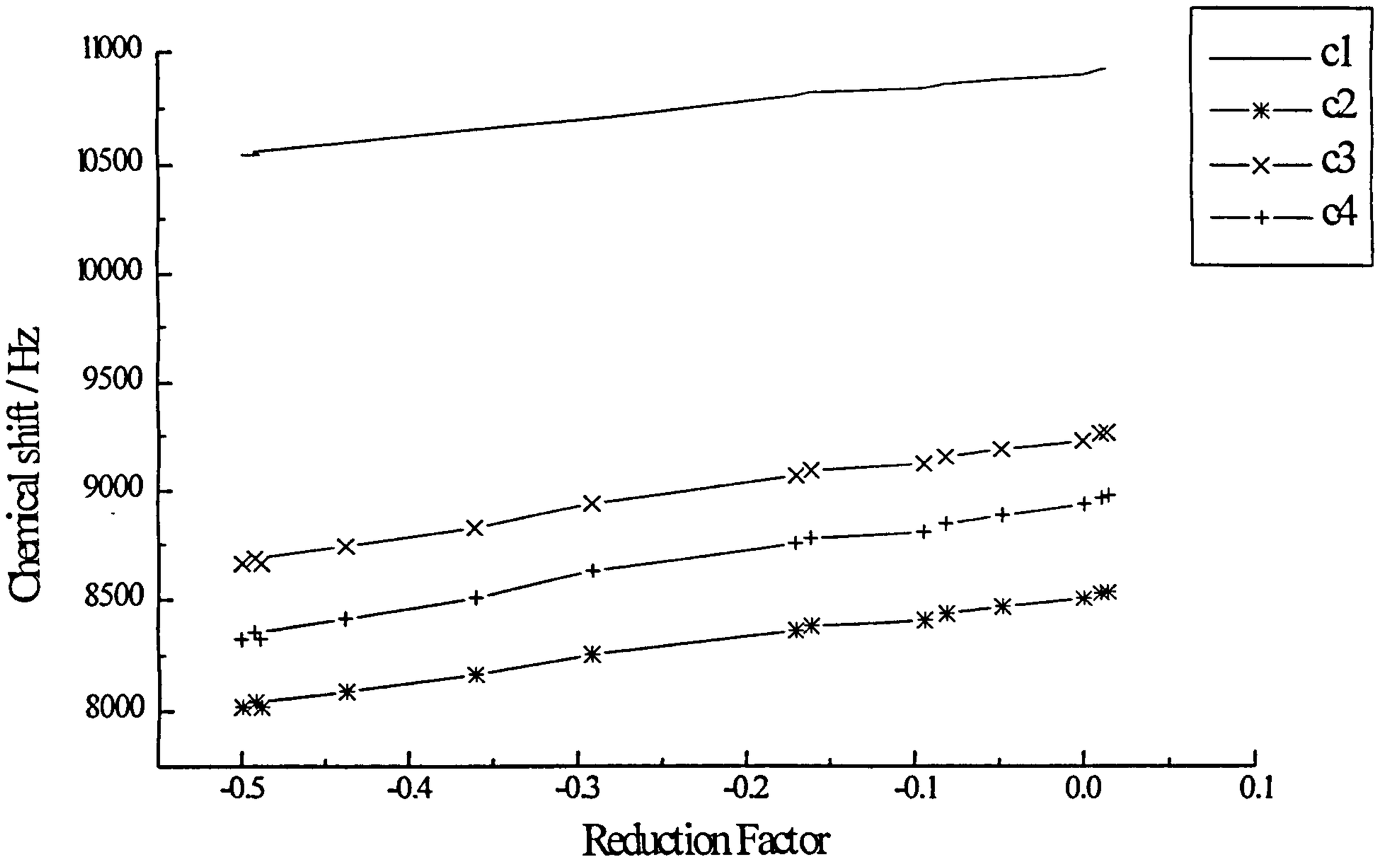

Figure 5 Chemical Shift Anistropy of ^{13}C of fluorobenzene dissolved in ZLI 1167 at 300K

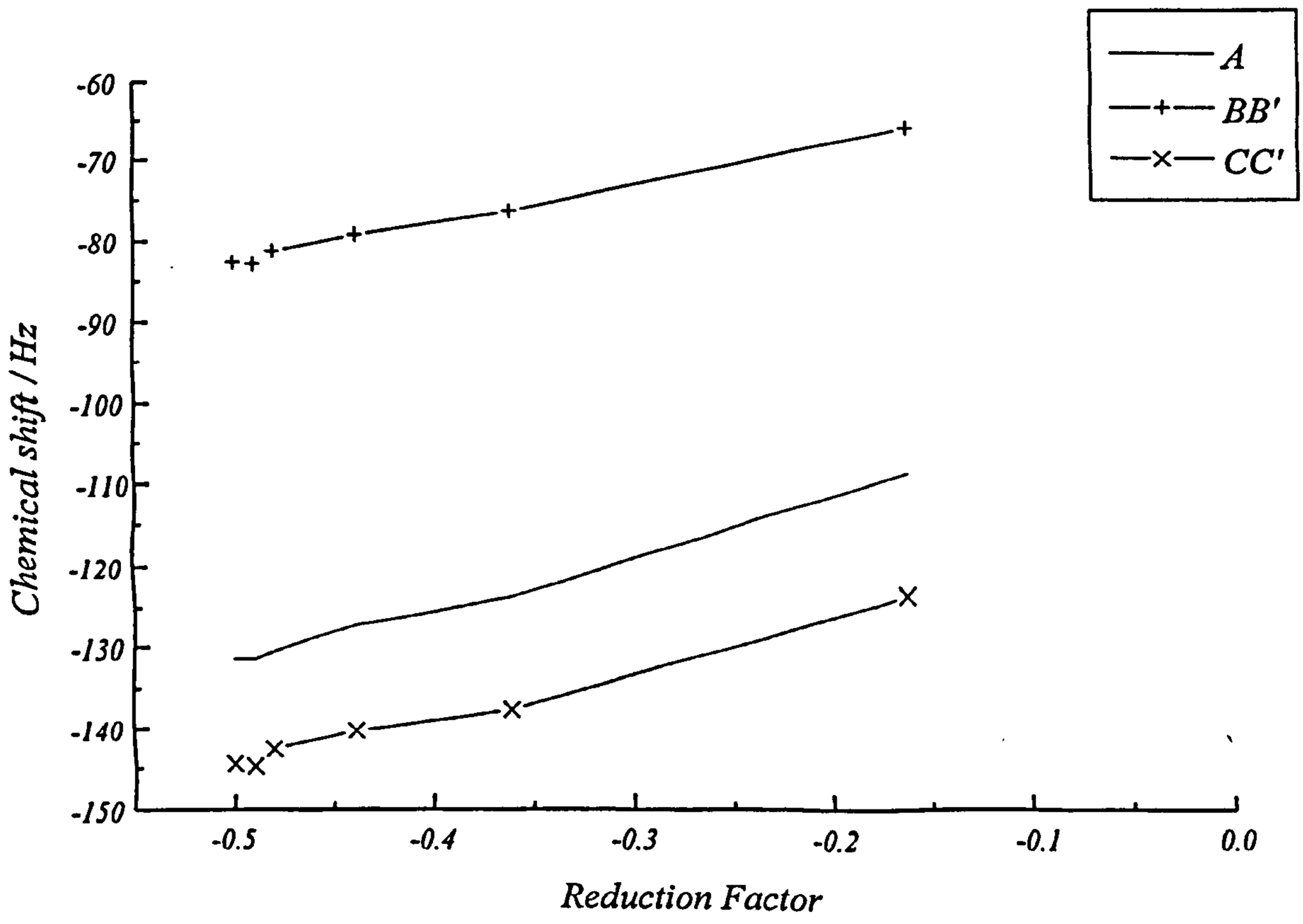

Figure 6 Chemical Shift anistropy of ^{1}H of fluorobenzene dissolved in ZLI 1167

parameters for comparison with our experimental, non vibrationally corrected, D_{ij} obtained from the VASS experiments. The order parameters and selected atomic positions were varied until a good agreement between the experimental and calculated D_{ij} was obtained.

There are eight independent variables which determine the nine values of D_{ij}^{HH} and D_{ij}^{HF}. For the determination of the structure from the D_{ij}^{HH} and D_{ij}^{HF}, seven of the nine variables were chosen, S_{XX}-S_{YY}, S_{ZZ}, X(7) = X(11), Z(7) = Z(11), Z(8) = Z(10), Z(9) and Z(12). The distance $r_{8,10}$ was held fixed at 4.2888 Å [13] and others distances allowed to vary.

For the determination of the structure from the D_{ij}^{CF}, two of the four variables were chosen, Z(4) and Z(12). The order parameters remained fixed from the ^1H data above. The positions of C2 and C3 could not be varied as they require two variables which depend on only one D_{CF} each. The error in the fit gives an indication of how good the VASS data is compared to that published by Jokisaari [13].

The final carbon, proton and fluorine positions and order parameters are given in table 4. These are translated into bond lengths and angles and show that the dipolar couplings obtained here through VASS predicted a molecular structure close to that obtained by Jokisaari. There are differences that may be explained through the use of vibrational corrections on the D_{ij} made by Jokisaari. In particular the comparison between the ratios of $D_{1,12} : D_{4,12}$, which are independent of the order parameters, can be made. This value was found to 26.7±0.1, from this work, compared to 26.87, from uncorrected D_{CF}, and 27.59, from corrected couplings. The difference to r_{14}, on comparison with the VASS to the vibrationally corrected structure, is 0.045Å. Jokisaari showed that vibrational corrections do not, however, have a large effect on the C-F couplings except $^1D_{CF}$, less than 1%, and only have a slightly larger effect on the H-H and H-F couplings, on average around 1%.

Uncorrected H-H and H-F couplings will give rise to slightly incorrect order parameters and molecular structure. These incorrect order parameters are then translated to the structure determined from the D_{CF}. $^1D_{CF}$ only really becomes significant in regards to r_{CF}, and Jokisaari shows a large deviation in the determination of this value, 1.355Å in ZLI 1132 and 1.371Å in ZLI 1167, however the magnitude of the anisotropic contribution is such that a more probable r_{CF} = 1.353Å is suggested. The structure determined here gives r_{CF} = 1.344Å. These compare with the value obtained by microwave studies of r_{CF} = 1.354Å [18]. The

Table 4 Order parameters and molecular geometry of fluorobenzene in ZLI 1167.

	This work	Jokisaari [13]
$S_{XX} - S_{YY}$	-0.0395 - 0.0966	-0.0499 - 0.1226
S_{ZZ}	-0.0570	-0.0726

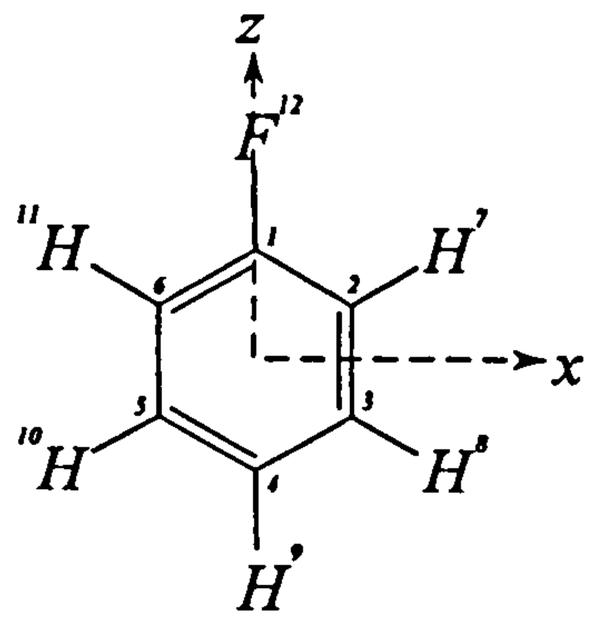

i	X	Z	i	X	Z
1	0.0	0.0	7	-2.1243	0.0808
2	-1.2175	0.6427	8	-2.1444	2.5508
3	-1.2097	2.0347	9	0.0	3.7745
4	0.0	2.6732	10	2.1444	2.5508
5	1.2097	2.0347	11	2.1243	0.0808
6	1.2175	0.6427	12	0.0	-1.3442

Bond Lengths / Å	This Work	Jokisaari [13]
$r_{1,2}$	1.377	1.377
$r_{2,3}$	1.392	1.392
$r_{3,4}$	1.368	1.398
$r_{1,12}$	1.344	1.371 / 1.353
$r_{2,7}$	1.067	1.078
$r_{3,8}$	1.068	1.077
$r_{4,9}$	1.101	1.076
Bond Angles / °		
12-1-2	117.8	117.8
1-2-3	117.5	117.5
2-3-4	118.1	120.4
3-4-5	124.3	119.8
6-1-2	124.3	124.3
1-2-7	120.4	120.4
2-3-8	118.6	119.5
3-4-9	117.8	120.1

order parameters are consistent with those calculated by Jokissari and are all reduced by 79%.

3.4 Conclusions

We can conclude that vibrational corrections are important to make, in the determination of very accurate molecular geometries, but their neglect still leads to reasonable geometries and it has been shown here that the uncorrected D_{ij} obtained from VASS NMR spectroscopy are accurate enough for the purposes we require.

The experimental proof of the absolute values of J_{CF} in fluorobenzene has also been presented here. It is the first such proof of the signs of these couplings in aromatic systems. The results agree with all previous assumptions and calculations especially with respect to the values of the $^1J_{CF}$ which is found to be large and negative. It will be shown in chapters 4 and 6 how this technique has proved to be robust in the determination of the absolute signs of the J_{CF} in 2,2'-difluorobiphenyl and the liquid crystals I35 and I52.

3.5 References

[1] J.W.Emsley, L.Phillips, V.Wray, "Fluorine Coupling Constants" Pergamon Press 1977.

[2] R.Freeman. "A Handbook Of Nuclear Magnetic Resonance". Longman Scientific and Technical, New York 1987.

[3] G.V.D.Tiers and P.C.Lauterbur, *J.Chem.Phys.*, **36**, 1110, (1962) ; G.V.D.Tiers, *J.Phys.Chem.*, **67**,928 (1963)

[4] J.W.Emsley, L.Phillips, V.Wray, "Fluorine Coupling Constants" Pergamon Press 1977, pp 112, table 12.

[5] J.W.Emsley, J.C.Lindon, *Chem.Phys.Lett.*, **26**, 361, (1974)

[6] J.W.Emsley, J.C.Lindon, *Mol.Phys.*, **28**, 1253, (1974)

[7] J.Courtieu, D.W.Alderman, D.M.Grant, J.P.Bayles, *J.Chem.Phys.*, **77**, 723, (1982)

[8] F.J.Weigert and J.D.Roberts, *J.Amer.Chem.Soc.*, **93**, 2361, (1971)

[9] V.Wray, L.Ernst and E.Lustig, *J. Mag. Reson.*, **27**, 1, (1977)

[10] V.A.Chertkov and N.M.Sergeyev, *J.Mag.Reson.*, **21**,159, (1976)

[11] L.C.Snyder, *J.Chem.Phys.*, **43**,4041, (1965)

[12] R.C.long, E.E.Babcock, J.H.Goldstein, *J.Phys.Chem.* **85**, 1165, (1981)

[13] J.Jokisaari, J.Kuonanoja, A.Pulkkinen, T.Vaananen, *Mol.Phys.*, **44**, 197, (1981)

[14] K.V.Schenker, D.Suter, A.Pines, *J.Magn.Reson.*, **73**, 99, (1987)

[15] G.Celebre, G.De Luca, M.Longeri, E.Sicilia, *J.Chem.Inf.Comp.Sci.*, **34**, 539, (1994)

[16] S.Castellano, A.A.Bothner-By, *J.Chem.Phys.*, **41**, 3863, (1964)

[17] Anisotropies in the chemical Shielding and spin-spin coupling in LC samples, "Encyclopedia of NMR" (D.M.Grant and R.K.Harris, Eds.), Wiley, Chichester (1996)

[18] L.Nygaard, I.Bojesen, T.Pedersen and J.Rastrup-Andersen, *J.Molec.Struct.*, **2**, 209, (1968)

Chapter 4

^{13}C NMR Spectroscopy of 2,2'-difluorobiphenyl

4.1 Introduction

2,2'-difluorobiphenyl, shown in figure 1, is another example of a liquid crystal fragment. However, unlike phenyl benzoate (chapter 2) it is not nearly so commonly used in liquid

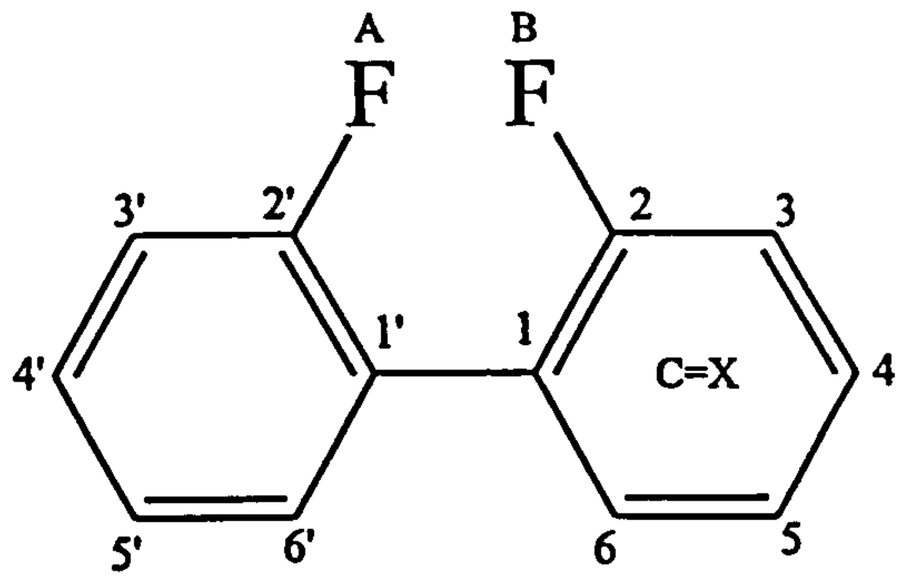

Figure 1 The structure of 2,2'-difluorobiphenyl

crystalline materials. Hird *et al.* [1] synthesised several terphenyls containing this group and discussed the relationship between the mesomorphic properties and the molecular structure of a range of difluoro substituted terphenyls, while a few years earlier Vauchier *et al.* [2] synthesised 'a new family of bifluorinated liquid crystals' and suggested that compounds exhibited broad mesomorphic ranges due to the presence of this group.

However, 2,2'-difluorobiphenyl is an interesting molecule in its own right, and the analysis of which through ^{13}C-{^{1}H} NMR spectroscopy has provided some interesting and very important results. It is actually a little studied group, with most attention being placed on the other 2,2'-halobiphenyls as well as other difluorobiphenyls, such as 3,3' and 4,4' substituted.

A concerted effort has been made in Southampton to determine the structure of 2,2'-difluorobiphenyl in the crystalline, liquid states and as an isolated molecule. Webster [3] carried out the X-ray study and has determined the crystal structure while MO calculations have been performed on an isolated molecule by Edgar [4] using Gaussian 92. This interest has spread to another group in Edinburgh who have also performed calculations on an isolated molecule[5]. Here we concentrate purely in the analyses of the ^{13}C-{^{1}H} NMR

spectra in the isotropic and liquid crystal phases the results of which are required for the conformational analysis discussed in chapter 5.

2,2'-difluorobiphenyl is an example of an ABX spin system [6]. Weigert and Roberts [7] described the ^{13}C-{^{1}H} spectra of the three isomers of difluorobenzene, themselves ABX spin systems, and showed that all the spectral parameters could be obtained providing that all 6 theoretically possible lines, shown in table 1, can be detected, and that both the line intensities and frequencies must be used in the analysis. Some of the lines are of very low intensity and not easily observed, which in turn leads to ambiguities in the analysis of the spectrum. However, improvements in signal to noise that can be obtained since Weigert and Roberts' experiments, mean that it is now possible to observe these very weak transitions, which as we will see are crucial in correctly determining the relative values for the scalar couplings and chemical shifts in the isotropic phase. The ^{13}C-{^{1}H} NMR spectrum of 2,2'-difluorobiphenyl in $CDCl_3$ shown in figure 2 demonstrates the ABX spin system for six different X displaying three types of multiplet, shown in figures 3 a) - c). Analysis of the isotropic ABX spectrum potentially yields the ^{19}F isotope shift, δ_{AB}, between the two fluorine nuclei, the chemical shift of the carbon, δ_X, the magnitude and relative signs of the

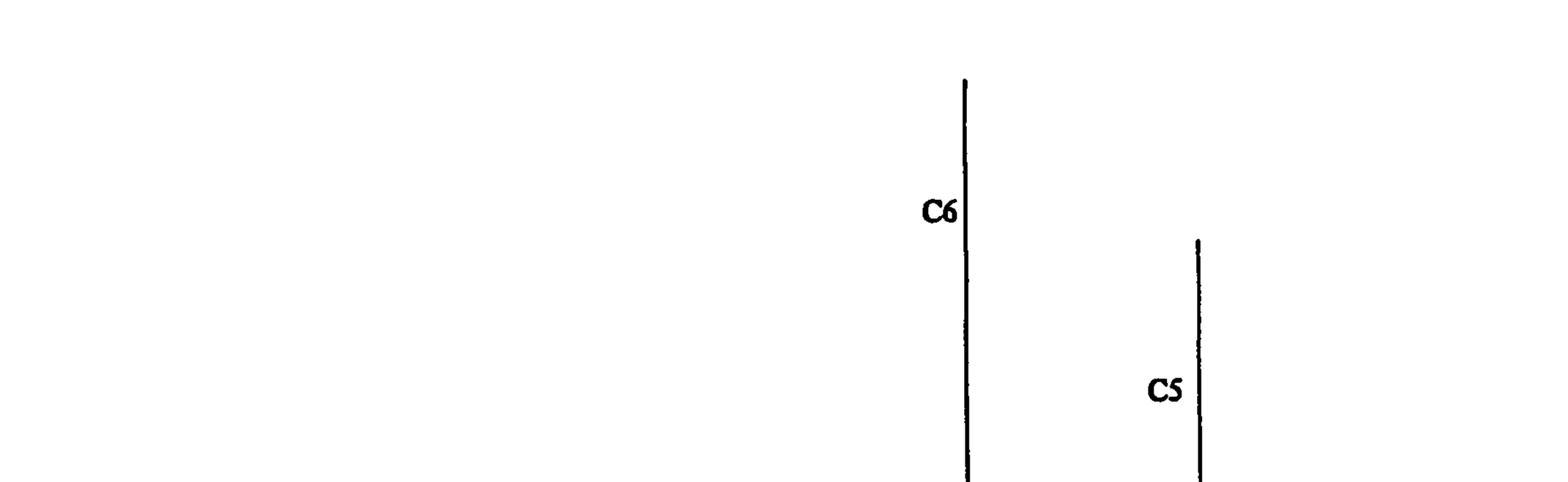

Figure 2 90.5 MHz ^{13}C - {^{1}H} spectrum of a solution of 2,2'-difluorobiphenyl dissolved in $CDCl_3$.

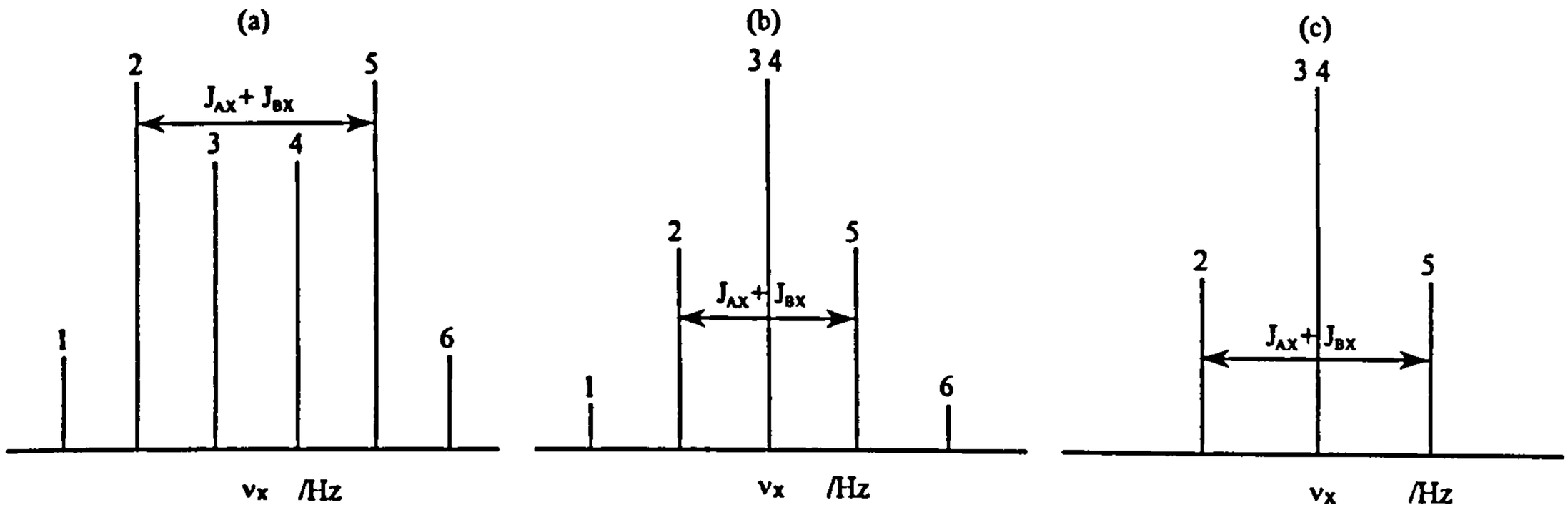

Figure 3 a) Splitting between 3 and 4. $\delta_{AB}\neq 0$. Appearence of 1 and 6. $J_{AX}\neq J_{BX}$. b) 3 and 4 not split. $\delta_{AB}=0$. Appearence of 1 and 6. $J_{AX}\neq J_{BX}$. c) 3 and 4 not split. $\delta_{AB}=0$. Non appearence of 1 and 6. $J_{AX}=J_{BX}$. $J_{AB} \gg \delta_{AB}$ and $(J_{AX}-J_{BX})/2$ [6]

scalar coupling constants J_{AX} and J_{BX} and the magnitude of J_{AB}. ABX spectra of samples in the LC phase, depend also on the anisotropic spin-spin couplings D_{AB}, D_{AX} and D_{BX}. The theoretical expressions for the line positions and intensities for the anisotropic ABX spin system are given in table 2. These suggest that the relative values of the J_{ij} and D_{ij} may be obtained provided that their relative magnitudes fall within certain narrow ranges of values. For any one sample it is unlikely that the correct range of values will be observed, however, it is possible to create the correct conditions by recording spectra of the oriented sample spinning about an axis making an angle, θ, to the magnetic field, B_0, as shown in figure 4. This technique of variable angle sample spinning (VASS) [8], discussed in chapter 1, was instrumental in the correct assignment and analysis of the liquid crystal spectrum. For the liquid crystal spectrum of 2,2'-difluorobiphenyl it will be shown that near the magic angle, $\theta=54.7°$, when the reduction factor $(3\cos^2\theta-1)/2$ is near zero, the relative signs of some of the pairs of D_{ij} and J_{ij} can be determined. The absolute signs of the J_{ij} can also be determined if, as in this case, the absolute signs of the D_{ij} are known. It will be shown here how the determination of the absolute signs of J_{CF} agrees with the results of the analysis of the VASS

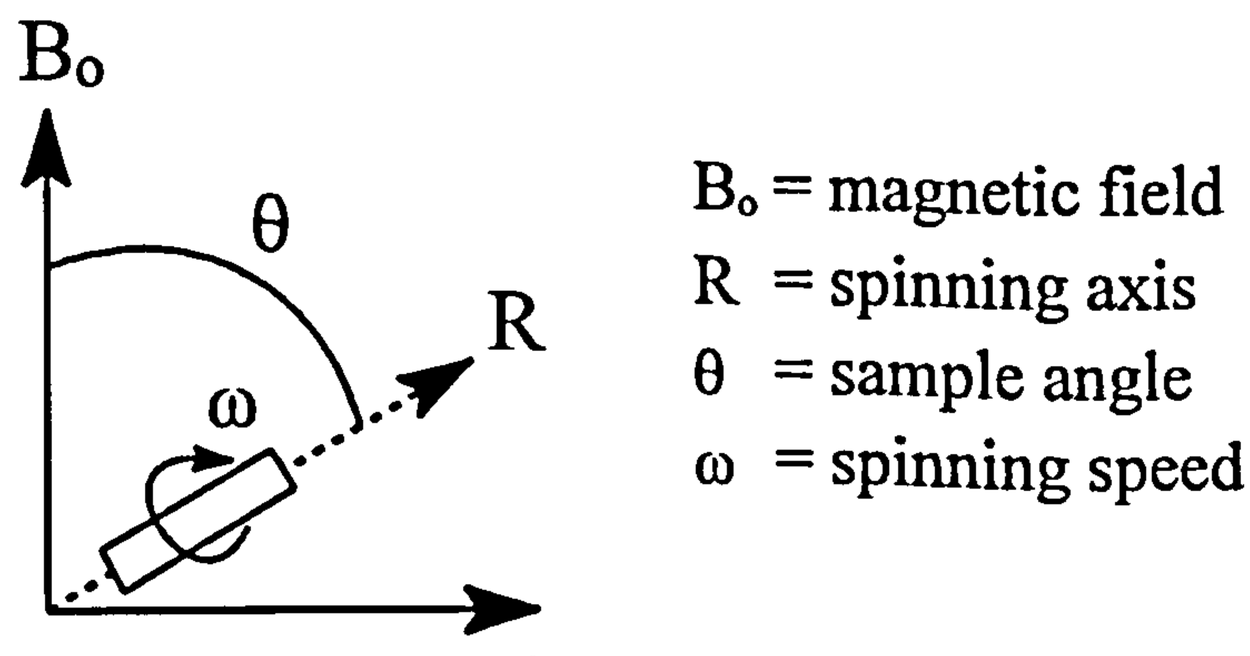

Figure 4 Schematic of the VASS Experiment

Table 1. Frequencies and intensities of the transitions in an isotropic ABX spin-½ system.

Line no.	frequency	Intensity
1.	$\nu_X - ½ (J_{AX} + J_{BX})$	1
2.	$\nu_X + (C_+ - C_-)$	$(1+Q_1Q_2)^2 / (1+Q_1^2)(1+Q_2^2)$
3.	$\nu_X - (C_+ + C_-)$	$(Q_1 - Q_2)^2 / (1+Q_1^2)(1+Q_2^2)$
4.	$\nu_X + (C_+ + C_-)$	$(Q_1 - Q_2)^2 / (1+Q_1^2)(1+Q_2^2)$
5.	$\nu_X - (C_+ - C_-)$	$(1+Q_1Q_2)^2 / (1+Q_1^2)(1+Q_2^2)$
6.	$\nu_X + ½ (J_{AX} + J_{BX})$	1

where

$C_+ = ½ [(\delta_{AB} + {}^1/_2 (J_{AX} - J_{BX}))^2 + J_{AB}^2]^{½}$

$C_- = ½ [(\delta_{AB} - {}^1/_2 (J_{AX} - J_{BX}))^2 + J_{AB}^2]^{½}$

and

$Q_1 = J_{AB} / [\delta_{AB} - {}^1/_2 (J_{AX} - J_{BX}) + 2C_-]$

$Q_2 = J_{AB} / [\delta_{AB} + {}^1/_2 (J_{AX} - J_{BX}) + 2C_+]$

Table 2. Frequencies and intensities of the transitions in an anisotropic ABX spin-½ system.

Line no.	frequency	Intensity
1.	$\nu_X - ½ (J_{AX} + 2D_{AX} + J_{BX} + 2D_{BX})$	1
2.	$\nu_X + (C_+ - C_-)$	$(Q_1 - Q_2)^2 / (1+Q_1^2)(1+Q_2^2)$
3.	$\nu_X - (C_+ + C_-)$	$(1+Q_1Q_2)^2 / (1+Q_1^2)(1+Q_2^2)$
4.	$\nu_X + (C_+ + C_-)$	$(1+Q_1Q_2)^2 / (1+Q_1^2)(1+Q_2^2)$
5.	$\nu_X - (C_+ - C_-)$	$(Q_1 - Q_2)^2 / (1+Q_1^2)(1+Q_2^2)$
6.	$\nu_X + ½ (J_{AX} + 2D_{AX} + J_{BX} + 2D_{BX})$	1

where

$C_+ = ½ [(\delta_{AB} + {}^1/_2 (J_{AX} + 2D_{AX} - J_{BX} - 2D_{BX}))^2 + (J_{AB} - D_{AB})^2]^{½}$

$C_- = ½ [(\delta_{AB} - {}^1/_2 (J_{AX} + 2D_{AX} - J_{BX} - 2D_{BX}))^2 + (J_{AB} - D_{AB})^2]^{½}$

and

$Q_1 = (J_{AB} - D_{AB}) / [\delta_{AB} - {}^1/_2 (J_{AX} + 2D_{AX} - J_{BX} - 2D_{BX}) + 2C_-]$

$Q_2 = (J_{AB} - D_{AB}) / [\delta_{AB} + {}^1/_2 (J_{AX} + 2D_{AX} - J_{BX} - 2D_{BX}) + 2C_+]$

spectra of oriented fluorobenzene [chaper 3]. The importance in determining the correct signs for the J_{ij} and D_{ij} is vital as analysis of the spectra may lead to different results if the relative signs of the couplings used in the analysis are incorrect. However, in some cases where $D_{ij} >> J_{ij}$ the errors are within the experimental error in determining the line positions from the spectra.

In this chapter the discussions will concentrate on the analysis of the sample of 2,2'-difluorobiphenyl in isotropic solution followed by the analysis of a sample in liquid crystalline solution followed by the method used to determine the absolute values of the isotropic and anisotropic couplings within the molecule.

4.2 Experimental

2,2'-difluorobiphenyl was purchased from Fluorochem Ltd. The ^{13}C-{^{1}H} spectrum of a sample of 2,2'-difluorobiphenyl (6mg) dissolved in $CDCl_3$ (54mg) was obtained on a Bruker AM 360 NMR spectrometer. The liquid crystal spectra were obtained from a sample of 2,2'-difluorobiphenyl dissolved as a 5% by weight solution in the nematic solvent ZLI 1167, (Merck) on a Bruker MSL 200 spectrometer. ZLI 1167, was chosen as it does not contain any aromatic carbons.

The sample for the VASS experiments was contained in a glass bottle sealed by epoxy resin which fits into a Zirconium rotor of 7mm o.d. (figure 5) for use in a VASS probe type MAS200 SB BL7. The spinning rate used has to be above the threshold at which the directors align along the spinning axis, and not to the magnetic field. In this case we chose to spin at 1000 Hz. Proton decoupling was achieved on the liquid crystalline sample using

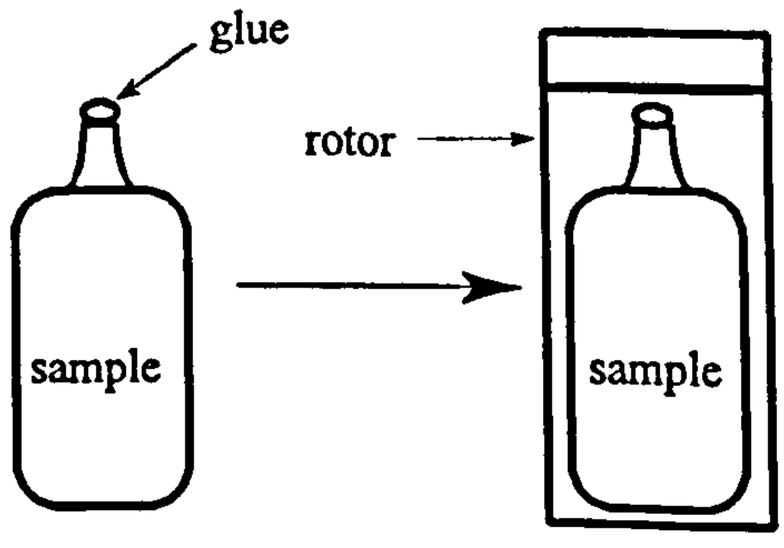

Figure 5 Sample containment for liquid VASS NMR.

NANZ-2 [9] pulse sequence based on COMARO2 [10] with a 90° pulse of 6.7μs. For ZLI 1167, as explained in chapter 1, the anisotropy in the magnetic susceptibility, $\Delta\chi$, is negative. The directors therefore align perpendicular to the magnetic field direction. For the VASS experiments we spin the sample at angles to the field in the range $54.7° < \theta \leq 90°$. Practically, angles of θ greater than 75.5° could not be exceeded for this sample. The VASS experiment is represented in figure 5.

The sample for the static experiment was contained in a glass tube held horizontally, perpendicular to the magnetic field. Proton decoupling was achieved using NANZ-2 with a 90° proton pulse of 6.1μs.

4.3 Results and Discussion

4.3.1 ^{13}C-{^{1}H} NMR spectra of the isotropic solution.

The reason that this system is an ABX and not as perhaps we might expect an AA'X where both fluorines should have identical chemical shifts as they themselves appear equivalent, is that each carbon atom is not equivalently located with respect to the two fluorine atoms. In any one 2,2'-difluorobiphenyl molecule we expect only one ^{13}C atom to be present at one time (in practice the probability of one ^{13}C atom in 2,2'-difluorobiphenyl is 0.132 as the natural abundance of ^{13}C is 1.1%), therefore the molecule is asymmetric and the fluorines are no longer equivalent. This means that when we observe the carbon resonances, there is a ^{13}C isotope effect on the chemical shift of the fluorines, δ_{AB}, in this molecule [6] which depends on their location relative to the ^{13}C.

The experimental spectrum of 2,2'-difluorobiphenyl in $CDCl_3$ is shown in figure 2. It is a superposition of the spectra from the six different isotopomers containing a single ^{13}C per molecule that we observe here, where the ^{13}C are the X part of an ABX spin system. On inspection of all the ABX regions, fine structure becomes noticeable, from the interactions of the carbon nucleus with the two fluorine nuclei. We remind ourselves that 6 lines are theoretically possible (table 1), however this is only the case when $\delta_{AB} \neq 0$ and/or $J_{AX} \neq J_{BX}$. Three cases are illustrated in figures 3 a) - c).

The first step in the analysis is to obtain J_{AB}. This coupling is expected to be the same for each ABX spin system because isotope effects on J_{AB} are small, and the correct determination of this makes the correct analysis of the other ABX possible. From there we can obtain δ_{AB}, J_{AX} and J_{BX} for each ABX.

We start, therfore, by analysing those spectra which display all six lines, and then proceed to the other cases.

The best example of a spectrum which has all six lines of appreciable intensity is that from C1, and this is shown in Figure 6 a). We see that the spectrum consists of 3 pairs of lines centred about the carbon chemical shift, δ_X. However, the three splittings provide

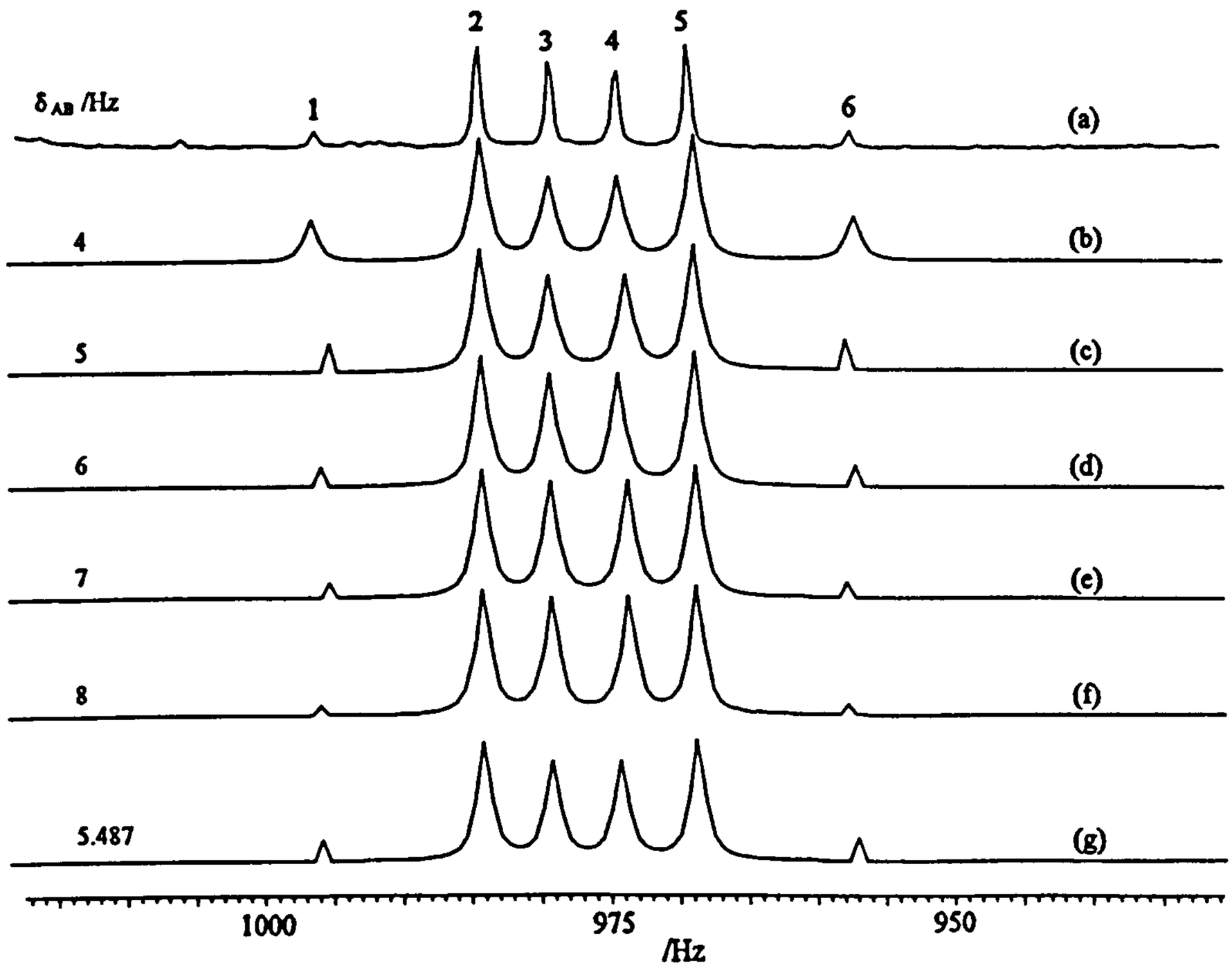

Figure 6 Expansion of the resonances in figure 1 given by C1. (a) Experiment, and (b) - (g) the results from iterative fits to the line positions with δ_{AB} fixed at the values marked against each spectrum.

insufficient data to fix the four remaining parameters J_{AX}, J_{BX}, J_{AB} and δ_{AB}. We need, therefore, to consider the intensities of these lines as well as their positions. The analysis of the spectrum was achieved using an iterative analysis program, PANIC (Bruker), based on LAOCOON [l2] which only considers the line positions, however, it is possible to determine quite accurately by eye the best result considering the line intensities. In order to begin the fitting of the experimental spectrum we require reasonable starting parameters.

From the equations in table 1 we know that from the appearance of the C1 region the splitting between lines 3 and 4 indicates that $\delta_{AB} \neq 0.0$Hz and that the presence of lines 1 and 6 indicates that $J_{AX} \neq J_{BX}$. From the splitting between lines 2 and 5 we also know the magnitude of $J_{AX}+J_{BX}$. The value for J_{AB} was taken from Servis *et al.*, 16.5 Hz [12]. Cooper *et al.* also measured this value, and found it to be 18.2 Hz [13]. The initial value adopted for J_{AX} was that obtained from an analysis of pure mono-fluorobenzene [14], $^2J_{CF}=20.98$Hz. This in turn sets our value for J_{BX} as the splitting between lines 2 and 5 is $|J_{AX}+J_{BX}|$. δ_{AB} was fixed at a reasonable 'guess' of 4.0 Hz from the approximate separation of lines 3 and 4. The parameters were varied through the iterative fitting procedure to determine the best values of J_{AB}, J_{AX} and J_{BX} which fit the line positions in the experimental spectrum, figure 6 a). A simulated spectrum is produced from these values determined by PANIC, to which we compare the line intensities from the experimental and calculated spectra. The fixed value of δ_{AB} was changed manually (5.0, 6.0, 7.0 and 8.0 Hz) and the fitting procedure repeated. The simulated spectrum shows how the relative line intensities, information which PANIC does not use in its calculations, depend on the value of δ_{AB} used in the simulations shown in figures 6 b)-f). It is then possible to choose a value for δ_{AB} from which the best fit including the line intensity information is obtained from the iterative calculations for the other three parameters. The value for J_{AB}, corresponding to the chosen δ_{AB}, is then fixed whilst δ_{AB}, J_{AX}

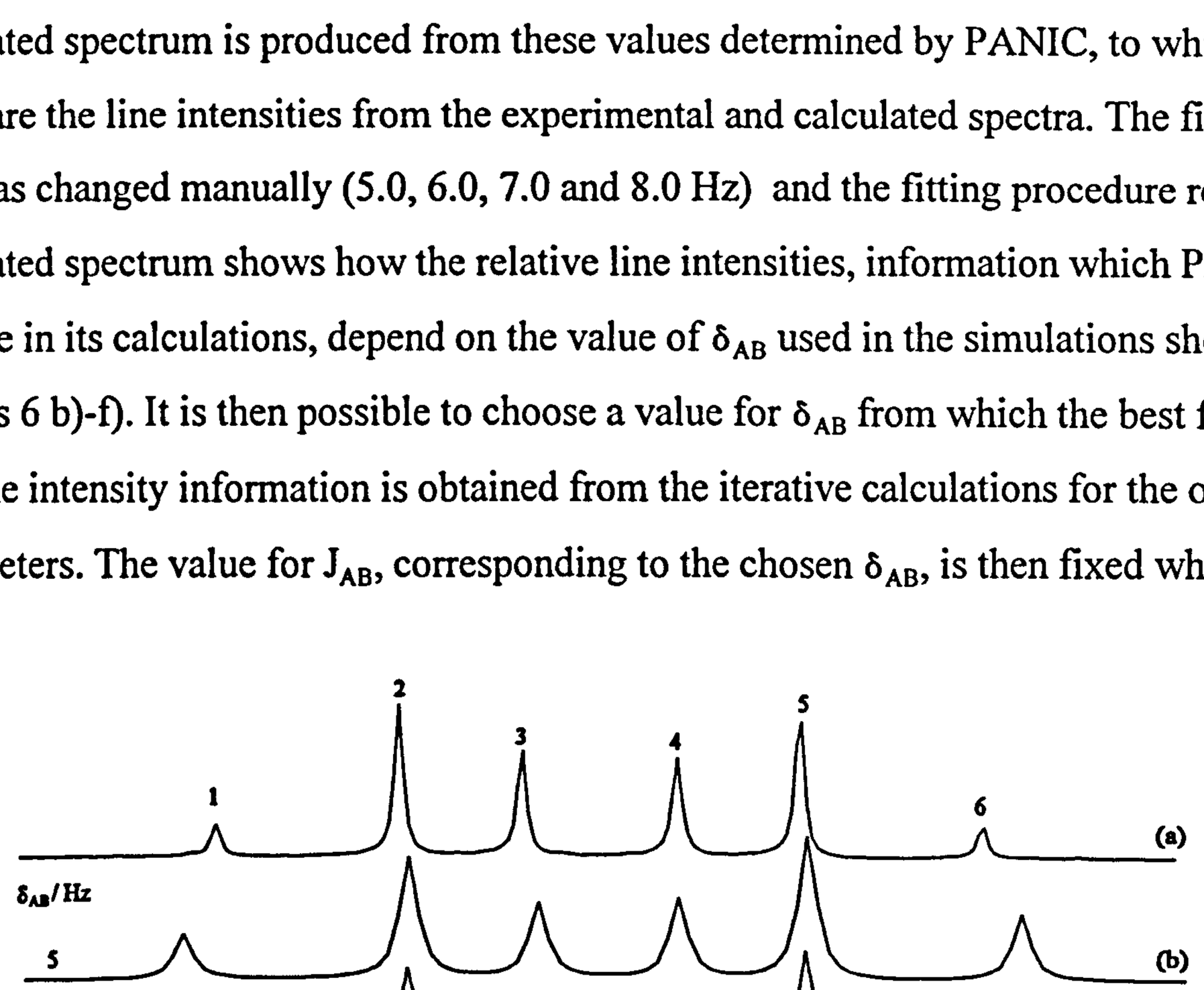

Figure 7 Expansion of the resonances in figure 1 given by C3. (a) Experiment, and (b) - (g) the results from iterative fits to the line positions with δ_{AB} fixed at the values marked against each spectrum.

and J_{BX} were allowed to vary in the final fitting procedure to produce the simulation shown in figure 6 g). We now possess a set of all 5 parameters, δ_X, δ_{AB}, J_{AX}, J_{BX} and J_{AB}, that best match the relative intensities and line positions in the experimental spectrum.

The procedure was repeated for the spectrum of C3, figure 7 a). The values for J_{AB} determined from the analyses of the spectra of C1 and C3 were compared and an average taken. The average value of J_{AB} was used, whilst kept fixed, in the analysis of the other four carbon multiplets. These multiplets were analysed by first determining δ_X as the centre frequency. δ_{AB}, J_{AX} and J_{BX} for each ABX were then determined by allowing them to vary until a good agreement between the calculated and experimental spectra were obtained.

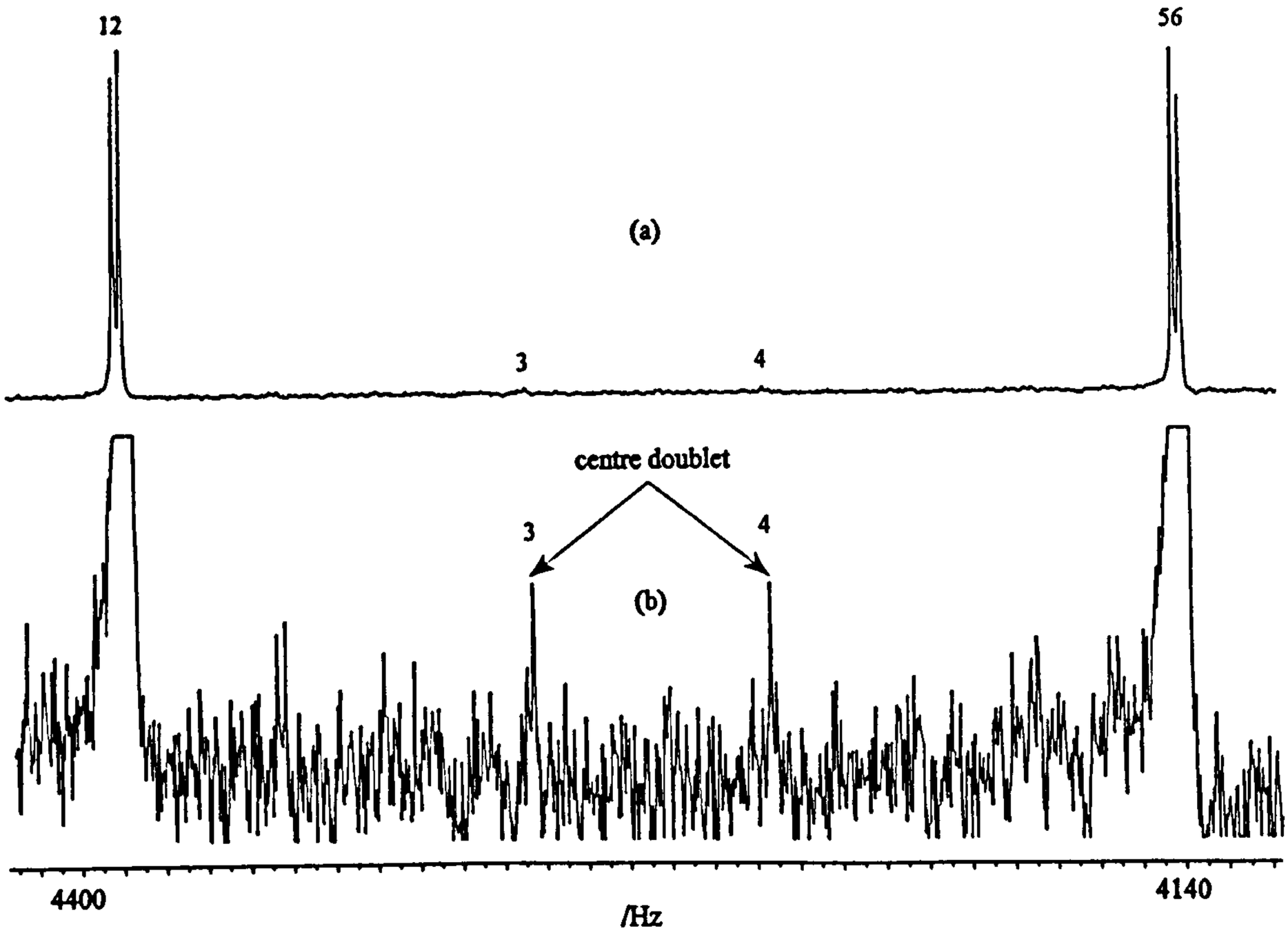

Figure 8 Horizontal expansion of the resonances in figure 1 given by C2, and (b) an additional vertical expansion (x 32) to show the weak pair of lines near the centre.

As mentioned earlier it is very important to locate the very weak intensities in each region. These are seen near the centre of C2, lines 3 and 4 in figure 8b), and at the outer parts, lines 1 and 6, of C4 shown in figure 9, and C5 shown in figure 10b). The intensity of the outer doublet, lines 1 and 6, depend on the ratio $|J_{AX}-J_{BX}|$ to $|J_{AB}|$. Even when the ratio is as large as 0.3, as in the case of C5, the lines are still easily overlooked. In the C6 region, figure 11, we do not see these lines, which is the case when $J_{AX}-J_{BX}$ and δ_{AB} are both zero, as illustrated in figure 3 c). The final results of the analysis of the $^{13}C-\{^1H\}$ NMR spectrum of 2,2'-difluorobiphenyl in isotropic solution are given in table 3.

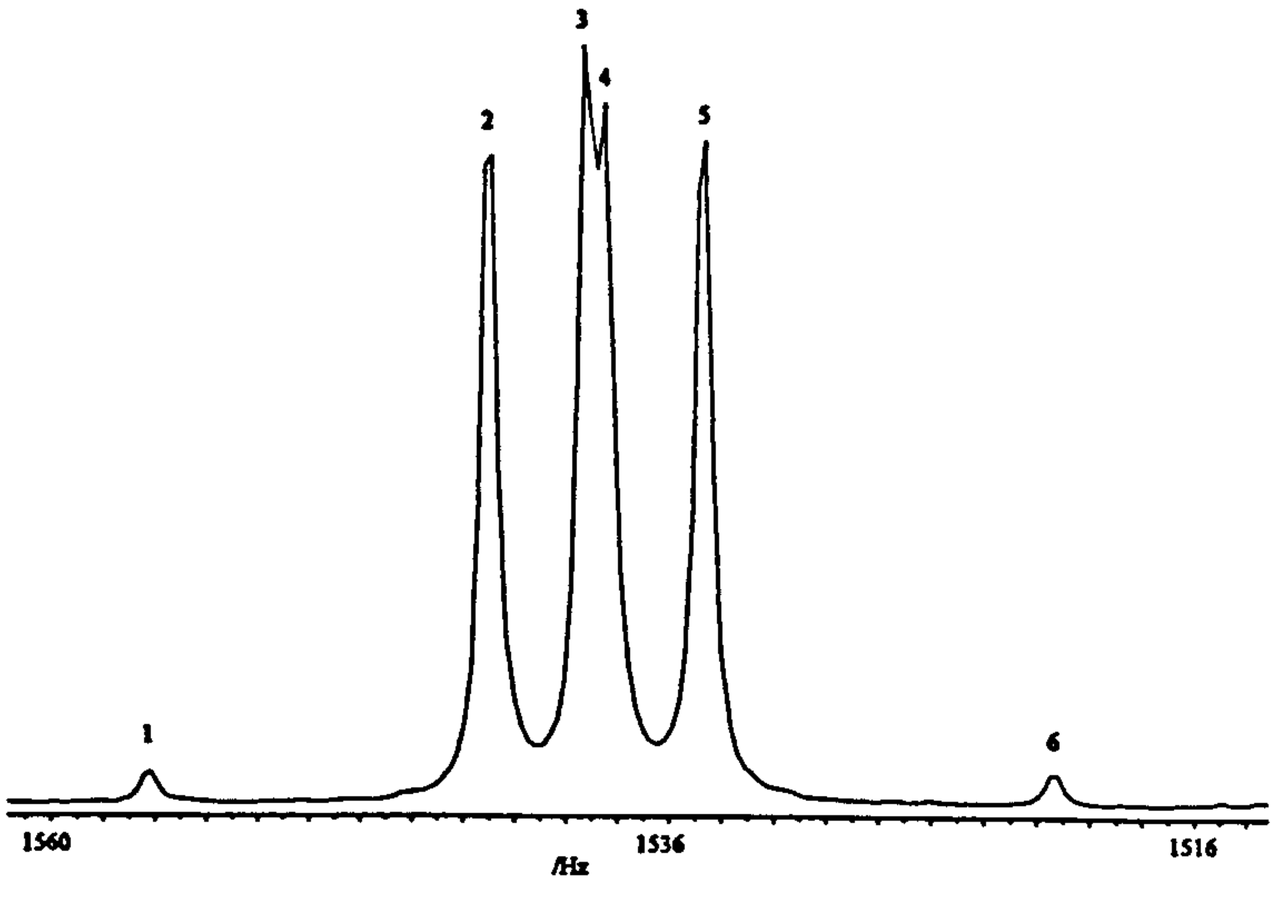

Figure 9 Horizontal expansion of the resonances in figure 1 of C4.

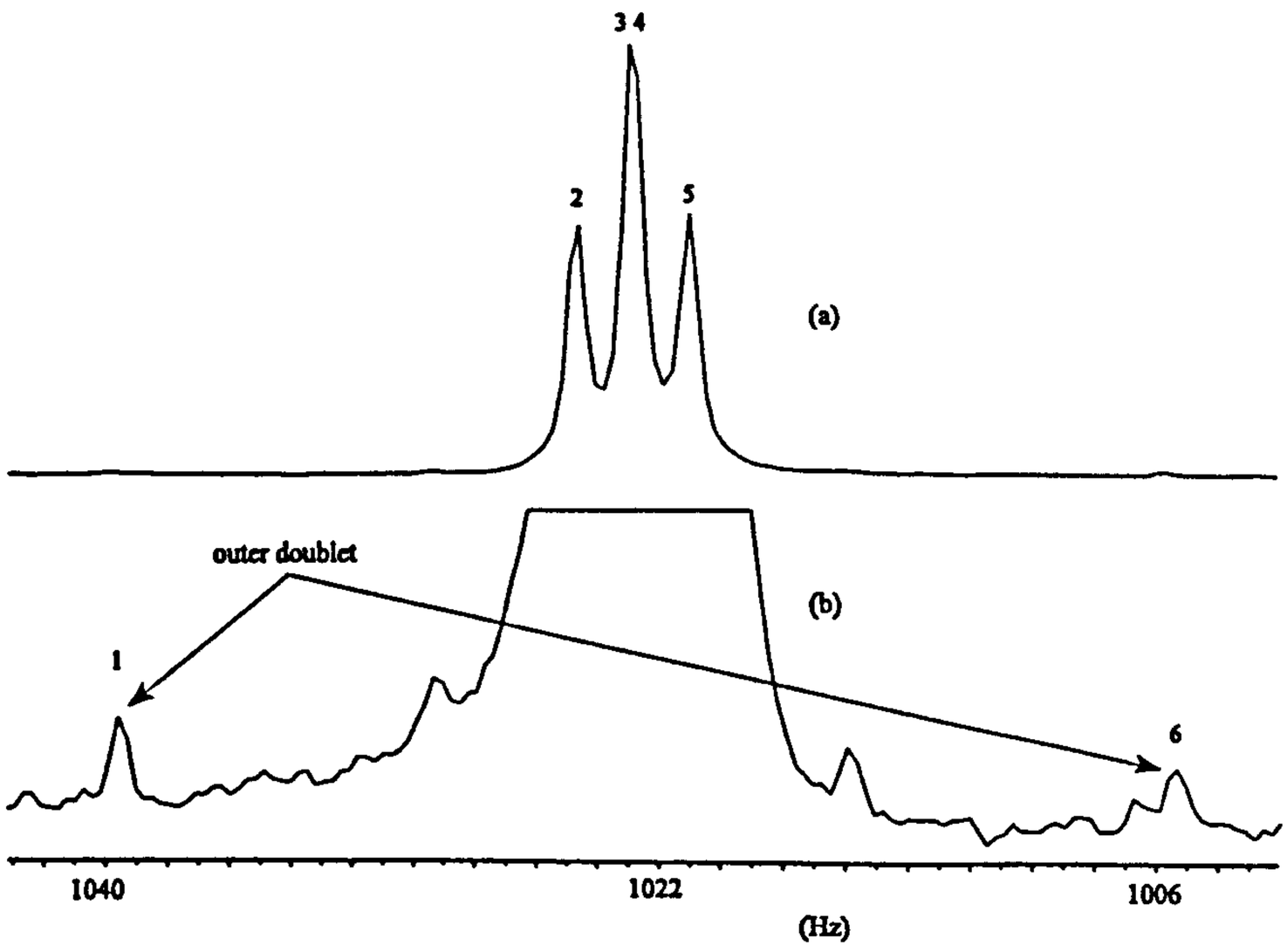

Figure 10 (a) Horizontal expansion of the resonances in figure 1 given by C5, and (b) an additional vertical expansion (x 32) to show the weak outer doublet.

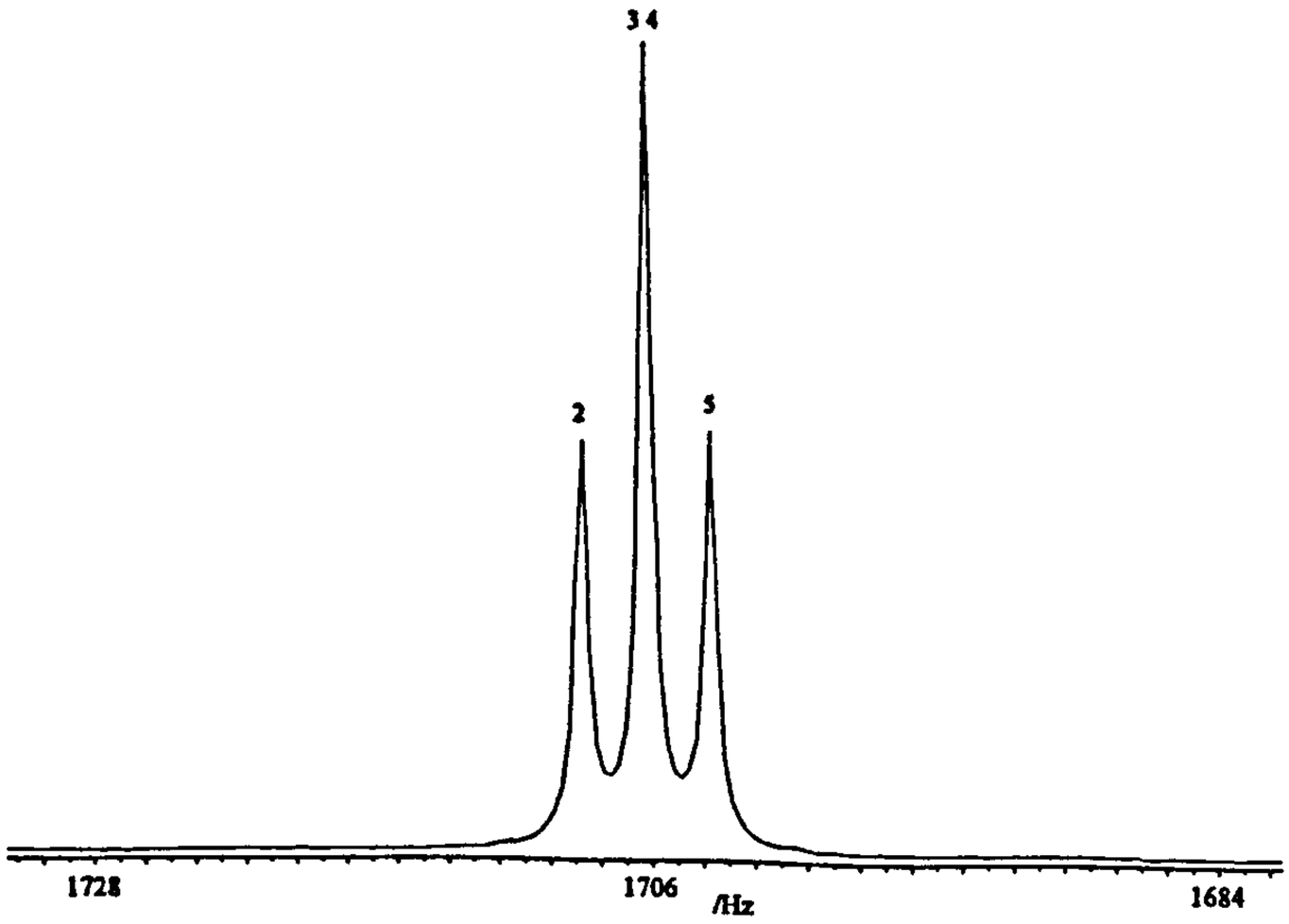

Figure 11 (a) Horizontal expansion of the resonances in figure 1 given by C6.

Table 3. ^{13}C chemical shifts, δ_i, relative to C3 , coupling constants, J_{ij}, and the fluorine isotope shift δ_i^{FF}, obtained from the analysis of the spectrum of 2,2'-difluorobiphenyl dissolved in $CDCl_3$.

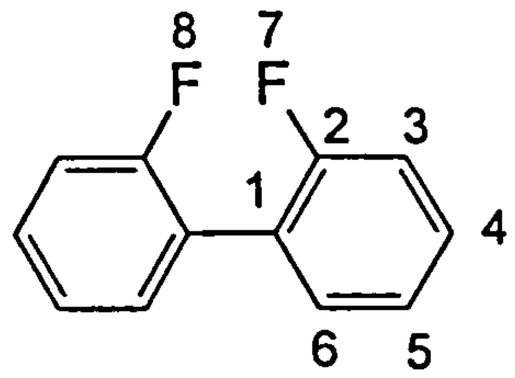

coupling constants / Hz

i,j	1,7	1,8	2,7	2,8	3,7	3,8
J_{ij}	16.2 ± 0.1	-1.2 ± 0.1	-248.5 ± 0.1	0.5 ± 0.1	23.3 ± 0.1	-0.8 ± 0.1
i,j	4,7	4,8	5,7	5,8	6,7	6,8
J_{ij}	8.8 ± 0.1	-0.8 ± 0.1	4.0 ± 0.1	-0.4 ± 0.1	2.5 ± 0.1	2.5 ± 0.1
i,j	7,8					
J_{ij}	16.5 ± 0.1					

^{13}C chemical shifts relative to C3 / ppm

i	1	2	3	4
δ_i	7.787 ± 0.001	44.096 ± 0.001	0.000 ± 0.001	14.000 ± 0.001
i	5	6		
δ_i	8.299 ± 0.001	15.850 ± 0.001		

^{19}F isotope shifts / ppm

i	1	2	3	4
δ_i^{FF}	0.0162 ± 0.0003	0.0735 ± 0.0003	0.0210 ± 0.0003	0.0044 ± 0.0003

4.3.2 ^{13}C-{^{1}H} NMR spectra of the anisotropic solution.

The theoretical expressions for the frequencies and intensities of the transitions derived from the X nucleus in the liquid crystal phase are given in table 2. We may remind ourselves at this point that ^{13}C-{^{1}H} NMR spectra in the liquid crystal phase depend not only on the isotropic interactions, the chemical shift, δ_x, and the scalar couplings, J_{ij}, but also on the anisotropic dipolar couplings, D_{ij} and the chemical shift anisotropy, δ_x^{aniso}. As in the isotropic solution, there are a maximum of six lines in the spectrum of each X group. Even if all six lines are detected we still have insufficient information to fix the 8 parameters (J_{AX}, J_{BX}, J_{AB}, D_{AX}, D_{BX}, D_{AB}, δ_X, δ_{AB}). We must therefore assume that the values for the isotropic interactions obtained from the NMR of the sample in isotropic solution remain unchanged in the liquid crystal solvent. There may be some solvent effects on the magnitude of these parameters, however, they should be very small compared to the magnitude of the D_{ij} and can be included in the error for the measurement of the D_{ij}. With δ_X still fixed as the centre of the multiplet we are left with only D_{AX}, D_{BX} and D_{AB} to determine which in theory, if all six transitions are resolved and detectable, is possible. In practice, however, the relative values of the parameters, the J_{ij} and the D_{ij}, are such that we are usually only able to observe four transitions. In these cases we must assume values for δ_{AB} and D_{AB} in addition to the three scalar couplings in order to determine D_{AX} and D_{BX}. If it were possible to observe six transitions in just one of the multiplets then D_{AB} could be determined and used throughout the analysis of the other multiplets. We denote this region in which the combinations of the parameters give rise to those further transitions as 'the sensitive region'. In the general case for a particular sample it is highly unlikely that the parameters for all carbons in the molecule lie in this region. In fact, the spectrum of C4 is in this sensitive region for the static sample. The first use of VASS is to assign the lines in the static spectrum, which revealed that the C4 multiplet consists of 5 lines and it is the analysis of C4 that is the key to analysing the other ABX. We also show here how we can bring the other carbon spectra into the sensitive region through the technique of Variable Angle Sample Spinning (VASS) and how this has enabled us to confirm the absolute values of the J_{CF}.

As was described in chapter 1, the liquid crystal directors, n , align along the spinning axis in a sample that is spun at a higher rate than a critical speed. In this case, the liquid crystal solvent, ZLI 1167, has $\Delta\chi$ negative and we spin the sample at an angle, θ, to the magnetic

field in the range $54.7° < \theta \leq 90°$.

Figure 12 shows the ^{13}C-{^{1}H} VASS spectra for a solution of 2,2'-difluorobiphenyl in the nematic solvent ZLI 1167 as the spinning axis is varied in the range $54.7° < \theta \leq 75.5°$. It is

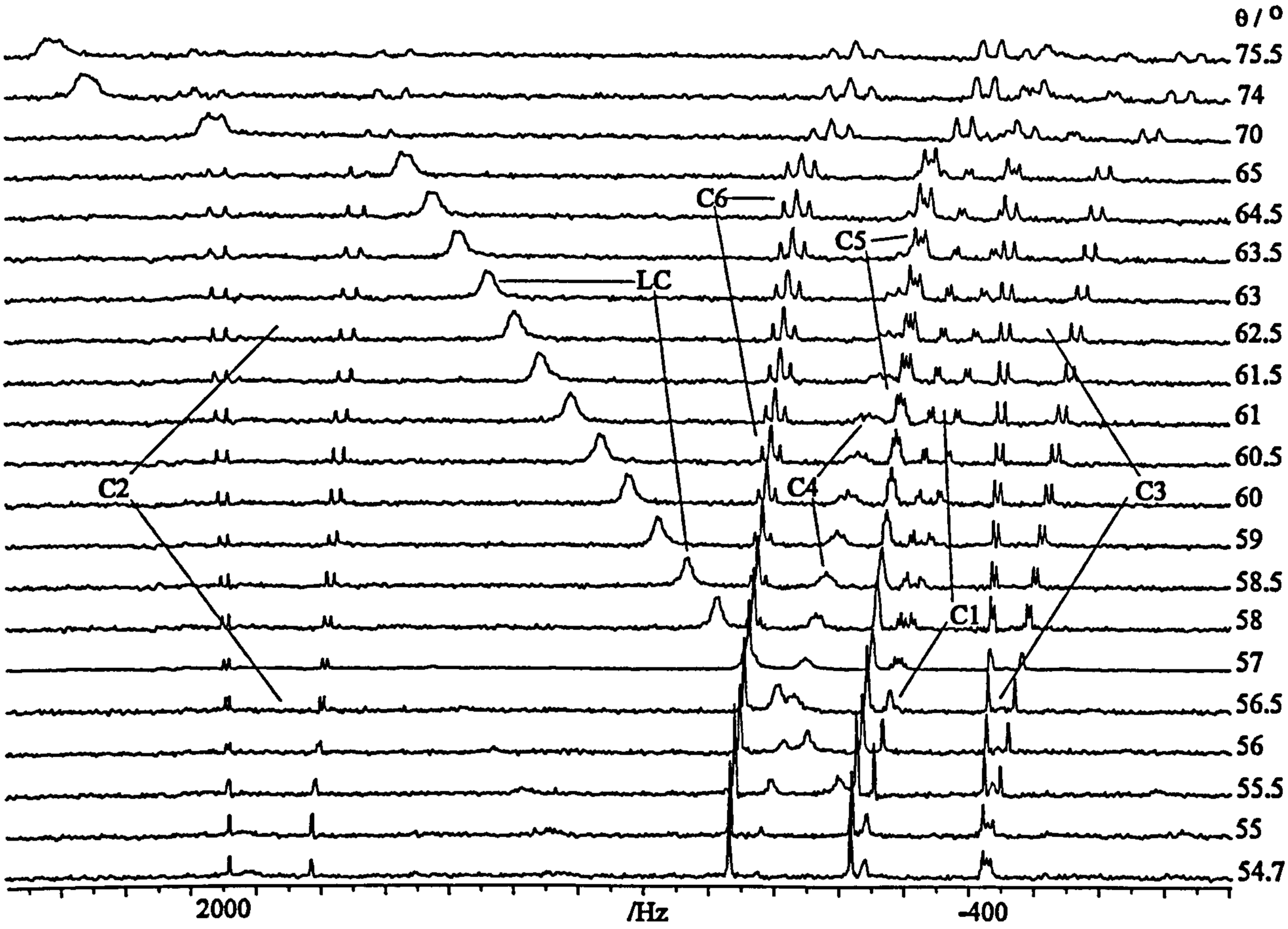

Figure 12 VASS 50.3 MHz ^{13}C - {^{1}H} spectra of a sample of 2,2'-difluorobiphenyl dissolved in the nematic solvent ZLI 1167. Most of the peaks from the solvent are at high field and are not shown. The angle, θ, between the spinning axis and B_0 is shown against each spectrum.

possible to assign all the transitions in the spectrum acquired at $\theta = 54.7°$, as it is almost identical, taking into account the greater linewidths, to the spectrum of 2,2'-difluorobiphenyl in isotropic solution, figure 2. This is because the spectrum recorded with the sample spinning at the magic angle, has the magnitude of the anisotropic interactions reduceed to zero, as shown in equation 1. As the spinning angle is moved away from the magic angle towards 75.5°, the magnitude of the anisotropic interactions, D_{ij}, increases and splittings begin to appear in the spectrum with respect to the isotropic interactions. The effect of the

$$D_{ij} = K_{ij}\left(\frac{3\cos^2\theta - 1}{2}\right) \qquad (1)$$

D_{ij} are initially observed through changing line shapes near to the magic angle emerging into doublets of doublets at later stages in the development.

4.3.3 The Variation of the ^{13}C Chemical Shift with θ

It is possible to follow each individual carbon multiplet in the spectrum as it shifts with changing θ, hence allowing the determination of the changing chemical shift, of X. The chemical shift in a liquid crystalline sample can be expressed as the contribution of δ_i^0, the isotropic value and δ_i^{aniso}, the anisotropic part. Thus,

$$\delta_i = \delta_i^0 + \delta_i^{aniso} \qquad (2)$$

The anisotropic part depends on the angle between the director and B_0, and so in the VASS experiment

$$\delta_i = \delta_i^0 + \delta_i^{aniso}\left(\frac{3\cos^2\theta - 1}{2}\right) \qquad (3)$$

A plot of δ_i against $(3\cos^2 - 1)/2$ should be linear with a slope of δ_i^{aniso}. Figure 13 shows that equation 3 is obeyed and yields the values of δ_i^{aniso} shown in table 4.

Table 4. The chemical shift anisotropies, δ_i^{aniso}, for the ^{13}C nuclei in 2,2'-difluorobiphenyl dissolved in the nematic solvent ZLI 1167.

i	1	2	3
δ_i^{aniso}/ppm	33.9 ± 0.6	5.0 ± 0.1	19.4 ± 0.5
i	4	5	6
δ_i^{aniso}/ppm	46.4 ± 1.4	21.6 ± 0.4	19.6±0.4

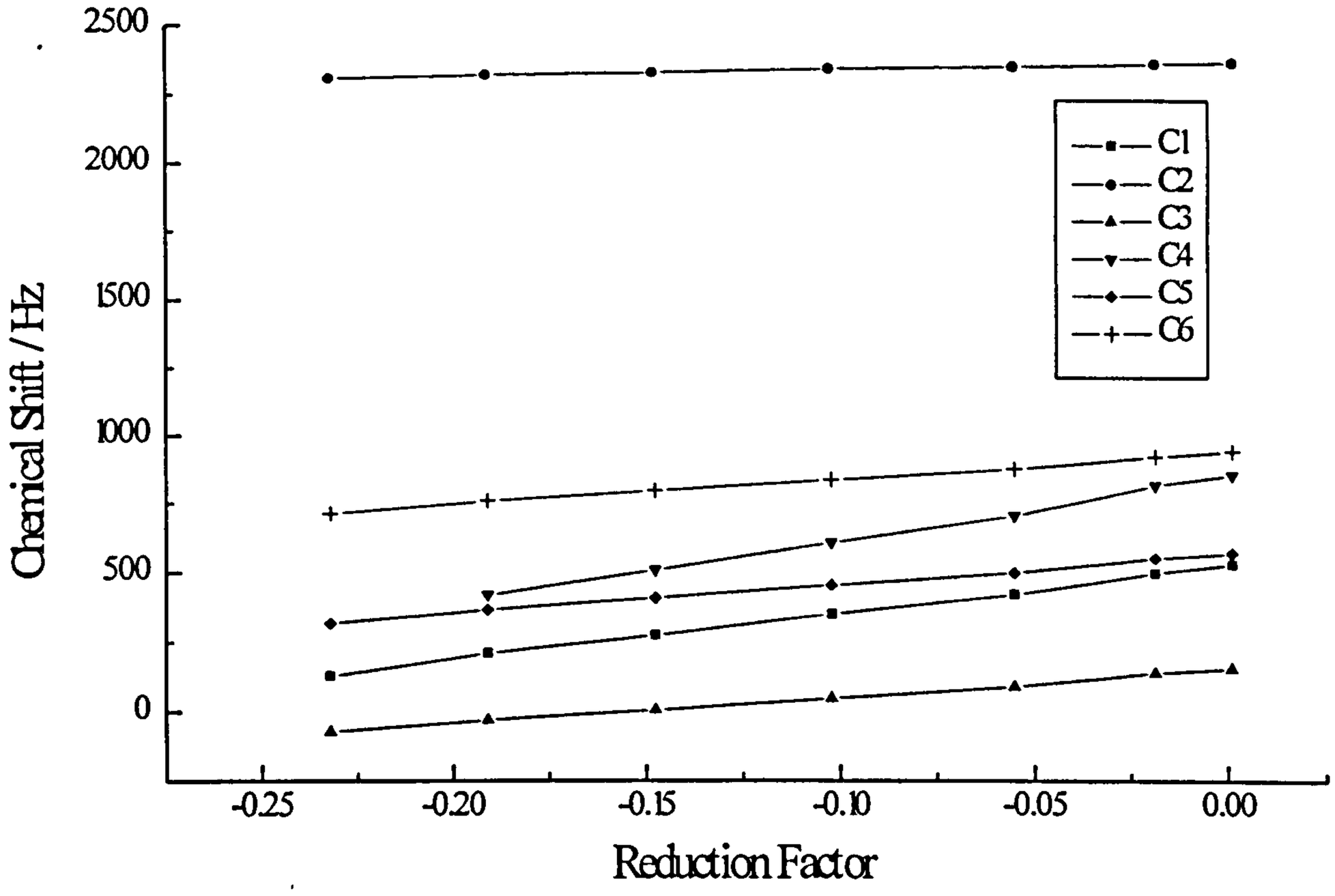

Figure 13 Variation with $R = (3\cos^2\theta - 1)/2$ of the centre of the resonances from the individual carbons in a sample of 2,2'-difluorobiphenyl dissolved in the nematic solvent ZLI 1167.

4.3.4 Analysis of the ^{13}C-{^1H} NMR Spectrum of the Static Liquid Crystalline Sample

The ^{13}C-{^1H} NMR spectrum of a static sample of 2,2'-difluorobiphenyl dissolved in the nematic solvent ZLI 1167 is given in figure 14. The static spectrum, which should be equivalent to the VASS spectrum when $\theta = 90°$ assuming all experimental conditions remain constant, can be assigned through extrapolation of the individual line positions from the VASS spectra, to the case at $\theta = 90°$. Through this method a good match was found and the static spectrum successfully assigned. The line assignments are also shown in figure 14. Having assigned the static spectrum it can be seen that all the carbons display a four line multiplet, except for carbon 4, which has five lines. We have already mentioned that more than four lines may be observed, if and only if the values of the parameters are bounded within 'the sensitive region'. Although we only observe five lines, the central line is in fact a superposition of two lines, with separation less than that of the experimental line widths. As δ_{AB} depends on this separation it is difficult to measure this parameter accurately here, so

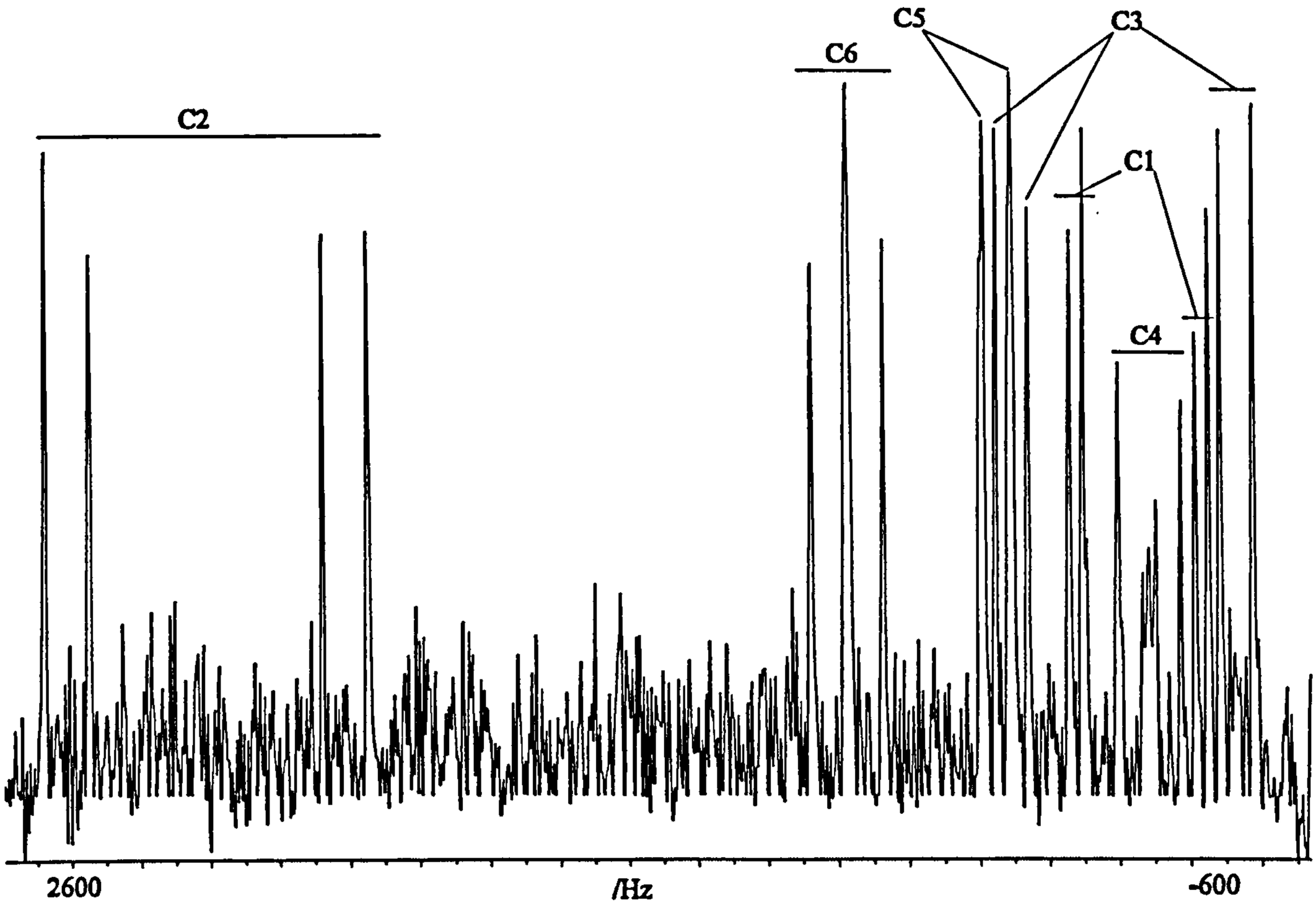

Figure 14 The 50.3 MHz ^{13}C - $\{^{1}H\}$ spectrum from a static sample of 2,2'-difluorobiphenyl dissolved in the nematic solvent ZLI 1167.

we must initially assume it to be the same as the value obtained from the analysis of the isotropic spectrum, however, we can still determine D_{AB}. In practice the magnitude of δ_{AB} for C4 is small enough as not to make any major differences to the line width of the central peak if there is a solvent effect to consider. Simulation of the carbon 4, as shown in figure 15, demonstrates the sensitivity of the relative magnitudes of J_{AB} and D_{AB} within a narrow range, hence the name 'the sensitive region'. The intensity of the centre line varies greatly with D_{AB} and is reduced to zero when $D_{AB} = J_{AB}$. Using the value of J_{AB} determined from the spectrum in the isotropic solution, $J_{AB} = 16.6$ Hz, it was then possible to determine the value of D_{AB} in the liquid crystal solution. The value of D_{AB} determined for carbon 4, remains constant for each carbon spectrum and was used in their respective analyses. It is important to note that there are in fact two values for D_{AB} that satisfy the line shape of the spectrum mirrored exactly about the value of J_{AB} where the line shape depends on $J_{AB} \pm D_{AB}$, however, in this case the lower value is disregarded, from evidence of the analyses of the ^{1}H-$\{^{2}H\}$ spectra in chapter 4 which require a larger value in order to satisfy the fit. Further VASS spectra have been recorded which demonstrate that the value of D_{AB} passes through a range of values including two stages in which five lines can be observed, which can only happen if the value of D_{AB} is the larger value (figure 16). As D_{AB} increases, the centre peak

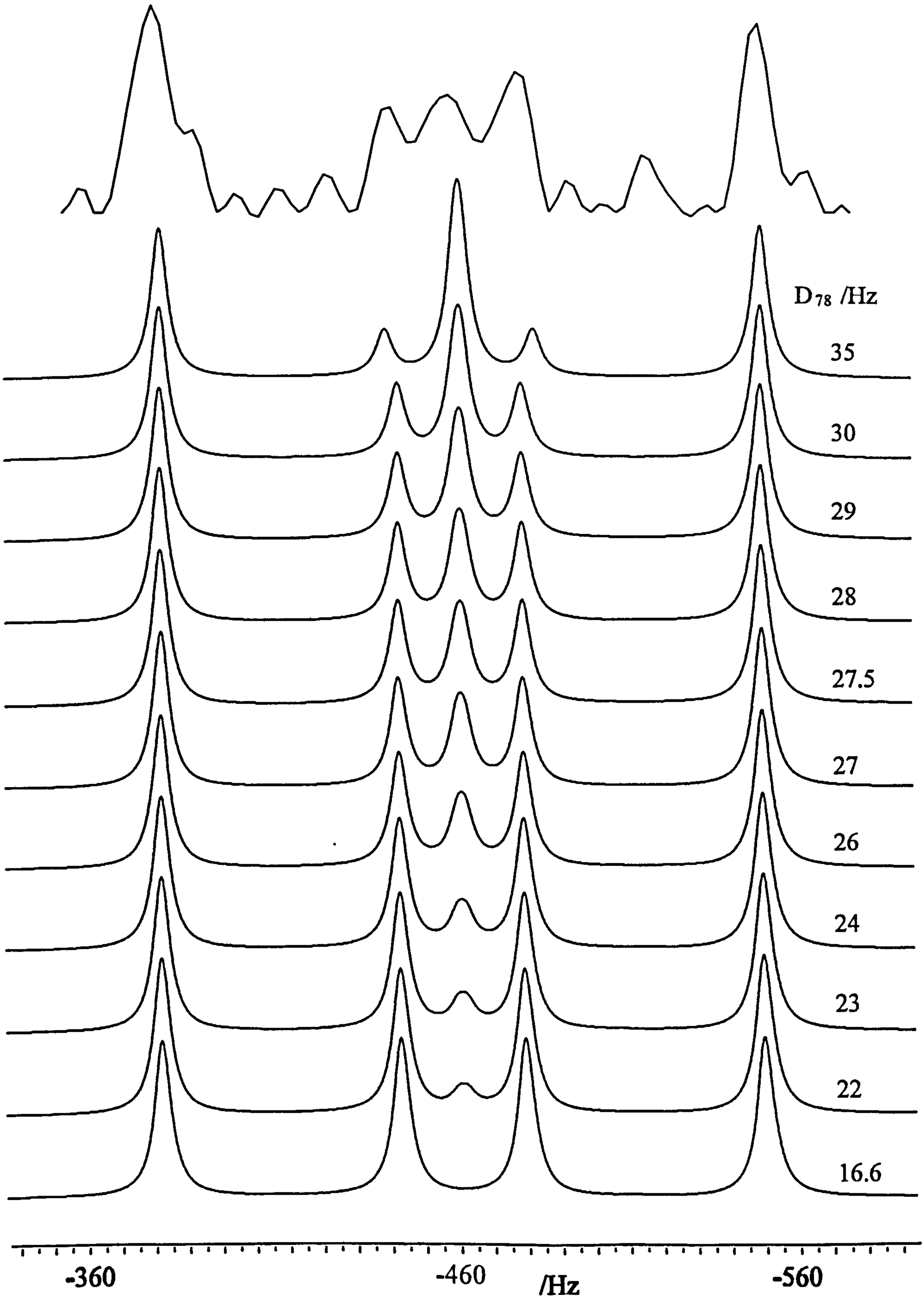

Figure 15 Experimental , top, and simulated ^{13}C - {^{1}H} spectra from C4 in a static sample of 2,2'-difluorobiphenyl dissolved in the nematic solvent ZLI 1167. The simulated spectra differ only in the value of D_{78} whose value is given alongside each spectrum.

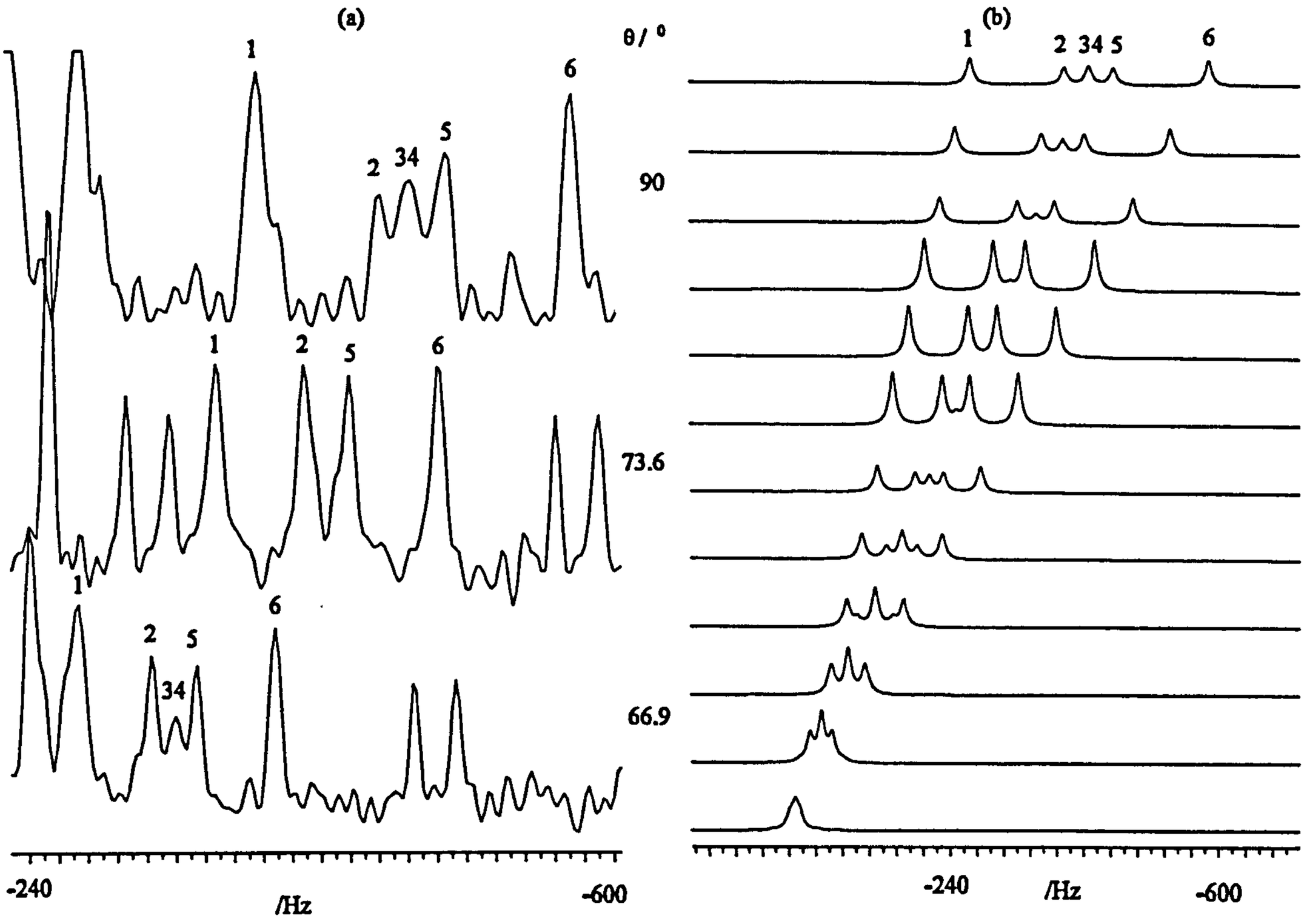

Figure 16 Experimental (a) and simulated (b) VASS ^{13}C-{^{1}H} spectra from C4 demonstrating dissappearence and reappearence of the centre line.

decreases in intensity as the following relationship applies, $D_{AB} < J_{AB}$. The centre peak increases again with D_{AB} when $D_{AB} > J_{AB}$. The results of the complete analysis of all six ABX spin systems are given in table 5.

Table 5. Chemical shifts, δ_i, and dipolar couplings, D_{ij}, obtained from the analysis of the ^{13}C - $\{^1H\}$ spectrum of a static sample of 2,2'-difluorobiphenyl dissolved in the nematic solvent ZLI 1167.

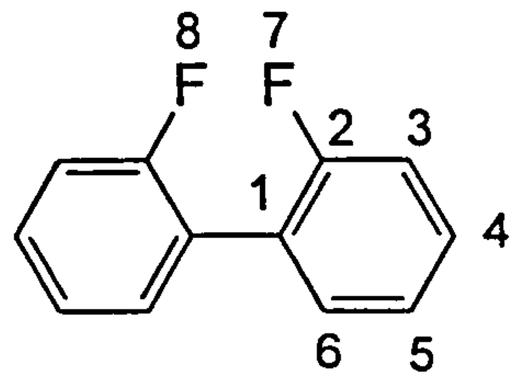

Dipolar couplings / Hz

i,j	1,7	1,8	2,7	2,8	3,7	3,8
D_{ij}	-186.2 ± 0.1	18.8 ± 0.1	-275.7 ± 0.1	63.7 ± 0.1	306.9 ± 0.1	46.9 ± 0.1
i,j	4,7	4,8	5,7	5,8	6,7	6,8
D_{ij}	47.5 ± 0.1	37.6 ± 0.1	-7.5 ± 0.1	41.1 ± 0.1	-48.6 ± 0.1	52.2 ± 0.1
i,j	7,8					
D_{ij}	27.5 ± 0.5					

^{13}C chemical shifts relative to C3 /ppm

i	1	2	3
δ_i	0.781 ± 0.001	50.365 ± 0.001	0.0 ± 0.001
i	4	5	6
δ_i	1.146 ± 0.001	7.955 ± 0.001	16.242 ± 0.001

^{19}F isotope shift/ppm

i	1	2	3	4	5	6
δ_i^{FF}	0.04 ± 0.02	0.40 ± 0.02	0.06 ± 0.02	0.0 ± 0.02	0.0 ± 0.02	0.0 ± 0.02

4.3.5 Absolute signs of the J_{ij}^{CF}

In order to obtain the D_{ij} it is necessary to know the magnitude and the sign of the J_{ij}. For the analysis of the ^{13}C-{^1H} NMR static spectrum of 2,2'-difluorobiphenyl in the liquid crystal phase, we used the values of J_{ij} determined from the analysis of the sample in isotropic solution, given in table 2. Here the absolute signs of the J_{CF} were assumed to be positive except for the directly bonded $^1J_{27}$. Our assumption is well founded, as the analysis of fluorobenzene in the liquid crystal phase, shown in chapter 3, demonstrates. However, we can test our results further by analysing the VASS spectra of 2,2'-diflurobiphenyl with respect to the changing line shapes of the multiplets as θ is changed.

It will now be shown how the relative signs of the J_{ij} and D_{ij} pairs can be obtained by observation of how the multiplets evolve as θ is changed in small steps from the magic angle. The absolute signs of the D_{CF} and D_{FF} for 2,2'-difluorobiphenyl dissolved in ZLI 1167 are known because the order parameters, $S_{\alpha\beta}$, have been obtained from the analysis of D_{HH} and D_{HF} of a partially deuterated sample also dissolved in ZLI 1167 at a similar concentration and temperature, discussed in chapter 5. We may first examine the multiplet associated with carbon 2, this being the unique case where the value of $^1J_{27}$ is large and negative. If we study the evolution of the C2 multiplet with θ, shown in figure 17, we notice

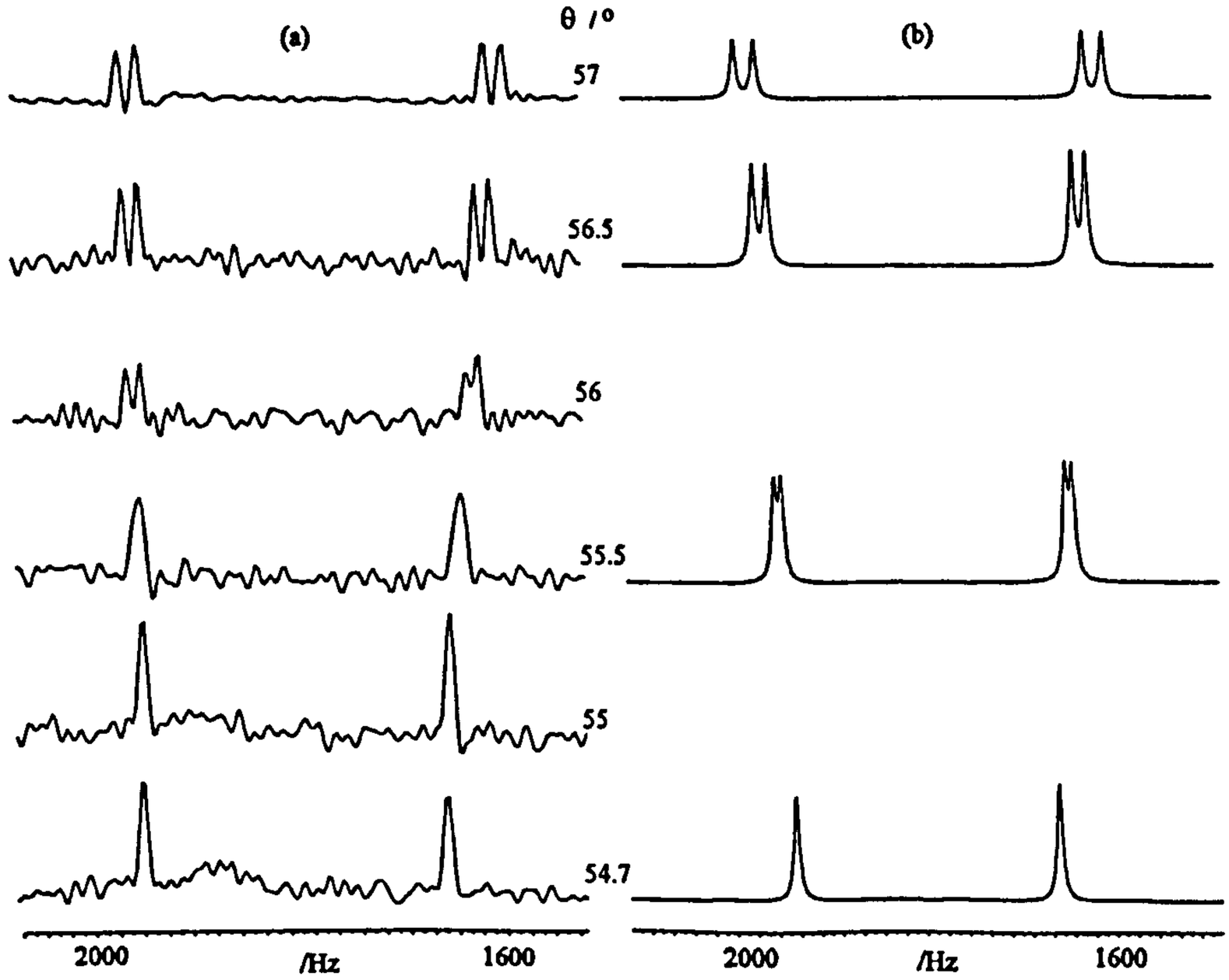

Figure 17 Experimental (a) and simulated (b) VASS ^{13}C - {^1H} spectra from C2 near the magic angle. The angle of the spinning axis with the field is given alongside each spectrum.

that the spectrum at the magic angle is dominated by the $^1J_{27}$ where the much smaller $^1J_{28}$ is unresolved in the liquid crystalline solution. In theory, table 3, the spectrum consists of 6 lines, figure 8, however, we only observe a doublet in this spectrum because of poor signal to noise compared to the spectrum acquired in the isotropic solution. As the spinning angle, θ, to the magnetic field is increased towards the horizontal, so the magnitude of the D_{ij} increase, as shown in equation 1. We observe this through the appearance of the minor splittings at θ=56.0°, corresponding to D_{28}, and an overall increase in the size of the major splitting corresponding to D_{27}. Since the magnitude of the splitting depends on the following addition of parameters, splitting = $2D_{ij} + J_{ij}$, we conclude that for C2 both $^1J_{27}$ and $^1D_{27}$ have the same sign and are therefore negative. This conclusion agrees with Tiers [15] and with our findings from the study of fluorobenzene in chapter 3. We now also know the absolute signs of the smaller, J_{28} and D_{28}. We can further test our findings with the other carbon multiplets, to confirm that our method for the determination of the absolute signs of the couplings is robust.

The evolution of C1 with θ is shown in figure 18. As in the C2 spectrum at the magic angle, the spectrum depends only on the isotropic interactions, the scalar couplings and the

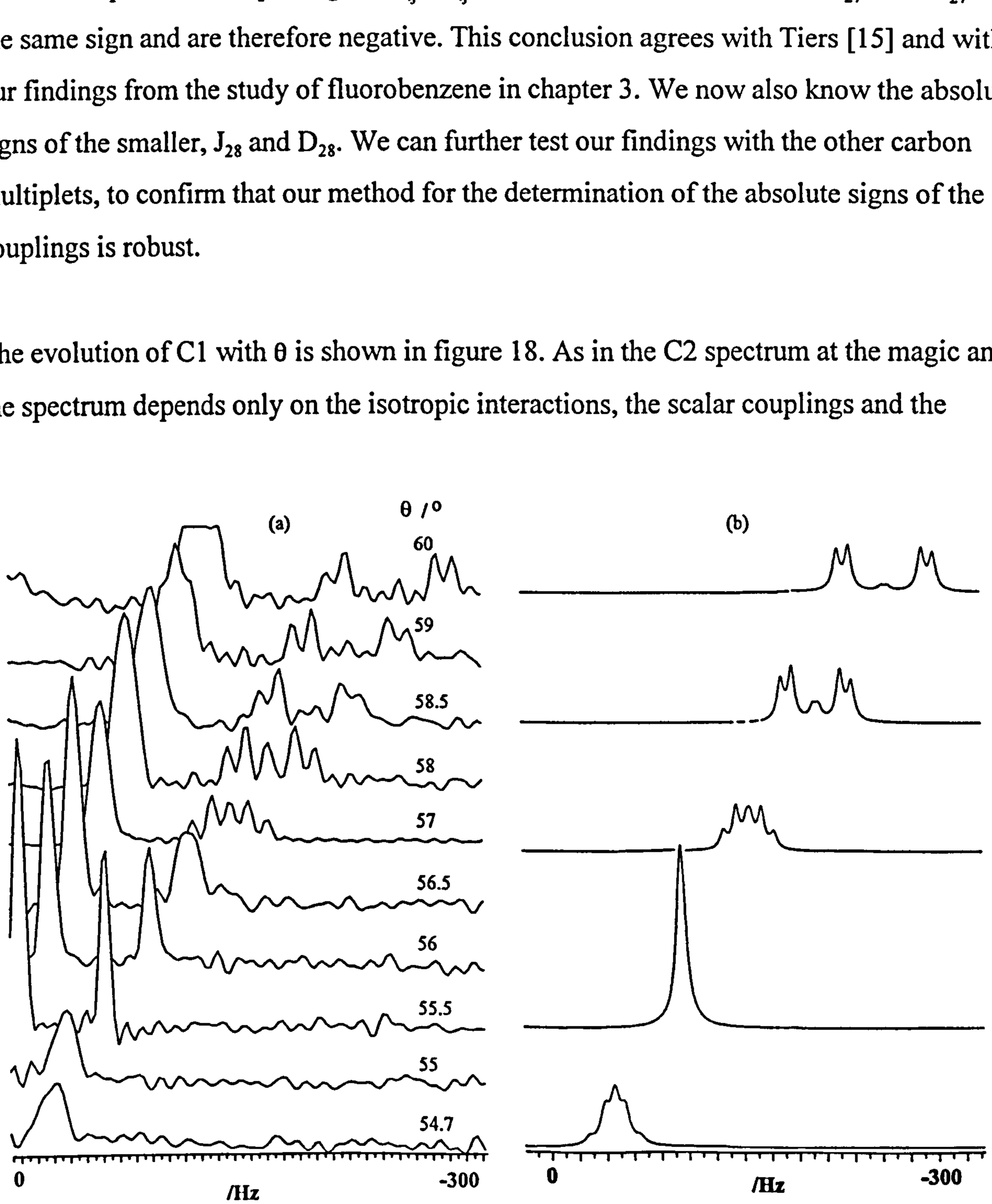

Figure 18 Experimental (a) and simulated (b) VASS ^{13}C - {^1H} spectra from C1 near the magic angle. The angle of the spinning axis with the field is given alongside each spectrum.

chemical shift. We would therefore expect to see six lines in the spectrum, equivalent to the spectrum given in figure 6a). Indeed simulation with zero line width, gives rise to the same spectrum, however, the experimental spectrum is not so well resolved and the line separations are smaller than the experimental line width, and we observe only one broad peak. Calculation of the $^2D_{17}$ from the order parameters obtained from the proton spectrum of 2,2'-difluorobiphenyl, gives the absolute sign of the coupling which is negative. This contrasts with the positive sign of $^2J_{17}$. We also know that the magnitude of the line splitting depend on the sum of the couplings. With this in mind we would expect the splittings to decrease initially as $R|^2D_{17}|$ approaches $|^2J_{17}|$, where R is the reduction factor, leading to an increase in the splitting with $R|^2D_{17}|$, as it increases and begins to dominate the spectrum. Figure 18 a) demonstrates this behaviour in the experimental spectra with the line narrowing to a minimum width at between θ=54.7° and 55.5° before increasing again after this angle. Figure 18 b) confirms this pattern through simulation of the growth of $|^2D_{17}|$. From θ=54.7° towards 75.5° the splittings initially collapse and then grow eventually evolving into a doublet of doublets similar to the spectrum of C2, where the major splitting depends on D_{17} and J_{17}, and the minor splittings on D_{18} and J_{18}.

Through θ=57.0° to 58.0°, the multiplet consists of five resolvable lines. The parameters appear to lie in 'the sensitive region' where it is possible to determine D_{AB} (D_{78}) and δ_{AB}. The centre line consists of two unresolved lines with splitting equal to δ_{AB}. Simulation of this region of the spectrum using the value for δ_{AB} determined in isotropic solution, gives a slightly different spectrum displaying resolution between the two central peaks. Reduction of the value of δ_{AB} in the simulation gives rise to a more reasonable simulation. We place an upper limit on the value of δ_{AB} = 2.0Hz in the liquid crystal solvent, which is significantly less than the value, δ_{AB} = 5.5Hz, in the isotropic solution. We have two possible explanations for this difference. There may be considerable anisotropic contributions to δ_{AB} of opposite sign to the isotropic contribution, or it could be a solvent affect on the isotropic value of δ_{AB}. It is not possible here to conclude which of these explanations is correct as we are restricted to measurements in the limited range of 'the sensitive region'.

The evolution of the spectrum of C3 with θ is shown in figure 19. We observe that the parameters appear to lie in 'the sensitive region' between θ=54.7° and θ=55.0°. The absolute values of the parameters are a different case than for C1 where the calculated absolute value for $^2D_{37}$ has the same sign as $^2J_{37}$. In this case we expect the addition of the parameters to

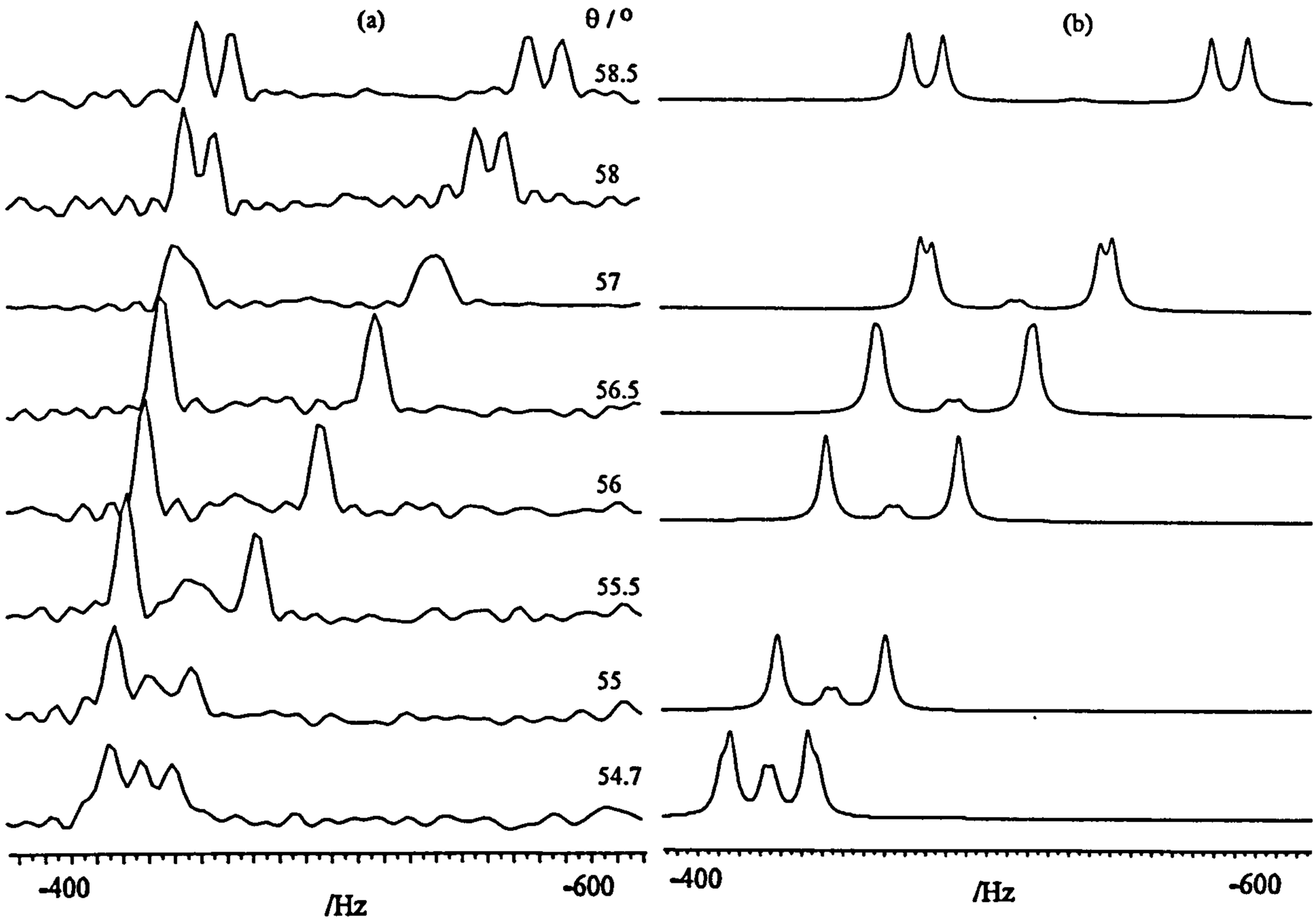

Figure 19 Experimental (a) and simulated (b) VASS ^{13}C - {^{1}H} spectra from C3 near the magic angle. The angle of the spinning axis with the field is given alongside each spectrum.

result in continued growth of the line splittings with $^{2}D_{37}$ through increasing θ, as with C2.

Examination of the experimental spectra in figure 19 a) confirms our predictions that the splittings increase constantly and eventually evolve into a doublet of doublets as in the case of C2 and C1 where the major splitting depends on D_{37} and J_{37} and the minor splittings depend on D_{38} and J_{38}. Figure 19 b) shows simulations of the spectra which illustrate this behaviour which only occurs using the correct absolute signs of the couplings. Incorrect relative signs for the parameter would result in a similar simulation to that for C1, shown in figure 18 b). As with the C1 spectrum, we can determine the values D_{78} and δ_{78}, in this case at θ=54.7° and θ=55.0°. Simulations of these spectra require us to place an upper limit on the value of δ_{78} of 3Hz, compared to 7.1Hz in isotropic solution.

The VASS spectra of C5 are shown in figure 20 a) on an expanded scale. The spectrum is not resolved at the magic angle, although it depends on J_{57}, and structure only starts to evolve at θ=59.0°, as $R|D_{57}|$ increases, due to poor resolution of the liquid crystal spectrum. We calculate, from the order parameters, that D_{57} has a small negative value and D_{58} a large positive value. From the analysis of the isotropic spectrum we know that the scalar couplings also have opposite signs, J_{57}=4.0Hz and J_{58}=-0.4Hz. Simulation of the spectra

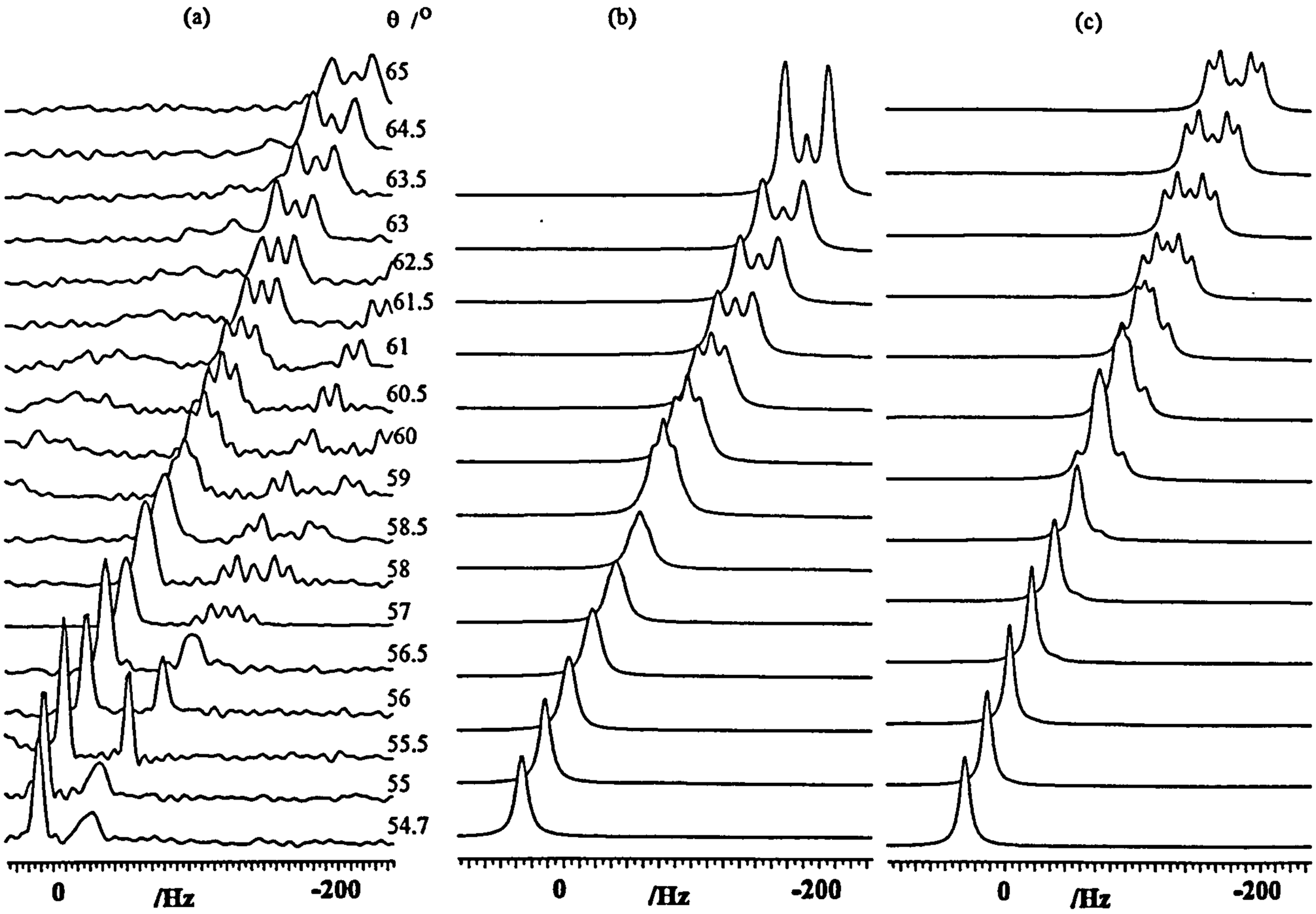

Figure 20 Experimental (a) and simulated (b) and (c) VASS ^{13}C - $\{^1H\}$ spectra from C5 near the magic angle. The simulations have (b) $J_{57} = 4.0$ and $J_{58} = -0.4$ Hz, whilst in (c) $J_{57} = -4.0$ and $J_{58} = 0.4$ Hz. In both cases the dipolar couplings are appropriate reductions of the static dipolar couplings $D_{57} = -7.5$ Hz and $D_{58} = 41.1$ Hz. The angle of the spinning axis with the field is given alongside each spectrum.

through changing θ using both sign combinations gives rise to two different sets of spectra, shown in figures 20 b) and c). We can clearly see on comparison of these simulations to the experimental spectra in figure 20 a) which sign combination correctly models the multiplet evolution. As θ is increased the spectra evolve into a doublet of doublets whose major splitting depends on J_{58} and D_{58} and the minor splitting on J_{57} and D_{57}.

The VASS spectra of C6 are clearly visible in figure 12. The scalar couplings for C6 are both equal and are relatively small at 2.5Hz. Changing the signs of these couplings does not make any significant differences to simulated spectra of C6 with changing θ. We cannot therefore guarantee the absolute signs of these couplings using our method. It appears that in this case we have surpassed the sensitivity of our method and so we assume the absolute signs for J_{67} and J_{68} to be positive, agreeing with all previous predictions and is further supported by the proof of the signs of the scalar couplings for carbons 1,2,3 and 5, here. Furthermore, we can accept our assumption if we include it as the error in the measurement of D_{67} and D_{68}.

The VASS spectra of C4, in figure 12, are poorly resolved, however, we can show that the evolution of the multiplet with θ is consistent with the signs of the couplings we have calculated from the previously determined order parameters (see figure 16 b) where the experimental spectra show no sign of a reduced set of line splittings resulting in a collapse of the C4 multiplet into a singlet. Therefore referring to our evidence with C1, C2 and C3, we may conclude that both D_{47} and J_{47} have the same sign, and are therefore both positive. From this conclusion we also know the absolute values of J_{48} and D_{48}.

We now have a complete set of the absolute values, given in table 4, for the scalar and dipolar couplings, that may be obtained from the ^{13}C-{^{1}H} NMR spectrum of 2,2'-difluorobiphenyl dissolved in the liquid crystal solvent ZLI 1167. As was mentioned earlier, the signs of the couplings have also been confirmed in fluorobenzene (chapter 3). The results of this piece of work coupled with the results of the analysis of the VASS spectra of fluorobenzene reported in chapter 3 lends further weight to our proof of the opposite signs of the directly bonded $^{1}J_{CF}$ compared to the indirectly bonded $^{n}J_{CF}$, where n=2-4, in aromatic systems.

4.4 Conclusions

In order to successfully analyse ABX spin systems in isotropic solution, it is necessary to resolve and assign very weak peaks that may otherwise be missed or ignored in order to obtain the correct values for the parameters. This approach has enabled us to fully analyse the ^{13}C-{^{1}H} NMR spectra of 2,2'-difluorobiphenyl in isotropic solutions. The fact that we are able to detect very small peaks shows the improvements that have been made in NMR technique since the studies by Weigert and Roberts on substituted fluorobenzenes [7].

The analyses of the spectra of carbon 5 and carbon 6 provide good examples of our progress, where the first impression might be that their spectra are identical and that only on closer inspection do we observe the very small outer peaks in the spectrum of C5. It is the assignment of these small peaks that differentiates between $^{4}J_{57} = 4.0$Hz and $^{5}J_{58} = 0.4$Hz, a difference we certainly expect as the two fluorines are inequivalent with regards to that carbon atom. If these peaks were not considered during the analysis, the results would have been quite different, with $J_{57} = J_{58} = 1.8$Hz, a result that is similar to that of C6. We cannot

resolve outer peaks in the spectrum of C6 and are therefore left to conclude that $^3J_{67} = {}^4J_{68} =$ 2.5Hz. In reality we would expect there to be a difference in these two couplings, however, we accept that the limit in resolution has been reached as the difference between them would be so small as to produce outer lines that are indistinguishable from the background noise level.

We may propose to improve the signal to noise ratio, through increasing the number of scans for the acquisition of the NMR spectra. However, this would be impractical with respect to the amount of spectrometer time required already, but also during this extra time subtle changes in the ambient conditions will begin to affect the spectrum resulting in line broadening leading to further loss of information and accuracy.

The analysis of the sample in the liquid crystal solvent has demonstrated that we may determine the absolute signs of all the parameters through experiment. The VASS technique has opened up a new door in spectral analysis, providing access to this previously unobtainable information. A major step forward must be in the proof through experimental evidence that the $^1J_{CF}$ is of opposite sign to the other longer range $^nJ_{CF}$. This is an observation that has not been previously made in an aromatic system.

4.5 References

[1] M.Hird, K.J.Toyne, G.W.Gray, D.G.McDonnell and I.C.Sage, *Liq. Cryst.*, **18**, 1, (1995)

[2] C.Vauchier, F.Vinet and N.Maiser, *Liq. Cryst.*, **5**, 141, (1989)

[3] B.Aldridge, G.De.Luca, M.Edgar, S.Edgar, J.W.Emsley, M.I.C.Furby and M.Webster, *Liq.Cryst.*, **24**, 569, (1998)

[4] M.Edgar personal communication

[5] C.J.Adam, S.J.Clark, G.J.Ackland, J.Crain, *Phys.Rev.E* , **55**, 5641, (1997)

[6] J.D.Roberts, "An introduction to the Analysis of Spin-Spin Splitting in Nuclear Magnetic Resonance," W.A.Benjamin, New York, N.Y., 1962, pp 71-85.

[7] F.J.Weigert and J.D.Roberts, *J.Amer.Chem.Soc.*, **93**, 2361, (1971)

[8] J.Courtieu, J.P.Bayle, B.M.Fung, *Prog.Nucl.Magn.Reson.Spectrosc.*, **26**, 141, (1994)

[9] D.Nanz, M.Ernst, M.Hong, M.A.Ziegeweid, K.Schmidt-Rohr, A.Pines, *J.Magn.Reson.*, **A113**, 169, (1995)

[10] K.V.Schenker, D.Suter, A.Pines, *J.Magn,Reson,*. **73**, 99, (1987)

[11] S.Castellano, A.A.Bothner-By, *J.Chem.Phys.*, **41**, 3863, (1964)

[12] K.L.Servis and K-N.Fang, *J. Amer. Chem. Soc.*, **90**, 6712, (1968)

[13] M.A.Cooper, H.E.Weber and S.L.Manatt, *J.Amer.Chem.Soc.*, **93**, 2369, (1971)

[14] V.Wray, L.Ernst and E.Lustig, *J. Mag. Reson.*, **27**, 1, (1977)

[15] G.V.D.Tiers and P.C.Lauterbur, *J.Chem.Phys.*, **36**, 1110, (1962) ; G.V.D.Tiers, *J.Phys.Chem.*, **67**,928 (1963)

Chapter 5

The Structure of 2,2'-difluorobiphenyl in the Liquid Crystal Phase

5.1 Introduction

There has been a number of studies of the structure of biphenyl and halosubstituted biphenyls, in various states of matter. The barrier for rotation about the centre bond is unusual in having a strong dependence on sample phase, and there is some dispute as to the conformational distribution of 2,2'-dihalobiphenyls, in particular whether there is only one minimum energy structure corresponding to the molecules being non planar where the rings are colinear with a dihedral angle between the planes of the rings where only the *-syn* or *-anti* (figure 1) conformer is probable or if there are two minimum energy structures where both *-syn* and *-anti* conformers are favourable, although not necessarily equal in probability.

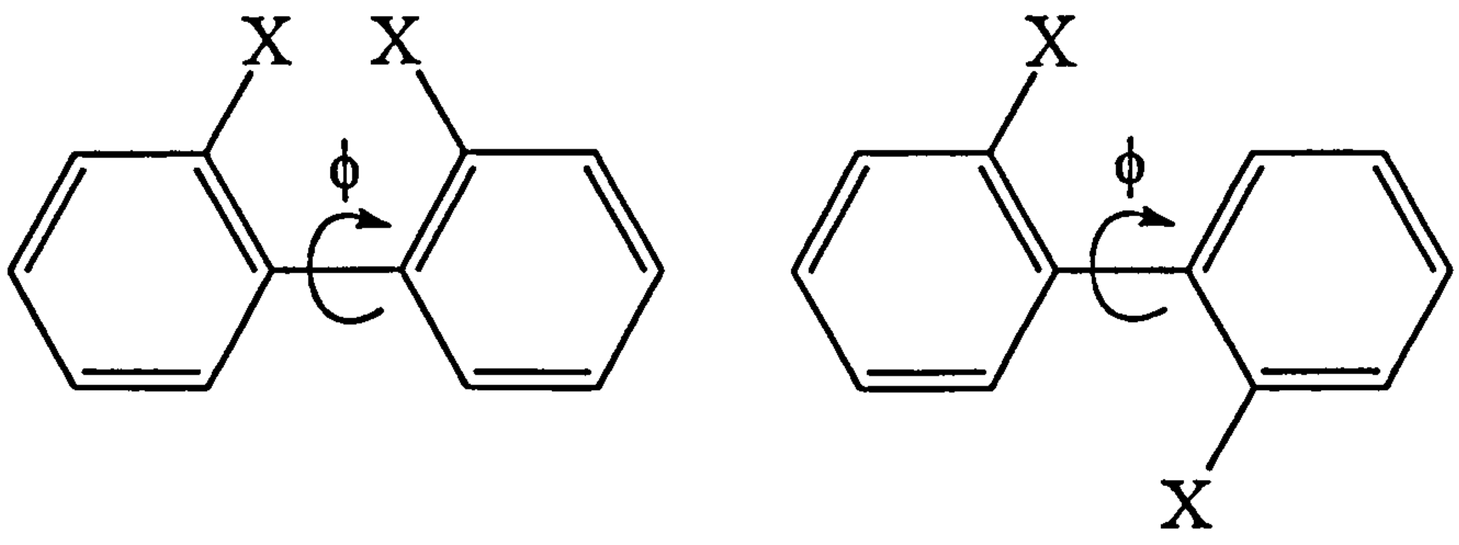

-syn *-anti*

Figure 1 *-syn* and *-anti* structures of 2,2'-dihalobiphenyls

A brief discussion of some of the studies of the structure of biphenyl and halobiphenyls in various states of matter along with their conclusions is given. The determination of the conformational distribution of 2,2'-difluorobiphenyl in the liquid crystal phase will be discussed in full in the following sections.

The structure of biphenyl has been the subject of a number of studies in various states of matter. In 1961, Trotter [1] showed through X-ray diffraction that the crystal structure of biphenyl is such that the two rings are colinear and the molecule is completely planar. This result greatly contrasts with the structure determined in the vapour phase by Bastiansen [2],

in 1949, who found that the two rings are also colinear but that the molecule is not planar, with a dihedral angle between the planes of the two rings of 45±10°. The structure of biphenyl has also been determined in the liquid crystal phase [3], through NMR spectroscopy, in which the dihedral angle between the two rings, using the additive potential method [4], was found to be 37.2±0.1°. The change in structure of biphenyl depending on the state of matter is one of the motivations for the study of similar molecules, and to determine whether this behaviour is repeated in the halo substituted biphenyls.

Bastiansen *et al.* [5] in 1950 carried out electron diffraction studies on halo substituted biphenyls in the gas phase and interpreted their results as follows. The dihedral angles between the planes of the two rings are 60°±5° for 2,2'-difluorobiphenyl, 74° for 2,2'-dichlorobiphenyl, 75° for 2,2'-dibromobiphenyl and 79° for 2,2'-diiodobiphenyl. Bastiansen and Smedvik, in 1954, [6] also determined dihedral angles of 49°±5° for 2-fluorobiphenyl and 44°±5°for 4,4'-difluorobiphenyl. The interesting point in Bastiansen's work is that he concludes that in the gas phase, the molecules investigated have only one favourable conformation, forming -*syn* only structures. In particular with the analysis of 2,2'-difluorobiphenyl Bastiansen considers a number of structures and calculates theoretical radial distribution curves with dihedral angles of 60°,65° and 120°between the planes of the two rings, where only the single best fitting theoretical curve to the experimental curve was considered. While this may seem sensible, it is apparent that the agreement between the experimental curve and individual calculated curves are not good. Bastiansen goes on to say that the discrepancies can be explained through normalisation uncertainties, and oscillations in the molecule from the equilibrium position will influence the curves. Perhaps the discrepancies between the calculated and experimental results can be additionally explained, in that the experimental curve is in fact a superposition of a number of curves, where the influence of each curve depends on the probability of each conformation. However, there is some supporting evidence for Bastiansen's conclusion. In 1975 Romming *et al.* [7] determined the structure of 2,2'-dichlorobiphenyl in the gas phase by electron diffraction and in the crystalline state by X-ray diffraction. They determined the dihedral angle to be approximately 70° and only slightly larger in the gas phase. They further conclude that only one stable conformer was detected in the gas phase at 300 °C which was contrary to a number of theoretical calculations at that time, predicting stable conformers at 42° and 143° [8].

Other X-ray crystal structure surveys of fluoro substituted biphenyl also have been carried out as follows. In 1995, Rajnikant and Watkin [9] determined the dihedral angle between the two rings to be 54±3° for 2-fluorobiphenyl. Hamor and Hamor [10], in 1978, determined the dihedral angle in 2H-nonafluorobiphenyl to be 59.5°, while Bowen-Jones and Brown in 1982 [11] determined an angle of 54.7° in 2H,2'H-octafluorobiphenyl. M.H.Lemee *et al.* [12], in 1987, determined that the two rings are coplanar in 4,4'-difluorobiphenyl. This is a similar case to biphenyl where the structure in the crystal phase in much different to that in the gas phase, determined by Bastiansen [6] with a dihedral angle between the rings of 44±5°.

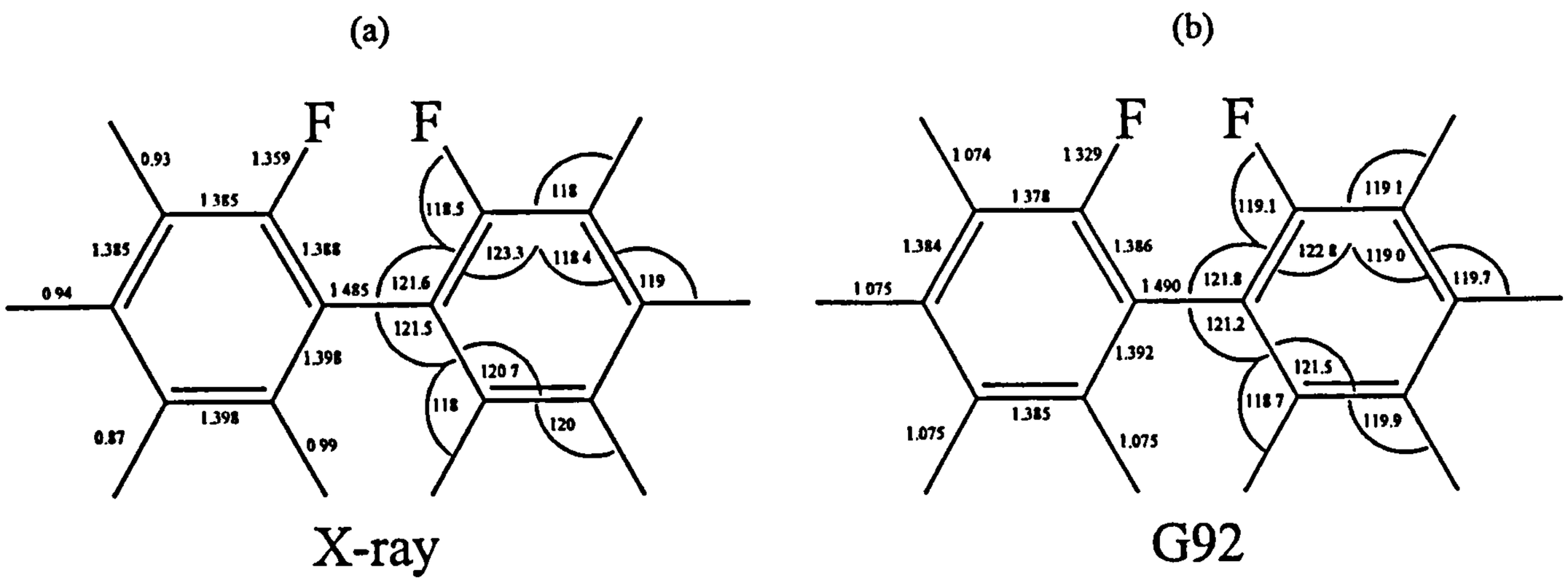

Figure 2 The a) X-ray and b) Gaussian 92 structures of 2,2'-difluorobiphenyl. Bond lengths / Å, bond angles / °.

Recently a concerted effort has been made in Southampton towards the analysis of 2,2'-difluorobiphenyl in various states of matter. An X-ray crystal structure study was performed by Webster [13] from which the molecular structure was determined, shown in figure 2a, in which the two rings have a dihedral angle of 58.42°. Egdar [14] performed a number of Molecular Orbital (MO) calculations on a single isolated molecule introducing geometry relaxation. The potential calculated for bond rotation has minima, corresponding to dihedral angles of 60°, the global minimum, and 120°, a less probable local minimum. This agrees well with earlier electronic structure calculations by Cioslowski and Mixon [15] who determined the global minimum at 54.7° and a local minimum at 128.7° through measurement of the steric hinderance of the molecule and the effect on the barriers to rotation. Crain and Adam [16] used a density functional method to calculate the minimum in the rotational potential, and their result is in agreement with that of Edgar. The structure determined by the MO method [14] is shown in figure 2b.

In this chapter we concentrate on the determination of the structure of 2,2'-difluorobiphenyl in the liquid crystal phase. 2,2'-difluorobiphenyl, shown in figure 3, is an example of a liquid crystal fragment, and it is the occurrence of this fragment recently in liquid crystals

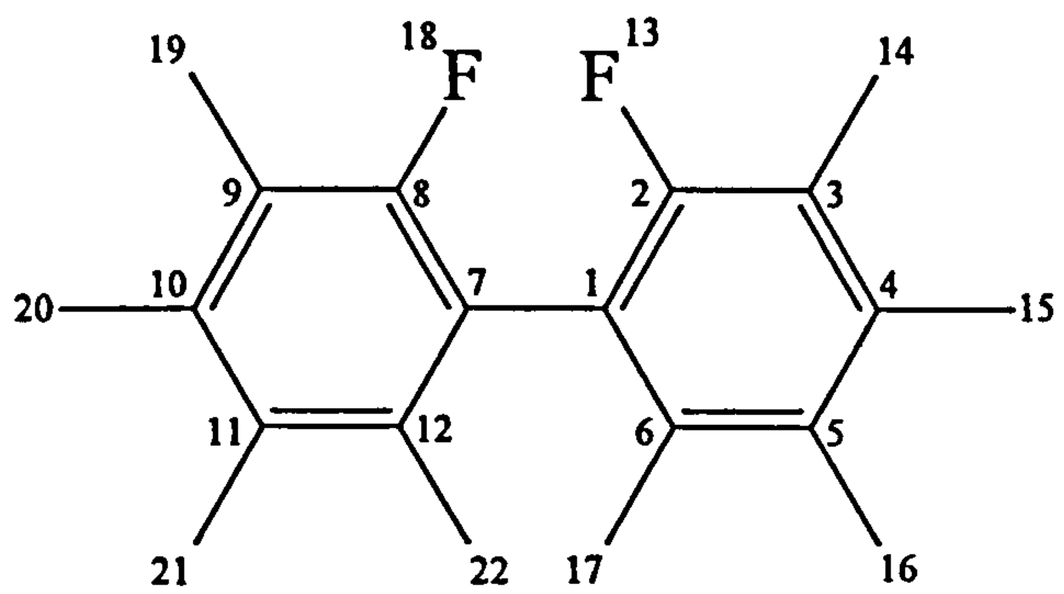

Figure 3 The structure of 2,2'-difluorobiphenyl

synthesised by Vauchier *et al.* [17] and Hird *et al.* [18], that has partly inspired this work to determine the conformational distribution of 2,2'-difluorobiphenyl in the liquid crystal phase. There is, however, further inspiration for this work. 2,2'-difluorobiphenyl is more complicated than other molecules that have been studied previously using the Additive Potential Method. The benzene rings unlike those in biphenyl [3], phenyl acetate [19] and phenyl benzoate [20][chapter2], for which their conformational distributions in the liquid crystal phase have already been determined, have lower symmetry due to the presence of the fluorine atom in the 2 position of the ring. This increases the complexity of the NMR spectra and the analysis becomes much more difficult. The ^{1}H NMR liquid crystal spectrum of 2,2'-difluorobiphenyl-d_0 depends on thirty one dipolar couplings compared to fifteen for biphenyl and twenty one for phenyl benzoate.

Probably the most important question that needs answering is whether 2,2'-difluorobiphenyl resides in one or two stable conformers. As has already been pointed out, X-ray studies suggest only single structure in the -*syn* conformation, which is expected to be the minimum energy structure to which the early electron diffraction work in the gas phase agreed. However, MO studies suggest that in an isolated molecule there are two stable conformers. It will be shown here that the conclusions reached by MO calculations give the true reflection of the structure of 2,2'-difluorobiphenyl in the liquid crystal phase.

5.2 Experimental

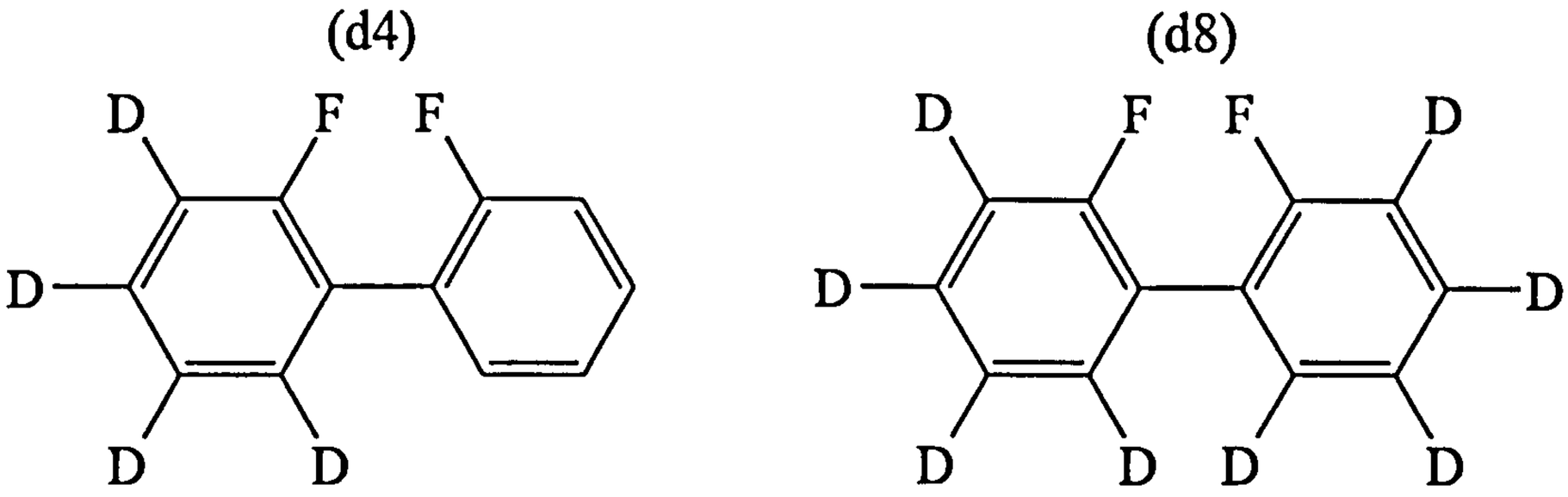

Figure 4 Deuterated isotopomers of 2,2'-difluorobiphenyl

Partially and fully deuterated 2,2'-difluorobiphenyls were synthesised by De Luca [13], to produce the isotopomers shown in figure 4. Samples of 2,2'-difluorobiphenyl-d_4 dissolved in the liquid crystal solvents ZLI 1132 and ZLI 1167 (Merck) were prepared at approximately 5% w/w and held in 5mm diameter short NMR tubes. ^2H and ^1H-$\{^2H\}$ NMR spectra were recorded on a Bruker MSL 200 NMR spectrometer at 300K for both samples.

The liquid crystal solvents used, both being mixtures, display a nematic phase at room temperature. ZLI 1132 has anisotropy in the magnetic susceptibility, $\Delta\chi$, positive so that the directors align parallel to the magnetic field direction, B_0. ZLI 1167 has $\Delta\chi$ negative and the directors align perpendicular to B_0. ZLI 1167 contains no aromatic groups which enabled the ^{13}C spectrum to be obtained, while ZLI 1132 was chosen as it gives good ^1H spectra.

A sample of 2,2'-difluorobiphenyl-d_8 dissolved in the liquid crystal solvent ZLI 1132 was prepared in the same way as the d_4 samples and ^2H and ^1H-$\{^2H\}$ NMR spectra were recorded.

2,2'-difluorobiphenyl (Fluorochem) dissolved in the liquid crystal solvent ZLI 1132 was prepared in the same way as the d_4 and d_8 samples and the ^1H and ^{19}F NMR spectra recorded.

The samples for the ^{13}C-$\{^1H\}$ NMR experiments of 2,2'-difluorobiphenyl dissolved in ZLI 1167, for both Variable Angle Sample Spinning and the static experiments, are described in Chapter 4.

5.3 Results and Discussion

The analysis of the ^{13}C-{^{1}H} NMR spectrum is reported in chapter 4 along with the parameters determined. The analysis of the ^{1}H and ^{19}F NMR spectra of 2,2'-difluorobiphenyl-d_0 have so far defied analysis and will no longer be referred to here. However, the spectra of the partially deuterated samples are much simpler and contain much of the information required.

5.3.1 Analysis of the -d_8 NMR spectra

The ^{1}H-{^{2}H} NMR spectrum and the ^{2}H NMR spectrum of 2,2'-difluorobiphenyl-d_8 are shown in figures 5 and 6 respectively.

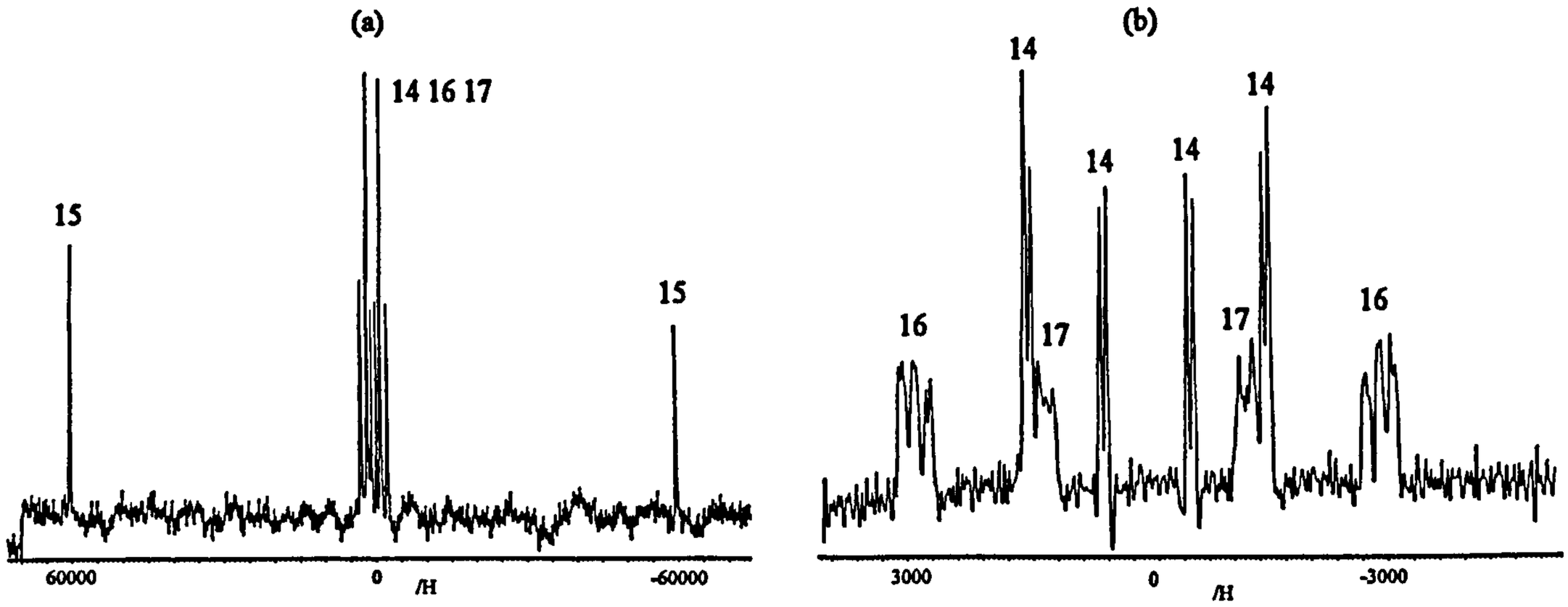

Figure 5 a) 30.7 MHz ^{2}H NMR spectrum of 2,2'-difluorobiphenyl-d_8 dissolved in ZLI 1132 at 300K. b) Horizontal expansion of the centre of the spectrum in a).

Analysis of the ^{2}H NMR spectrum, yields the deuterium quadrupole interactions, q_{CD} which are related to the corresponding doublet splittings, $\Delta\nu_i$, by equation 1.

$$\Delta\nu_i = \frac{3}{2} q_{CDi} S_{CDi} \qquad (1)$$

$\Delta\nu_i$ are related to the local order parameters, $S_{\alpha\beta}{}^{R}$ (see chapter1). In this case the geometry can be considered to be that of a regular hexagon, q_{CDi} can be set equal to 182 kHz and the asymmetry parameter, η_i, to zero. The relationship can be simplified thus

$$\Delta\nu_{14} = \Delta\nu_{17} = -34.125\, S_{ZZ}^{R} + 34.125\left(S_{XX}^{R} - S_{YY}^{R}\right) + 177.314\, S_{XZ}^{R}$$

$$\Delta\nu_{16} = -34.125\, S_{ZZ}^{R} + 34.125\left(S_{XX}^{R} - S_{YY}^{R}\right) - 177.314\, S_{XZ}^{R} \qquad (2)$$

$$\Delta\nu_{15} = 273.00\, S_{ZZ}^{R}$$

where $\Delta\nu_i$ is measured in kHz.

The ^{2}H NMR spectrum is assigned as follows. $\Delta\nu_{15}$ corresponds to the largest splitting since it can be confidently predicted that the molecule will align in the liquid crystal solvent as to give S_{ZZ}^{R} large and positive. The value of S_{ZZ}^{R} can be predicted and used throughout equation 2. The pairs of lines arising from position 14 will have a large dipolar coupling to the adjacent fluorine atom, F13, and a smaller splitting from the fluorine at position 18. This can be seen in the ^{2}H spectrum from the separations between the lines labelled 14 in figure 5, enabling the assignment of $\Delta\nu_{14}$. From equation 2, $\Delta\nu_{17} = \Delta\nu_{14}$, therefore we assign the quadrupole splitting closest in magnitude to that of $\Delta\nu_{14}$ to $\Delta\nu_{17}$. The remaining lines are assigned as $\Delta\nu_{16}$. The quadrupole splittings and the T_{ij}, the sum of the D_{ij} and J_{ij}^{aniso}, arising from D14 are reported in table 1.

Table 1. The magnitude of the quadrupolar splittings, $|\Delta\nu_i|$, and the total spin-spin coupling constants $|T_{ij}|$ for the deuterons in 2,2,'-difluorobiphenyl-d_8 dissolved in ZLI 1132.

i	$\lvert\Delta\nu_i\rvert$ / Hz
14	1925 ± 20
15	120055 ± 20
16	5478 ± 20
17	2547 ± 20

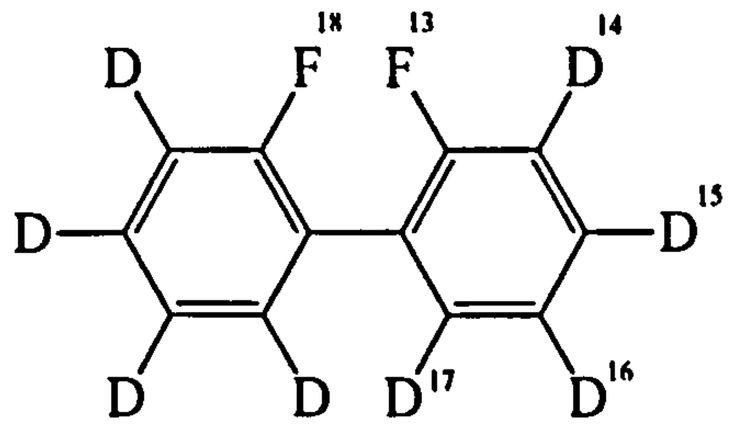

i,j	$\lvert T_{ij}\rvert$ (HF) / Hz	J_{ij} / Hz *
13,14	896.5 ± 0.5	1.5
14,18	76.0 ± 0.5	0.0

*scaled by 0.1535 ($=\gamma_D/\gamma_H$) from the values of J_{HF}.

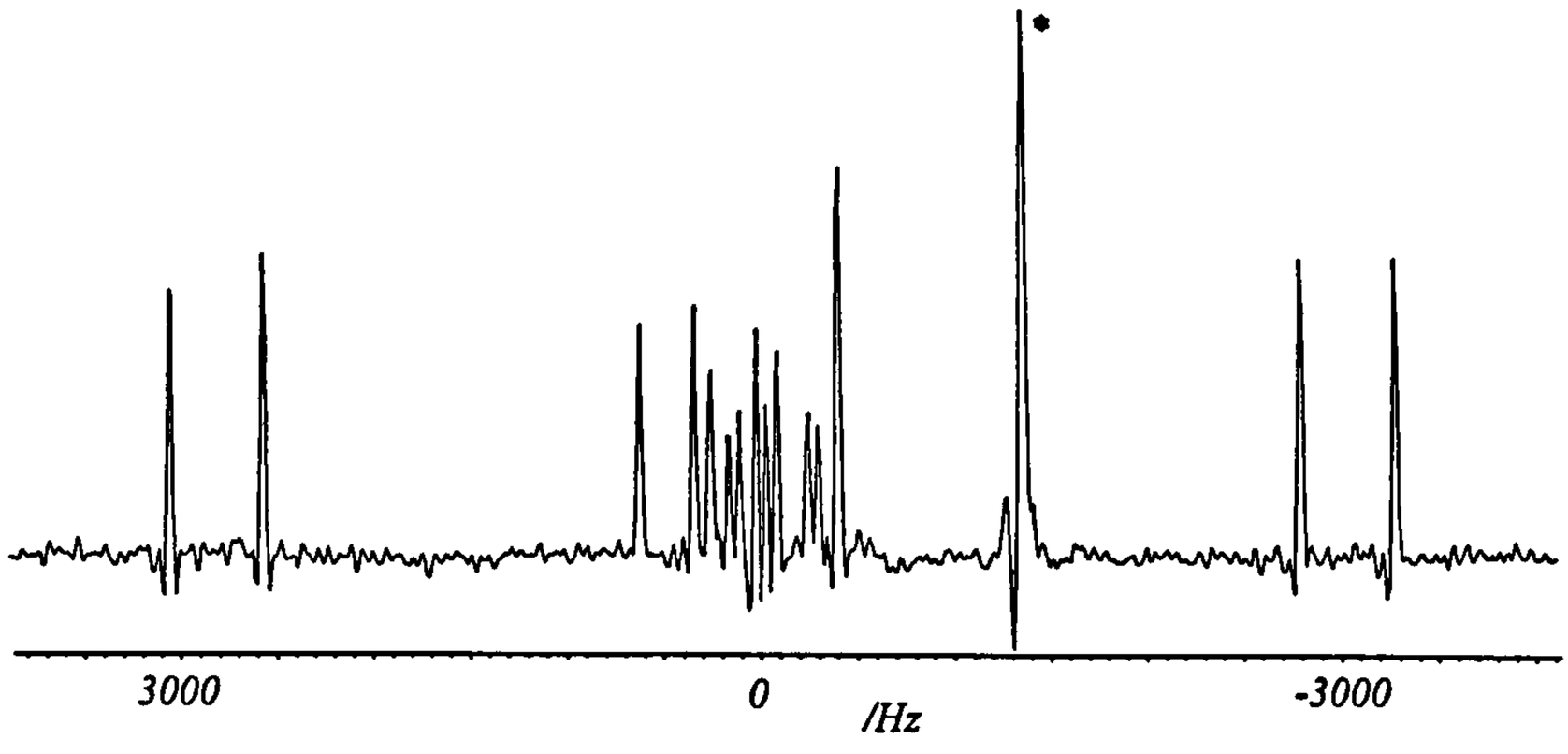

Figure 6 200 MHz ^{1}H-{^{2}H} NMR spectrum of 2,2'-difluorobiphenyl-d_8 dissolved in ZLI 1132 at 300K. The peak * is from an impurity.

The order parameters obtained are then used to determine a set of intra-ring dipolar couplings, D_{ij} (see chapter 1), to be used as starting parameters in the analysis of the ^{1}H-{^{2}H} NMR spectrum. The transitions observed in the ^{1}H-{^{2}H} NMR spectrum are associated with the residual protons in the (-d_8) isotopomer. In this case the spectrum is that of an ABX spin system, similar to that of the ^{13}C-{^{1}H} NMR spectrum in chapter 4, where the X part is the residual proton and AB are the fluorine atoms. Each ABX gives rise to four lines of measurable intensity, whose separations depend on $|(J_{AX} + 2D_{AX})|$ and $|(J_{BX} + 2D_{BX})|$. The values of J_{AX} and J_{BX} were those measured for 2,2'-difluorobiphenyl in $CDCl_3$ and were used to determine the dipolar couplings. The results are given in table 2.

Table 2. Magnitude, $|T_{ij}|$, of the total spin-spin coupling constants obtained from the ^{1}H-{^{2}H} NMR spectrum of the sample of 2,2'-difluorobiphenyl-d_8 dissolved in ZLI 1132.

i,j	$\|T_{ij}\|$ / Hz	J_{ij} / Hz
13,14	5847 ± 5	10.0
14,18	488 ± 5	0.0
13,15	654 ± 3	4.96
15,18	367 ± 3	0.0
13,16	54 ± 1	-0.16
16,18	405 ± 1	0.0
13,17	423 ± 2	8.34
17,18	318 ± 2	0.0

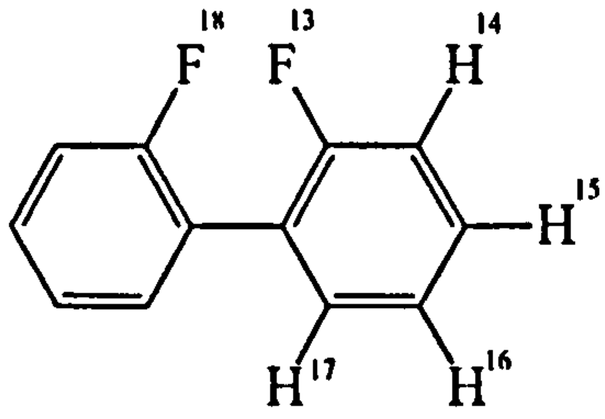

5.3.2 Analysis of (-d_4) Spectra

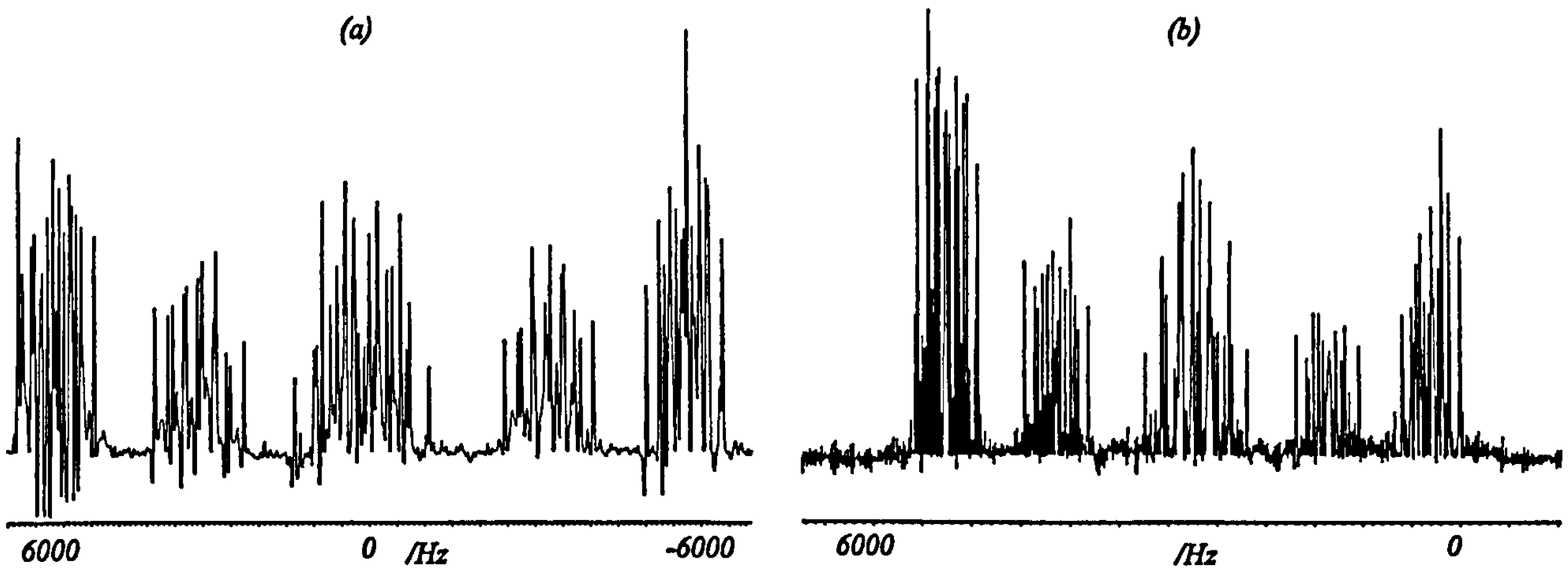

Figure 7 200 MHz ^{1}H-{^{2}H} NMR spectra of 2,2'-difluorobiphenyl-d_4 a) in ZLI 1132 and b) in ZLI 1167, at 300K.

The ^{1}H-{^{2}H} NMR spectra of 2,2'-difluorobiphenyl-d_4 dissolved in ZLI 1132 and ZLI 1167 are shown in figure 7. The scaled D_{ij} for the rigid fragment obtained from the analysis of the (-d_8) spectrum were used as starting parameters in the analysis of the (-d_4) spectra which proceeded as follows. The J_{ij}, from analysis in $CDCl_3$ (chapter 4), and D_{ij} were used to calculate a spectrum. The spectrum also depends on $D_{13,18}$ (D_{FF}) which cannot be predicted from the order parameters in the rigid fragment. However, a value for D_{FF} in ZLI 1167 was determined from the analysis of the ^{13}C-{^{1}H} spectra of 27.5Hz. This value was subsequently used in the analysis of the (-d_4) spectrum in ZLI 1167, and scaled by a ratio of the order parameters, approximately -2, for the analysis of the (-d_4) spectrum in ZLI 1132. This is a good approximation, but not exact. The calculated spectrum was assigned to the experimental spectrum and the parameters varied, using an iterative fitting program, ARCANA [21], based on LAOCOON [22] until a good agreement between the experimental and calculated spectra was obtained. Some pairs of D_{ij}, were found to be highly correlated and it was not possible to vary these individually, the consequences of which become apparent during the later structural calculations. Iterative analyses of both the ^{1}H-{^{2}H} spectra gave values for the intra-ring couplings which could then be compared, and a better ratio found to multiply the value of D_{FF} by. The ratio was found to be -2.3, giving a value of D_{FF} = -63.25Hz in ZLI 1132. The iterative fitting procedure was repeated for ZLI 1132 using this refined value of D_{FF} as input to obtain a new set of intra-ring couplings. The changes in the values of the intra-ring couplings are insensitive to small changes in the value of D_{FF}, which ensures that the data in table 3 is reliable.

Table 3. Chemical shifts, δ_i, dipolar couplings, D_{ij}^{HH}, D_{ij}^{HF} and D_{FF}, obtained from the analysis of the ^1H-{^2H} spectrum of samples of 2,2'-difluorobiphenyl-d_4 dissolved in the nematic solvents ZLI 1167 and ZLI 1132.

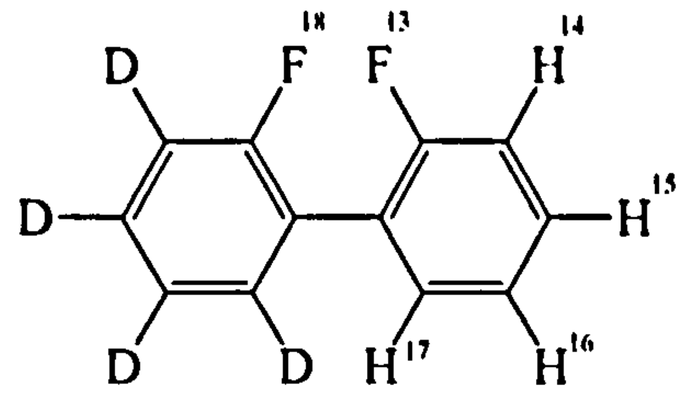

i		ZLI 1132 δ_i / Hz	ZLI 1167 δ_i / Hz
17		69.5 ± 3.5	38.2 ± 2.6
16		19.1 ± 4.0	-12.1 ± 2.6
15		215.9 ± 0.8	-42.5 ± 0.8
14		0.0 ± 0.7	0.0 ± 0.6
i j	**J_{ij} / Hz***	**D_{ij} / Hz**	**D_{ij} / Hz**
16,17	8.0	-3758.0 ± 0.8	1636.9 ± 0.5
15,17	2.0	-485.9 ± 0.4	212.3 ± 0.5
15,16	8.0	24.6 ± 0.4	-12.7 ± 0.5
14,17	0.0	5.8 ± 0.4	-2.9 ± 0.3
14,16	2.0	279.3 ± 0.4	-114.9 ± 0.3
13,17	8.34	222.3 ± 0.7	-97.6 ± 0.7
13,16	-0.16	38.8 ± 0.7	-12.6 ± 0.7
17,18	0.0	-180.1 ± 0.6	80.9 ± 2.5
16,18	0.0	-212.1 ± 0.6	96.5 ± 2.5
14,15	8.0	252.5 ± 0.4	-95.9 ± 0.4
13,15	4.96	-342.8 ± 0.6	153.3 ± 0.8
15,18	0.0	-201.7 ± 0.6	89.0 ± 0.8
13,14	10.0	-3155.2 ± 0.7	1377.9 ± 0.7
14,18	0.0	-269.6 ± 0.6	117.2 ± 0.6
13,18	16.6 [chap. 4]	-63.3 ± 1.2	27.5 ± 0.5 [chap. 4]

*from reference [23] and kept fixed in the analysis

5.3.3 Structure of the Rigid Fragment

The D_{ij}^{CF} data from the analysis of the ^{13}C-{^{1}H} NMR spectra (chapter 4) were used to optimise the structure of the rigid fragment given in figure 8. The data consists of seven D_{ij}^{CF}, which depend on sixteen coordinates and three order parameters, S_{ZZ}, S_{XX}-S_{YY} and S_{XZ}. We therefore have more variables than data and cannot vary the whole geometry. The geometry is assumed to be that from other evidence, in particular, the X-ray and MO

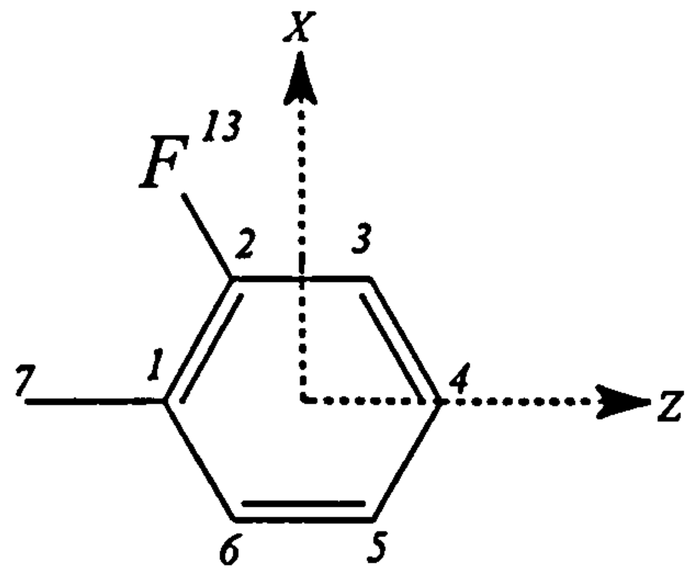

Figure 8 Rigid Fragment

geometries in figure 2. Calculations were done with all carbon positions kept fixed at either the X-ray or MO positions and the order parameters allowed to vary until the best agreement was found between the calculated and the experimental D_{ij}^{CF}. In both cases, the difference between the calculated and experimental D_{ij}^{CF} was found to be significant but small. The error in the fit could be further minimised by changing the position of the fluorine atom with respect to the carbon skeleton. This was done by fixing $r_{2,13}$ at 1.35Å and rotating the F atom about C2 in the XZ plane. The optimised geometries and the errors in the fit are reported in Table 4 with increased r_{CF} = 1.35Å and ∢ 1-2-13 = 119.6°.

Optimisation of the structure using the D_{ij} from the (-d_4) ^{1}H-{^{2}H} spectra was attempted for the corresponding rigid fragment. However, due to the high degree of correlation, we only have four well determined intra-ring D_{ij} with which to optimise the ^{1}H geometry. This means that there is insufficient data to determine the relative positions of the protons and fluorine in the ring. The carbon-proton bond lengths from the X-ray and MO geometries are very different (see figure 2). It has been pointed out that the positions of hydrogen atoms show a systematic difference when determined by X-ray rather than neutron diffraction, the X-ray scattering experiments yielding C-H bond lengths which are on average 0.096Å shorter [24]. This is because the scattering centre for X-rays is displaced from the

Table 4. The deviations $\Delta_{ij} = D_{ij}$(observed) -D_{ij}(calculated), the order parameters and the coordinates of the carbons and fluorine in the rigid fragment of 2,2'-difluorobiphenyl determined by bringing observed and calculated D_{ij}^{CF} and D_{FF} for the solution in ZLI 1167 into best agreement. The positions of the carbons were fixed at either those determined by X-ray, or MO calculation.

Geometry	X-ray		MO	
S_{XX}	0.088 ± 0.001		0.088 ± 0.001	
S_{XZ}	0.011 ± 0.001		0.009 ± 0.001	
S_{YY}	0.135 ± 0.001		0.134 ± 0.001	
S_{ZZ}	-0.223 ± 0.001		-0.221 ± 0.001	
i	X	Z	X	Z
1	0.0	0.7425	0.0	0.7448
2	-1.1822	1.4698	-1.1777	1.4748
3	-1.2233	2.8542	-1.2014	2.8522
4	-0.0251	3.5488	-0.0020	3.5446
5	1.1733	2.8713	1.1971	2.8504
6	1.1928	1.4735	1.1903	1.4657
7	0.0	-0.7425	0.0	-0.7448
13	-2.3711	-0.8114	-2.3627	0.8281
ij	Residual / Hz	D_{ij} / Hz	Residual / Hz	D_{ij} / Hz
1 13	0.1	-186.1	0.1	-186.1
2 13	-0.1	-275.7	-0.1	-275.7
3 13	-0.2	306.7	-0.2	306.7
4 13	1.2	48.7	1.1	48.6
5 13	-0.6	-8.1	-0.6	-8.1
6 13	-0.2	-48.8	-0.3	-48.9
7 13	0.1	18.8	0.1	18.8

Table 5. Results of bringing calculated D_{ij}^{HH} and D_{FF} into agreement with the experimental D_{ij} for 2,2'-difluorobiphenyl-d_4 in ZLI 1132 and ZLI 1167 using MO geometry.

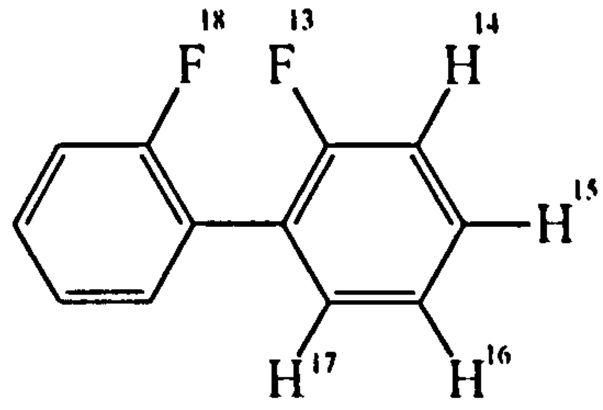

	ZLI 1132	ZLI 1167
S_{XX}	-0.182 ± 0.001	0.081 ± 0.001
S_{XZ}	-0.018 ± 0.001	0.004 ± 0.001
S_{YY}	-0.284 ± 0.001	0.122 ± 0.001
S_{ZZ}	0.466 ± 0.001	-0.203 ± 0.001

	X	Z	X	Z
17	2.1174	0.9224	2.1174	0.9224
16	2.1311	3.3819	2.1311	3.3819
15	-0.0076	4.6185	-0.0076	4.6185
14	-2.1535	3.3642	-2.1535	3.3642
13	-2.3627	0.8281	-2.3627	0.8281

i j	Weight	Residual	D_{ij}(calc)	Residual	D_{ij}(calc)
16 17	1	0.1	-3757.9	-0.2	1636.7
15 17	0	-10.5	-496.4	2.1	210.2
14 17	0	-1.0	6.8	5.0	-7.9
13 17	0	6.28	228.5	4.3	-101.9
15 16	0	7.2	31.8	40.4	-53.1
14 16	0	1.8	277.5	9.1	-124.0
13 16	0	6.6	32.2	0.0	-12.6
14 15	1	-0.1	252.5	0.1	-95.9
13 15	1	0.2	-342.6	-0.5	152.9
13 14	1	-0.1	-3155.3	0.3	1378.2

position of the the hydrogen nucleus, which is not the case, to such a great extent, with other atoms. Fixing the proton positions as in the X-ray structure and the fluorine position from the optimisation using D_{ij}^{CF} and varying the three order parameters to fit the four D_{ij}^{HF} gave large errors, Δ_{ij}^{HF}, between the calculated and experimental couplings. The same calculation using the proton position from MO calculation [14] gave much smaller errors in the fit, shown in table 5. No further optimisation of the proton positions was required, and so the structure used for all further calculations using D_{ij}^{HH} and D_{ij}^{HF} was that of the MO geometry with optimised fluorine position determined from the D_{ij}^{CF}.

5.3.4 Conformational Analysis

The three sets of dipolar couplings, the single set obtained from the analysis of the ^{13}C-{^{1}H} spectrum in ZLI 1167, and those obtained from the analysis of the ^{1}H-{^{2}H} spectra of the (-d_4) isotopomer in both ZLI 1167 and ZLI 1132, are used separately to determine the conformational distribution of 2,2'-difluorobiphenyl and its bond rotation potential in the

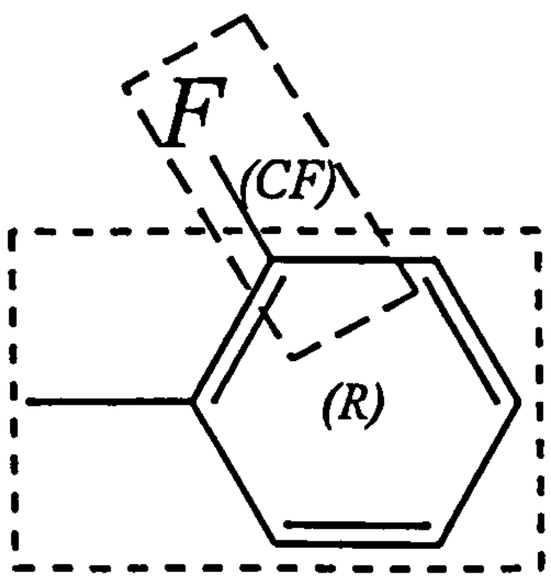

Figure 9 Fragment definition

liquid crystal phase. The procedure used, however, is identical in each case, using the optimised molecular structure and the full set of couplings. To do this we need to consider how the D_{ij} are averaged over the whole motion of the molecule relative to the liquid crystal director, and the internal motion about the bond between the two rings. The relationship is the following

$$D_{ij} = \int D_{ij}(\beta,\gamma,\phi)\, P_{LC}(\beta,\gamma,\phi) \sin\beta \; d\beta d\gamma d\phi \qquad (3)$$

where $D_{ij}(\beta,\gamma,\phi)$ is the value of the dipolar coupling in a fixed conformation, ϕ, and orientation, specified by polar angles β and γ, of the liquid crystal director with respect to axes fixed in the molecule. $P_{LC}(\beta,\gamma,\phi)$ is the probability density for this particular conformation and orientation. The model adopted for $P_{LC}(\beta,\gamma,\phi)$ is the additive potential method [4] to calculate the averaged couplings with equation 3. The additive potential method considers the total energy, U_{LC}, of the molecule in two parts, the external energy, $U_{ext}(\beta,\gamma,\phi)$, which depends on the orientation of the molecule and therefore disappears in the isotropic phase, and the internal energy, $U_{int}(\phi)$, which does not. For 2,2'-difluorobiphenyl, we may consider the molecule to be constructed from two identical sub-units, shown in figure 9, which must be considered when constructing U_{ext} from equations

$$U_{LC} = U_{ext}(\beta,\gamma,\phi) + U_{int}(\phi) \qquad (4)$$

38 and 39 in chapter 1. It is convenient to split the rigid fragment into two parts, where the biaxial benzene ring is described by $\epsilon^{R}_{2,0}$ and $\epsilon^{R}_{2,2}$, and the uniaxial C-F bond by $\epsilon^{CF}_{2,0}$. These are translated into Cartesian tensors for the purposes of the calculations, thus

$$\epsilon^{R}_{2,0} = \sqrt{(3/2)}\,\epsilon^{R}_{ZZ}$$

$$\epsilon^{R}_{2,2} = \frac{1}{2}\left(\epsilon^{R}_{XX} - \epsilon^{R}_{YY}\right) \qquad (5)$$

$$\epsilon^{CF}_{2,0} = \sqrt{(3/2)}\,\epsilon^{CF}_{aa}$$

where *a* is directed along the C-F bond. The internal potential, $U_{int}(\phi)$, is expressed as :

$$U_{int}(\phi) = V_1\cos\phi + V_2\cos 2\phi + V_4\cos 4\phi + U_{steric} \qquad (6)$$

with

$$U_{steric} = \sum_{ij} E_{ij}\left[\left(\frac{A_{ij}}{r_{ij}}\right)^{12} - \left(\frac{A_{ij}}{r_{ij}}\right)^{6}\right] \qquad (7)$$

which allows for short range repulsive and attractive forces. where A_{ij} and E_{ij} are constructed from values of A_i and E_i [26, 27].

$$A_{ij} = A_i + A_j$$
$$E_{ij} = \left(E_i E_j\right)^{1/2} \quad (8)$$

The general procedure is to vary ϵ^R_{ZZ}, $(\epsilon^R_{XX} - \epsilon^R_{YY})$, ϵ^{CF}_{aa}, V_1, V_2 and V_4 in order to bring the calculated D_{ij} into agreement with the experimental D_{ij}. The value of D_{FF} is not directly yielded from the analysis of the ^1H-$\{^2H\}$ spectra and so the conformational analysis was carried out with and without the inclusion of this coupling in the data set. Up to four models were therefore proposed for each data set which accounted for all the combinations including or not including U_{steric} and/or D_{FF} depending on the data set used.

5.3.5 Investigation of the Conformational distribution using D_{ij}^{CF} and D^{FF}.

The calculations from D_{ij}^{CF} and D_{FF} data in ZLI 1167 were performed using both the optimised X-ray and MO geometries, as these were found to both be reasonable with regards to the structure of the rigid fragments. A comparison can be made to determine the effect of differences in the structure to the final result. Models were considered with and without the steric term included into the rotational potential. Given that we expect steric hinderance to occur throughout full rotation about ϕ, an attempt was made to determine the effect on $P_{LC}(\phi)$ by also allowing some bond relaxation as ϕ changes. To do this θ_F, which equals ∢1-2-13 or θ_H, which equals ∢1-6-17, was made to depend on ϕ, figure 10, by

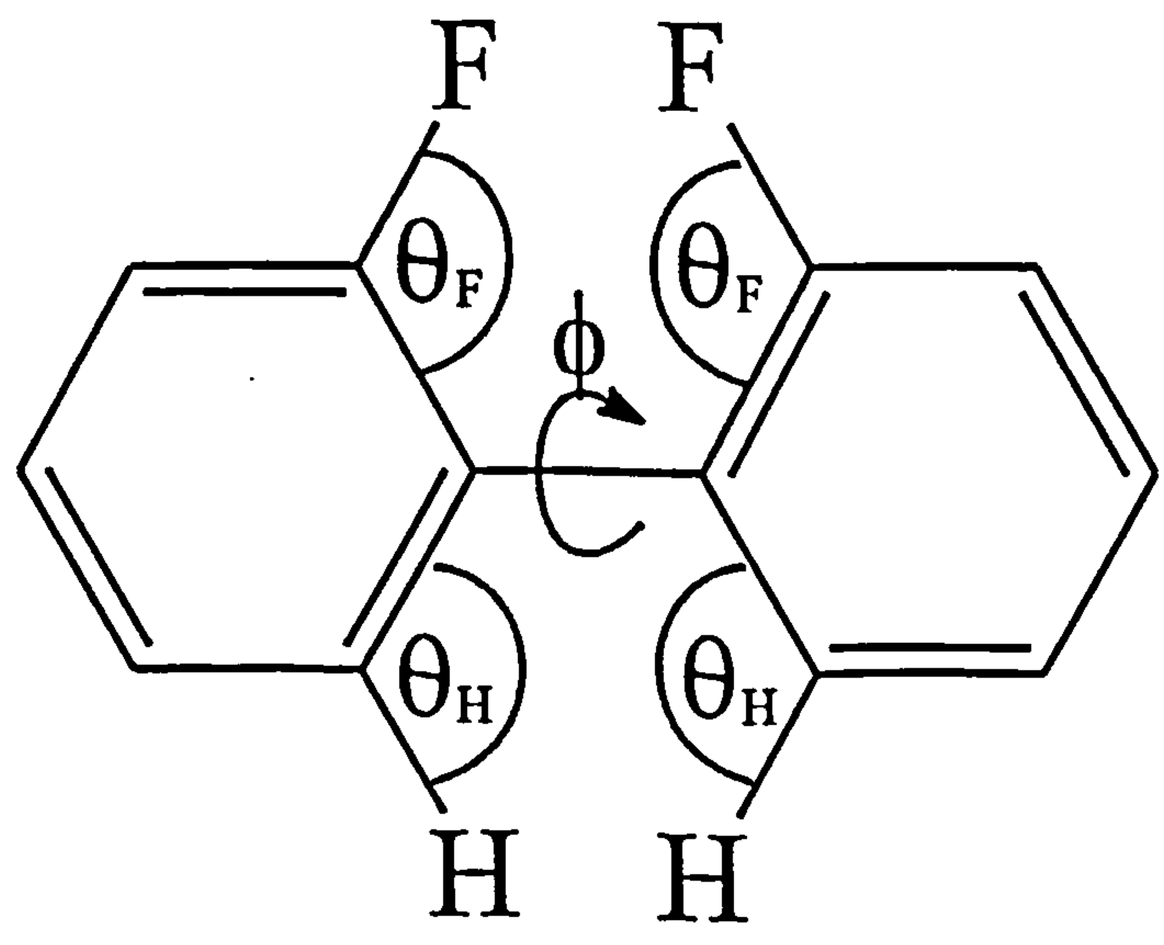

Figure 10 Bond Angles to be varied during geometry relaxation

expressing as a Fourier series, thus

$$\theta_a = \theta_a^0 + 0.5 + 0.45\cos\phi + 1.6\cos2\phi + 0.3\cos3\phi + 0.35\cos4\phi \qquad (9)$$

Where a = H or F and θ_a^0 is the original bond angle. Equation 9 is the best model of the variation of θ with ϕ, shown in figure 11, determined through the MO calculations by Edgar [14]. The true shape of the curve could not be exactly simulated with only 4 terms, so this is an approximation. The final results of the conformational analyses are reported in table 6 and given in figures 12 and 13, which show the P_{LC} obtained from the X-ray and MO structures respectively.

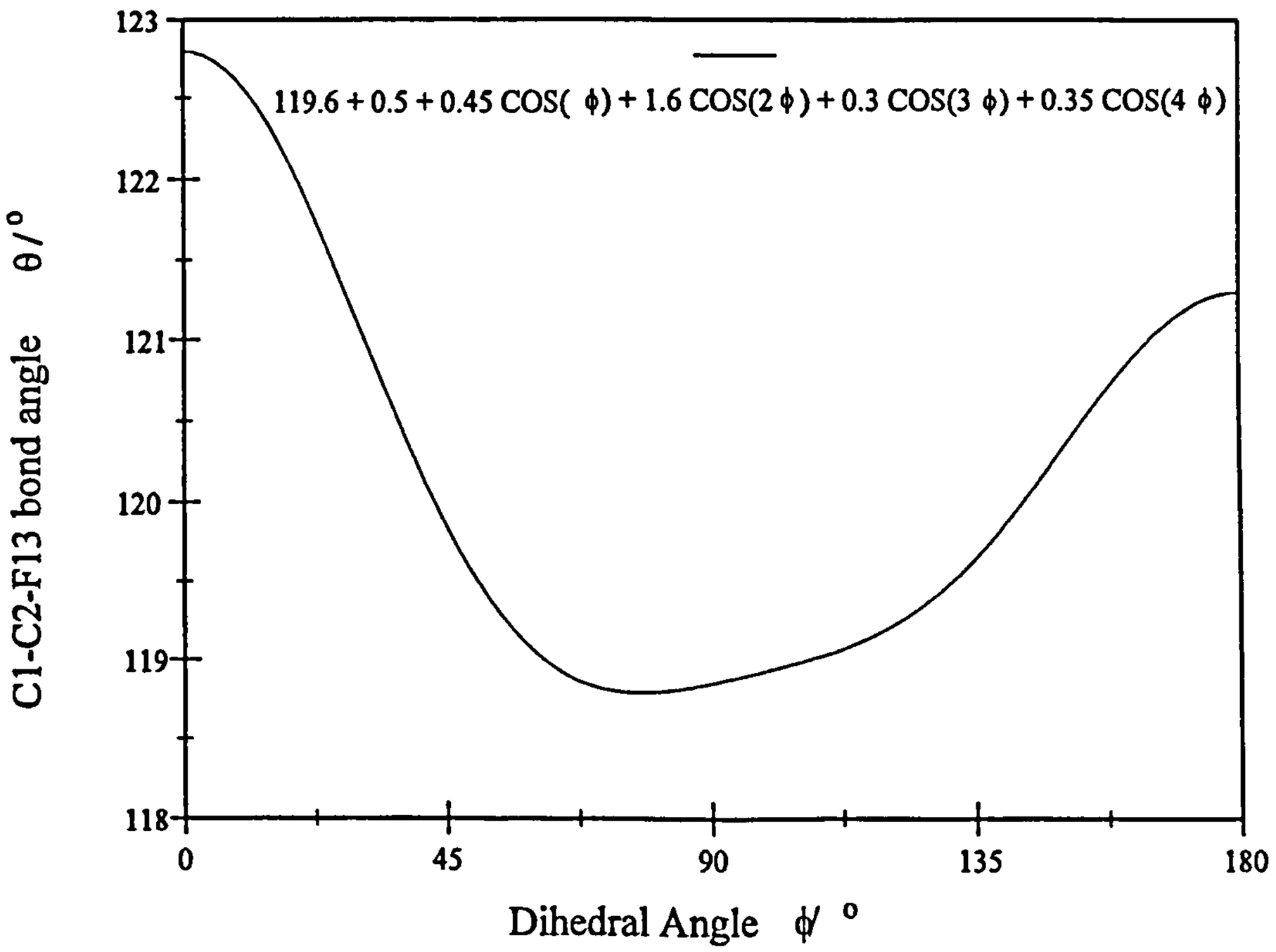

Figure 11 Fourier series in equation 9 representing geometry relaxation for ∢1-2-13

From the shapes of the potential curves in figure 12, for the X-ray structure, it can be seen that the effect of the steric term is to sharpen the probability distribution curve. However, both models, with (-x-) or without (—) U_{steric}, give similar results as to the positions of the maxima and proportions of -*syn* and -*trans* conformers 55.5% : 44.5% on average. The greatest difference is in the position of the maximum probability of the -*anti* conformer where the position is shifted by 3° from 128 to 131°, this is compared to only a 1° difference from 50° to 51° for the -*syn* form.

Table 6. Results of bringing observed and calculated D_{ij}^{CF} and D^{FF} obtained for the sample in ZLI 1167 into agreement by varying ϵ_{ZZ}^{R}, $\epsilon_{XX}^{R} - \epsilon_{YY}^{R}$, ϵ_{aa}^{CF}, V_1, V_2 and V_4.

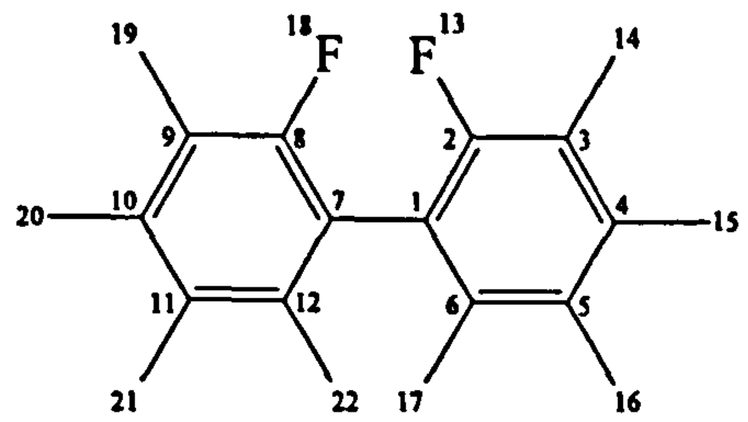

Geometry		X-ray		MO		
		A	B	A	B	C
i	j	D_{ij} (obs) / Hz		$\Delta_{ij} = D_{ij}(obs) - D_{ij}(calc)$ / Hz		
1	13	-186.2	0.2	-0.5	0.2	0.2	-0.7
2	13	-275.7	-0.1	0.2	-0.1	-0.1	0.2
3	13	306.9	-0.1	-1.3	0.1	-0.1	-0.5
4	13	47.5	1.3	1.1	1.2	1.2	1.0
5	13	-7.5	-0.4	-0.4	-0.6	-0.6	-0.8
6	13	-48.6	-0.2	-0.3	-0.2	-0.2	-0.5
7	13	18.8	-0.1	-1.6	0.1	0.1	0.7
8	13	63.7	-0.1	2.5	0.1	0.1	0.1
9	13	46.9	0.1	0.7	-0.4	-0.2	-0.1
10	13	37.6	-0.2	-0.6	-0.9	-0.9	-0.6
11	13	41.1	0.1	0.3	-0.2	-0.6	-0.3
12	13	52.2	-0.1	2.1	0.1	0.3	0.2
13	18	27.5	0.1	-0.5	-0.1	-0.1	-0.1
V_1 / kJ mol^{-1}			-0.17	-0.47	-0.17	-0.58	-0.50
V_2 / kJ mol^{-1}			2.93	4.77	5.28	-2.85	-1.91
V_4 / kJ mol^{-1}			3.22	12.87	6.37	1.31	1.66
ϵ_{ZZ}^{R} / kJ mol^{-1}			-0.71	-0.70	-0.70	-0.70	-0.70
$\epsilon_{XX}^{R}-\epsilon_{YY}^{R}$ / kJ mol^{-1}			-0.37	-0.32	-0.33	-0.34	-0.35
ϵ_{aa}^{CF} / kJ mol^{-1}			0.11	0.11	0.10	0.10	0.11

S_{ZZ}	-0.223	-0.221	-0.221	-0.221	-0.222
S_{XX}-S_{YY}	-0.046	-0.044	-0.046	-0.046	-0.046
S_{XZ}	-0.011	-0.010	-0.009	-0.009	-0.009
ϕ (*-syn*) / °	51	50	51	50	50
% *-syn* *	54.9	56.0	55.3	57.6	56.8
ϕ (*-anti*) / °	128	131	129	132	131
% *-anti* *	45.1	44.0	44.7	42.4	43.2

A Without steric term (U_{steric}). Including D_{FF}.

B With steric term (U_{steric}). Including D_{FF}.

C With steric term ($-U_{steric}$). Including D_{FF}. Including bond relaxation.

* % -syn and -anti are the areas from 0-90° and 90-180° respectively of $P_{LC}(\phi)$

The Additive Potential method also yields the probability distribution in the isotropic phase, by simply removing the U_{ext} term from equation 4. The distributions obtained are almost identical to those in the liquid crystal phase so will not be shown here.

Figure 13 shows the $P_{LC}(\phi)$ obtained from the conformational analysis using the MO geometry. Unlike the X-ray structure results, the effect of the steric terms appears to be that it flattens the probability distribution, however, as with the X-ray geometry the final results show that the models predict similar positions of the maxima and the proportions of the *-syn* and *-anti* conformers, 56.5% : 43.5% on average.

Inclusion of bond relaxation in the model (-∗-) with the steric term does not significantly effect the probability distribution. MO calculations showed that the greatest change in θ away from the optimum angle, $\theta = 119.6°$, with ϕ occurs when the molecule resides in a planar form. These conformers are not significantly probable in the liquid crystal phase and therefore the effect of geometry relaxation is minimal. We may therefore neglect this term in future calculations.

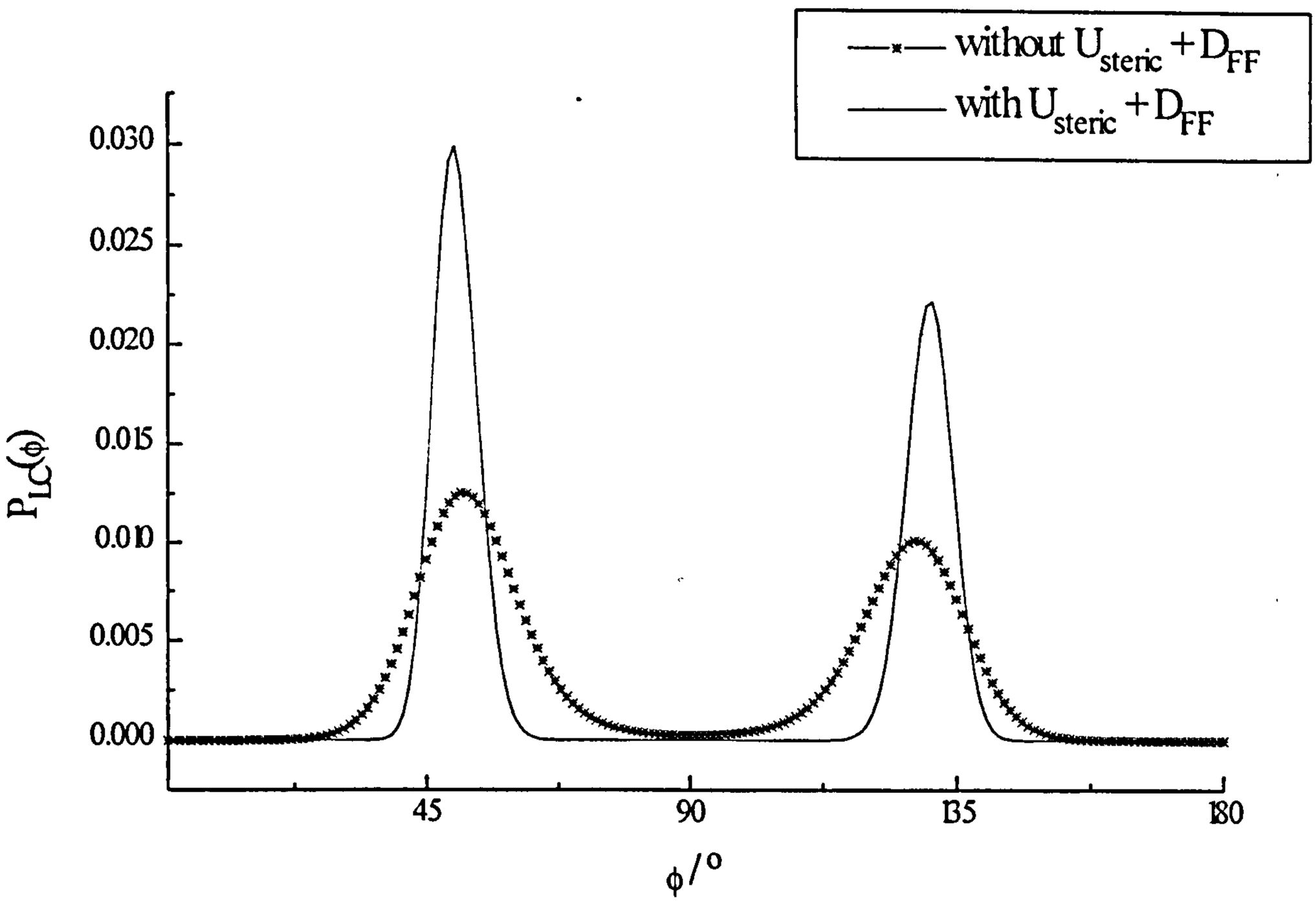

Figure 12 The probabilty of conformation in the liquid crystal phase for motion about ϕ for 2,2'-difluorobiphenyl / ZLI 1167 at 300K. Optimised X-ray geometry obtained from D_{ij}^{CF}.

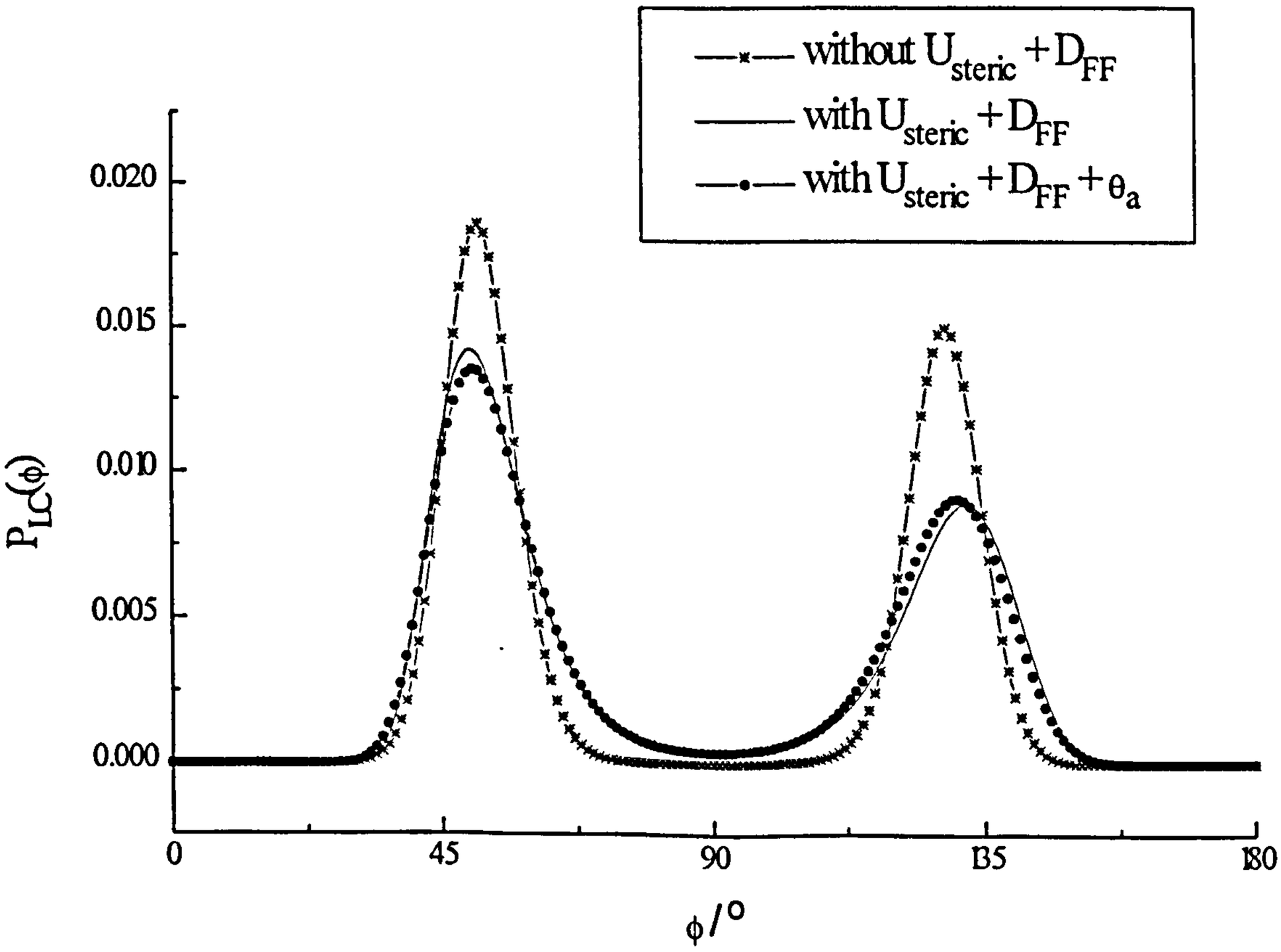

Figure 13 The probabilty of conformation in the liquid crystal phase for motion about ϕ for 2,2'-difluorobiphenyl-d_4 / ZLI 1167 at 300K. Optimised MO geometry obtained from D_{ij}^{CF} including bond relaxation.

5.3.6 Investigation of the Conformational distribution using D_{ij}^{HH} and D_{ij}^{HF}.

As already discussed, the proton geometry was found to be unreasonable in the X-ray structure, therefore only the optimised MO structure was considered during the conformational analysis using the D_{ij}^{HH} and D_{ij}^{HF} extracted from 2,2'-difluorobiphenyl-d_4 in ZLI 1132 and ZLI 1167. The inter-ring D_{ij}^{HF} and D_{FF} and the four well determined intra-ring D_{ij} were used to determine the conformational distribution of 2,2'-difluorobiphenyl in both solvents. As noted earlier, the analysis of the spectra do not directly yield a value for D_{FF} and so the conformational analysis was carried out with and without D_{FF} included for comparison. The calculated D_{ij} were brought into agreement with the experimental D_{ij} through the variation of the same parameters as for the ^{13}C analysis. The full set of results are reported in tables 7 and 8 and the probability distributions shown in figures 14 and 15 for 2,2'-difluorobiphenyl-d_4 dissolved in ZLI 1167 and ZLI 1132 respectively.

Figure 14 shows the $P_{LC}(\phi)$ for 2,2'-difluorobiphenyl-d_4 dissolved in ZLI 1167 at 300K. The two P_{LC}, with (-x-) and without (-+-) U_{steric}, closely agree on the positions of the two maxima, both at 48° for the -syn form and 132° and 133° for the -anti form respectively.

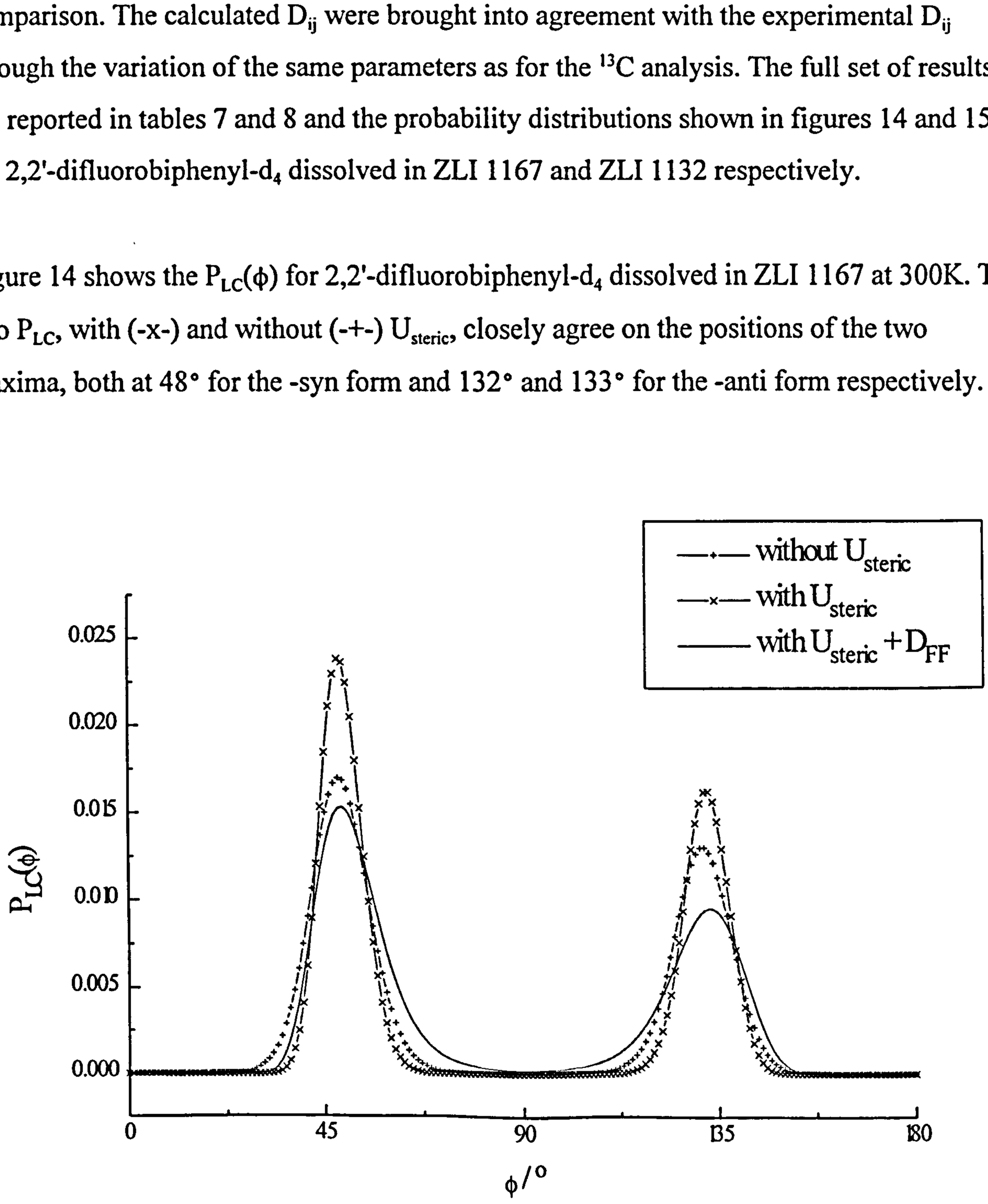

Figure 14 The probabilty of conformation in the liquid crystal phase for motion about ϕ for 2,2'-difluorobiphenyl / ZLI 1167 at 300K obtained from D_{ij}^{HH} and D_{ij}^{HF}

Inclusion of the steric term sharpens the probability distribution increasing the potential barrier for rotation about the centre bond. The value of D_{FF} is also calculated from the final parameters in both models. In both cases the value is found to be higher than expected from comparison with the value extracted from the analysis of the ^{13}C NMR spectra (chapter 4). Without U_{steric}, D_{FF} is found to be greater by a factor of 2.2 while with U_{steric} the factor is only 1.5. This suggests that the model with the steric term included gives a truer representation of $P_{LC}(\phi)$ as we would not expect a great difference in the calculated value of D_{FF} to the observed value from the analysis of the ^{13}C spectra as the order parameters shown in tables 6 (D_{ij}^{CF} and D_{FF}) and 7 (D_{ij}^{HH} and D_{ij}^{HF}) are very similar. Inclusion of D_{FF} without the steric term gave rise to an unreasonable potential for rotation about the centre bond, the energy barriers were such that the structure was restricted to only a few degrees of motion about the two maxima. The corresponding model with the steric term included gave the distribution shown in figure 12 (—), the positions of the maxima were shifted by 1°, however the proportions of *-syn* and *-anti* forms remain almost the same at 57.9% : 42.1%. The effect on the shape of the distribution is to slightly flatten the curve, reducing the potential barrier for rotation about the centre bond.

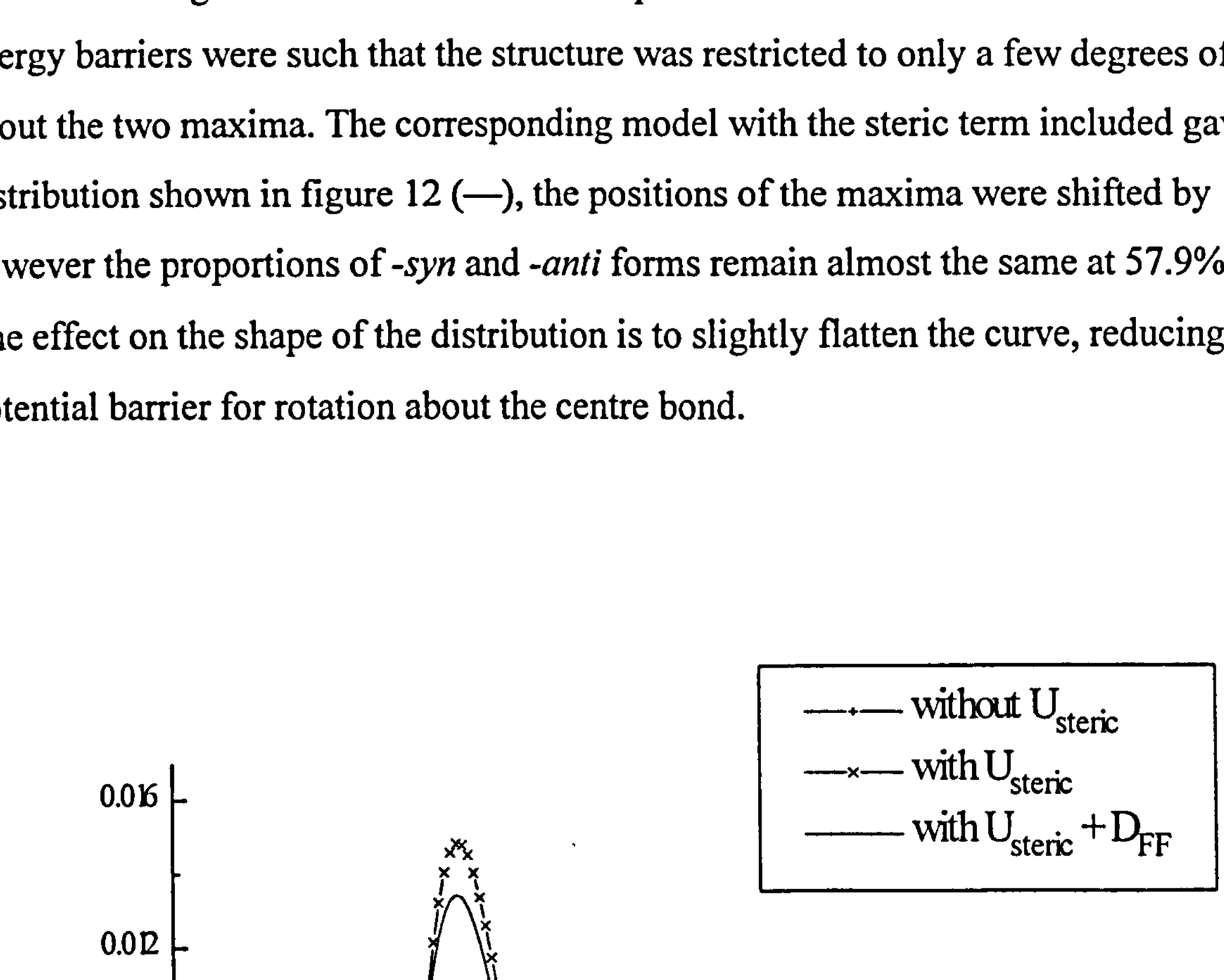

Figure 15 The probabilty of conformation in the liquid crystal phase for motion about ϕ for 2,2'-difluorobiphenyl / ZLI 1132 at 300K obtained from D_{ij}^{HH} and D_{ij}^{HF}

Figure 15 shows $P_{LC}(\phi)$ for 2,2'-difluorobiphenyl-d_4 dissolved in ZLI 1132 at 300K. The positions of the maxima are slightly different between the two models, with (-x-) or without (-+-) the steric term included, where the -*syn* form is predicted to occur at 50° and 48° and the -*anti* form at 130° and 134° respectively. The effect of the steric term, as with the sample in ZLI 1167, is to sharpen the distribution. The value of D_{FF} calculated from the final parameters also shows that both models find this to be higher than expected. Without U_{steric}, D_{FF} is found to be greater by a factor of 3.1 while with U_{steric} the factor is only 1.2. Again, this demonstrates that the model including the steric term gives a truer representation of $P_{LC}(\phi)$. Inclusion of D_{FF} as data, has a similar effect to the sample in ZLI 1167, in that the result without the steric term gives rise to an unreasonable potential barrier for rotation about the centre bond. With U_{steric} included (-x-), the distribution is also slightly flattened, however the proportions of -*syn* : -*anti* conformers remains the same at 59.8% : 40.2%.

Table 7. Results of bringing observed and calculated D_{ij}^{HH}, D^{HF} and D_{FF} obtained for the sample in ZLI 1167 into agreement by varying ϵ_{ZZ}^{R}, $\epsilon_{XX}^{R} - \epsilon_{YY}^{R}$, ϵ_{aa}^{CF}, V_1, V_2 and V_4.

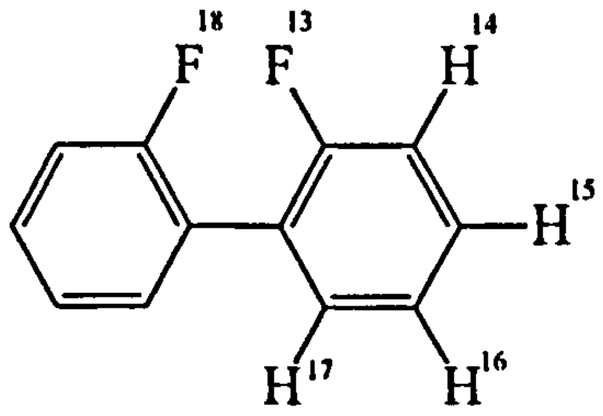

i j	Wt	D_{ij} (obs) / Hz	$\Delta D_{ij} = D_{ij}(obs) - D_{ij}(calc)$ / Hz			
			A	B	C	D
13 14	1	1377.9	-1.1	0.1	-1.1	-1.8
13 15	1	153.3	-0.7	-0.6	-0.6	-1.5
13 16	0	-12.6	-0.5	-0.5	-0.5	-0.4
13 17	0	-97.6	-6.7	-9.0	-6.7	-4.8
13 18	1/0	27.5	32.7	4.0	15.1	0.8
14 15	1	-95.9	0.1	0.6	0.1	0.4
14 16	0	-114.9	-12.7	-15.6	-15.1	-10.2
14 17	0	-2.9	-8.3	-11.3	-8.3	-5.9
14 18	1	117.2	0.1	-6.3	0.1	-2.4
15 16	0	-12.6	-62.9	-86.5	-62.9	-43.6

15 17 0	212.3	-5.7	8.9	-5.7	-3.1
15 18 1	89.0	-3.2	-4.1	-3.2	-2.5
16 17 1	1636.9	1.2	0.4	1.2	2.0
16 18 1	96.5	-0.1	4.3	0.1	-1.1
17 18 1	80.9	-0.1	-3.4	0.1	-0.2
rms		13.5	103.7	13.5	23.4
ϵ_{ZZ}^{R} / kJ mol^{-1}		-0.63	-0.63	-0.63	-0.63
ϵ_{XX}^{R}-ϵ_{YY}^{R} / kJ mol^{-1}		-0.19	-0.15	-0.19	-0.24
ϵ_{aa}^{CF} / kJ mol^{-1}		0.03	0.01	0.03	0.05
V_1 / kJ mol^{-1}		-0.20	-0.10	-0.54	-0.61
V_2 / kJ mol^{-1}		2.31	85.75	-1.20	-3.20
V_4 / kJ mol^{-1}		5.00	193.70	6.42	1.48
S_{ZZ}		-0.202	-0.202	-0.202	-0.202
S_{XX}-S_{YY}		-0.035	-0.031	-0.035	-0.039
S_{XZ}		-0.003	-0.001	-0.003	-0.004
ϕ (*-syn*) / °		48	48	48	49
% *-syn* *		56.5	-	57.4	57.9
ϕ (*-trans*) / °		132	132	133	133
% *-anti* *		43.5	-	42.6	42.1

A Without steric term (U_{steric}).

B Without steric term (U_{steric}). Including D_{FF}.

C With steric term (U_{steric}).

D With steric term (U_{steric}). Including D_{FF}.

* % -syn and -anti are the areas from 0-90° and 90-180° respectively of $P_{LC}(\phi)$

Table 8. Results of bringing observed and calculated D_{ij}^{HF}, D_{ij}^{HH} and D_{FF} obtained for the sample in ZLI 1132 into agreement by varying ϵ_{ZZ}^{R}, $\epsilon_{XX}^{R} - \epsilon_{YY}^{R}$, ϵ_{aa}^{CF}, V_1, V_2 and V_4.

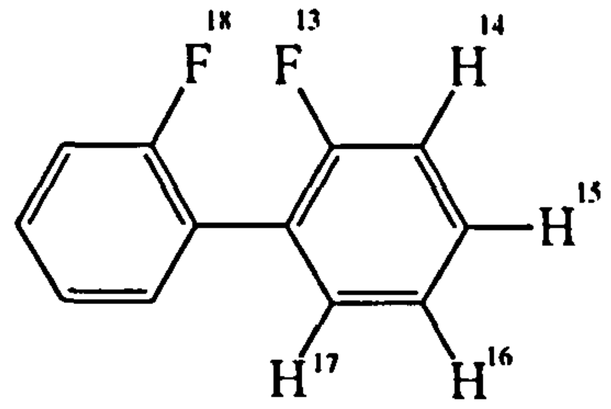

i j	Wt	D_{ij} (obs) / Hz	$\Delta D_{ij} = D_{ij}(obs) - D_{ij}(calc)$ / Hz		
		A	B	C	D
13 14	1	-3155.2	1.9	-0.9	1.9	2.7
13 15	1	-342.8	-1.2	-4.4	-1.2	-0.3
13 16	0	38.8	5.5	5.5	5.5	5.5
13 17	0	222.3	-15.4	-21.7	-15.4	-13.3
13 18	1/0	-63.3	-131.1	-10.9	-11.9	-0.7
14 15	1	252.5	0.1	-1.1	0.1	-0.3
14 16	0	279.3	-11.1	-19.1	-11.1	-8.5
14 17	0	5.8	-13.3	-21.6	-13.3	-10.7
14 18	1	-269.6	-0.1	12.3	-0.1	2.0
15 16	0	24.6	-96.0	-160.8	-96.1	-75.5
15 17	0	-485.9	2.8	11.6	2.8	0.1
15 18	1	-201.7	2.4	4.8	2.3	1.6
16 17	1	-3758.0	-1.6	0.9	-1.6	2.5
16 18	1	-212.1	-0.1	-18.7	0.1	0.7
17 18	1	-180.1	0.1	10.6	0.1	0.2
rms			13.4	778.5	13.4	21.2
ϵ_{ZZ}^{R} / kJ mol^{-1}		1.11	1.10		1.11	1.11
ϵ_{XX}^{R}-ϵ_{YY}^{R} / kJ mol^{-1}		1.50	1.15		1.49	1.61
ϵ_{aa}^{CF} / kJ mol^{-1}		-0.10	-0.05		-0.09	-0.10

V_1 / kJ mol^{-1}	-0.25	-0.10	-0.70	-0.73
V_2 / kJ mol^{-1}	1.40	84.36	-3.58	-3.93
V_4 / kJ mol^{-1}	1.98	171.26	0.97	0.42
S_{ZZ}	0.464	0.463	0.464	0.464
S_{XX}-S_{YY}	0.085	0.074	0.085	0.088
S_{XZ}	0.012	0.008	0.012	0.014
ϕ (*-syn*) / °	50	49	48	48
% *-syn*	57.5	-	59.8	59.8
ϕ (*-trans*) / °	130	131	134	135
% *-anti*	42.5	-	40.2	40.2

A Without steric term (U_{steric}).

B Without steric term (U_{steric}). Including D_{FF}.

C With steric term (U_{steric}).

D With steric term (U_{steric}). Including D_{FF}.

* % -syn and -anti are the areas from 0-90° and 90-180° respectively of $P_{LC}(\phi)$

5.4 Conclusion

The conformational analysis of 2,2'-difluorobiphenyl in the liquid crystal phase using NMR data clearly answers the question as to whether this molecule exists exclusively in only one conformer as suggested by the electron diffraction work of Bastiansen [6] or if the molecule resides mainly in two major conformations as suggested by MO calculations[14, 16]. The results here show the latter to be the case in the liquid crystal and indeed isotropic solutions. The three sets of data yield very similar probability distributions with slightly different potentials for the barrier of rotation about the centre bond of 2,2'-difluorobiphenyl. A comparison is made in figure 16 of the NMR results with the results of the MO calculation

[14]. The Additive Potential method, as used here, predicts the conformation of 2,2'-difluorobiphenyl in the liquid crystal phase as being most likely at $\phi = 50° \pm 2°$ for -*syn* and $\phi = 131° \pm 4°$ for -*anti* with the -*syn* form being most likely, populated at 55 - 60%. The results of the AP method (—), (-+-) and (-x-) can be compared to the result of MO calculation (-◆-), shown in figure 16, and X-ray diffraction. MO finds the most probable conformers at $\phi = 57.2°$ and 129° while the minimum energy structure in the crystal phase finds $\phi = 58.42°$. The differences in ϕ for the -*syn* form may well be due to differences in the structure according to the phase. We would expect there to be differences in the X-ray structure as it has been shown here to be different to the structure in the liquid phase. Palke *et al.* [28] attempted an assessment of the precision by which the AP method can obtain P_{LC}. Their results showed that the AP method was indeed accurate in the case of biphenyl dissolved in a liquid crystal solvent to within 2°. This therefore suggests that the difference in the structures determined in the liquid crystal and isotropic phases is real.

Geometry relaxation is an important factor to consider, however, in this example it has been shown that the NMR data was sufficient to exclude conformers which require large deviations in the C1-C2-F13 bond angle.

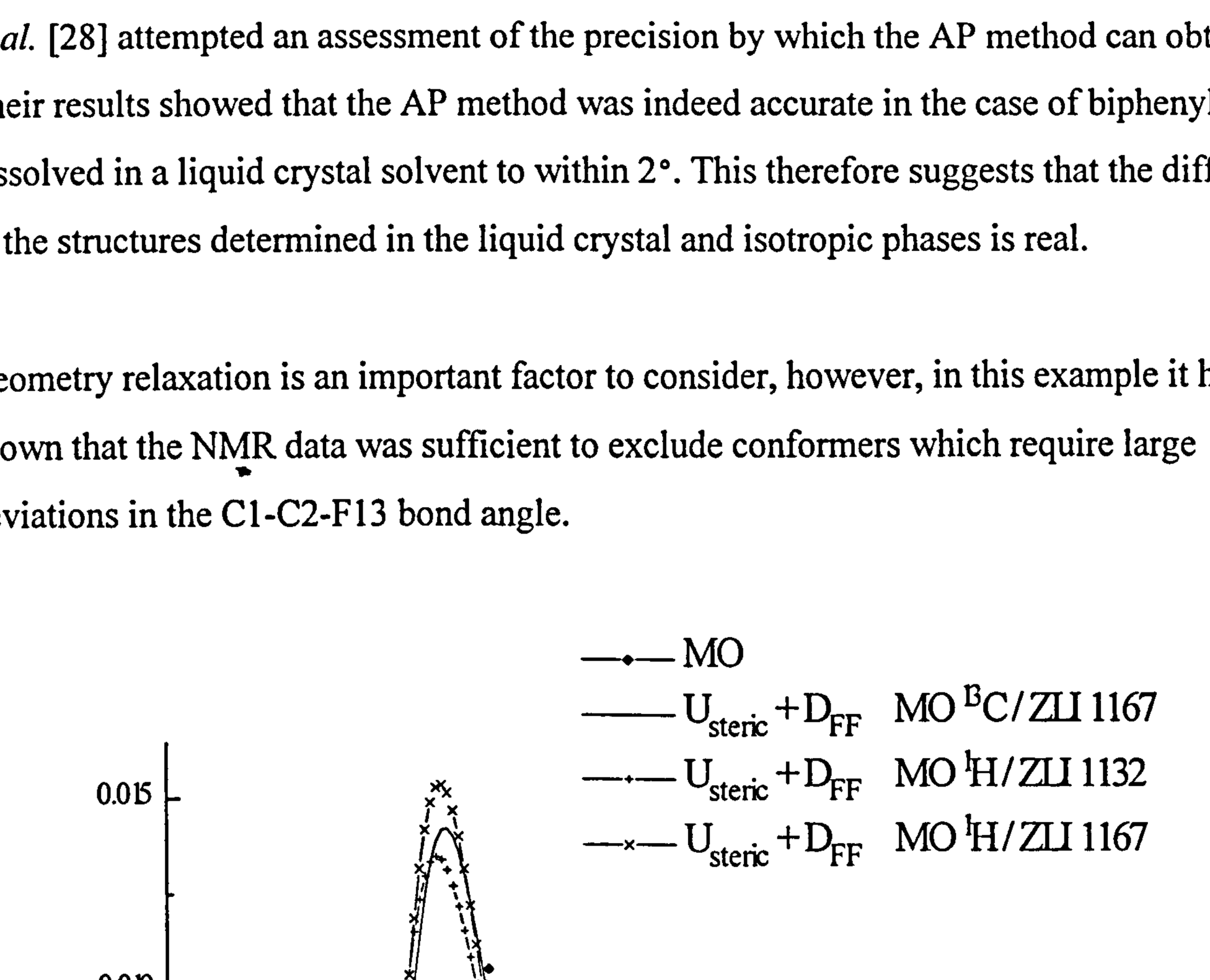

Figure 16 Comparison of MO calculation with the Additive Potential Method

The results also suggest that inclusion of the steric term is also very important. It was shown that the models without the value of D_{FF} included as data did not calculate this value to within reasonable precision to the value extracted from the ^{13}C-{^{1}H} NMR spectra in ZLI 1167. The inclusion of the steric term allowed the exploration of rotation potential energy curves that cannot be modelled using four terms of a Fourier series only, hence we perhaps have been able to model more accurately the real shape of the curve.

5.5 References

[1] J.Trotter, *Acta.Cryst.*, **14**, 1135, (1961)

[2] O.Bastiansen, *Acta.Chem.Scand.*, **3**, 408, (1949)

[3] G.Celebre, G.De Luca, M. Longeri, D.Catalano, C.A.Veracini, J.W.Emsley. *J.Chem.Soc.Faraday Trans.*, **87**, 2623, (1991)

[4] J.W.Emsley, G.R.Luckhurst, C.P.Stockley, *Proc. R. Soc. London, A*, **381**, 117, (1982)

[5] O.Bastiansen, *Acta.Chem.Scand,*. **4**, 926, (1950)

[6] O.Bastiansen, L.Smedvik, *Acta.Chem.Scand,*. **8**, 1593, (1954)

[7] C.Rømming, H.M.Seip, I.-M.Aanesen Øymo, *Acta.Chem.Scand.*, **A28**, 507, (1974)

[8] A.Almenningen, O.Bastiansen, L.Fernholt, S.Gundersen, E.Kloster-Jensen, *J.Mol.Struct.*, **128**, 77, (1985)

[9] Rajnikant, D.Watkin, *Acta.Cryst.*, C**51**, 1452, (1995)

[10] M.J.Hamor, T.A.Hamor, *Acta.Cryst.*, B**34**, 863, (1978)

[11] J.Bowen Jones, D.S.Brown, *Acta.Cryst.*, B**38**, 317, (1982)

[12] M.H.Lemée, L.Toupet, Y.Délugeard, J.C.Messager, H.Calleau, *Acta.Cryst.*, B**43**, 466, (1987)

[13] B.Aldridge, G.De Luca, M.Edgar, S.Edgar, J.W.Emsley, M.I.C.Furby, M.Webster, *Liq.Cryst.*, **24**, 569, (1998)

[14] M.Edgar, Personal Discussions

[15] J.Cioslowski, S.T.Mixon, *J.Am.Chem.Soc.*, **114**, 4382, (1992)

[16] S.J.Clark, C.J.Adam, D.J.Cleaver, J.Crain, *Liq.Cryst.*, **22**, 477, (1997)

[17] C.Vauchier, F.Vinet, N.Maiser, *Liq.Cryst.*, **5**, 141, (1989)

[18] M.Hird, K.J.Toyne, G.W.Gray, D.G.McDonnell, I.C.Sage, *Liq.Cryst.*, **18**, 1, (1995)

[19] E.K.Foord, J.Cole, M.J.Crawford, J.W.Emsley, G.Celebre, M.Longeri, J.C.Lindon,

Liq.Cryst. **18**, 615, (1995)

[20] J.W.Emsley, M.I.C.Furby, G.De Luca, *Liq.Cryst.*, **21**, 877, (1996)

[21] G.Celebre, G.De Luca, M.Longeri, E.Sicilia, *J.Chem.Inf.Comp,Sci.*, **34**, 539, (1994)

[22] S.Castellano, A.A.Bothner-By, *J.Chem.Phys.*, **41**, 3863, (1964)

[23] J.W.Emsley, L.Phillips, V.Wray, "Fluorine Coupling Constants" Pergamon Press 1977.

[24] F.H.Allen, *Acta Crystallogr.*, **B42**, 515, (1986)

[25] A.Domenicano, I.Hargittai (Ed.) "Accurate Molecular Structures" Oxford University Press 1992.

[26] W.L.Jorgensen, D.L.Severance, *J.Am.Chem.Soc.*, **112**, 4768, (1990)

[27] E.M.Duffy. PhD thesis (1990) Yale University

[28] W.E.Palke, D.Catalano, G.Celebre, J.W.Emsley, *J.Chem.Phys.*, **105**, 7026, (1996)

Chapter 6

The Analysis of the Liquid Crystals I35 and I52 through Variable Angle Sample Spinning

6.1 Introduction

^{13}C-{^{1}H} Variable Angle Sample Spinning (VASS) NMR has been successfully employed in the study of small molecules dissolved in liquid crystalline solvents. The analyses of fluorobenzene and 2,2'-difluorobiphenyl are reported in chapters 3 and 4 respectively, along with the determination of their molecular structures. It was concluded that the same technique could be applied to the analysis of the ^{13}C-{^{1}H} NMR spectra of larger more complicated molecules such as liquid crystals themselves.

The nature of the experiments reported in chapters 3 and 4 was to analyse the liquid crystal spectra of the solute molecules in order to extract the carbon-fluorine dipolar couplings, D_{ij}^{CF}. These ^{13}C-{^{1}H} NMR spectra were shown to be reasonably simple compared to the corresponding ^{1}H NMR spectra, where the spectrum of fluorobenzene, an AX spin system, consists of doublets centred about the carbon chemical shift, δ_X. The spectrum of 2,2'-difluorobiphenyl, an ABX spin system, is more complicated and consists of multiplets with a maximum of six lines centred about δ_X, but is still relatively simple. The liquid crystal I35 and I52, whose structures are shown in figure 1, are examples of AX spin systems. The natural abundance of ^{13}C (1.1%) is such that a single molecule will contain only one ^{13}C

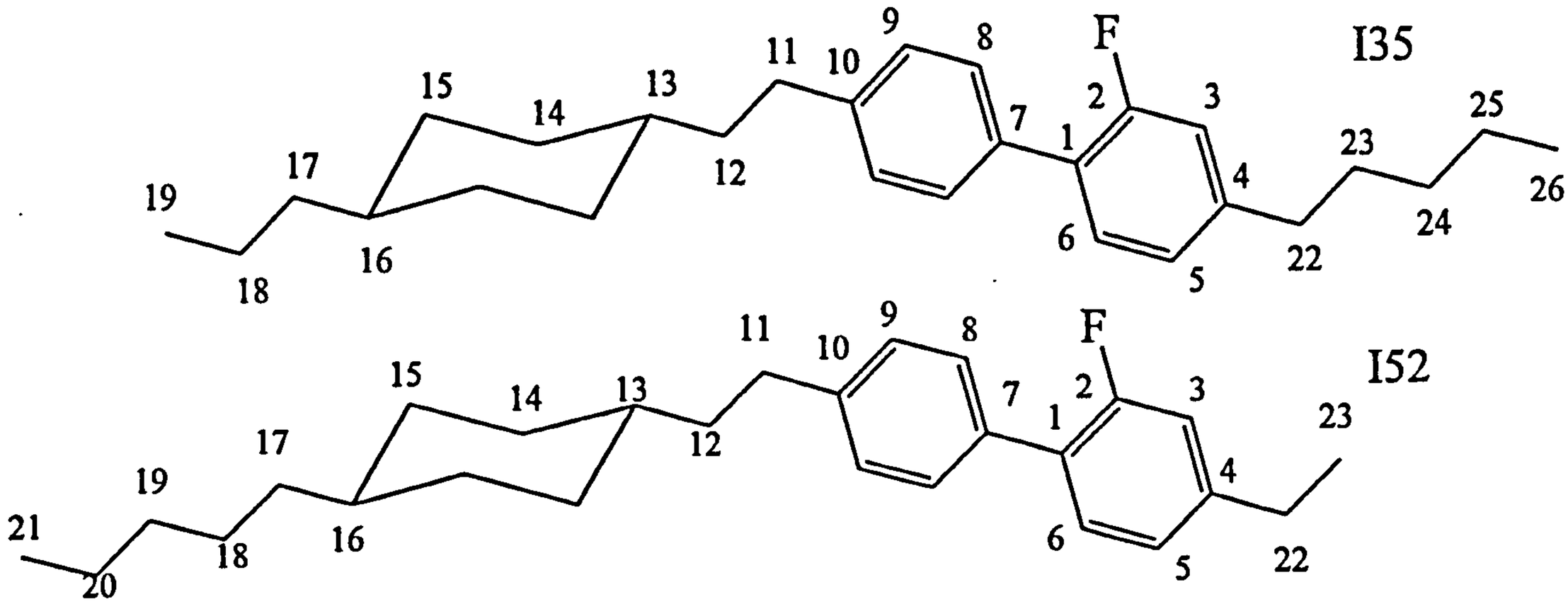

Figure 1 The structures of I35 and I52

atom on average. The spectra therefore consist simply of doublets centred about δ_X, whose splitting equals $2D_{ij}^{CF} + J_{ij}^{CF}$. In theory the liquid crystal spectrum of I35 should consist of 24 doublets (23 for I52) if all the transitions are well resolved and do not overlap. This, however, will be shown not to be the case in these examples and we must therefore follow a similar procedure for the analysis of the liquid crystal spectra of I35 and I52 as was used for the analysis of the liquid crystal spectra of fluorobenzene and 2,2'-difluorobiphenyl.

The first step is to assign the ^{13}C-{^1H} NMR spectra in isotropic solution. Once completed it becomes possible to assign the liquid crystal spectra if we are able to understand how the anisotropic interactions have affected the positions of the transitions. The successful analysis of the liquid crystal spectra yields a set of dipolar couplings, from which it is possible to determine the molecular structure and orientational order of I35 and I52, in particular the conformational distributions. We may consider I35 and I52 to be composed of fragments, some of whose structures have been investigated both experimentally, or theoretically. Both liquid crystal molecules contain the same aromatic core, which should be similar in structure to 2-fluorobiphenyl. In 1995 Rajnikat and Watkin [1] reported an X-ray diffraction study of 2-fluorobiphenyl of the crystal form. They determined the dihedral angle between the two rings to be 54±3°, however, they report an unusually short r_{CF} = 1.319Å. An earlier X-ray diffraction study of 4-acetyl-2'-fluorobiphenyl, in 1968 by Young *et al.* [2], found the dihedral angle to be 50.5°. They determined r_{CF} = 1.369Å which compares more reasonably to the r_{CF} = 1.359Å found in 2,2'-difluorobiphenyl [3]. 2-fluorobiphenyl has also been the subject of a Molecular Orbital calculation on a single isolated molecule [4], here the dihedral angle was found to be 49°. The structure of aliphatic chains connected to aromatic groups have been the subject of the a number of studies. Thus, Celebre *et al.* [5] determined the structure of 4-chloroethylbenzene in a liquid crystal phase and concluded that the lowest energy conformation has the chain orthogonal to the ring plane, a result that is in agreement with earlier Molecular Orbital calculations by Caminati *et al.* [6]. De Luca and Emsley [7] come to the same conclusion concerning the relative orientation of the ring and chain in 4-n-pentyl-4'-cyanobiphenyl (5CB) both as the pure liquid crystal and dissolved in I35, as do Clark *et al.* [8] through Molecular Orbital calculations of an isolated molecule. There is less information to guide us on the orientation of the rest of the molecule relative to the aromatic core, however, some work has been carried out in the determination of the structure of cyclohexylcyclohexanes (CCH's) which contain aliphatic chains attached to cyclohexyl groups. Haase and Paulus [9] determined the

crystal structures of CCH3, CCH5 and CCH7, from X-ray data, and showed that the cyclohexyl rings assumed the chair conformation while the chains adopted the *trans* conformation. Wilson and Allen [10] have reported a molecular dynamics computer simulation on the nematogen CCH5. They used potentials for internal motions which meant that the chain adopts mainly the all *trans* conformation in the liquid crystal phase with small amounts of *gauche(+)* and *gauche(-)* forms. The conformation of the chain with the cyclohexyl group is such that the molecule adopts two *gauche* forms and a small percentage of the *trans* form.

Here the NMR data is used to determine the potential barriers for rotation within I35 and I52 and to compare them with those determined from the study of other similar examples mentioned above.

6.2 Experimental

The liquid crystals I35 and I52 were purchased from Merck and used without further purification in the following experiments.

6.2.1 Sample Preparation

I35 was dissolved in $CDCl_3$ and the ^{13}C-{^1H} NMR spectra recorded with 512 scans on a Bruker AM360 NMR spectrometer at 297K. Proton decoupling was achieved using the WALTZ-16 [11] decoupling sequence.

2A -2A

where

$A = (270_{-x}\ 360_x\ 180_{-x}\ 270_x\ 90_{-x}\ 180_x\ 360_{-x}\ 180_x\ 270_{-x})$

A sample of I35 with 10 % w/w dissolved hexamethyldisiloxane (HMDSO), was used for VASS and static ^{13}C-{^1H} NMR experiments. The sample for VASS was contained in a glass bottle sealed with epoxy resin. The bottle fits into a Zirconium rotor of 7mm o.d for use in a VAS probe type BL-7. The spinning rate used has to be above the threshold at

which the directors align along the spinning axis, and in the present case it was convenient to use 1000 Hz. The purpose of the HMDSO was to reduce the viscosity, therefore reducing the line broadening in the spectra. The VASS spectra were recorded in the range $42.0° < \theta < 54.7°$ where θ is the sample spinning angle to the magnetic field, B_0, using 400 scans at 300K. The proton decoupling pulse was set at 8.0 μs. The static spectrum was recorded using COMARO-2 [12] decoupling sequence using 12,827 scans at 300K with proton decoupling pulse at 5.5 μs.

(385°y 320°-y 25°y 385°x 320°-x 25°x)$_3$ (385°-y 320°y 25°-y 385°x 320°-x 25°x)$_3$

A sample of I35 with 10% w/w dissolved benzene, was also used for VASS and static ^{13}C-{^1H} NMR experiments. Again benzene was used to reduce the viscosity, however, the ^1H spectra of benzene in the liquid crystal phase were used to optimise the homogeneity of the magnetic field. A range of VASS NMR spectra were recorded using the SL-2 [13] decoupling sequence with a proton decoupling pulse of 1.5ms.

(Dx Dy D-x D-y)

D=1.5ms

^{13}C-{^1H} NMR spectra of a similar sample of I52 / HMDSO were recorded. Proton decoupling in both VASS and static experiments was achieved using NANZ-2 [14] decoupling sequence with a proton decoupling pulse of 7.75 μs using 400 scans. A repeat set of experiments were carried out with the same sample using the SL-2 pulse sequence with ^1H decoupling pulse of 1.5ms. More static spectra were recorded using WALTZ-16, COMARO-2, SL-1 [13], NANZ-1 [14] decoupling sequences for comparison.

(270°y 270°-x 270°y) = A (270°x 270°y 270°x) = B

2A -3A 2A -3A 3A -2A A -2B 3B -2B 3B -3B 2B -B

6.2.2 Decoupling Protons from Carbon

The success of the ^{13}C NMR experiments is dependent on removing spin coupling between ^{13}C and ^1H nuclei so that the remaining lines are narrow enough that the ^{13}C-^{19}F couplings

can be resolved. Heteronuclear decoupling in isotropic liquids is effectively achieved using the WALTZ-16 pulse sequence [11], however, Schenker *et al.* [12] designed the COMARO sequences specifically for heteronuclear decoupling in solids and liquid crystals, in which the decoupling of ^{1}H from ^{13}C is designed to overcome both the scalar, J_{CH}, and dipolar, D_{CH}, interactions. The decoupling of ^{1}H from ^{13}C in liquid crystal samples has been studied more recently by Nanz *et al.* [14] and by Sandström and Levitt [13]. Nanz *et al.* used I52 as their test molecule. They applied a number of multi-pulse decoupling sequences, and concluded that the most efficient sequence is NANZ-2. Their best results, however, were not very impressive. Sharp lines for the aromatic carbons, and some for the aliphatic carbons, were obtained. However, some of the aliphatic carbons gave very broad lines. They were also unable to assign any of their lines in the aliphatic region to particular ^{13}C nuclei and did not actually analyse the aromatic region of the spectrum. Sandström and Levitt applied two multi-pulse schemes to 5CB. Their main purpose was to record 2D double quantum ^{13}C spectra in order to determine dipolar couplings between pairs of ^{13}C nuclei. They succeeded in obtaining sharp lines for the aromatic carbons only. Both groups concluded that there is some unknown problem preventing good decoupling of aliphatic carbons in liquid crystalline samples.

The efficiency of the COMARO type pulse sequences, including WALTZ-16 was re-examined. The MSL 200 NMR spectrometer, used here, has more decoupler power available than the high resolution spectrometers used by both Nanz *et al.* and Sandström and Levitt, which is very important when considering the power required to overcome the large geminal ^{1}H-^{1}H dipolar couplings present in the aliphatic chains. It was found that COMARO-2 or WALTZ-16 gave good decoupling of the aromatics, but not of the aliphatics, in agreement with Nanz *et al.* However, Sandström and Levitt's scheme, SL-2, gave excellent decoupling of aliphatics, providing the proton offset frequency, O2, was carefully optimised and the delay between pulses was sufficiently large to avoid heating of the sample, typically 10-20s for SL-2 and 4-8s for others. Poor optimisation of O2 gives rise to inefficient decoupling of protons resulting in line broadening, especially when the dipolar couplings are large. The results of COMARO-2 versus SL-2 for I35 / HMDSO are shown in figure 2, while the results of a range of sequences for I52 / HMDSO and I52 / benzene are given in figure 3. Note, however, that lines are missing in the aromatic region of the spectra using the SL-2 sequence. It was concluded that good decoupling of aromatic and aliphatic carbons could not be achieved with a single decoupling scheme. The analysis of the spectra

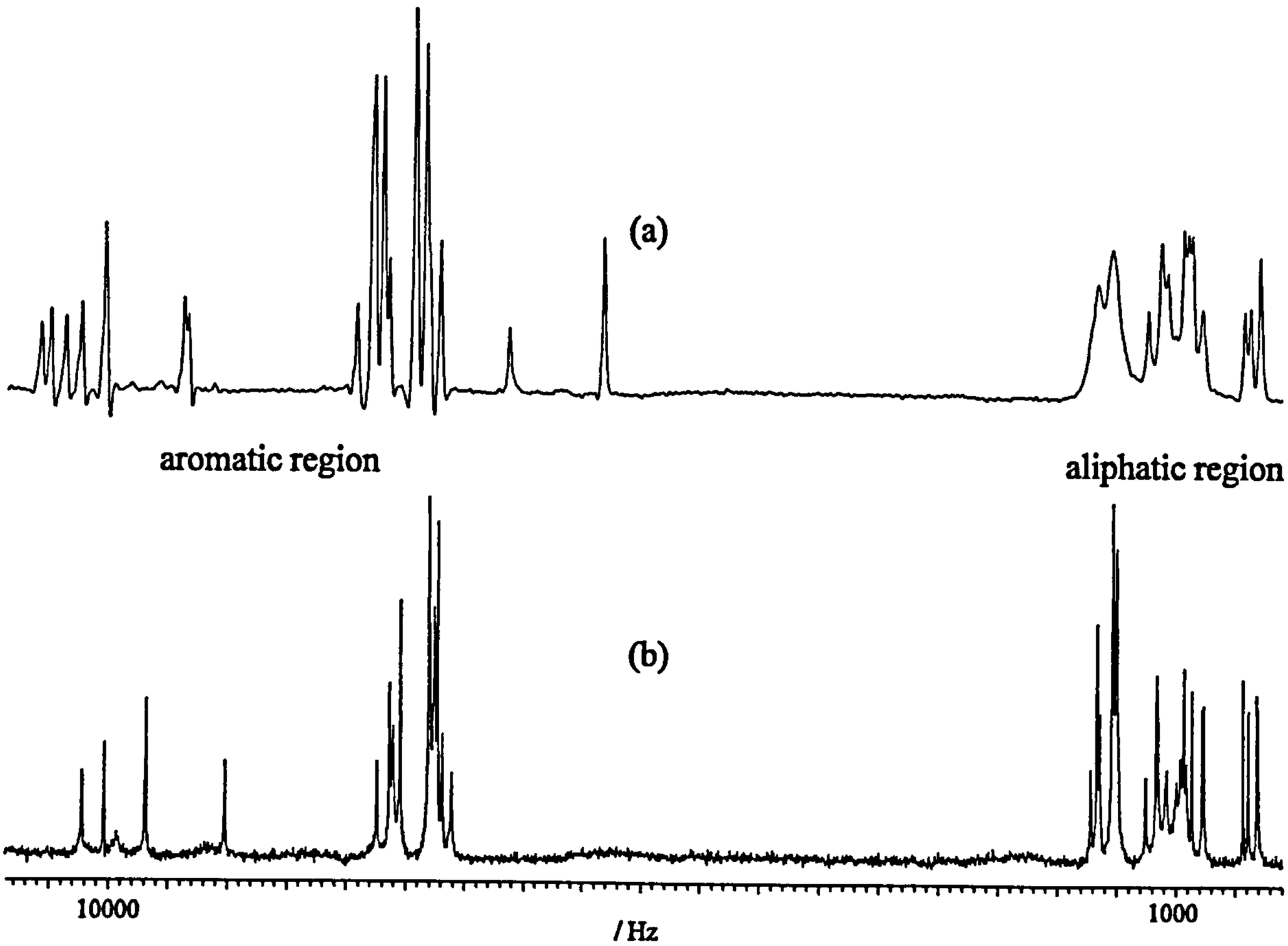

Figure 2 50.3 MHz ^{13}C-{^{1}H} NMR spectra of a) I35 / HMDSO 10% w/w - COMARO-2 ^{1}H decoupling. b) I35 / benzene 10% w/w - SL-2 ^{1}H decoupling.

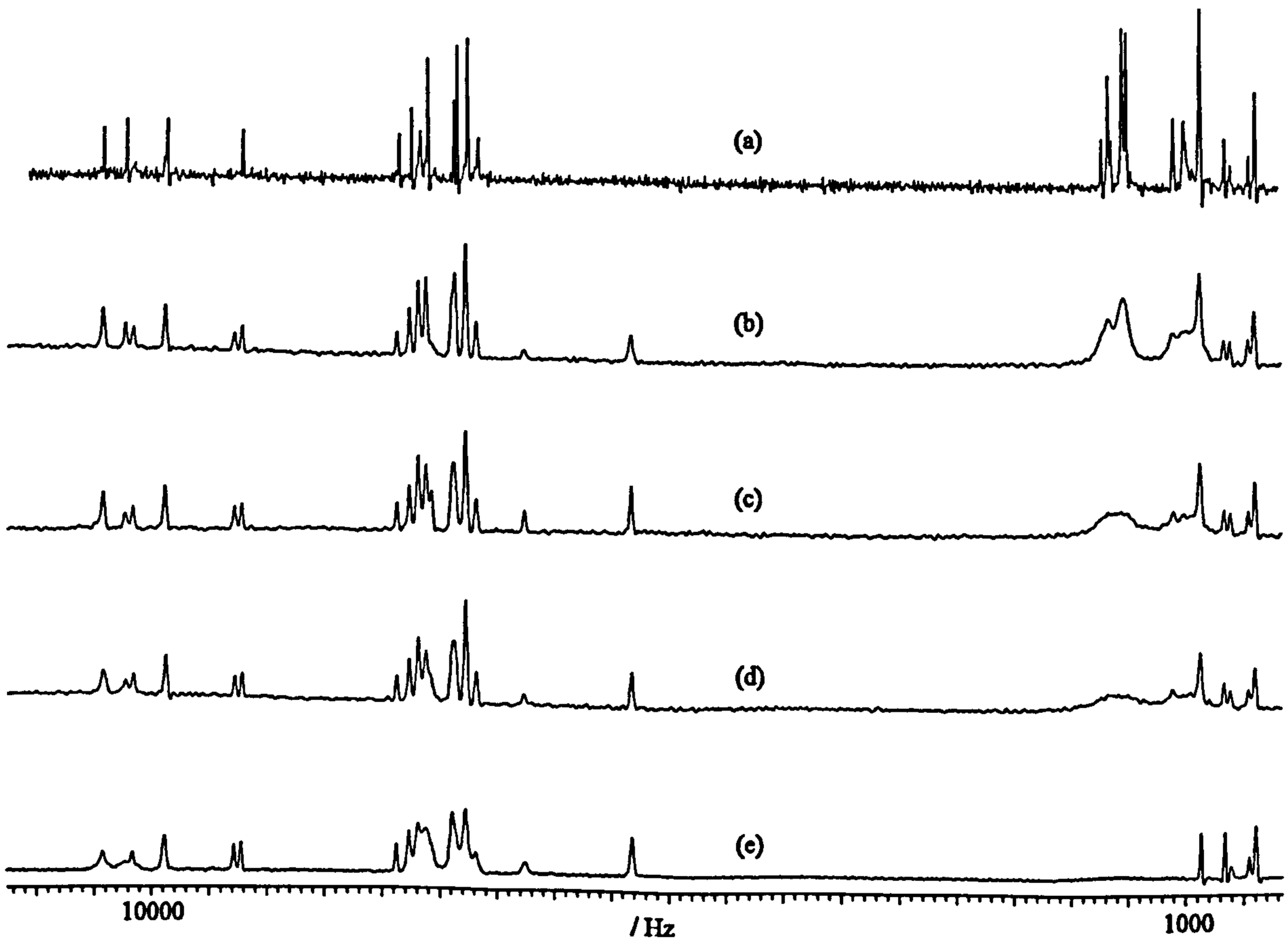

Figure 3 50.3 MHz ^{13}C-{^{1}H} NMR spectra of I52 at 300K. Using a) SL-2 b) SL-1 c) NANZ-2 d) COMARO-2 e) WALTZ-16 ^{1}H decoupling sequences. a) I52 / benzene b) - e) I52 / HMDSO

in figures 2 and 3 will be discussed later.

6.2.3 The ^{13}C-{^{1}H} NMR Spectrum of I35 in Isotropic Solution

The full ^{13}C-{^{1}H} NMR spectrum of I35 in $CDCl_3$ is given in figure 4. The assignment of the lines, according to the numeration in figure 1, are shown in the horizontal expansions, figures 5 and 6, of the aromatic and aliphatic regions respectively. The aromatic carbon atoms all have large downfield chemical shifts and so are immediately recognisable from the aliphatic carbon atoms. It is also possible to determine the scalar couplings, J_{ij}^{CF}, in this region which helps us to assign the spectrum.

The spectrum of the aliphatic carbons consists of singlets and are therefore difficult to assign to particular locations in the molecule. It is possible to partly assign some transitions, due to their intensities and chemical shifts, however, these are not completely certain. The assignment of this region was achieved by a combination of NMR techniques. DEPT spectra of I35 / $CDCl_3$ were used to show which carbon transitions were of type C, CH, CH_2

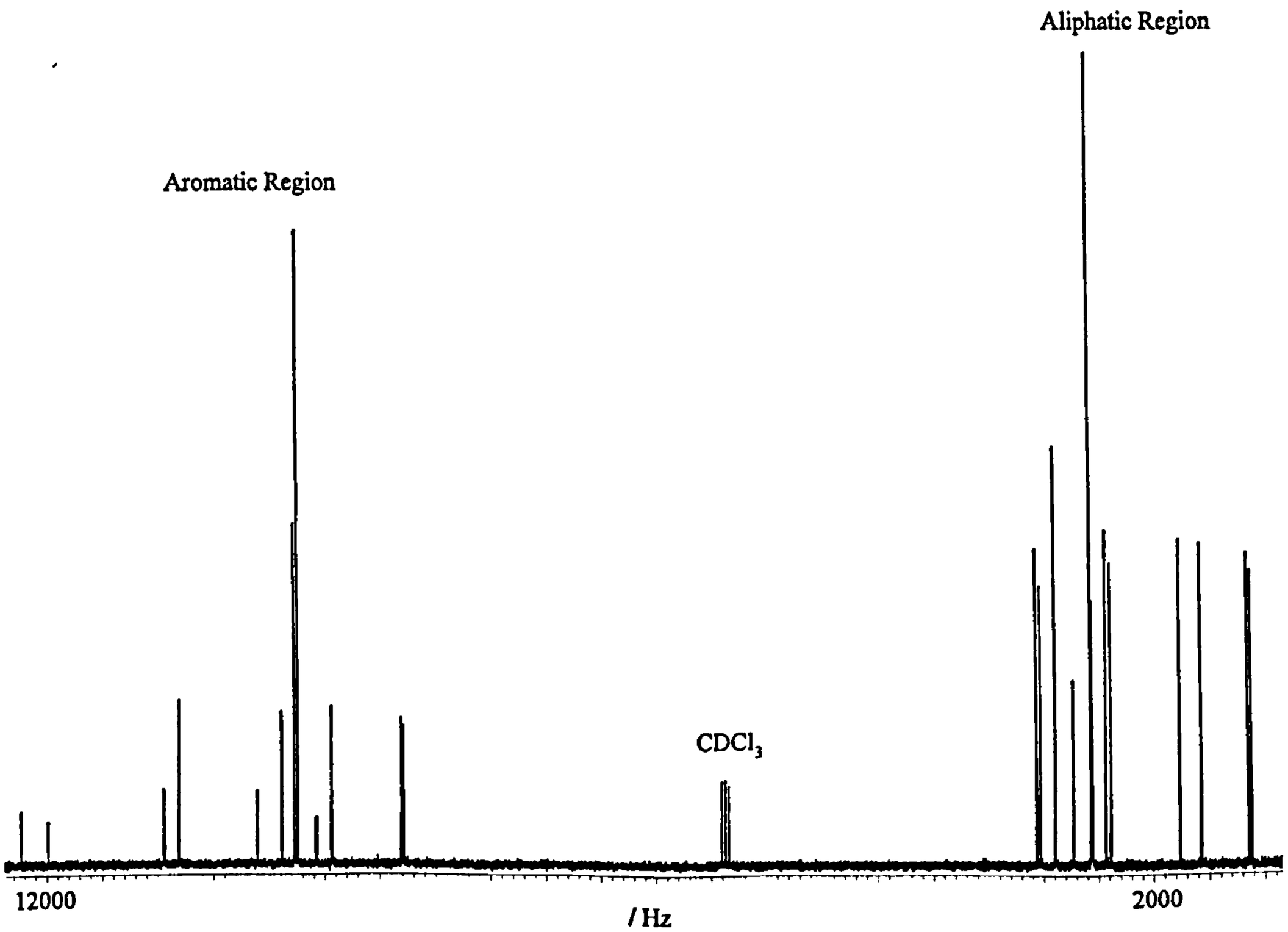

Figure 4 75.5 MHz ^{13}C-{^{1}H} spectrum of I35 / $CDCl_3$ at 300K

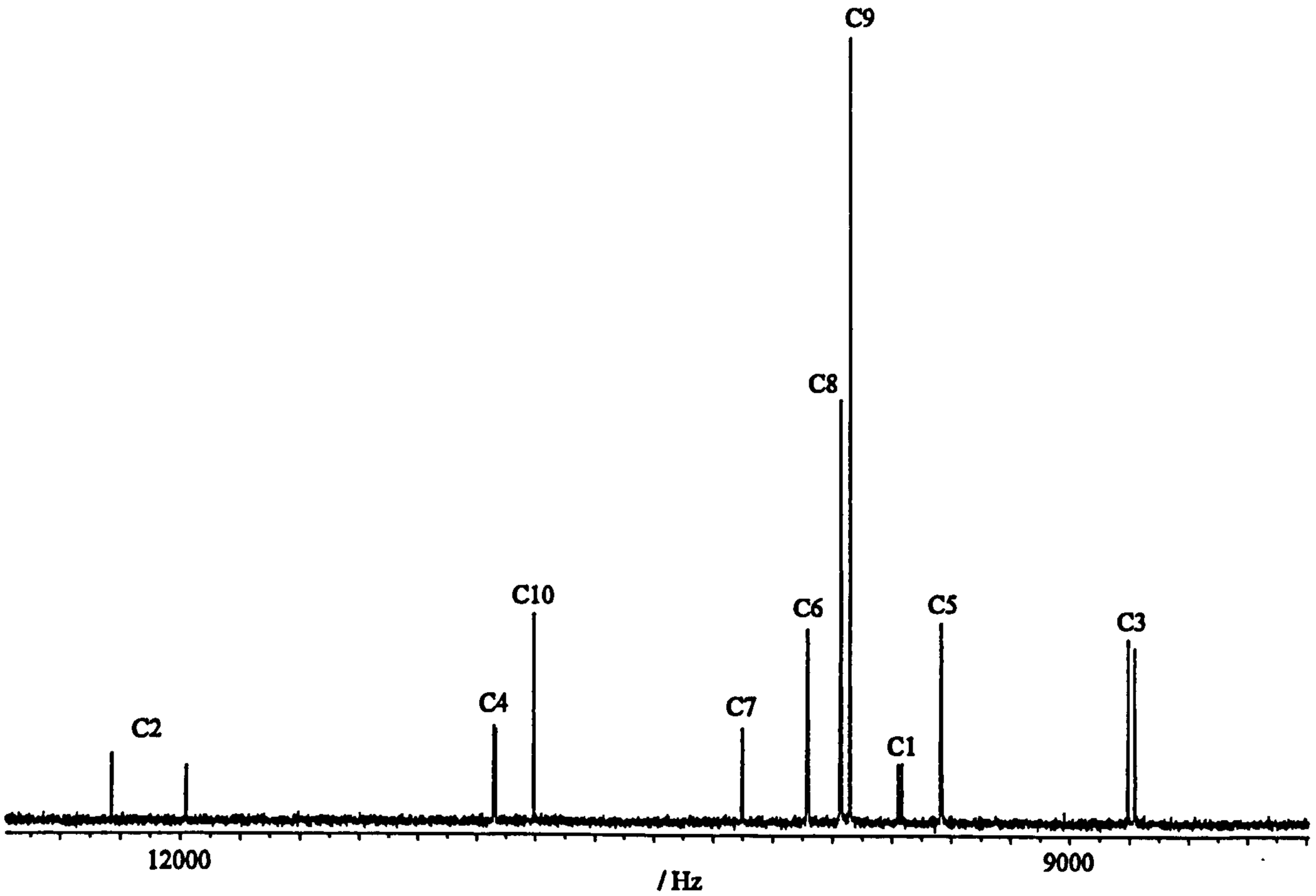

Figure 5 Horizontal expansion of the aromatic region from figure 4.

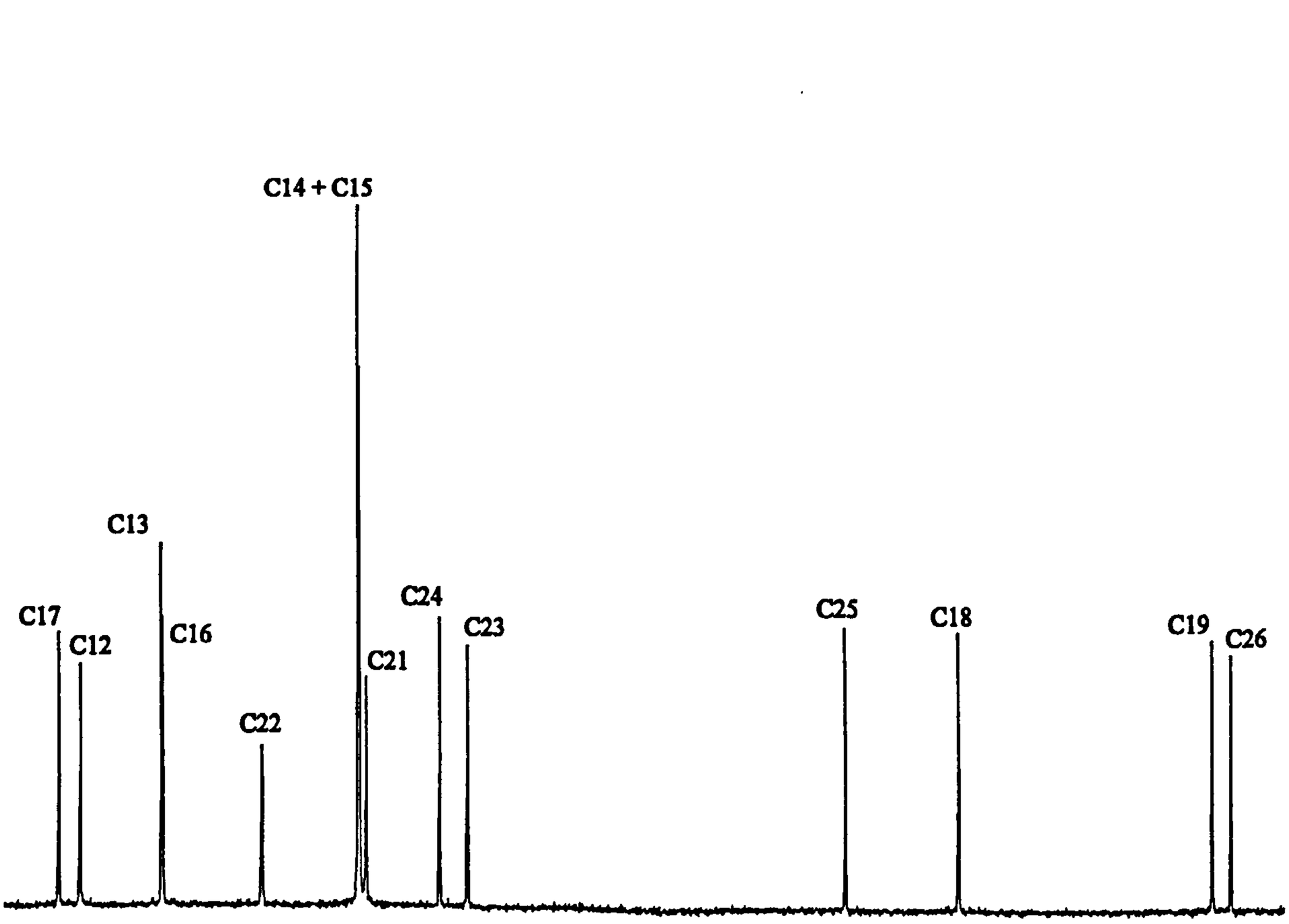

Figure 6 Horizontal expansion of the aliphatic region from figure 4.

or CH_3 (examples are given in section 6.2.4). Partial assignment of the lines was based on DQF-COSY proton spectra, combined with HSQC proton-carbon correlation spectra [15]. However, some ambiguities remained in the cases where lines are not well resolved. The assignments were completed through examination of all the sets of NMR data that had been obtained so far.

Complete analysis of the ^{13}C-{^1H} NMR spectrum in isotropic solution, yields the chemical shift, δ_C, and the scalar coupling constants, J_{ij}^{CF}, of those with resolved doublets, as reported in table 1.

6.2.4 The ^{13}C-{^1H} NMR Spectrum of I52 in Isotropic Solution

The full ^{13}C-{^1H} NMR spectrum of I52 in $CDCl_3$ is given in figure 7. The assignment of the lines, according to the numeration in figure 1, are shown in the horizontal expansions, figures 8 and 9, of the aromatic and aliphatic regions respectively. The assignment of the

Figure 7 90.6 MHz ^{13}C-{^1H} spectrum of I52 / $CDCl_3$ at 300K

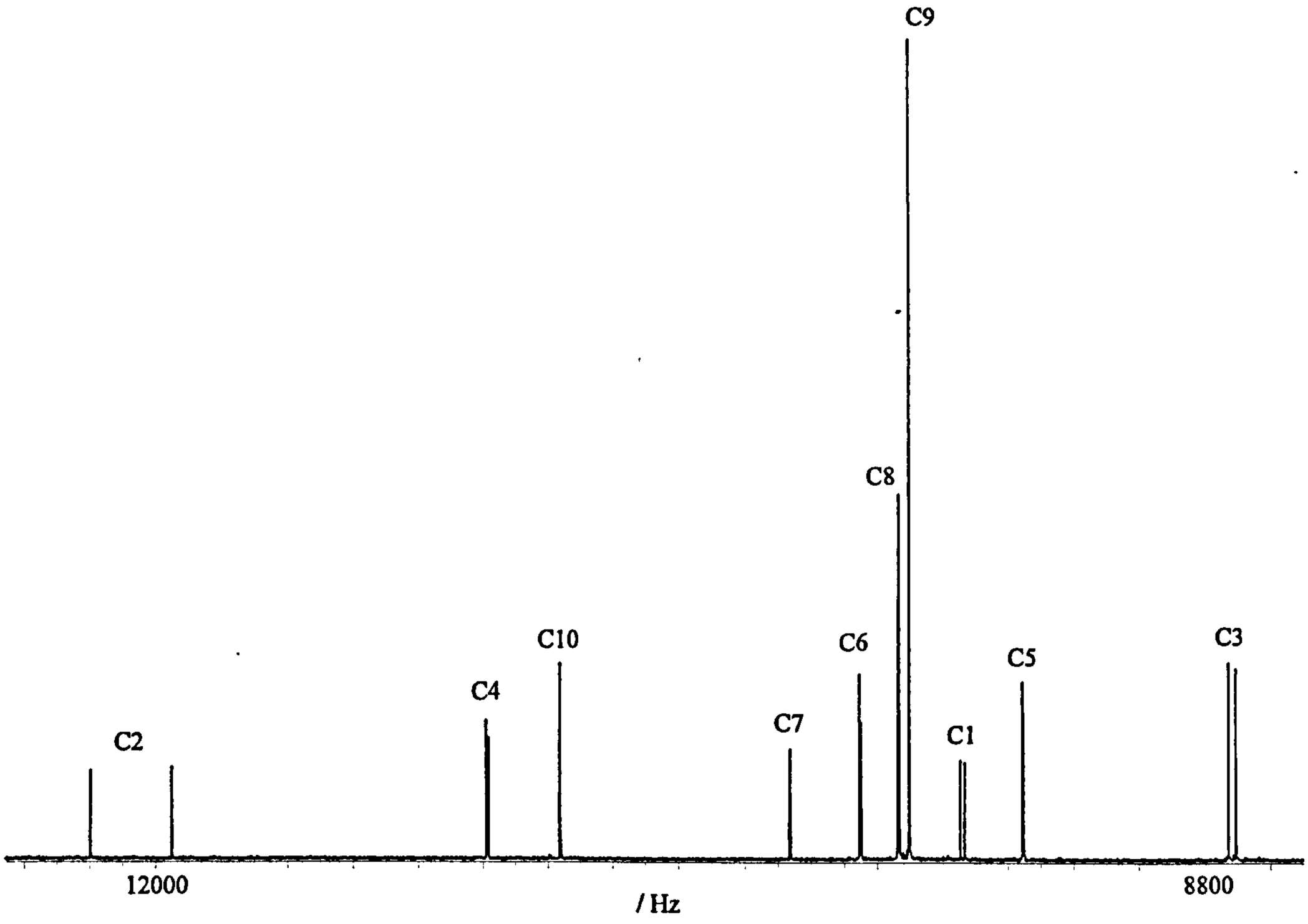

Figure 8 Horizontal expansion of the aromatic region from figure 7.

Figure 9 Horizontal expansion of the aliphatic region from figure 7.

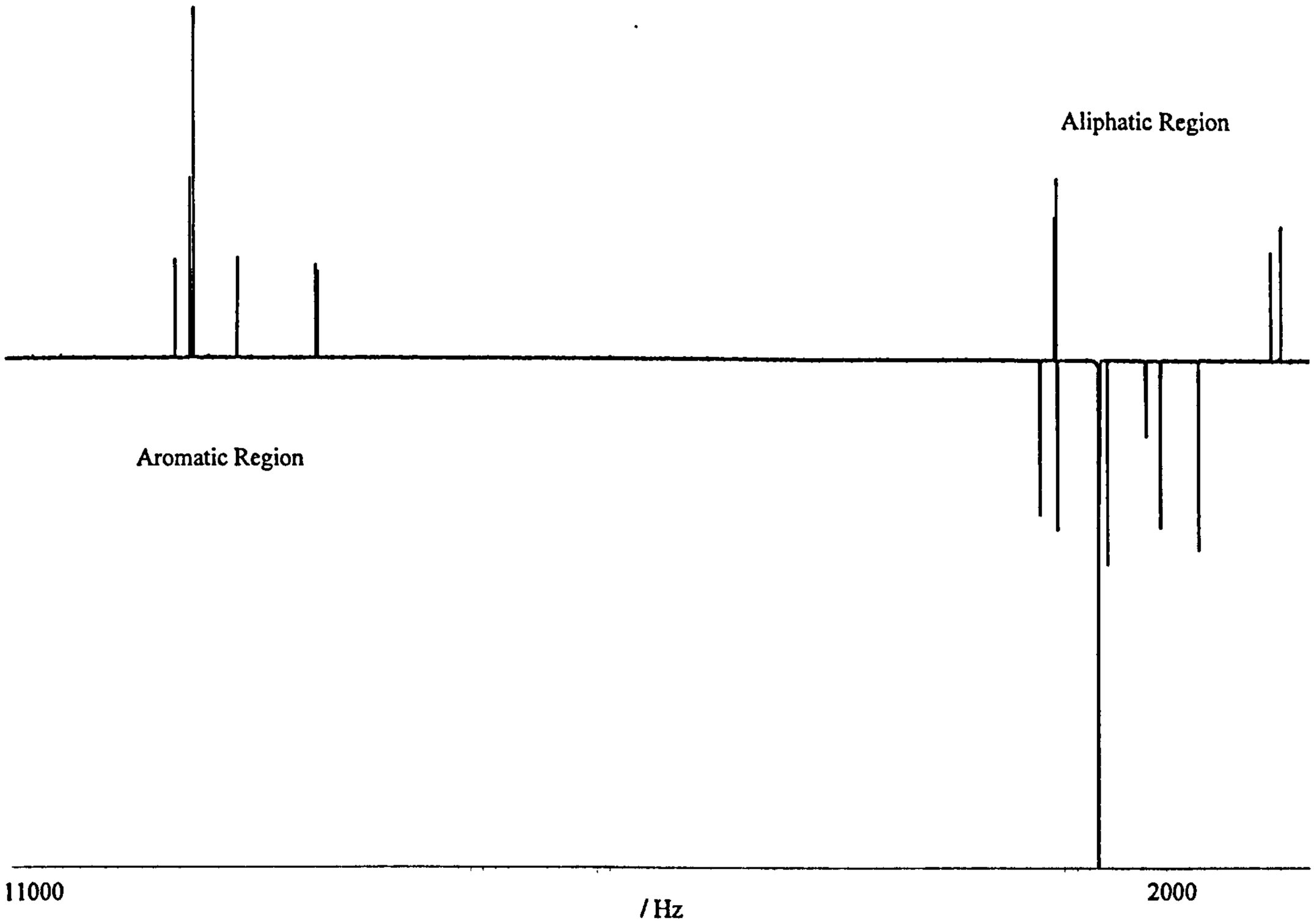

Figure 10 ^{13}C-{^{1}H} DEPT 135° I52 / $CDCl_3$. CH_2 reversed C removed.

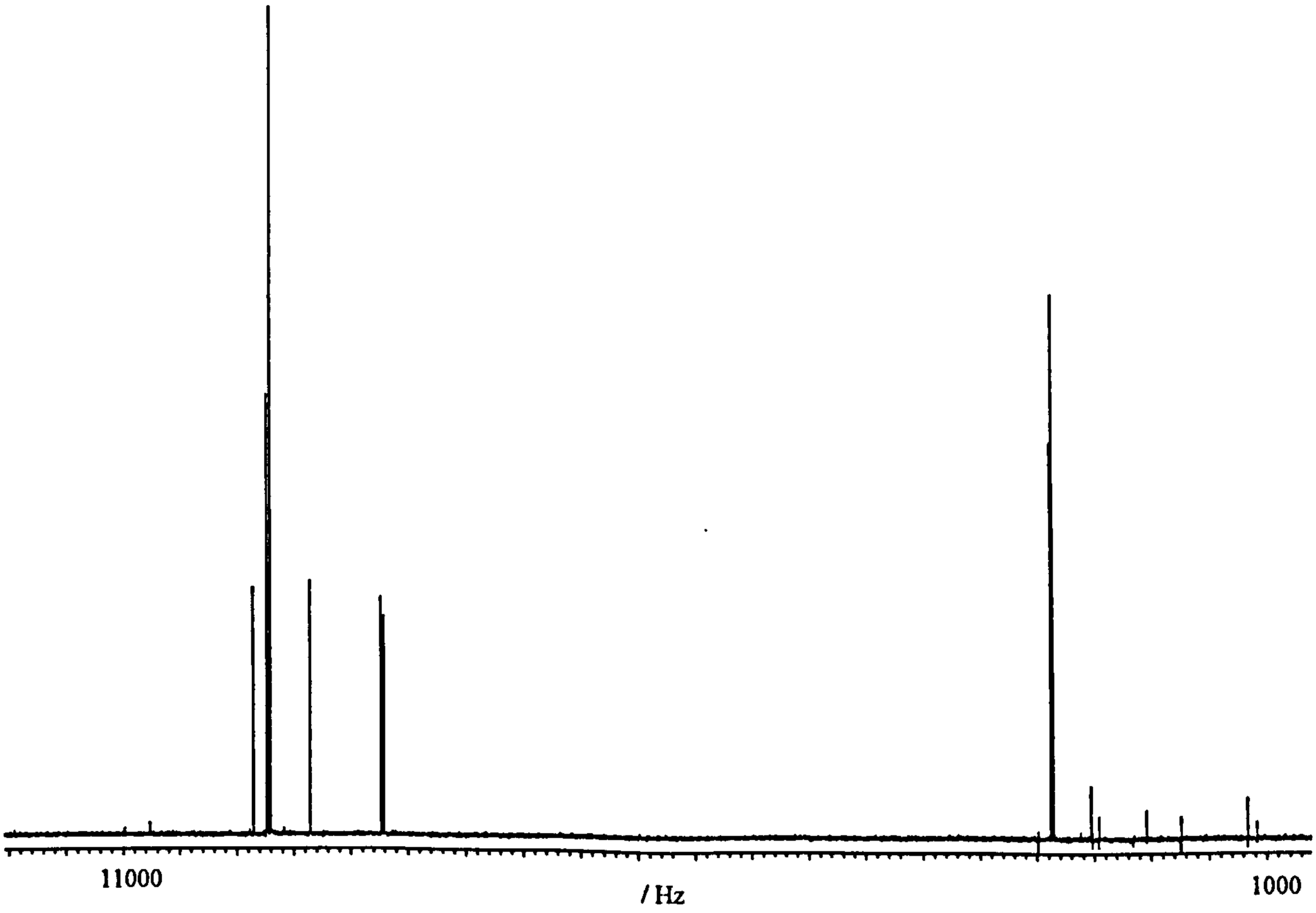

Figure 11 ^{13}C-{^{1}H} DEPT 90° I52 / $CDCl_3$. CH_1 only.

spectra was completed in the same way as for I35. The DEPT spectra which were used to assign the types of carbon atom are given in figures 10 and 11.

6.2.5 The ^{13}C-{^{1}H} NMR Spectra of I35 in the Nematic Phase.

Two different samples of I35 were used, one with 10% w/w HMDSO and one with 10% w/w benzene. The crystal-nematic transition T_{NK} for pure I35 occurs at >300K, and so it is necessary to perform NMR at higher than room temperature for the nematic phase. The sample, once nematic, is viscous and so alignment is slow in the magnetic field. This may lead to line broadening if the spectra are acquired too soon after sample insertion into the magnetic field and so hexamethyldisiloxane (HMDSO) was added to reduce the viscosity of the sample. Addition of HMDSO also results in the lowering of T_{NK} which prevents recrystallisation of the sample at room temperature and so it is possible to record spectra at lower temperatures, which consequently increases the magnitudes of the splittings in the liquid crystal spectrum. HMDSO also gives rise to a sharp single peak in the ^{13}C-{^{1}H} NMR spectrum which may be used for reference. Another sample was prepared which contained benzene, again to lower the melting point, but it also gives a strong ^{1}H signal with sharp lines from which it is possible to optimise the homogeneity of the magnetic field more effectively. On the down side, benzene also gives rise to strong line in the ^{13}C-{^{1}H} NMR spectrum which interferes with the aromatic region of I35. Once the conditions were optimised a range of ^{13}C-{^{1}H} NMR spectra of I35 were acquired.

Figure 2 compares the ^{13}C-{^{1}H} NMR spectra of I35 / HMDSO using COMARO-2 proton decoupling and I35 / benzene using SL-2 proton decoupling. Here the importance of the choice of the correct decoupling sequence is vital in the acquisition of useful NMR spectra depending on which type of carbon atom we are interested in, aliphatic or aromatic. From Figure 2 it can be seen that SL-2 decoupling sequence gives good NMR spectra for the aliphatic region compared to the spectrum using COMARO-2 ^{1}H decoupling. The lines from the aromatic region also appear to be well resolved, however, there are pairs of lines missing from this spectrum corresponding to C2, C3 and C4. It is uncertain why this should happen, however, it may be due to the large values of both C-F and H-F dipolar couplings. It is suspected that the missing lines have been broadened beyond detection from the baseline. Enough information can be extracted, however, so that the data from the SL-2

experiment may be scaled to the data from COMARO-2 to give a consistent set of D_{ij}^{CF} by comparing the magnitude of the splittings measured in both experiments.

Given that we have well resolved spectra in both regions, it is possible to proceed with the assignment and subsequent analysis to determine the dipolar couplings, D_{ij}^{CF}. As discussed in chapters 3 and 4, VASS spectra may be used to achieve the assignment of the spectrum of a static sample, through observation of the shifting line positions with θ, and extrapolating to their positions in the static sample. In this case, however, the extrapolation of the shifting transitions through $0° < \theta < 54.7°$, is more difficult as the VASS probe only allows the exploration of the range $40° < \theta < 54.7°$, the spectra from which are shown in figures 12 and 13. The evidence in chapters 3 and 4 suggests that the anisotropy in the chemical shifts, δ_C^{aniso}, is linear with respect to the reduction factor, $R=(3\cos^2\theta-1)/2$, and it should therefore be possible to extrapolate from $\theta = 40°$ to $\theta = 0°$. Figures 14 and 15 show the chemical shift anisotropy, measured as the centre of the ^{13}C-^{19}F doublets, from I35 through the range $40° < \theta < 54.7°$, which shows the linearity of the data as expected.

The extrapolation of the transitions from the VASS spectra to the static spectrum was, however, not precise. The final values of the couplings were obtained by fitting the spectral envelope to the superposition of the doublets using the program WINFIT (Bruker). In the case of the aromatic region, only slight adjustments were required and the spectrum was successfully assigned, as shown in figure 16. Although the VASS spectra using SL-2 ^1H decoupling are relatively well resolved in the aliphatic region, some peaks are of low intensity and are not easily observed, which leads to ambiguities in the assignment, especially in areas of overlapping peaks. The best assignment of the static spectrum is given in figure 17, and was achieved through cross examination of the NMR experiments and the results of the conformational distribution modelling as described later.

Once the complete assignment was achieved, the line splittings were measured and the total interaction, T_{ij}, was obtained. Although there may be some solvent effects on the value of the scalar couplings and an anisotropy in the scalar coupling constant, these are assumed to be small and are neglected. The final D_{ij}^{CF} for the whole molecule are reported in table 1.

The VASS spectra from the aromatic region also confirm the absolute signs of the couplings. The magnitude of J_{ij}^{CF} are measured directly from the spectrum of I35 in

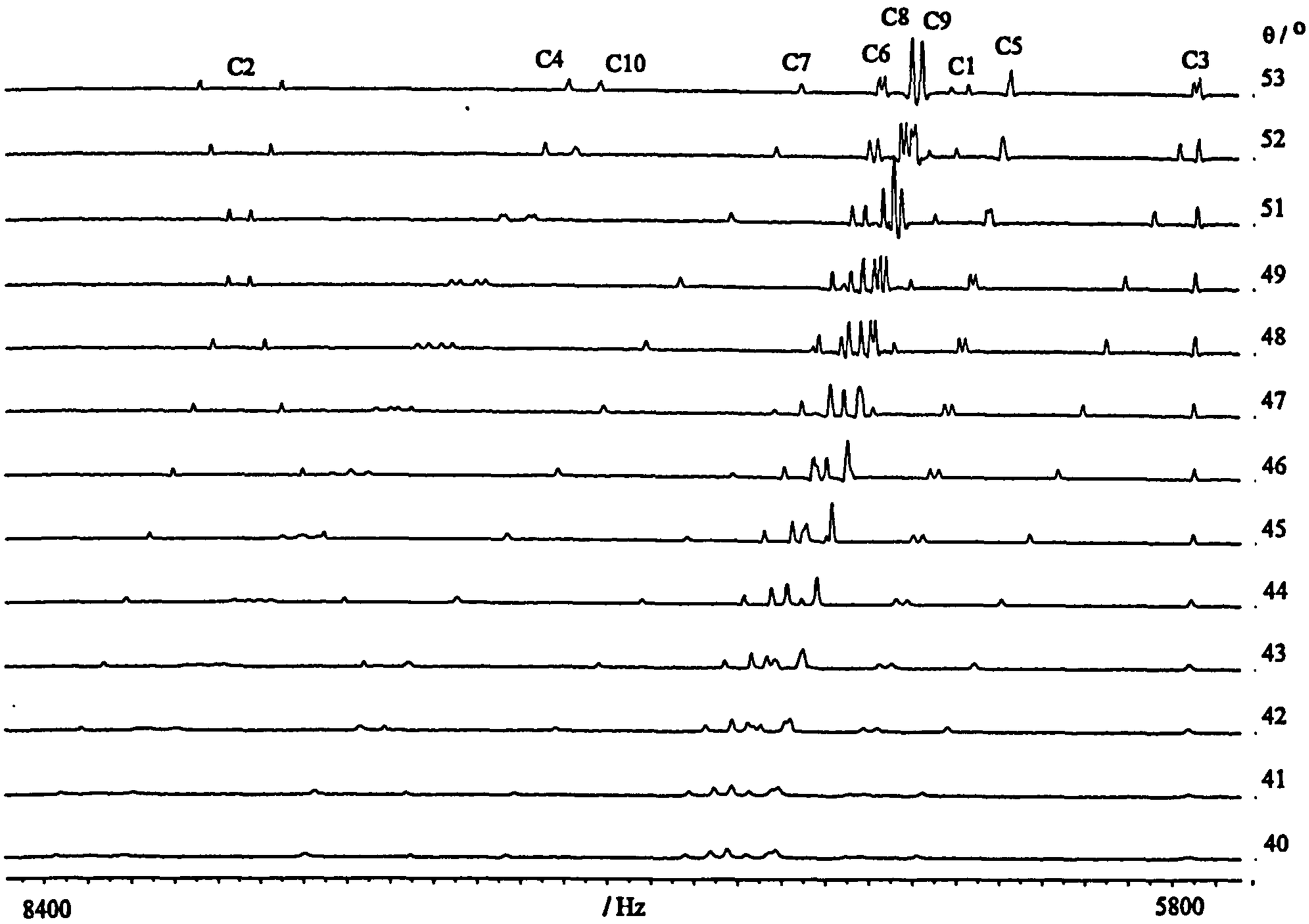

Figure 12 50.3 MHz ^{13}C-{^{1}H} VASS NMR spectra of I35 / HMDSO - expansion of the aromatic region.

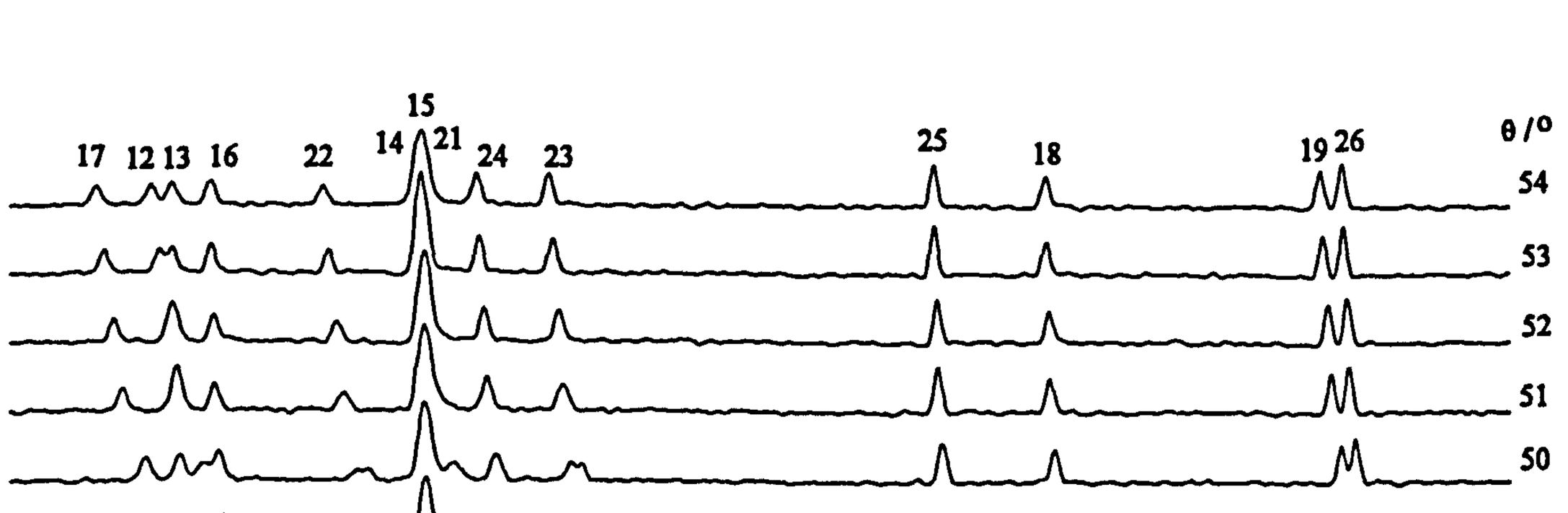

Figure 13 50.3 MHz ^{13}C-{^{1}H} VASS NMR spectra of I35 / benzene using SL-2 pulse sequence - expansion of the aliphatic region.

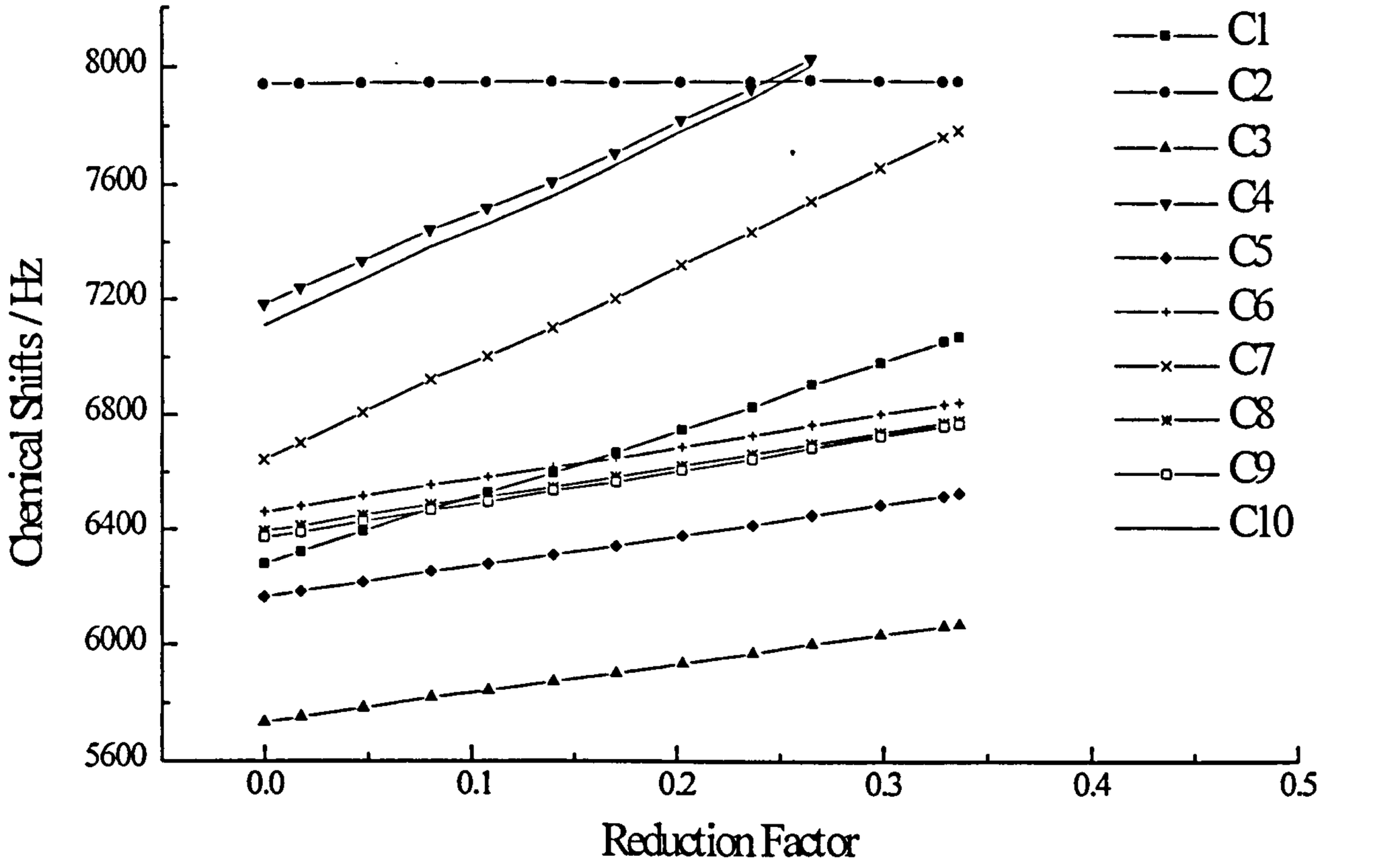

Figure 14 Anisotropy in the aromatic ^{13}C chemical shifts of I35.

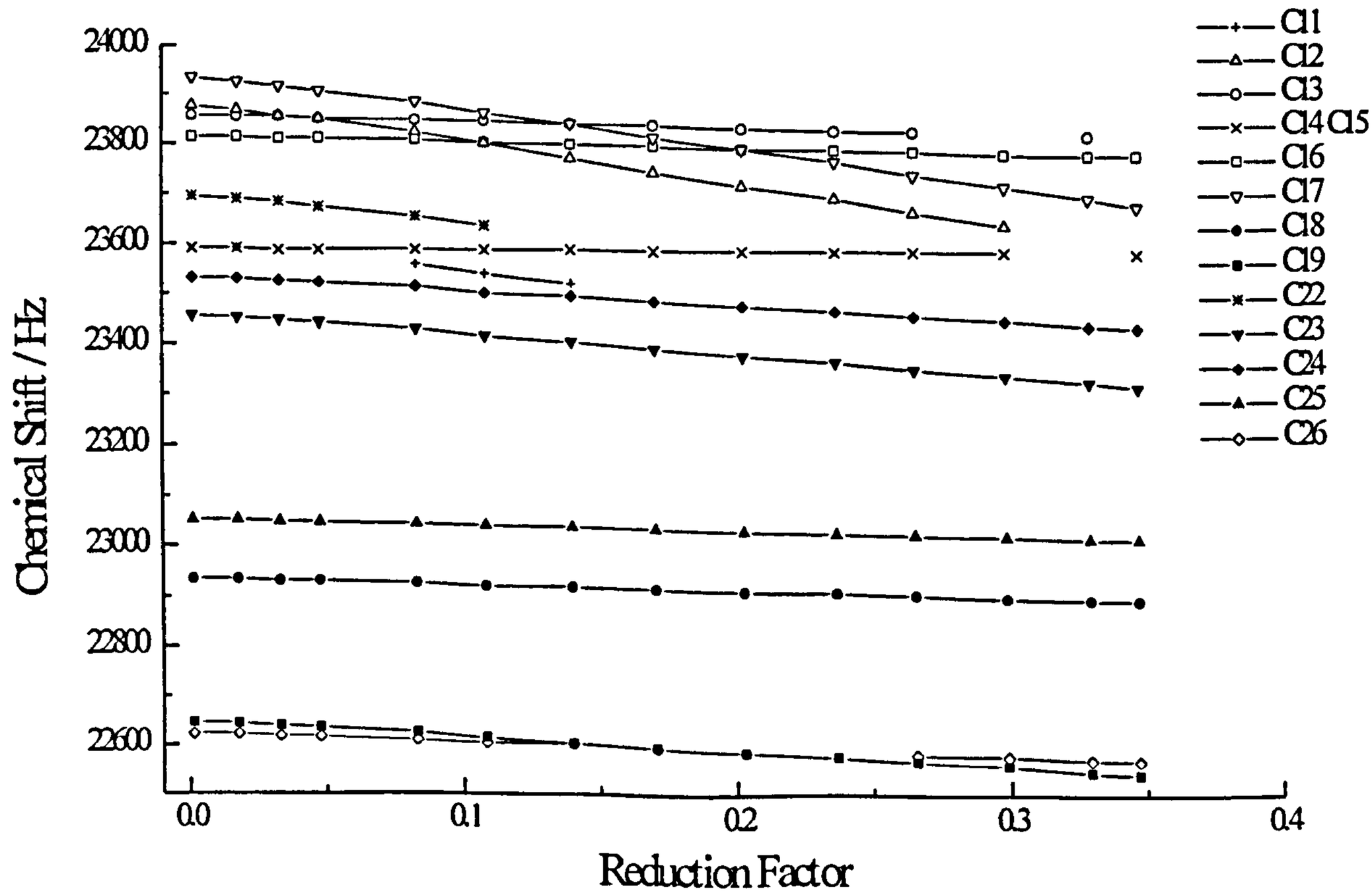

Figure 15 Anisotropy in the aliphatic ^{13}C chemical shifts of I35.

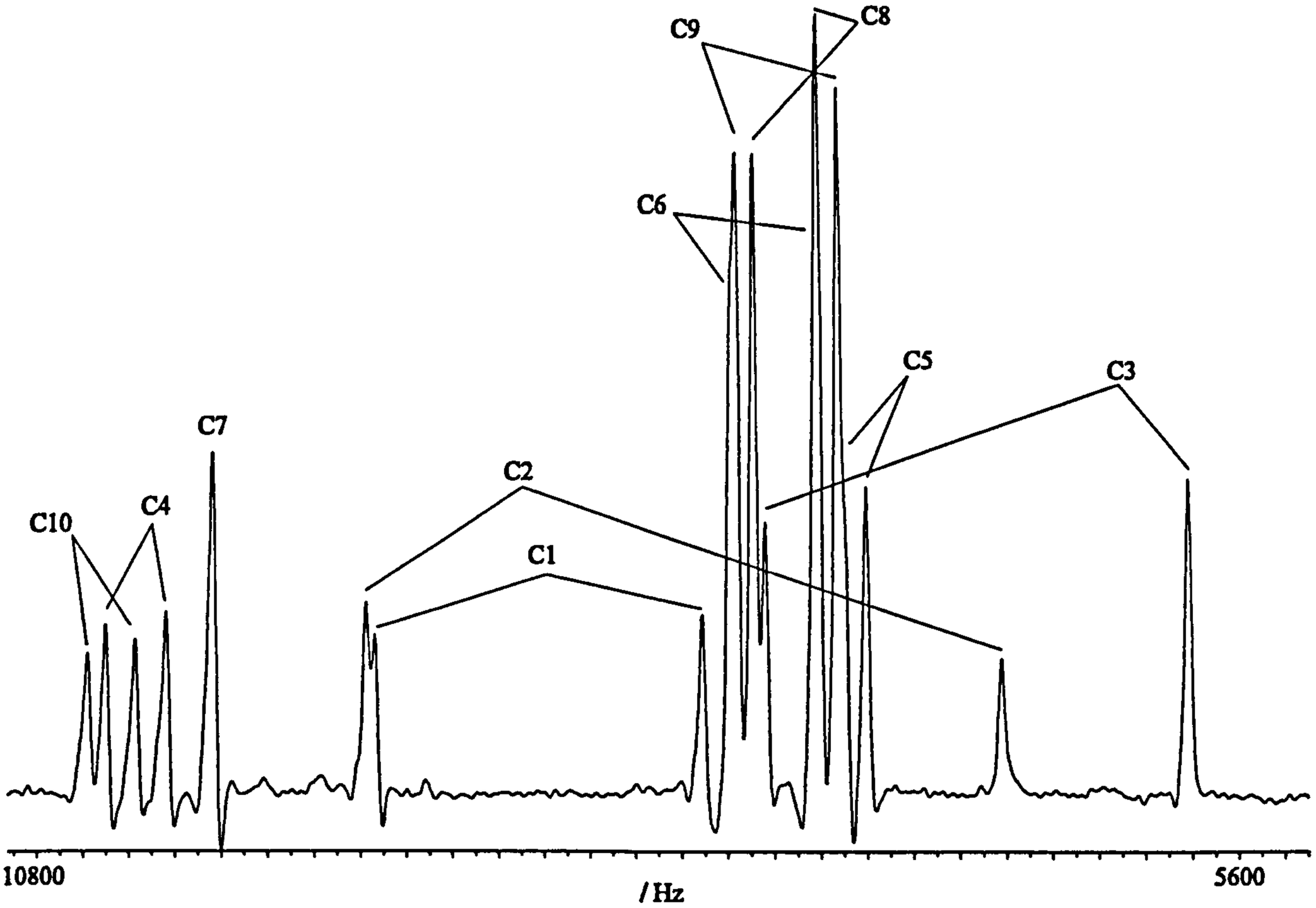

Figure 16 Assignment of the ^{13}C-{^{1}H} NMR spectrum of the aromatic region in the static sample of I35 / HMDSO using COMARO-2 decoupling sequence.

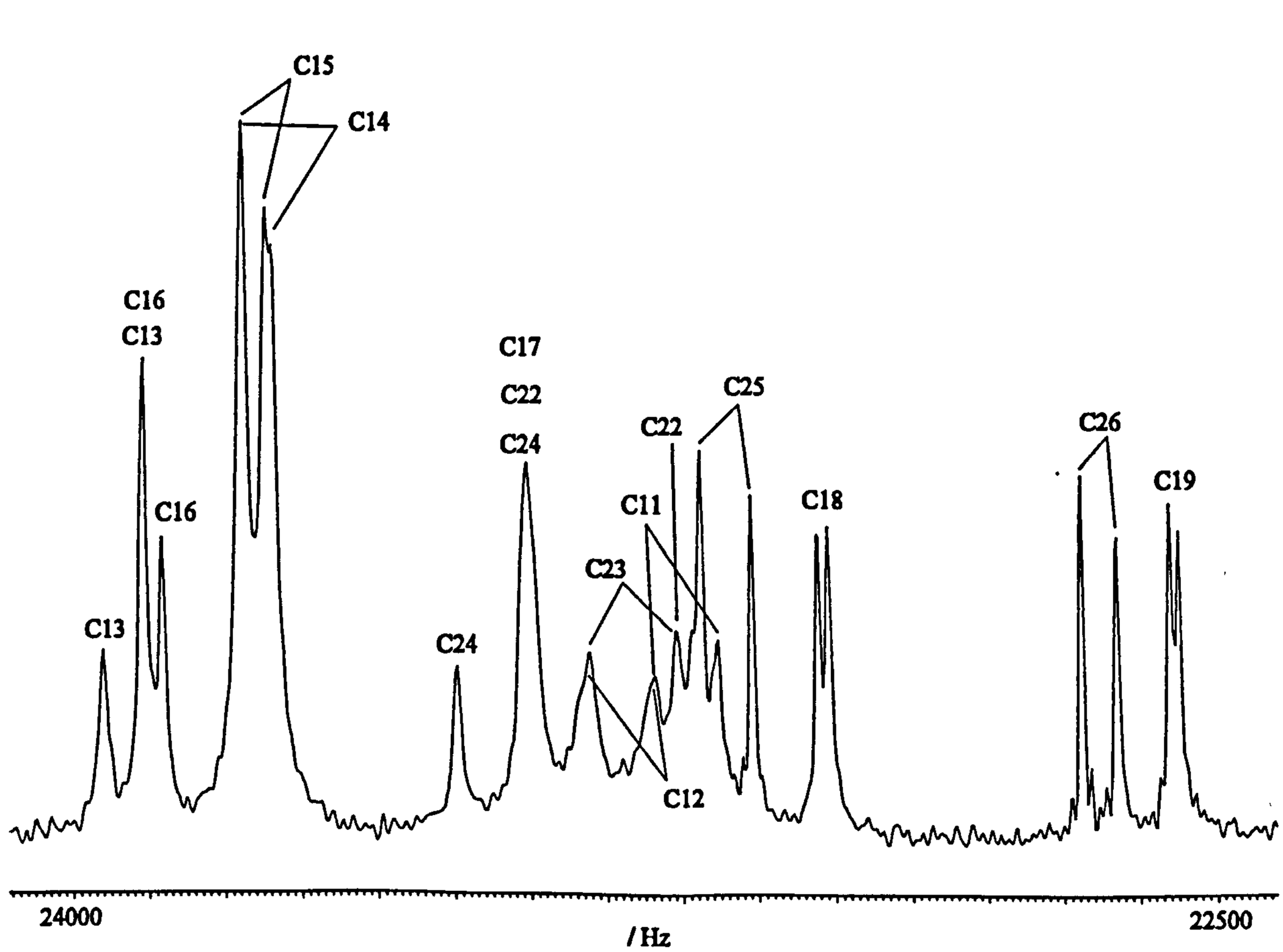

Figure 17 Assigment of the ^{13}C-{^{1}H} static NMR spectrum of the aliphatic region of I35 / benzene using SL-2 proton decoupling.

isotropic solution, however, information regarding the sign of these couplings is not obtained. In chapters 3 and 4, it has been shown that the evolution of the carbon multiplets through changing θ yields the relative signs of the D_{ij}^{CF} and the J_{ij}^{CF}. As mentioned earlier the spectrum of I35, an AX spin system, consists simply of doublets whose splitting, T_{ij}^{CF}, is

$$T_{ij}^{CF} = 2D_{ij}^{CF} + J_{ij}^{CF} \qquad (1)$$

In cases where D_{ij}^{CF} and J_{ij}^{CF} are of opposite sign, T_{ij}^{CF} decreases and passes through zero as θ moves away from the magic angle as $|D_{ij}|$ increases before re-emerging as a doublet dominated by $|D_{ij}^{CF}|$. This is clearly the case for C2 as can be seen in figure 7. The same behaviour should be also be seen with C3 and C4, however, the range of VASS spectra do not clearly show this behaviour. This behaviour can, however, be confirmed by comparing the splitting in the isotropic spectrum to the splittings in the VASS spectrum at θ=53°. The splittings are reduced for C3 and C4 in the VASS spectrum which shows that D_{ij}^{CF} has reduced $|T_{ij}^{CF}|$ and is therefore of opposite sign to J_{ij}^{CF}. In cases where D_{ij}^{CF} and J_{ij}^{CF} are of the same sign, T_{ij}^{CF} increases with θ. The splitting of C1 and C6 show definite increases in the splitting at θ=53° compared to those in isotropic solution. In the cases where no J_{ij}^{CF} is measurable from the spectrum of I35 in isotropic solution, it is not possible to determine the absolute signs of the D_{ij}^{CF}. This problem is dealt with in the structure determination from which order parameters are obtained from which it is possible to calculate the absolute values of D_{ij}^{CF}.

6.2.6 The ^{13}C-{^{1}H} NMR Spectra of I52 in the Nematic Phase.

The analysis procedure of the spectrum of the static sample of I52 was completed in a similar fashion to that of I35. Further experiments were carried out on a static sample of I52 / HMDSO using a range of ^{1}H decoupling pulse sequences, shown in figure 3. From these results it was decided that the NANZ-2 pulse sequence gave the best spectra in the aromatic region while SL-2 remained the best sequence to obtain good spectra for the aliphatic region. As with I35, the data obtained using SL-2 is scaled to match the data obtained from the spectrum using NANZ-2, in order to obtain a consistent set of couplings.

Table 1. The values of J_{ij}^{CF}, D_{ij}^{CF} and δ_C^{aniso} obtained from the analysis of the ^{13}C-{^1H} NMR spectra of I35 with 10% HMDSO.

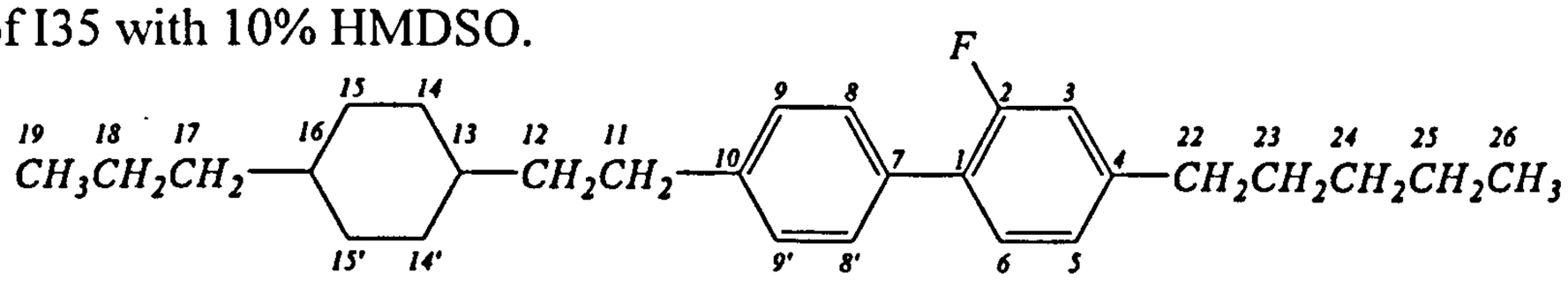

i	J_{iF} / Hz	D_{iF} / Hz	δ_C^{aniso} / Hz
1	13.3 ± 0.5	705.4 ± 2.0	2361.8 ± 15.2
2	-247.3 ± 0.5	1502.1 ± 2.0	54.8 ± 5.7
3	22.3 ± 0.5	-922.7 ± 2.0	1002.0 ± 6.7
4	7.6 ± 0.5	-135.8 ± 2.0	3167.5 ± 29.2
5	3.1 ± 0.5	45.4 ± 2.0	1089.2 ± 8.0
6	4.2 ± 0.5	179.9 ± 15.0	1152.5 ± 6.7
7	1.1 ± 0.5	0.0 ± 10.0	3414.3 ± 22.1
8	2.8 ± 0.5	-216.5 ± 15.0	1167.1 ± 8.5
9	-	-139.9 ± 2.0	1197.5 ± 7.5
10	-	-105.1 ± 2.0	3351.6 ± 30.4
11	-	(-)42 ± 20.0	-595 ± 32
12	-	(-)38.5 ± 5.0	-832 ± 12
13	-	(-)26 ± 2.0	-136 ± 3
14	-	(-)21.5 ± 2.0	-33 ± 2
15	-	(-)13.5 ± 2.0	-33 ± 2
16	-	(-)12.5 ± 2.0	-128 ± 3
17	-	(-)1 ± 10.0	-766±7
18	-	(-)7 ± 2.0	-132±2
19	-	(-)6 ± 2.0	-306±4
22	-	(-)102 ± 5.0	-574 ± 35
23	-	(-)73.5 ± 2.0	-419 ± 4
24	-	(-)51.5 ± 2.0	-304 ± 4
25	-	(-)33.5 ± 2.0	-122 ± 2
26	-	(-)23 ± 2.0	-158 ± 5

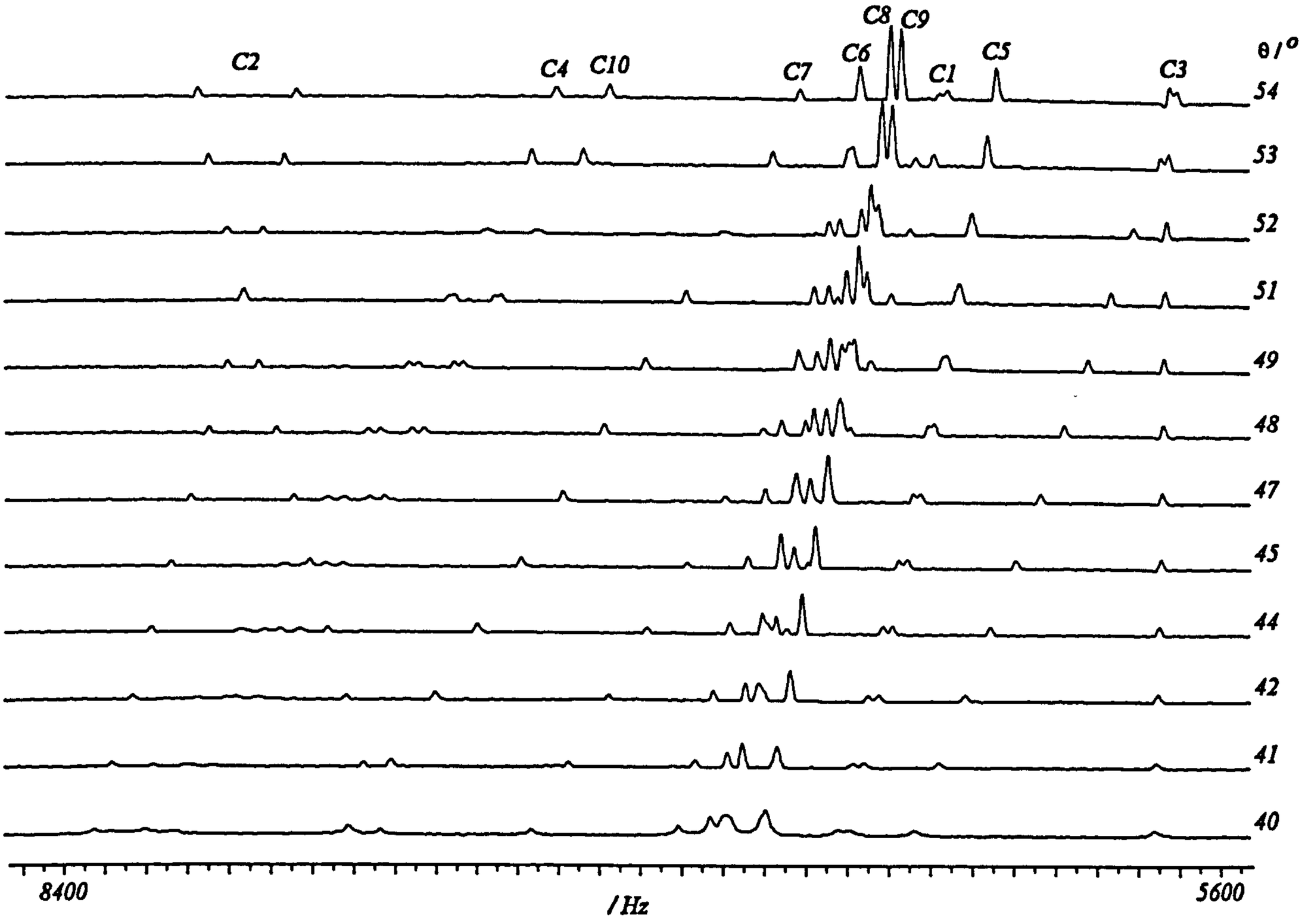

Figure 18 50.3 MHz 13C-{1H} VASS NMR spectra of the sample of I52 / HMDSO using NANZ-2 proton decoupling. Expansion of the aromatic region.

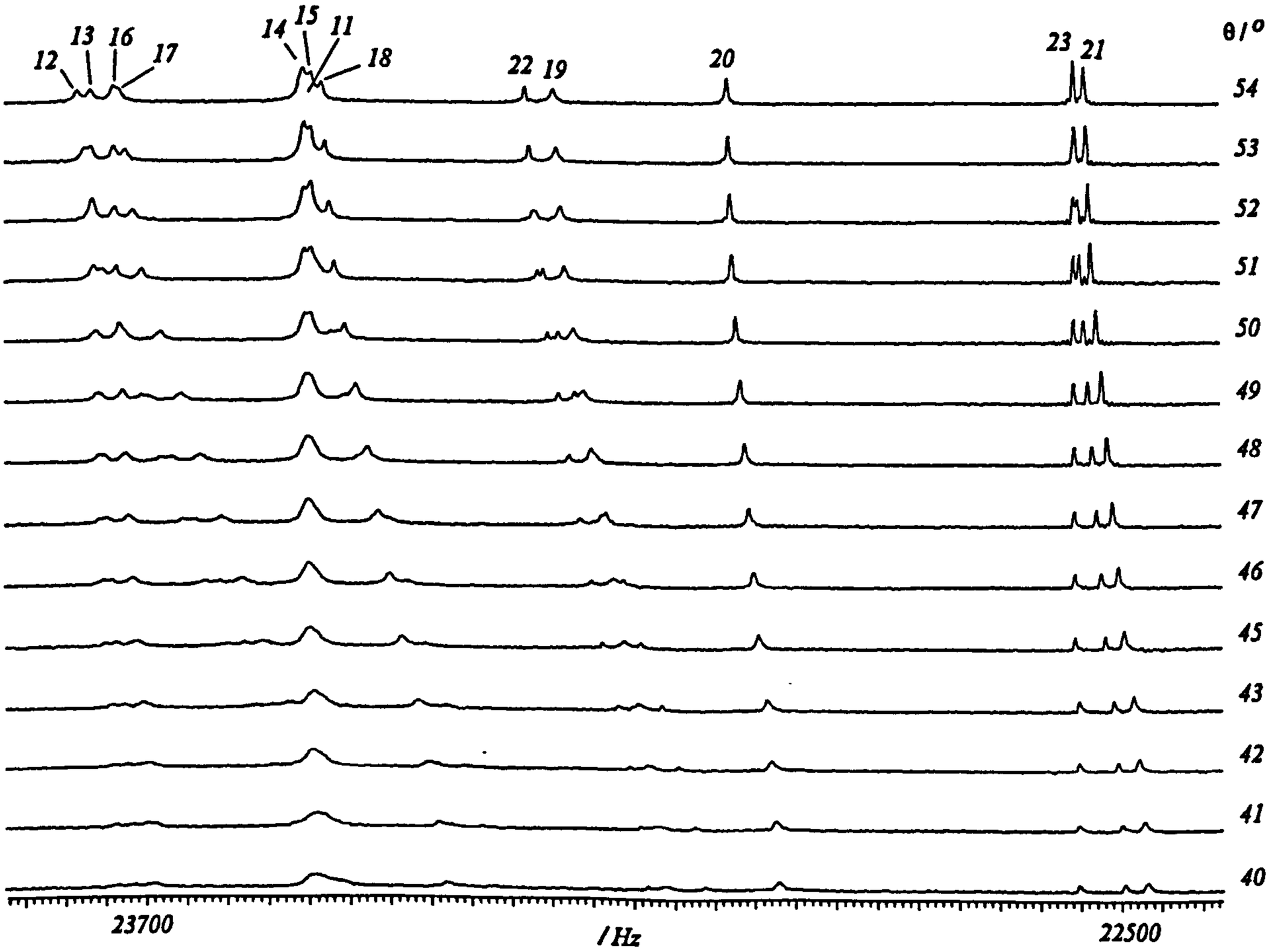

Figure 19 50.3 MHz ^{13}C-{^{1}H} VASS NMR spectra of the sample of I52 / HMDSO using SL-2 proton decoupling. Expansion of the aliphatic region.

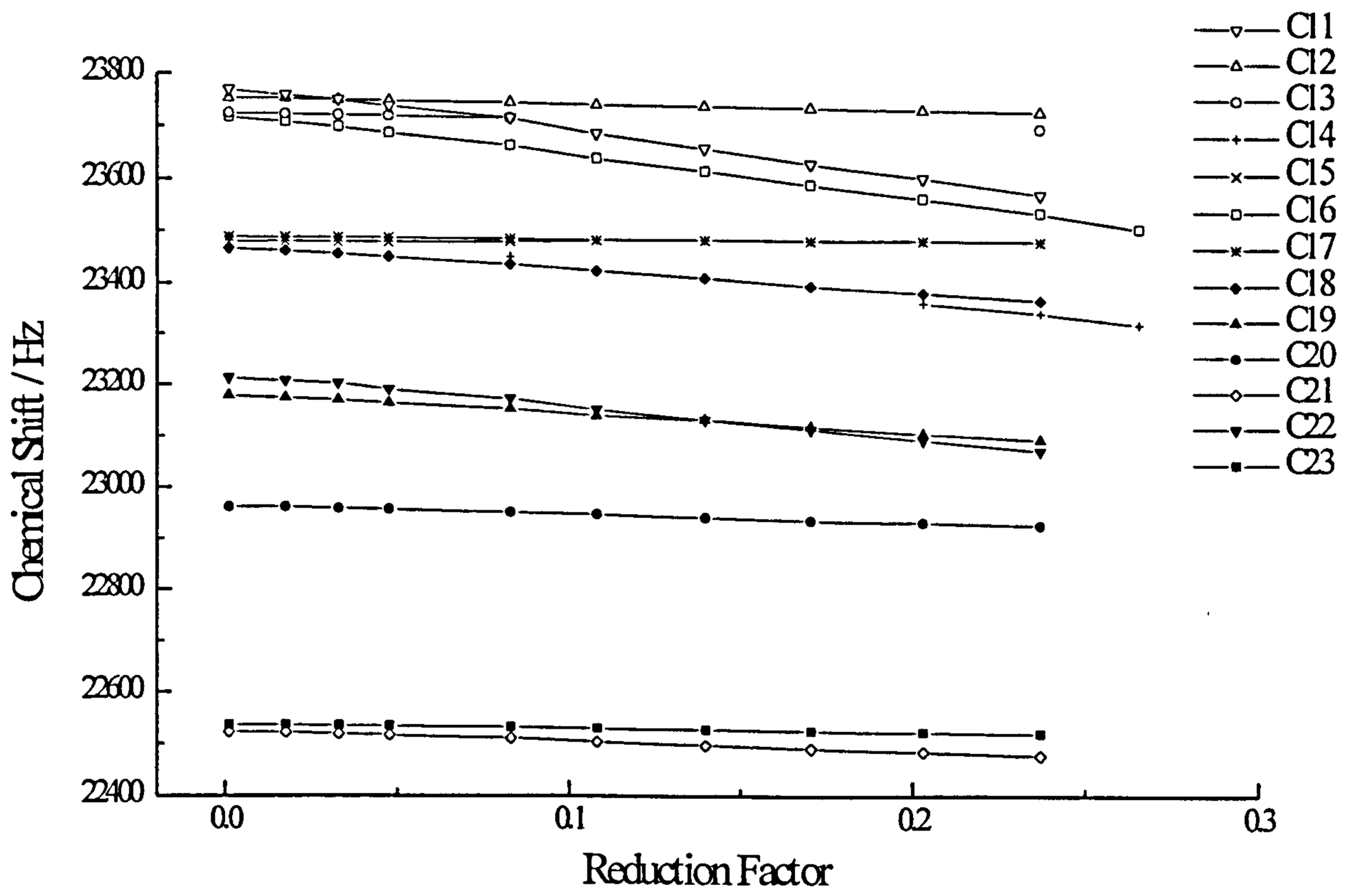

Figure 20 Anisotropy in the aliphatic ^{13}C chemical shifts of I52.

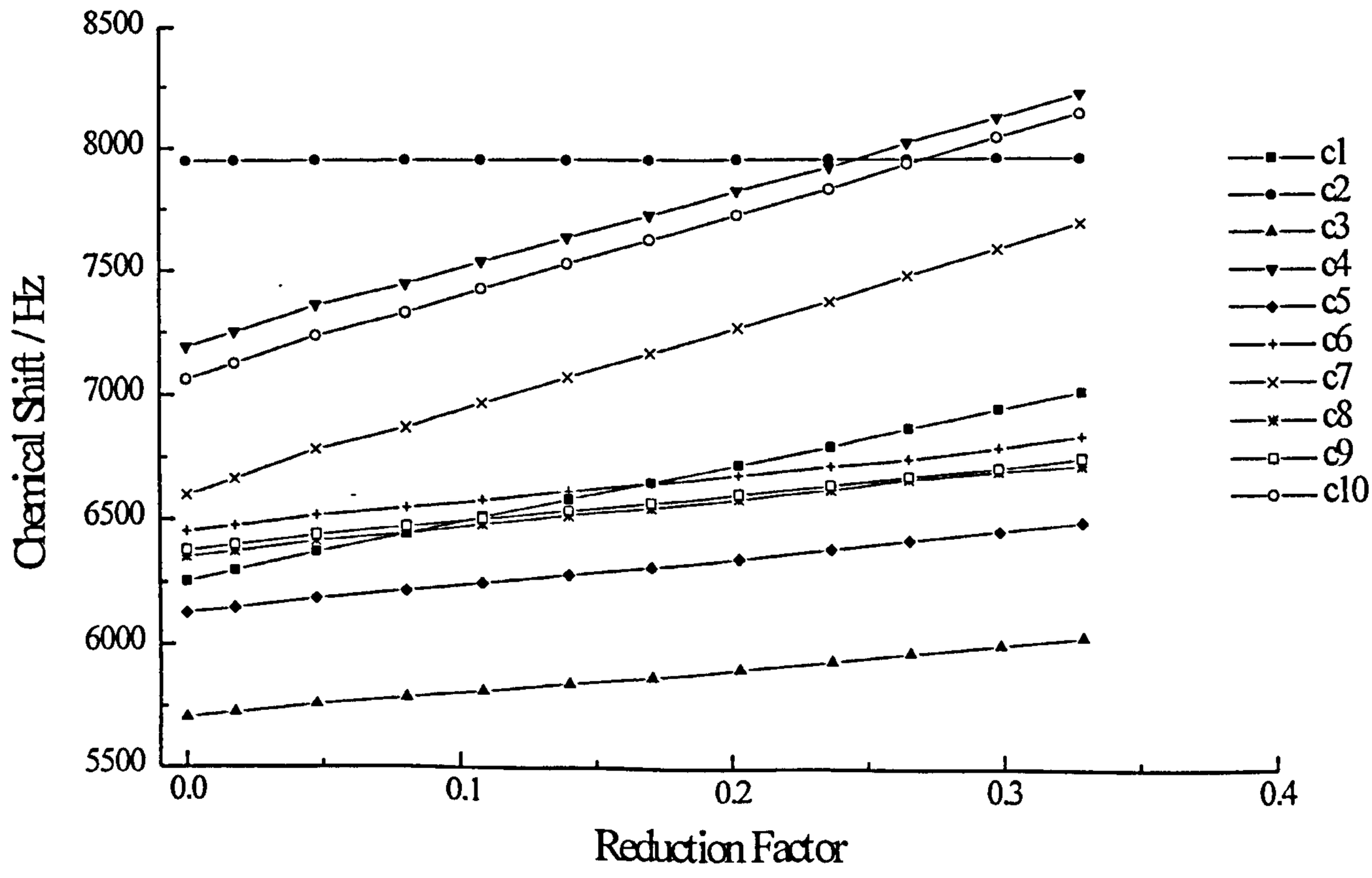

Figure 21 Anisotropy in the aromatic ^{13}C chemical shifts of I52.

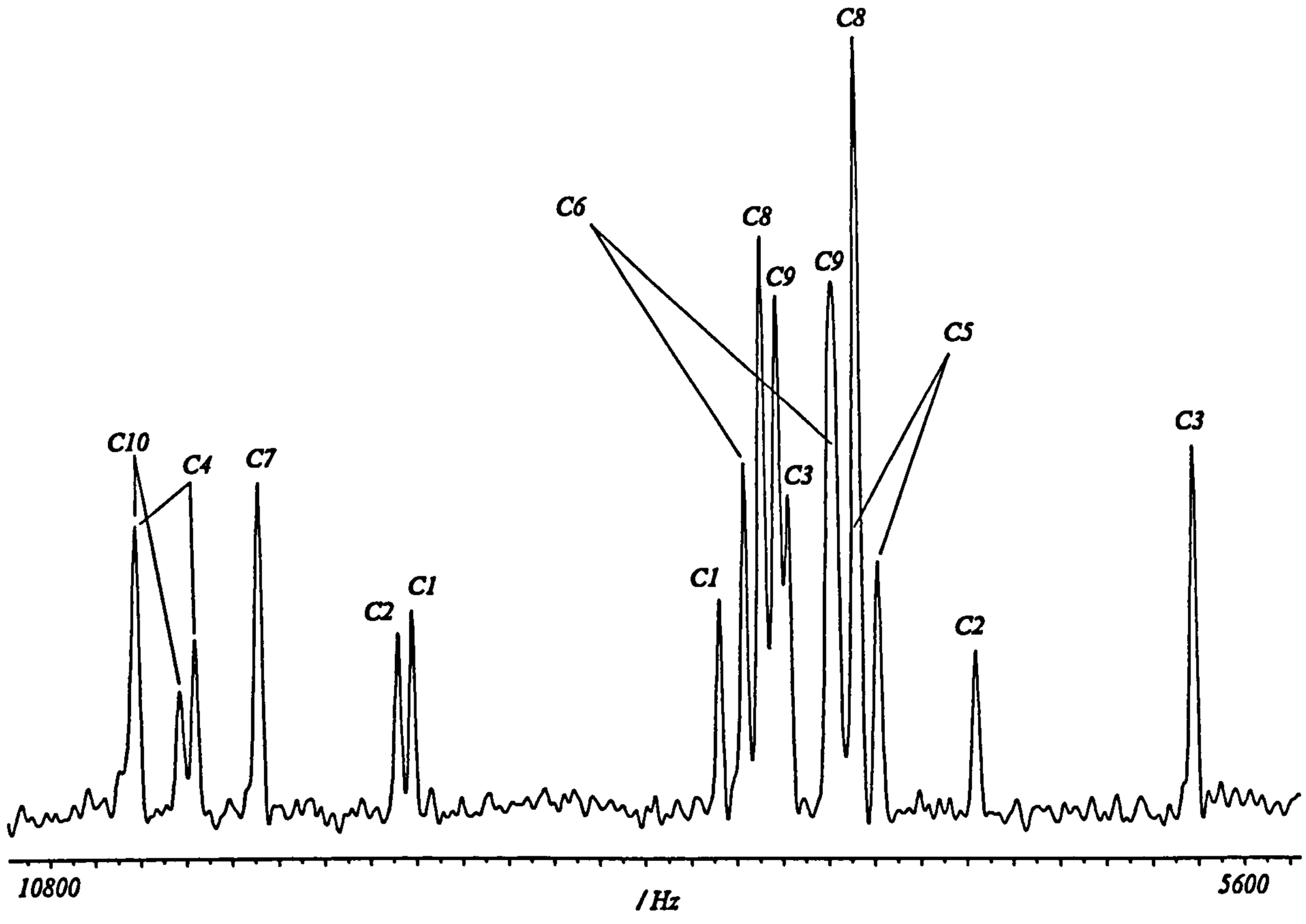

Figure 22 Assignment of the ^{13}C-{^{1}H} NMR spectrum of the aromatic region in the static sample of I52 / HMDSO using NANZ-2 decoupling sequence.

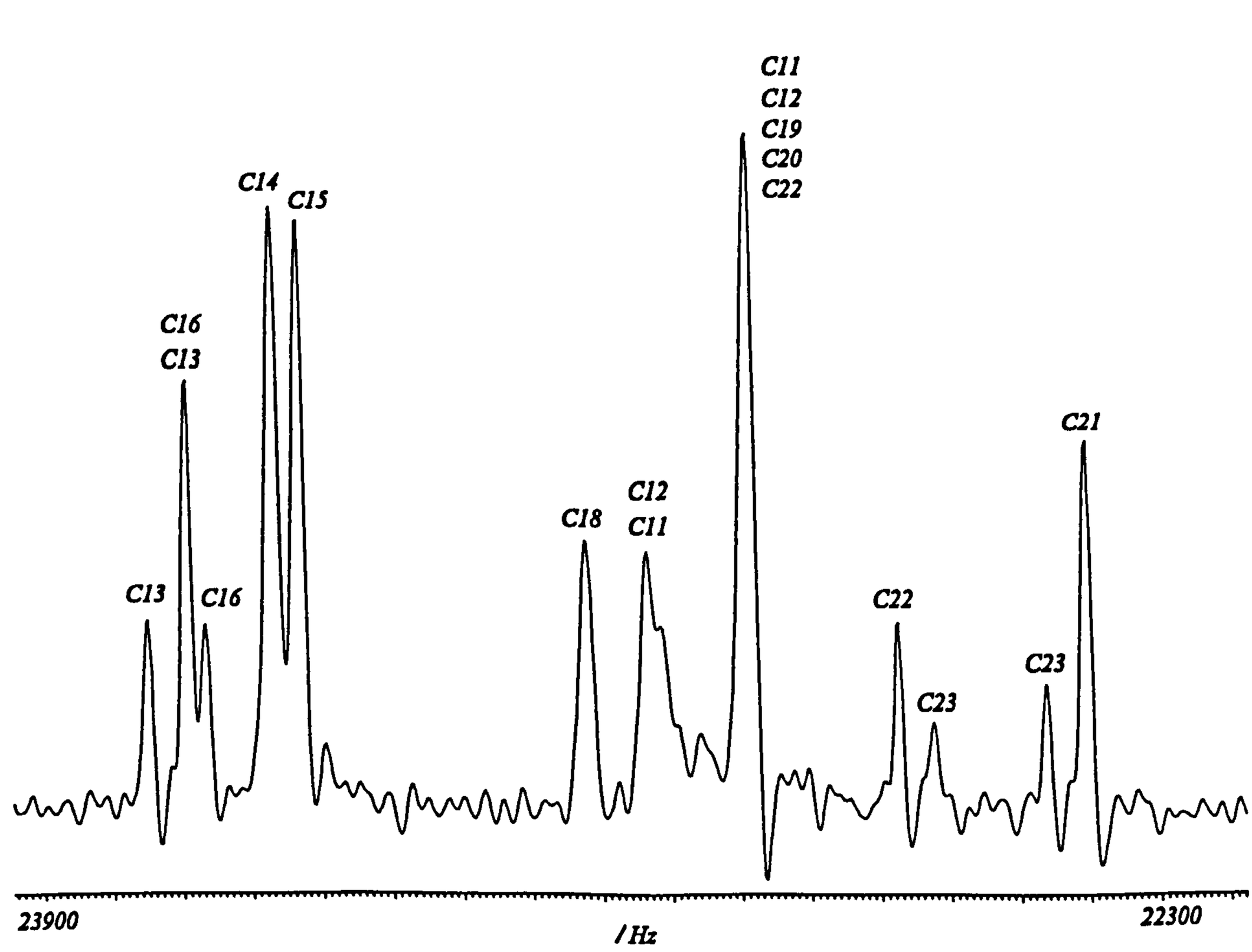

Figure 23 Assigment of the ^{13}C-{^{1}H} static NMR spectrum of the aliphatic region of I52 / hmdso using SL-2 proton decoupling.

Table 2. The values of J_{ij}^{CF}, D_{ij}^{CF} and δ_C^{aniso} obtained from the analysis of the ^{13}C-{^1H} NMR spectra of I52 with 10% HMDSO.

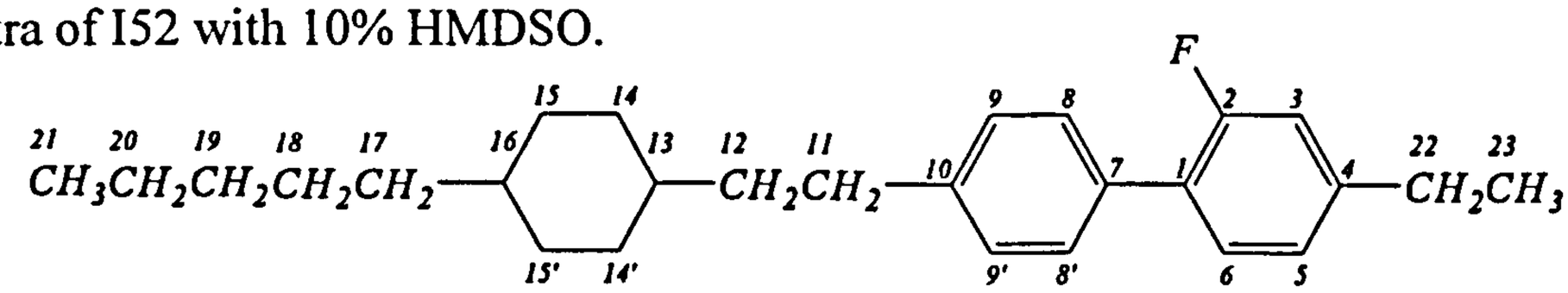

i	J_{iF} / Hz[a]	J_{iF} / Hz[b]	D_{iF} / Hz	δ_C^{aniso} / Hz
1	13.1 ± 0.5	13.3 ± 2.0	666.1 ± 2.0	2312.1 ± 9.8
2	-247.3 ± 0.5	-246.0 ± 2.0	1381.9 ± 2.0	65.1 ± 3.1
3	22.1 ± 0.5	22.6 ± 2.0	-888.4 ± 2.0	1004.5 ± 6.6
4	7.3 ± 0.5	7.3 ± 2.0	-131.4 ± 2.0	3137.1 ± 17.1
5	2.5 ± 0.5	-	41.6 ± 2.0	1105.1 ± 6.6
6	3.3 ± 0.5	3.4 ± 2.0	183.1 ± 2.0	1141.8 ± 12.6
7	-	-	0.0 ± 10.0	3309.8 ± 19.7
8	2.6 ± 0.5	-	-205.4 ± 2.0	1142.0 ± 12.3
9	-	-	-126.8 ± 2.0	1118.5 ± 7.8
10	-	-	-102.0 ± 2.0	3293.0 ± 15.3
11	-	-	(-)25 ± 5.0	-706 ± 17
12	-	-	(-)53 ± 5.0	-846 ± 19
13	-	-	(-)27 ± 2.0	-106 ± 3
14	-	-	(-)23 ± 2.0	-28 ± 1
15	-	-	(-)15 ± 2.0	-28 ± 1
16	-	-	(-)12 ± 2.0	-120 ± 3
17	-	-	(-)10 ± 3.0	-792 ± 13
18	-	-	(-)6 ± 2.0	-423 ± 6
19	-	-	(-)10 ± 3.0	-363 ± 7
20	-	-	(-)2.5 ± 2.0	-155 ± 4
21	-	-	(-)4.5 ± 2.0	-222 ± 5
22	-	-	(-)104 ± 4.0	-614 ± 12
23	-	-	(-)82 ± 2.0	-71 ± 2

[a] measured from isotropic sample of I52 dissolved in $CDCl_3$ at 300K

[b] measured from isotropic sample of I52 / HMDSO at 350K

The assignment of the static spectrum, however, must be analysed using the same technique of VASS NMR to extrapolate the line positions from the assigned spectrum in isotropic solution. Figures 18 and 19 show the ^{13}C-{^{1}H} VASS NMR spectra in the range $40° \leq \theta \leq 54°$. The shifting line positions were monitored and the anisotropy in the chemical shifts determined, as shown in figures 20 and 21. These were used to extrapolate the line positions to and adjusted to match the static spectrum, as shown in figures 22 and 23. The splittings were measured and the D_{ij}^{CF} obtained are reported in table 2.

6.3 Derivation of the Structure of I35 and I52

The structure chosen for I35 and I52 was based on the Molecular Orbital structure of 2-fluorobiphenyl, determined by Edgar and shown in figure 24, for the aromatic region and an average of the bond lengths and angles found for aliphatic chains, in ethylbenzene and 5CB, the structure of the cyclohexyl group and attached chains was that from the X-ray study of CCH3.

$$\rho = \begin{matrix} 1.332 \text{ X } MO \\ 1.35 \text{ X } optimised \end{matrix} \qquad X = Å$$

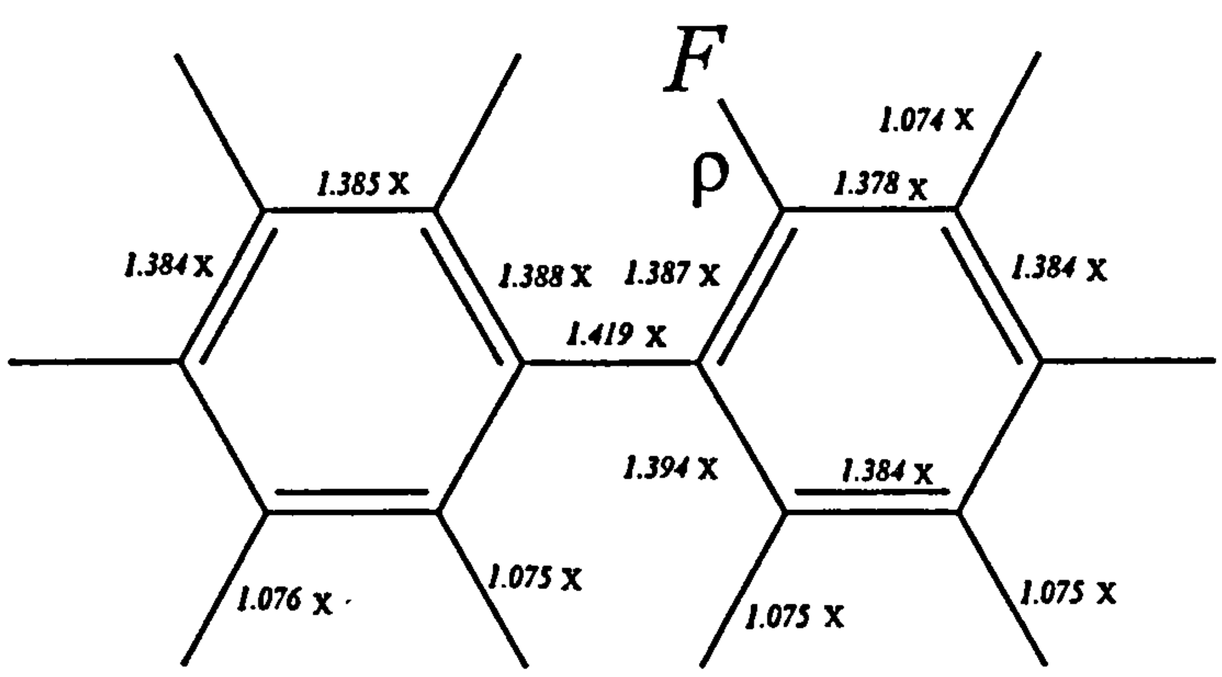

$$\gamma = \begin{matrix} 119.4° \ MO \\ 120.2° \ optimised \end{matrix}$$

Figure 24 The structure of the 2-fluorobiphenyl sub unit from MO calculation, and subsequent optimisation of the fluorine position from D_{ij}^{CF} obtained from both I35 and I52.

6.3.1 The Structure of the Rigid Fragment Containing the F atom

The rigid fragment is shown in figure 25. Ten D_{iF}^{CF} were measured, but these depend on fifteen atomic coordinates and three order parameters. We clearly do not have enough data to allow all these to vary, so the carbon geometry is assumed to be correct while an attempt was made to optimise the geometry by changing the fluorine position and the order

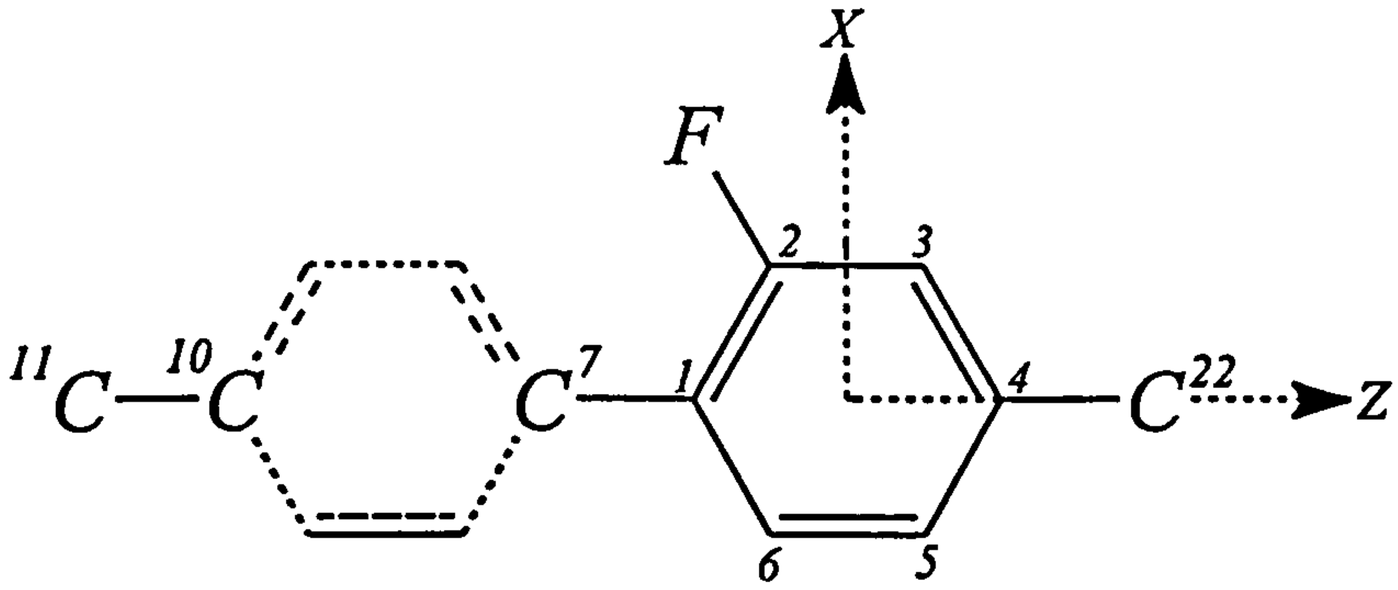

Figure 25 Structure of the rigid fragment

parameters only. For the optimisation r_{CF} was kept fixed at 1.35Å and allowed to rotate about C2 in the XZ plane. The ring-chain C-C bond lengths $r_{4,22}$ and $r_{10,11}$ were kept fixed at 1.53Å .The optimised geometry is given in table 3. The indication that the optimised geometry, for I35, is correct comes from the calculated value of $D_{7,F}^{CF}$. The line from C7 was not resolved in the liquid crystal spectrum and so $D_{7,F}^{CF} = 0 \pm 10$ Hz. The original MO structure requires this value to equal 27Hz, while the optimised structure gives 2 Hz without being included as a constraint in the fit. For the I35 data, two large errors are observed with $D_{6,F}^{CF}$ and $D_{11,F}^{CF}$. These errors are found to remain consistent throughout and are therefore unweighted in future calculations. In fact, these errors can be put down to errors in the fitting of the spectral envelope in the static spectrum as the corresponding transitions are not well resolved. The results of both calculations from the I35 and I52 data are given in table 3.

6.4 Conformational Analysis

There are ten bonds in I35 and 9 in I52 rotation about which move the carbons relative to the fluorine atom. The approach adopted was to find which is the simplest conformational model which will fit the data. Thus, the rotation potentials about each bond are assumed to independent of one another.

Table 3. Optimised geometry of the rigid fragment using both D_{iF}^{CF} obtained from the analysis of the ^{13}C-{^{1}H} NMR spectra of I35 / HMDSO and I52 / HMDSO.

	I35		**I52**	
S_{ZZ}	0.682 ± 0.001		0.653 ± 0.001	
S_{XX}-S_{YY}	0.011 ± 0.001		0.018 ± 0.001	
S_{XZ}	-0.013 ± 0.001		-0.010 ± 0.001	

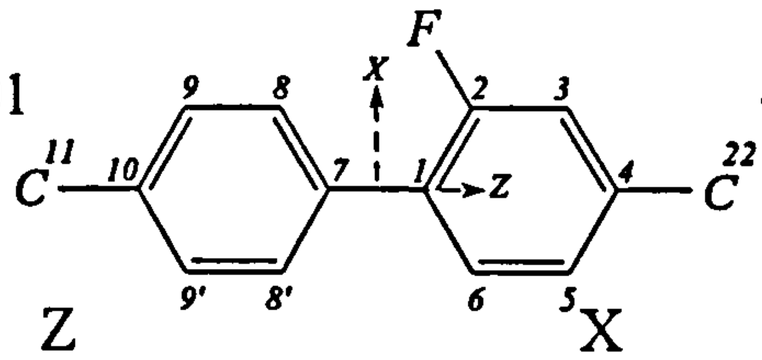

i	X	Z	X	Z
1	0.0	0.746	0.0	0.746
2	-1.171	1.490	-1.171	1.490
3	-1.186	2.867	-1.186	2.867
4	-0.015	3.553	-0.015	3.553
5	1.209	2.850	1.209	2.850
6	1.193	1.467	1.193	1.467
7	0.0	-0.746	0.0	-0.746
10	0.0	-3.540	0.0	-3.540
11	0.0	-5.083	0.0	-5.083
22	0.017	5.070	0.0165	5.070
F	-2.370±0.001	0.869±0.001	-2.370±0.001	0.869±0.001

i,F	$\Delta D_{iF} = D_{iF}$(calc-obs)	Weight	$\Delta D_{iF} = D_{iF}$(calc-obs)	Weight
1	0.1	1	0.9	1
2	0.1	1	0.1	1
3	0.1	1	0.1	1
4	0.2	1	-0.5	1
5	-1.1	1	-1.0	1
6	7.9	0	-4.0	1
7	1.7	0	-0.3	1
10	-0.3	1	1.4	1
11	-18.0	0	-4.2	1
22	-4.1	1	1.8	1

Both I35 and I52 can be treated as a flexible molecules consisting of a number of rigid fragments, the geometry of which have been optimised or assumed as previously discussed. This geometry is then kept fixed, and the set of D_{ij}^{CF} used to test models for the conformational distribution.

To do this it is necessary to consider how the D_{ij} are averaged by the combination of the motion of the entire molecule within the bulk sample relative to the liquid crystal director, **n**, and the internal motion through the relationship

$$D_{ij} = \int D_{ij}(\beta,\gamma,\Phi)\ P_{LC}(\beta,\gamma,\Phi)\sin\beta\ d\beta d\gamma d\Phi \qquad (2)$$

where $D_{ij}(\beta,\gamma,\Phi)$ is the D_{ij} in a fixed conformation, specified by the set of angles $\Phi = \phi_1, \phi_2$ ...., and orientation, β and γ, defined as the orientation of the liquid crystal director to molecule-fixed axes, and $P_{LC}(\beta,\gamma,\Phi)$ is the probability density for that conformation and orientation. $D_{ij}(\beta,\gamma,\Phi)$ is simply calculated from the geometry and order parameters, however, $P_{LC}(\beta,\gamma,\Phi)$ must be modelled so that the calculated dipolar couplings are in good

$$U_{LC}(\beta,\gamma,\Phi) = U_{ext}(\beta,\gamma,\Phi) + U_{int}(\Phi) \qquad (3)$$

agreement with the experimental couplings. In order to model P_{LC} we use the Additive Potential method [16], which considers the total energy, U_{LC}, of the molecule in two parts, the external energy, $U_{ext}(\beta,\gamma,\Phi)$, which depends on the orientation and the conformation of the molecule and the internal energy, $U_{int}(\Phi)$, which depends only on the conformation.

6.4.1 The Aromatic Inter-ring Bond

Both I35 and I52 contain the aromatic 2-fluorobiphenyl group. The model used to study the motion within the group is therefore the same.

The fragment

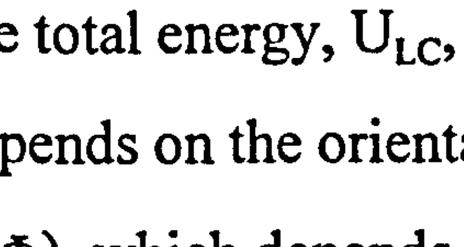

is assigned non-zero values of ϵ_{ZZ}^{FR} and $\epsilon_{XX}^{FR}-\epsilon_{YY}^{FR}$, and the fragment C^2-F requires only

ϵ_{aa}^{CF}. This means that the total fragment has three non-zero epsilon values. It is not necessary to make any assumptions about the conformations adopted by A = C_5H_{11}, the contributions from which are now absorbed into ϵ_{aa}^{CF}.

The fragment

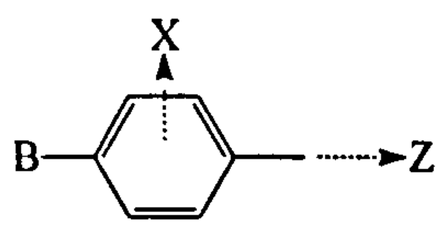

is assumed to require only ϵ_{ZZ}^{UR} and ϵ_{XX}^{UR}-ϵ_{YY}^{UR}. This means that B is assumed to have conformations in pairs of equal energy related either by YZ or XZ planes. However, in reality there will be a small deviation from this symmetry because of correlation between the conformations of B and A.

In practice the model also cannot distinguish between ϵ_{ZZ}^{UR} and ϵ_{ZZ}^{FR} since the Z axes are parallel, so these are made equal to $\epsilon_{2,0}^{R}$. Likewise, both ϵ_{XX}^{UR}-ϵ_{YY}^{UR} and ϵ_{XX}^{FR}-ϵ_{YY}^{FR} are made equal to ϵ_{XX}^{R}-ϵ_{YY}^{R}. It is worth noting that keeping these parameters unequal does not improve the fit.

The internal potential, $U_{int}(\phi_1)$ is expressed as

$$U_{int}(\phi_1) = V_2\cos 2\phi_1 + V_4\cos 4\phi_1 + U_{steric} \qquad (4)$$

which are the minimum number of terms required to describe the correct symmetry about ϕ_1, and U_{steric} describes the short range repulsive and attractive forces given in equation 8 chapter 5. The general procedure was to vary ϵ_{ZZ}^{R}, ϵ_{XX}^{R}-ϵ_{YY}^{R}, ϵ_{aa}^{CF}, V_2 and V_4 in order to bring the calculated D_{ij}^{CF} into close agreement with the experimental D_{ij}^{CF}. Note that $\epsilon_{\alpha\alpha}^{R}$ and ϵ_{aa}^{CF} obtained contain contributions from the groups A and B.

The probability distribution in the liquid crystal phase, $P_{LC}(\phi_1)$, of the inter-ring bond, for I35, is shown in figure 26 and the final values for the parameters are reported in table 4. The results of the analysis give a maximum value for the dihedral angle , $\phi_1 = 42°$ in the model without inclusion of the steric term (—) and 37° with the steric term included (-+-). Similar results are found for I52, and are reported in table 5. The $P_{LC}(\phi_1)$ of the inter-ring bond is shown in figure 27, where the minimum value of ϕ_1 is found to be 42° without inclusion of the steric term (—) and 37° with the steric term included (-+-). The dihedral angle between

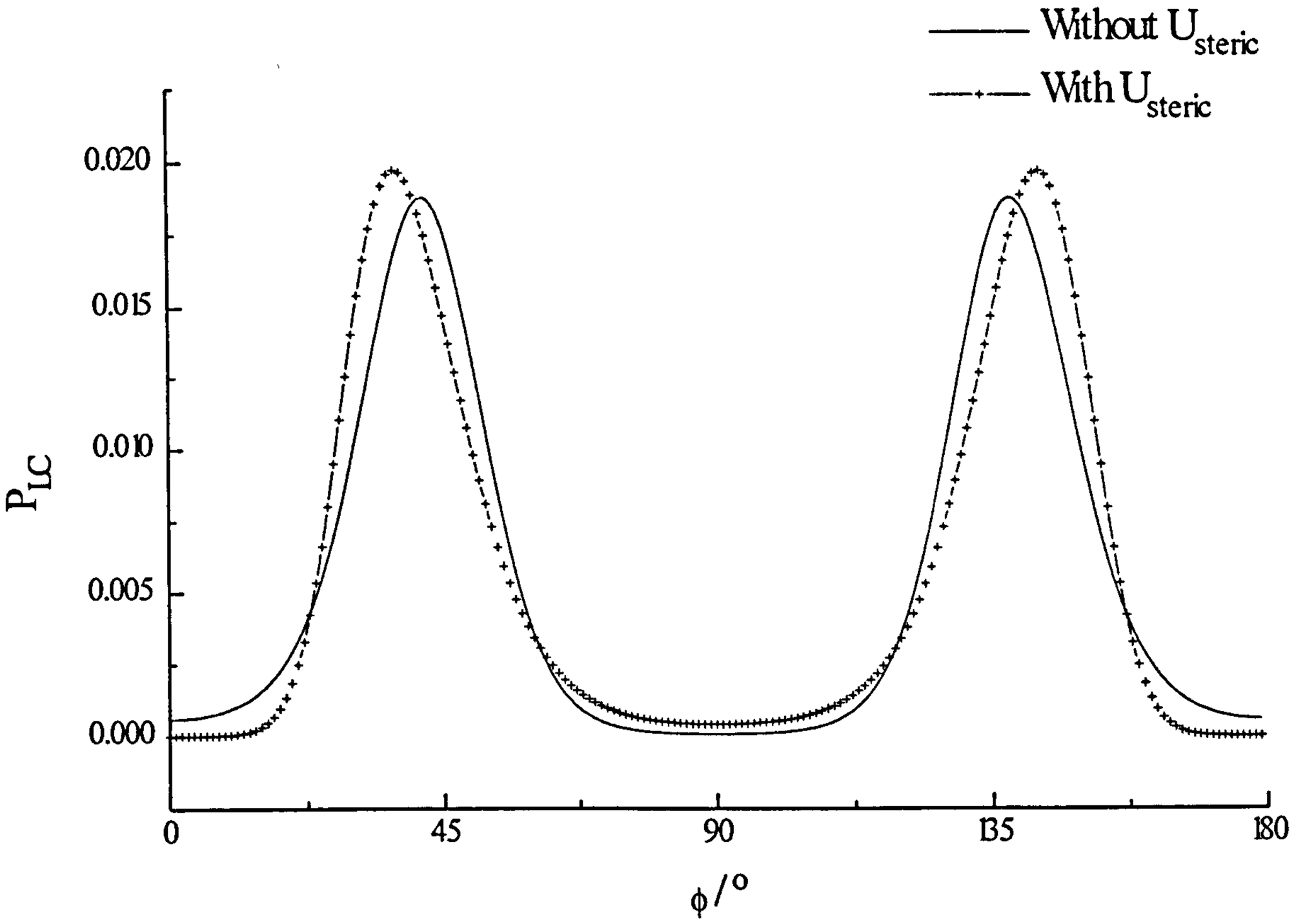

Figure 26 The probability in the liquid crystal phase (P_{LC}) for the conformation of the 2-fluorobiphenyl fragment of I35 with 10% w/w HMDSO at 300K.

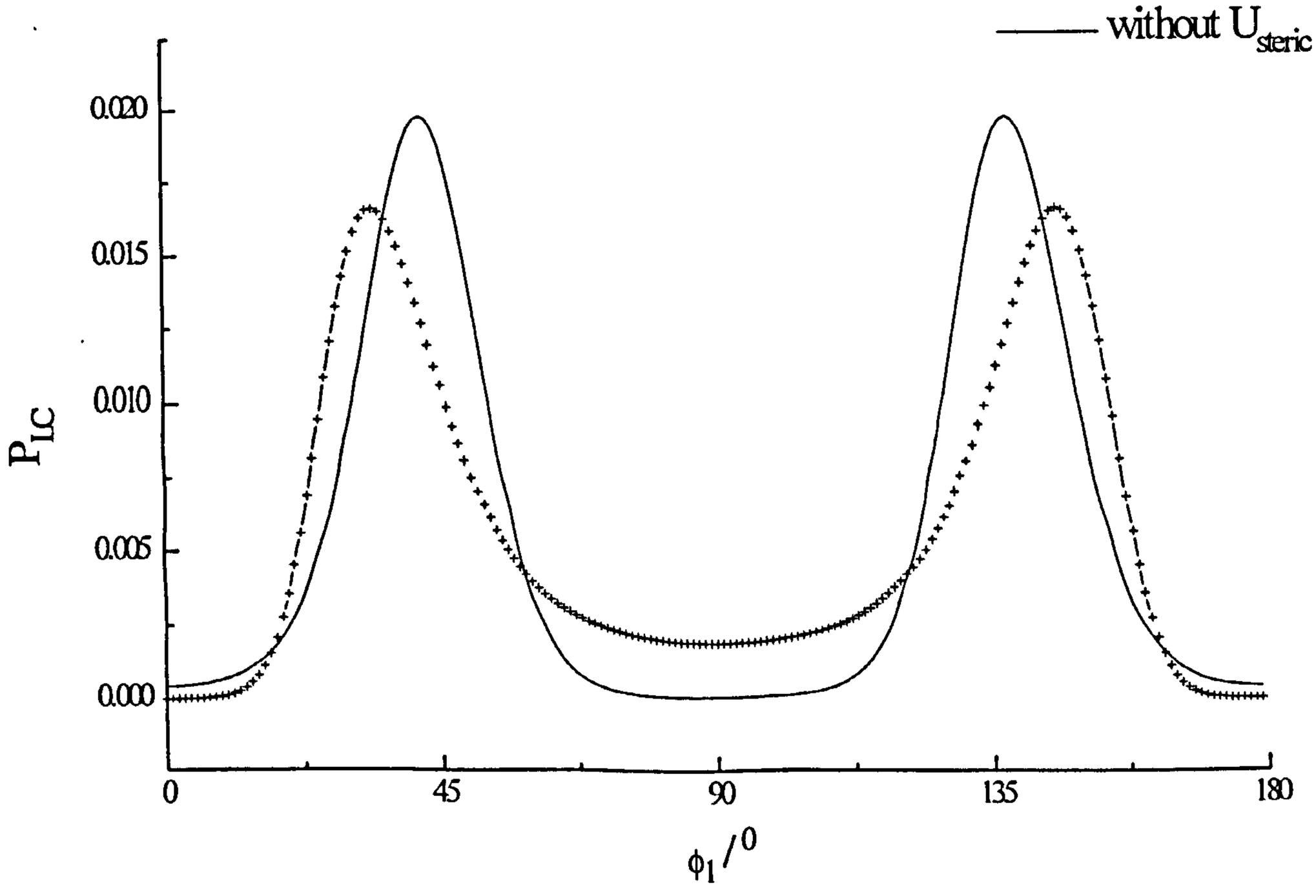

Figure 27 The probability in the liquid crystal phase (P_{LC}) for the conformation of the 2-fluorobiphenyl fragment of I52 with 10% w/w HMDSO at 300K.

Table 4. Results of bringing observed and calculated D_{ij}^{CF} obtained for The biphenyl fragment in I35 into agreement by varying ϵ_{ZZ}^{R}, $\epsilon_{XX}^{R}-\epsilon_{YY}^{R}$, ϵ_{aa}^{CF} and V_4. V_2 is kept fixed.

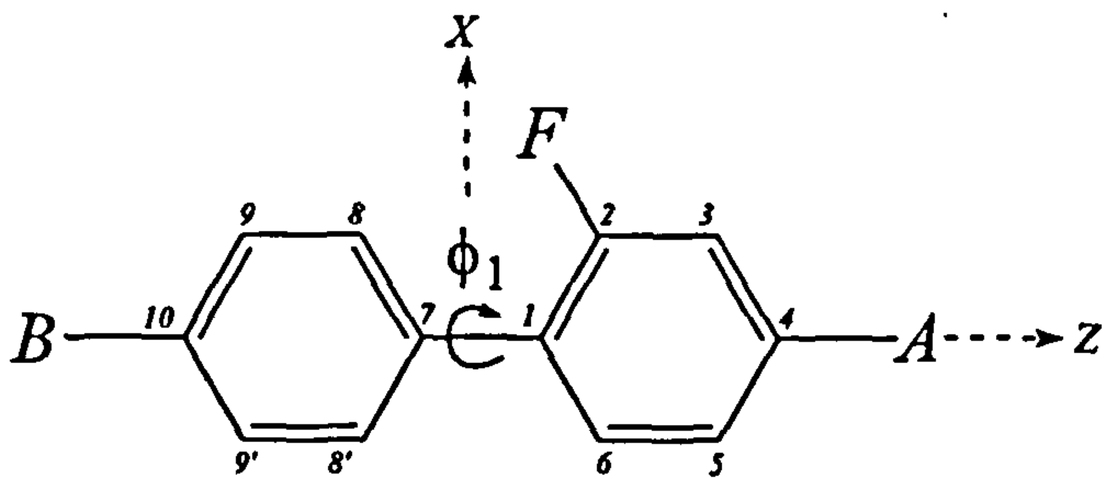

i	D_{iF}(obs) / Hz	$\Delta_{iF} = D_{iF}$(calc)-D_{iF}(obs) / Hz	
		Without U_{steric}	Including U_{steric}
1	705.4	-0.8	-1.1
2	1502.1	0.3	0.3
3	-922.7	-0.9	-1.1
4	-135.8	0.1	0.1
5	45.5	-1.2	-1.2
6	179.9	8.8	8.8
7	0.0	0.9	0.5
8	-216.5	-0.5	-0.2
9	-139.9	2.9	2.8
10	-105.1	-0.4	-0.5
V_2 / kJ mol^{-1}		-2.5	-11.2
V_4 / kJ mol^{-1}		5.5 ± 0.3	0.7 ± 1.7
ϵ_{ZZ}^{R} / kJ mol^{-1}		4.6 ± 0.03	4.6 ± 0.02
$\epsilon_{XX}^{R}-\epsilon_{YY}^{R}$ / kJ mol^{-1}		1.2 ± 0.2	1.2 ± 0.2
ϵ_{aa}^{CF} / kJ mol^{-1}		-0.3 ± 0.02	-0.3 ± 0.02
ϕ_1 / °		42 ± 1	37 ± 1

Table 5. Results of bringing observed and calculated D_{ij}^{CF} obtained for the biphenyl fragment in I52 into agreement by varying ϵ_{ZZ}^{R}, ϵ_{XX}^{R}-ϵ_{YY}^{R}, ϵ_{aa}^{CF} and V_4. V_2 is kept fixed.

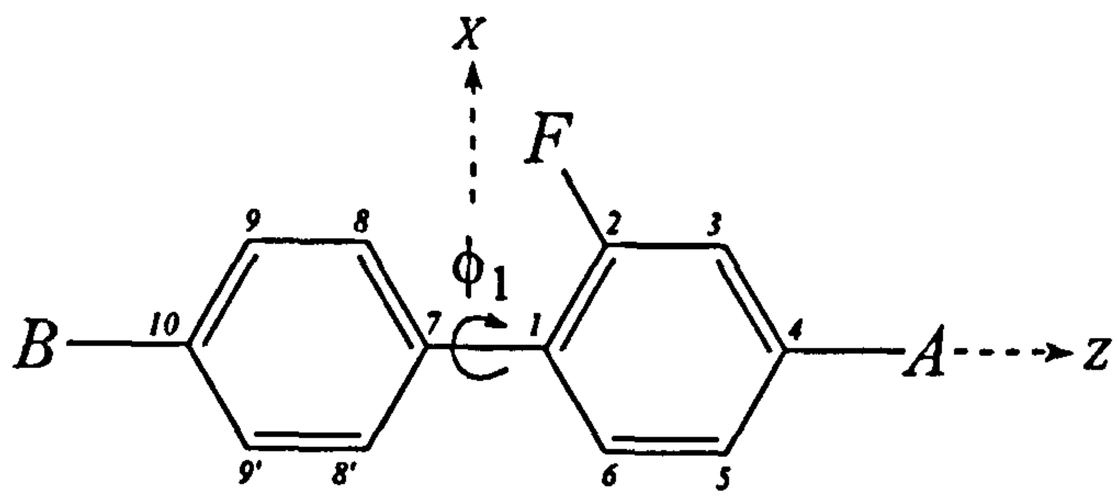

i	D_{iF}(obs) / Hz	$\Delta_{iF} = D_{iF}$(calc)-D_{iF}(obs) / Hz	
		Without U_{steric}	Including U_{steric}
1	666.1	1.1	0.9
2	1381.9	-0.1	0.1
3	-888.4	0.4	0.1
4	-131.4	-0.4	-0.5
5	41.6	-1.0	-1.0
6	181.0	-4.0	-4.0
7	0.0	0.1	-0.3
8	-205.4	0.6	0.9
9	-126.8	-3.3	-2.9
10	-102.0	1.5	1.4
V_2 / kJ mol^{-1}		-2.5	-11.0
V_4 / kJ mol-1		5.9 ± 0.4	-1.5 ± 0.8
ϵ_{ZZ}^{R} / kJ mol^{-1}		4.2 ± 0.02	4.2 ± 0.02
ϵ_{XX}^{R}-ϵ_{YY}^{R} / kJ mol^{-1}		0.73 ± 0.08	0.75 ± 0.08
ϵ_{aa}^{CF} / kJ mol^{-1}		-0.27 ± 0.02	-0.27 ± 0.01
ϕ_1 / °		42 ± 1	37 ± 1

the two rings for both liquid crystals is found to be less than the angle reported for the crystal structures of the 2-fluorobiphenyl group and that of the MO calculation. The difference in structure with phase is consistent with previous studies on similar systems such as 2,2'-difluorobiphenyl where the dihedral angle in the crystal structure was found to be 58° and the liquid crystal structure was found to be 50° [3][chapter 5].

The probability distribution in isotropic solution, P_{ISO}, is also calculated for both I35 and I52, however, it is found to be almost identical to that in the liquid crystal phase and is not shown here.

6.4.2 The aromatic ring - alkyl chain (A') conformations

6.4.2.1 n-pentyl chain of I35

In theory it should be possible to determine P_{LC} over all internal motions within the chains of the molecule given that a complete set of D_{ij}^{CF} have been obtained. Ideally, to begin the conformational analysis, we require optimised chain coordinates. However, in practice this is not possible as each carbon position depends on three coordinates and one interaction parameter, ϵ_{aa}^{CC}, for which we only have one D_{ij}^{CF}. The geometry of the chain must therefore be assumed and the only variable allowed being ϵ_{aa}^{CC} which is assumed equal for all C-C bonds. The assumed geometry of the chain remains fixed and the D_{ij}^{CF} used to attempt to determine the P_{LC} over all internal motions. The aliphatic chains are expected to have little effect on the potential for rotation about ϕ_1 in the liquid crystal phase and so this is kept fixed at the value determined from the analysis of the aromatic inter-ring bond in all further analyses.

The fragment now being considered is

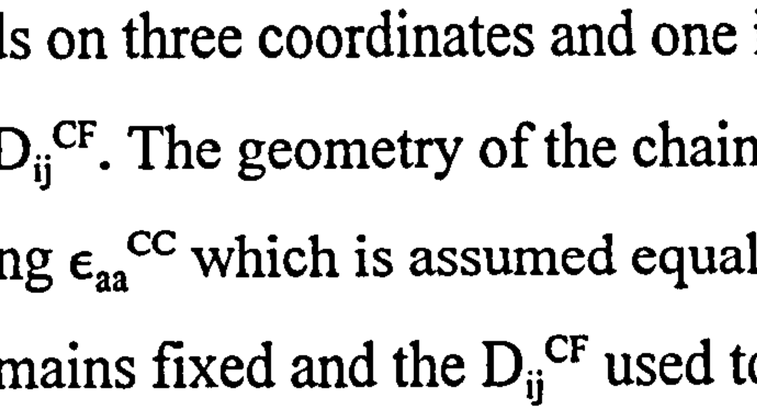

Evidence from previous studies show that the chains, A', prefer to lie at 90° to their

neighbouring rings, where the barrier for rotation depends on the length of the chain. It is found to be high for 5CB, ϕ_2=10 kJmol^{-1} [7] and low for 4-chloroethylbenzene, ϕ_2=3 kJmol^{-1} [5]. The n-pentyl chain of I35 is similar to that of 5CB and so we expect the barrier for rotation about ϕ_2 to be high. We can therefore treat the analysis as a jump model where only a few values of ϕ_2 are explored. The possibility of the chain lying in the plane of the ring was tested, by comparing two jump models, the first allowing only the two orthogonal structures at ϕ_2=90° and 270°, and the second allowing only the two planar structure at ϕ_2=0° and 180° whilst in both cases allowing ϵ_{ZZ}^{R}, ϵ_{XX}^{R}-ϵ_{YY}^{R}, ϵ_{aa}^{CF}, ϵ_{aa}^{CC} to vary. The results showed that an acceptable fit was obtained for the orthogonal structure only. The internal rotation potentials about the ring-chain bond, $U_{int}(\phi_2)$ are therefore expressed as

$$U_{int}(\phi_2) = V_2\cos 2\phi_2 \qquad (6)$$

which gives the correct symmetry with minimum potential at ϕ_2=90°.

In the case of I52, the problem is analogous to 4-chloroethylbenzene as A' is only 2 carbon atoms in length. The jump model is therefore too simplified to measure the conformational distribution as there will be a broader spread of populated forms. We also have insufficient information to model the continuous potential about ϕ_2 , or indeed for the jump model, as only one D_{ij}^{CF} depends on the motion about ϕ_2.

Internal motion within the chain may also be explored using a jump model which assumes that the chain carbons only occupy the three positions with respect to each other as shown in figure 28. Evidence for the potential barrier of rotation [17] within the flexible chain shows that the three conformations are possible, with the most likely at ϕ_{chain} = 0°, a *trans*

G(+) *-trans* *G(-)*

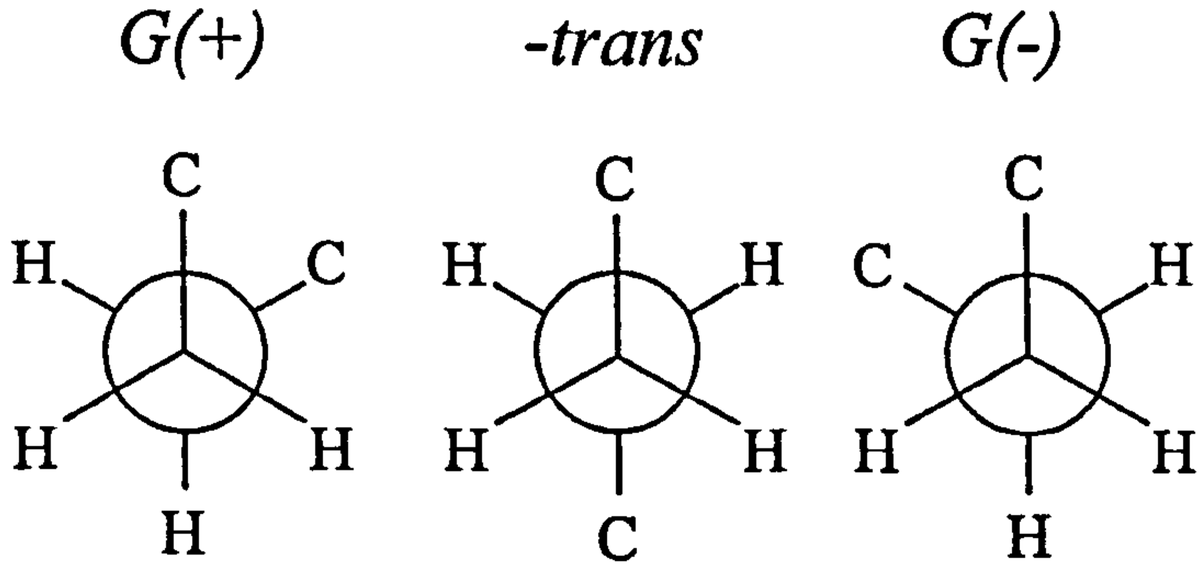

Figure 28 Conformations adopted in the jump model of the aliphatic chains.

conformer, and two less probable *gauche* conformers at 113° and -113°. Rotation about the bonds 22-23, 23-24 and 24-25 are assumed as jumps between *gauche*+, *trans* and *gauche*- (g+,t,g-). The barriers for rotation about the C-C bonds are such that the curve should be

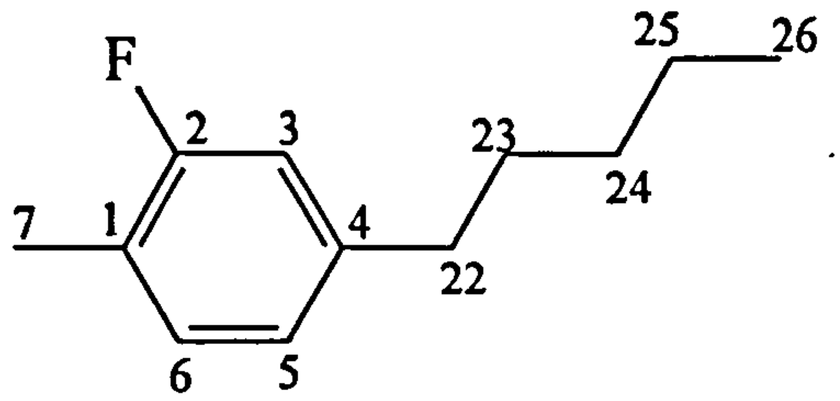

modelled by using a large, between 3 and 5, number of terms in a Fourier series. However, as we are only interested in the relative energy difference of the three conformers explored in the jump model, E_{tg}, it is only necessary to model the energy curve with the first term of the Fourier Series which produces the simplest possible fit between 3 points. The potential barrier for rotation within the n-pentyl chain is therefore expressed as

$$U_{int}(\phi_{cc}) = V_1 \cos\phi_{cc} \qquad (7)$$

Where a small negative value for V_1 gives the correct symmetry with a minimum energy at 0°. Increasing V_1 simply increases the relative energy difference between the *trans* and *gauche* conformers. The energy difference between *trans* and *gauche* conformers is expected to be in the region of E_{tg} = 3-4 kJmol^{-1}. A value of E_{tg} = 3.44 kJmol^{-1} was chosen for convenience. It is not possible to include V_1 as a variable whilst considering ϵ_{aa}^{CC} as a variable, due to lack of data.

The calculations testing the conformation of the chain relative to the rings was repeated, this time including the internal motion of the n-pentyl chain. The fit for the orthogonal model is further improved by considering internal chain motion. Conversely the fit from the planar model is worsened. We may now discount the possibility of the chain lying in the plane of its neighbouring aromatic ring and concentrate on the orthogonal model.

In order to determine the potential barrier for rotation about the ring-chain bond it was necessary to extend the orthogonal jump model to a continuous potential orthogonal model. $V_2(\phi_2)$ was initially chosen to be +10kJmol^{-1} as found in 5CB [7] and allowed to vary along with the parameters ϵ_{ZZ}^{R}, ϵ_{XX}^{R}-ϵ_{YY}^{R}, ϵ_{aa}^{CF}, ϵ_{aa}^{CC} until a good agreement between the

experimental and calculated D_{ij}^{CF} was obtained. The fit is not expected to be perfect as some of the chain dipolar couplings are subject to large errors. This perhaps shows up in the results which found the value of $V_2(\phi_2)$ to be higher than 200 kJmol^{-1}. We already know that the value of $V_2(\phi_2)$ is expected to be in the order of 10 kJmol^{-1} [5, 7] and so the model was repeated by fixing $V_2(\phi_2)$ at the lowest value possible whilst maintaining a good agreement between the experimental and calculated dipolar couplings. The minimum value $V_2(\phi_2)$ required to maintain a good fit was 10kJmol^{-1}.

The continuous potential surface for motion about ϕ_1 and ϕ_2 is shown in figure 29; the rest of the chain is confined to the fully *trans* form. The probability distribution in isotropic solution shows a slight difference to that in the liquid crystal phase, figure 30. The difference between the two curves may be explained by the larger distribution of probable conformers with flexible chains in the isotropic phase where the *gauche* forms are more probable. Zero order in the isotropic phase does not constrain the conformation of the molecule as the liquid crystal phase does. The model finds that the most likely forms in the liquid crystal phase are indeed the most highly ordered. The final results are reported in table 6.

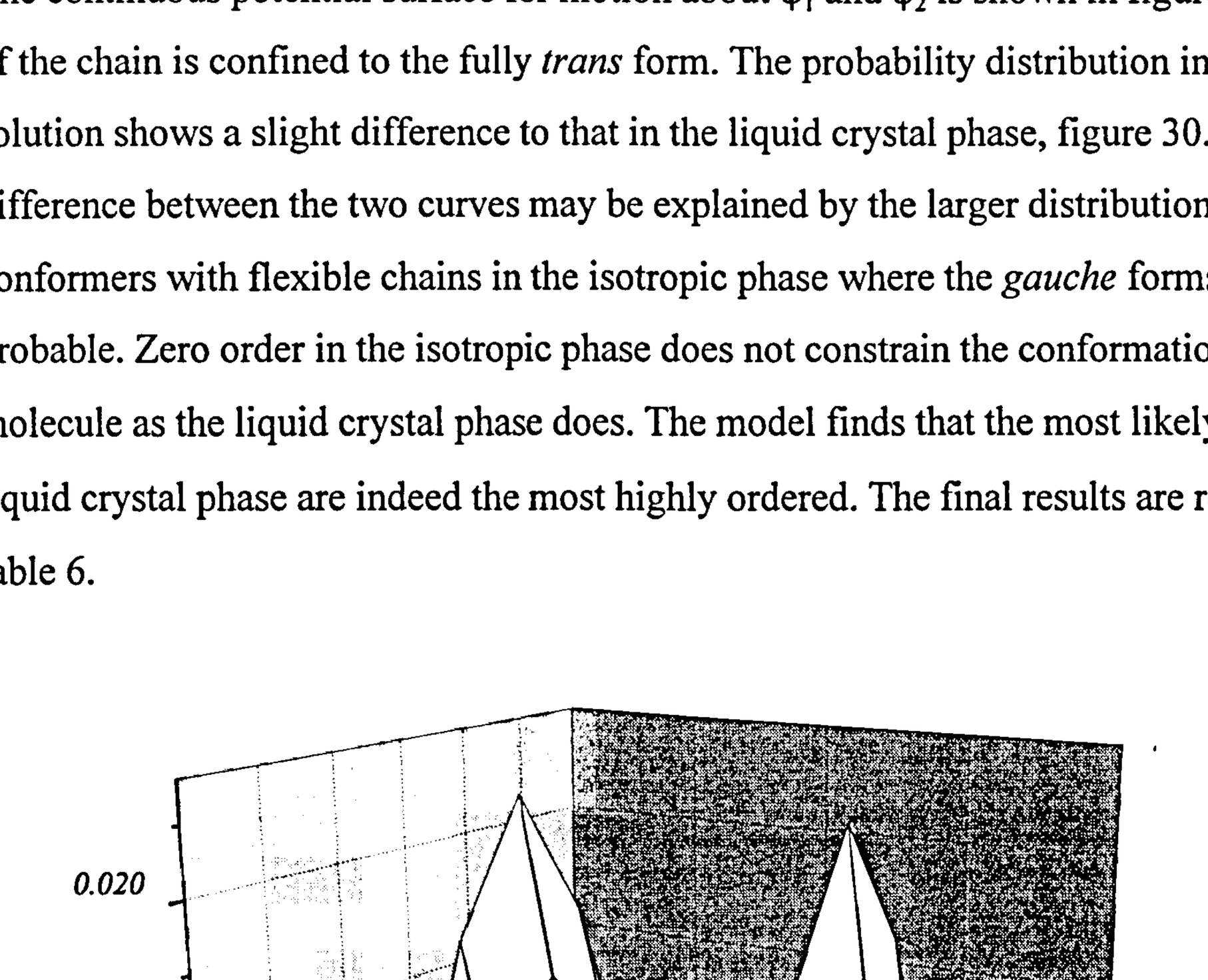

Figure 29 Probability density in the liquid crystal phase for rotation about ϕ_1 and ϕ_8. ϕ_9, ϕ_{10} and ϕ_{11} are in the most probable *trans* forms.

Table 6. Results of bringing observed and calculated D_{ij}^{CF} obtained for I35 into agreement by varying ϵ_{ZZ}^{R}, ϵ_{XX}^{R}-ϵ_{YY}^{R}, ϵ_{aa}^{CF} and ϵ_{aa}^{CC} whilst maintaining $V_2(\phi_1)$, $V_4(\phi_1)$, $V_2(\phi_8)$, E_{tg} $(\phi_9)(\phi_{10})(\phi_{11})$ fixed.

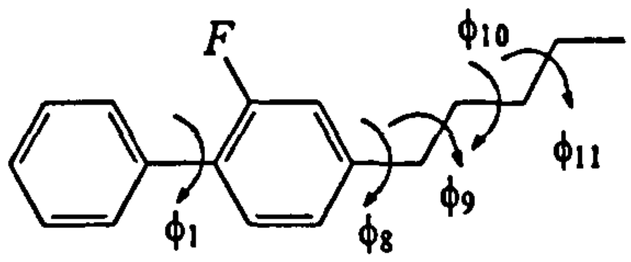

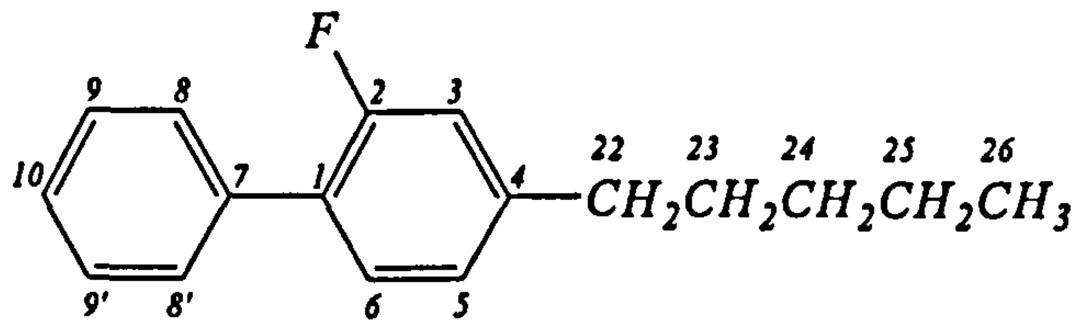

i	D_{iF}(obs) / Hz	$\Delta_{iF} = D_{iF}$(calc)-D_{iF}(obs) / Hz
1	705.4	-0.6
2	1502.1	0.2
3	-922.7	-0.5
4	-135.8	0.6
5	45.5	-0.5
6	179.9	8.3
7	0.0	-5.0
8	-216.5	-0.9
9	-139.9	3.5
10	-105.1	-0.02
22	-102	-4.2
23	-73.5	-0.4
24	-51.5	3.2
25	-33.5	-0.2
26	-23.0	-1.6

$V_2(\phi_1)$ / kJ mol^{-1}	-2.5
$V_4(\phi_1)$ / kJ mol^{-1}	5.5
$V_2(\phi_8)$ / kJ mol^{-1}	10.0
$E_{tg}(\phi_9)(\phi_{10})(\phi_{11})$ / kJ mol^{-1}	-3.44
ϵ_{ZZ}^{R} / kJ mol^{-1}	4.2 ± 0.2
ϵ_{XX}^{R}-ϵ_{YY}^{R} / kJ mol^{-1}	3.4 ± 1.1
ϵ_{aa}^{CF} / kJ mol^{-1}	-0.25 ± 0.03
ϵ_{aa}^{CC} / kJ mol^{-1}	1.52 ± 0.7

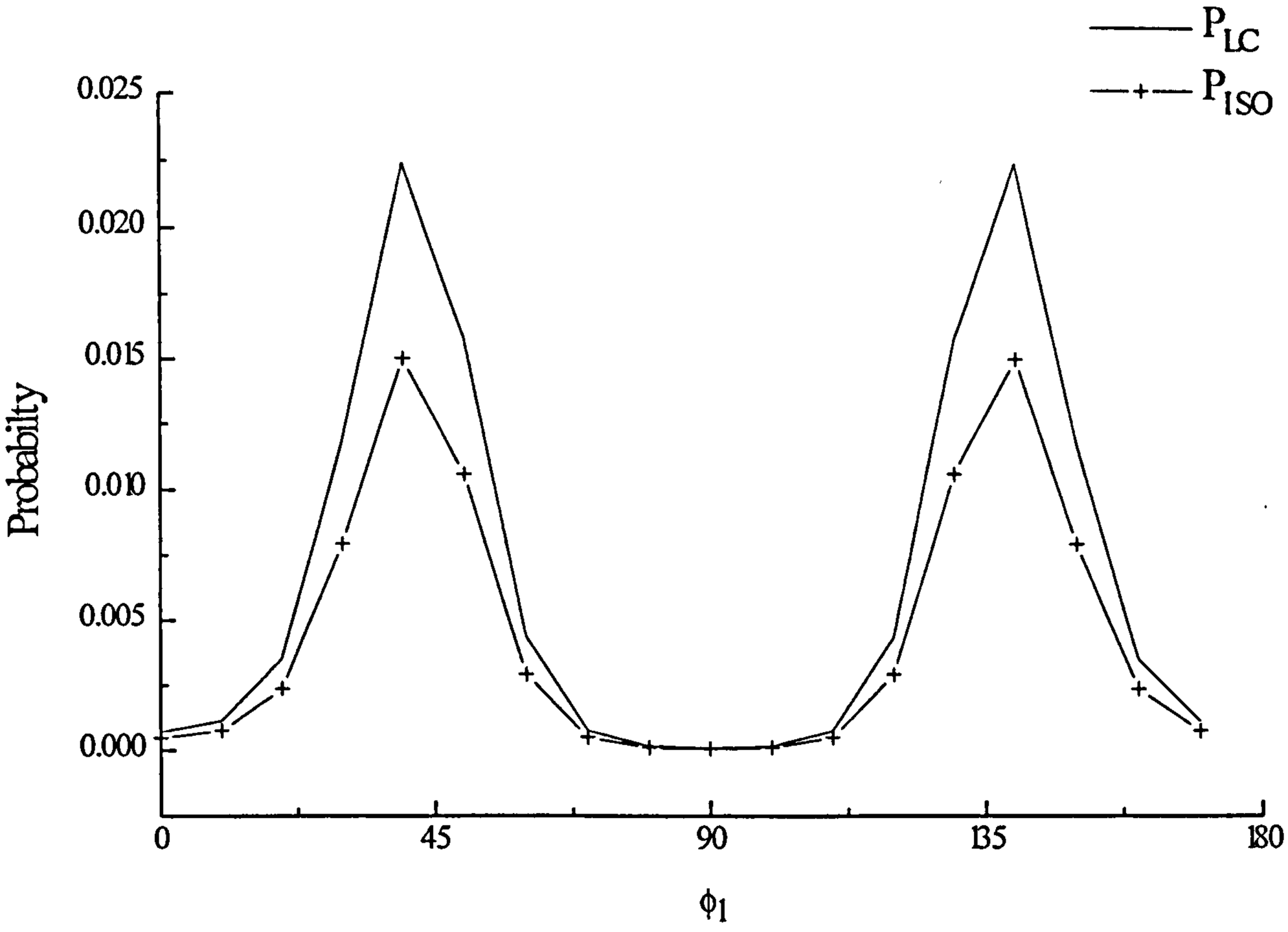

Figure 30 Comparison of the probability density in the liquid crystal and isotropic phases about ϕ_1 at the point where ϕ_2 is orthogonal and ϕ_4, ϕ_5 and ϕ_6 are *trans*.

6.4.2.2 Ethyl chain of I52

While this appears simpler than the n-pentyl chain model of I35, with only one rotor to consider, we do not have enough data relating the A' ethyl chain to the fluorine atom on the ring to determine the conformational distribution about ϕ_2. The study of the analogous rotor in 4-chloroethylbenzene [7] shows that for shorter chains lengths the barrier for rotation is low, and therefore the spread of highly populated conformers is broad compared to that of the n-pentyl chain. We only have one D_{ij}^{CF} that depends on motion about ϕ_2 and so it is unrealistic to model the continuous potential barrier. We therefore must make an assumption as to the form of the barrier for rotation about ϕ_2 based on 4-chloroethylbenzene, where the most probable conformers are when the chain is orthogonal to the ring plane. This assumption will be used when the whole I52 molecule is modelled.

6.4.3 The aromatic ring - alkyl chain (B') conformations

The fragment now being considered is

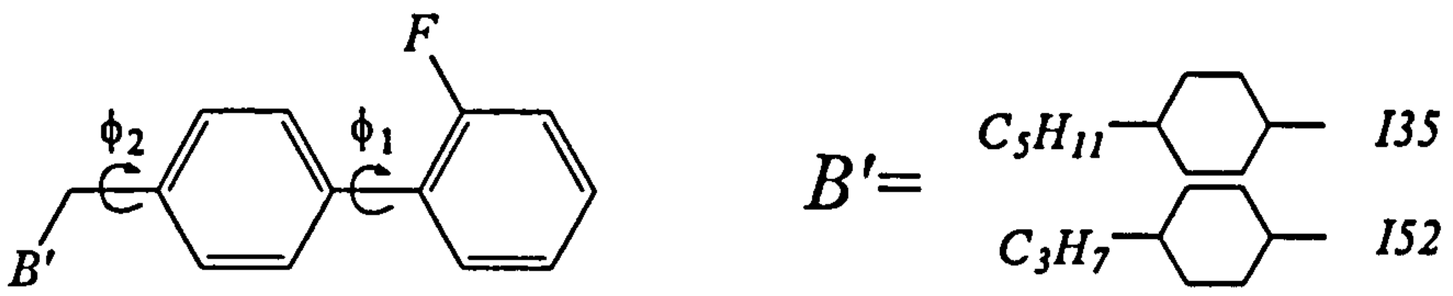

The same jump conformational model as applied to the analysis of the conformation of A' can be applied to the analysis of B' for all C-C bonds in the chain including those connected to the cyclohexyl ring. The cyclohexyl group can be considered to be a rigid fragment, as interconversion between axial and equatorial substitution, is energetically unfavourable considering the large groups attached to the ends of the cyclohexane ring. The chair form is the lowest energy structure and as such is assumed to be the only form adopted in I35 and I52 in the liquid crystal phase.

We may consider the results from the analysis of A' to be applicable to B', where the chains prefers to lie orthogonal to the ring plane, in a fully *trans* arrangement. There is an added complication, however, in consideration of the motion about the bond connecting the chain to the cyclohexyl group. The potential barrier for rotation about such a bond is subject to a double degeneracy at $\phi = 113°$ and 293°which both produce *gauche* forms of the structure of approximately equal energy, shown in figure 31 [10]. A third, higher energy, form occurs at $\phi = 180°$. The potential barrier for rotation may, therefore, be modelled in the same way as the chains, where we only require the first term of a Fourier series to model the relative energies of the three probable conformers in much the same way as for the 5 membered chain, A' for I35. The C-C bonds within the cyclohexyl group also contribute to the total ϵ^{CC} tensor. Given that the chain, B', is expected to lie orthogonal to the ring plane and the reduced

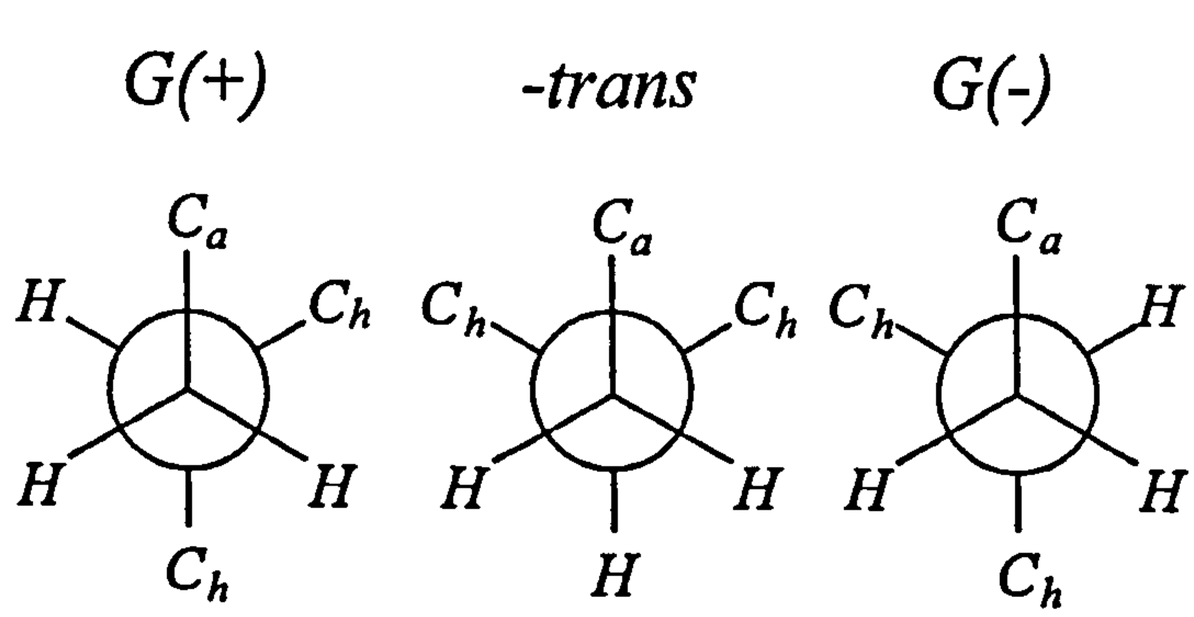

Figure 31 Conformations adopted in the jump model of the aliphatic chains directly attatched to the cyclohexy group. C_a is an alkyl carbon atoms and C_h are the cyclohexyl carbon atoms

accuracy of the D_{ij}^{CF} from the analysis of the NMR spectra, it was decided that this chain should be modelled as part of the whole molecule rather than as a fragment. The results should then give an indication of the preferred orientation of the chains relative to one another as well as the fluorine atom, to give an idea of the structure of I35 and I52 in the liquid phase.

6.4.4 The Complete Structure of I35 and I52

To completely model the conformation distribution of I35 and/or I52 we should consider all internal motions. For I35 we have ten internal motions to consider and nine for I52. In the case of I35, if we assume the jump model for the alkyl chain conformations, it is still necessary to model 1.6 million conformations. This calculation is not feasible due to limitations in computer power and time. The quality of the data also is not sufficient to correctly determine all these conformations. Further assumptions are therefore necessary. The motion occurring at the extreme ends of I35 may be neglected due to their limited affect on the orientation of the whole molecule. This assumption reduces the number of conformations to a still unfeasible 180,000. We must therefore reduce the step size about ϕ_1. Motion about ϕ_1 is now also treated as a jump model where only the most probable values are considered, $\phi_1 = 40$ and 140°. This reduces the number of conformations examined to a more reasonable 1944.

In the final model, all values for the V terms required to model the potential barrier for rotation, were those determined in previous models or those assumed from previous studies and kept fixed in the calculation of the structure of the whole molecule. The parameters ϵ_{ZZ}^{R}, ϵ_{XX}^{R}-ϵ_{YY}^{R}, ϵ_{aa}^{CF}, ϵ_{aa}^{CC} were allowed to vary until a good agreement between the experimental and calculated D_{ij}^{CF} was obtained. The results are reported in tables 7 for I35. Allowing the same parameters to vary for I52 leads to a very different value for ϵ_{XX}^{R}-ϵ_{YY}^{R} (16.4 kJ mol^{-1}) and ϵ_{aa}^{CC} (10.7 kJ mol^{-1}). The predicted conformational distribution is also found to be substantially different. The different ϵ values are probably in part a reflection of the assumption of a single value for ϵ_{aa}^{CC} for each C-C bond. Making ϵ_{aa}^{CC} equal to that found for I35 reduces the difference between the ϵ values, and makes the conformational distributions very similar. It also increases $\Delta D_{23,F}$ to 12.0 Hz, but this can be understood in that the barrier to rotation about the C4-C22 bond in I52 is probably much smaller than in

I35, meaning that the assumption of there being only two populated values of ϕ_2 of 90° and 270° in I52 too severe. In the calculation on I52, therefore, the coupling $D_{23,F}$ was not included in the data set and ϵ_{aa}^{CC} was fixed at the value found for I52. The results are shown in table 8.

6.4.5 The Interdependence of the Conformational Distribution and the Orientational Order

We can examine more closely the results of the modelling in terms of the orientation and structure, through examination of the conformational distributions. It is impractical to present the entire distribution so we concentrate on the most important features within the distributions. Tables 9 and 10 give the probabilities, $P_{LC}(\phi_i)$ and $P_{ISO}(\phi_i)$ of some of the conformations of I35 and I52, including the corresponding orientational order matrix elements, expressed in the molecular axis frame, X, Y and Z.

We can see that the most probable conformers are those in which the minimum energy structures are adopted within the aliphatic chains. The 16 most populated conformers have the same probability in the isotropic phase of 0.0144, and correspond to each CCCC fragment in the aliphatic chains being in the *trans* state, whilst the rings also adopt their minimum energy form. In the liquid crystal phase, we see some differences in the probability as the importance of orientational ordering affects increases the $U_{ext}(\beta,\gamma,\Phi)$ term with respect to $U_{int}(\phi)$. This effect is large for I35 and I52 as they are both highly ordered molecules. The least probable conformer, number 16, in this subset has the chains at either end of the biphenyl core on the same side of the attatched phenyl ring. Repulsive effects over this range between the end chains are negligible and are not the reason for this lowering of favourability, rather it is due to the preference of straighter conformers in the nematic phase that causes this slight difference in energy. Even so, conformer 16 is 20% less probable than conformer 1, in the liquid crystal phase for both I35 and I52. The large difference between $P_{LC}(\phi)$ and $P_{ISO}(\phi)$ is also a consequence of the strong orientational ordering of the molecules is to be expected in these examples, however, some credit can be given to the assumptions made in the model used to predict the conformational distribution, such as ε^{CC} is the same for all aliphatic C-C bonds.

Table 7. Results of bringing observed and calculated D_{ij}^{CF} obtained for I35 into agreement by varying ϵ_{ZZ}^{R}, $\epsilon_{XX}^{R}-\epsilon_{YY}^{R}$, ϵ_{aa}^{CF} and ϵ_{aa}^{CC} whilst maintaining $V_2(\phi_1)$, $V_4(\phi_1)$, $E_{tg}(\phi_3)(\phi_4)(\phi_5)(\phi_9)(\phi_{10})$ fixed.

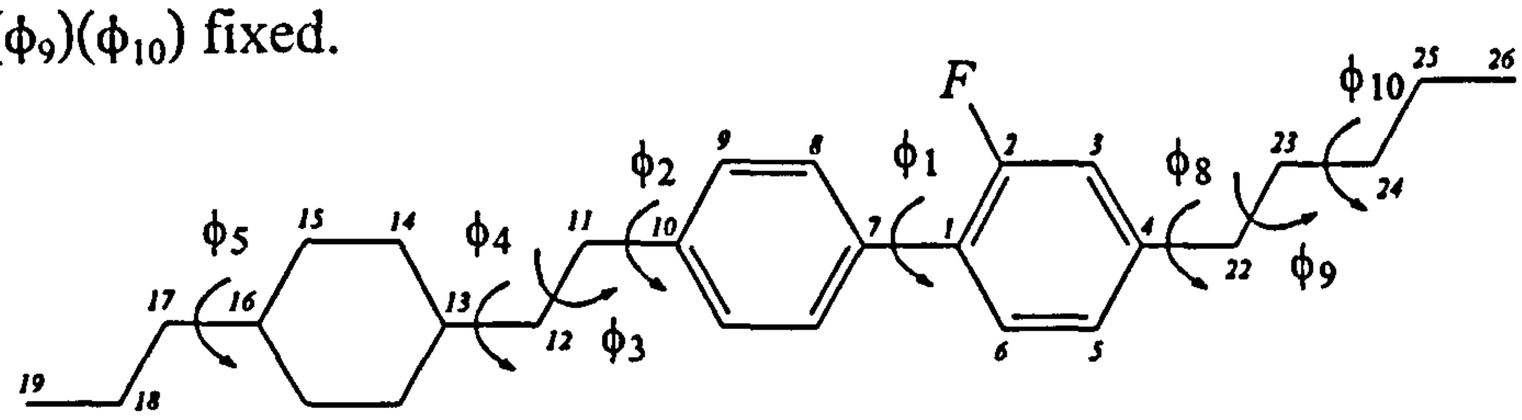

i,F	D_{iF}(obs) / Hz	weight	$\Delta_{iF} = D_{iF}$(calc)-D_{iF}(obs) / Hz
1	705.4	1	-0.7
2	1502.1	1	-0.3
3	-922.7	1	0.3
4	-135.8	1	0.2
5	45.5	1	-1.1
6	179.9	0	7.8
7	0.0	0	1.6
8	-216.5	1	-0.1
9	-139.9	1	2.4
10	-105.1	1	-0.2
11	-42.0	0	-18.0
12	-38.5	1	-7.4
13	-26.0	1	-1.0
14	-21.5	1	-1.6
15	-13.5	1	-1.8
16	-12.5	1	-1.0
17	-1.0	0	-8.3
18	-7.0	1	-0.6
19	-6.0	1	0.4
22	-102.0	1	-4.1
23	-73.5	1	-1.9
24	-51.5	1	3.6
25	-33.5	1	0.5
26	-23.0	1	2.3

$V_2(\phi_1)$ / kJ mol^{-1}	-2.5
$V_4(\phi_1)$ / kJ mol^{-1}	5.5
$E_{tg}(\phi_3)(\phi_4)(\phi_5)(\phi_9)(\phi_{10})$ / kJ mol^{-1}	3.44
ϵ_{ZZ}^{R} / kJ mol^{-1}	2.8 ± 0.03
$\epsilon_{XX}^{R}-\epsilon_{YY}^{R}$ / kJ mol^{-1}	3.5 ± 0.1
ϵ_{aa}^{CF} / kJ mol^{-1}	-0.3 ± 0.03
ϵ_{aa}^{CC} / kJ mol^{-1}	1.4 ± 0.05

Table 8. Results of bringing observed and calculated D_{ij}^{CF} obtained for I52 into agreement by varying ϵ_{ZZ}^{R}, $\epsilon_{XX}^{R}-\epsilon_{YY}^{R}$ and ϵ_{aa}^{CF} whilst maintaining $V_2(\phi_1)$, $V_4(\phi_1)$, $E_{tg}(\phi_3)(\phi_4)(\phi_5)(\phi_6)(\phi_7)$ and ϵ_{aa}^{CF} fixed.

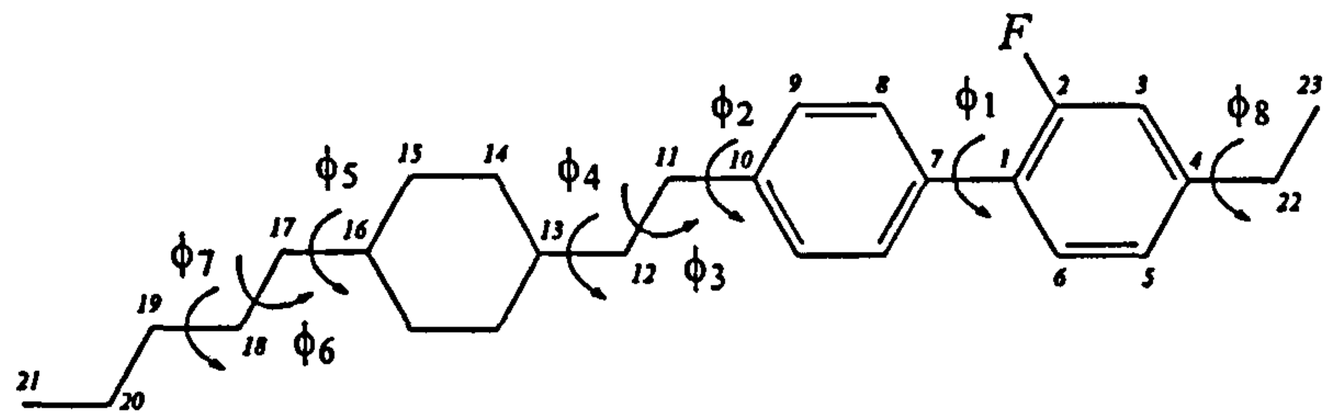

i,F	D_{iF}(obs) / Hz	weight	$\Delta_{iF} = D_{iF}$(calc)-D_{ij}(obs) / Hz
	666.1	1	1.1
2	1381.9	1	-0.0
3	-888.4	1	0.6
4	-131.4	1	-0.5
5	41.6	1	-1.1
6	183.1	1	-4.0
7	0.0	1	2.2
8	-205.4	1	-0.6
9	-126.8	1	-4.0
10	-102.0	1	1.8
11	-25.0	0	32.0
12	-53.0	1	8.8
13	-27.0	1	-0.1
14	-23.0	1	0.8
15	-15.0	1	0.3

16	-12.0	1	-2.9
17	-10.0	1	1.1
18	-6.0	1	-1.3
19	-10.0	1	4.4
20	-2.5	1	-2.1
21	-4.5	1	0.9
22	-104.0	1	1.9
23	-82.0	0	12.0

$V_2(\phi_1)$ / kJ mol^{-1}	-2.5
$V_4(\phi_1)$ / kJ mol^{-1}	5.5
$E_{tg}(\phi_4)(\phi_5)(\phi_6)(\phi_7)(\phi_8)$ / kJ mol^{-1}	3.44
ϵ_{ZZ}^{R} / kJ mol^{-1}	1.9 ± 0.02
$\epsilon_{XX}^{R}-\epsilon_{YY}^{R}$ / kJ mol^{-1}	9.9 ± 0.1
ϵ_{aa}^{CF} / kJ mol^{-1}	-0.04 ± 0.02
ϵ_{aa}^{CC} / kJ mol^{-1}	1.4

The first real change occurs between conformers 16 and 17, in which we observe a jump in the values of $P_{LC}(\phi)$ and $P_{ISO}(\phi)$. From the description of the structure, it is shown that the chains have adopted an energetically unfavourable single *trans* form about the chains attached to the cyclohexyl ring, for example, about ϕ_8 for I35 and ϕ_5 for I52. While this is energetically unfavourable, the molecule has still retained its elongated structure. Motions, such as the one about these bonds are parallel to the molecular long axis and therefore do not greatly affect the ordering. A little further down within this second grouping of probability, the introduction of *gauche* forms within the aliphatic chains causes the lowering of probability. For example conformer 19 of I35 about ϕ_5 and conformer 23 of I52 about ϕ_{11}. Again, like the the examples of a single *trans* form given above, motion about these bonds does not greatly affect the shape of the molecule, just the internal energy, and so the molecules remain highly ordered.

On the adoption of a *gauche* form in ϕ_4, as we see for conformer 65 of I35 we again observe

a large fall in the value of $P_{LC}(\phi)$ from conformers 64 and higher to roughly a half that of conformer 64. A jump in the value of P_{ISO} is however not observed, as motion about ϕ_4 affects the ordering which is not a factor in the isotropic phase where only changes in internal energy matter. Motion about this bond greatly affects the shape of the molecule as this bond does not lie in the same direction of the molecular long axis. Now the molecule is kinked and this change of shape can be observe in the order matrix where S_{ZZ} has fallen from 0.76 to 0.57. The same behaviour is observed for I52 with motion about ϕ_{10}.

6.5 Conclusion

The conformational distribution of the mesogenic core of I35 and I52 has been determined in the nematic phase at 300K. The results are consistent with earlier work on mesogenic fragments such as biphenyl [18] and 2,2'-difluorobiphenyl [3][chapter3] where the dihedral angle between the two ring planes is found to lie between 39° and 42°, less than those determined in the crystal structure of 54° [1] and in the isolated molecule of 49° [4]. The results of the analysis of the chains on either side of the mesogenic core is also consistent with previous work on 5CB [7], in which the chains are found to lie mainly orthogonal to the rings planes on which they are attached. A jump model was employed for the analysis of the internal motions of the chains, and a distribution of *trans* and *gauche* conformers found, where the *trans* forms are found to be most probable for n-alkyl chains and the *gauche* forms are found to be most probable for the chain to cyclohexyl bonds.

Combining the two chains with the mesogenic core showed that the chains prefer to adopt a *trans* form to each other. This is to be expected, however, it must be pointed out that the difference between some *trans* forms and some *cis* are small, and the change can be brought about by motion in only one of ϕ_1, ϕ_2 or ϕ_3. The results also show that, in general, the probability is reduced when the alkyl chains adopt the internal *gauche* form or the chain - cyclohexyl bond adopts the *trans* form.

It is concluded that the information content is not great enough to accurately model the complete molecule. Although we have measured long range dipolar couplings across the entire length of I35 and I52, the magnitudes are so small as to be greatly affected by line broadening. In the extreme cases we can expect errors of 50-100%, especially in areas of the spectra where overlapping lines occur and where lines are poorly resolved.

Table 9. Selected conformations of I35 and their probabilities and orientational order parameters. The conformers are labelled according to their probabilities. In all conformers the value of ϕ_1 is 40°, and ϕ_6 and ϕ_{10} are 0°.

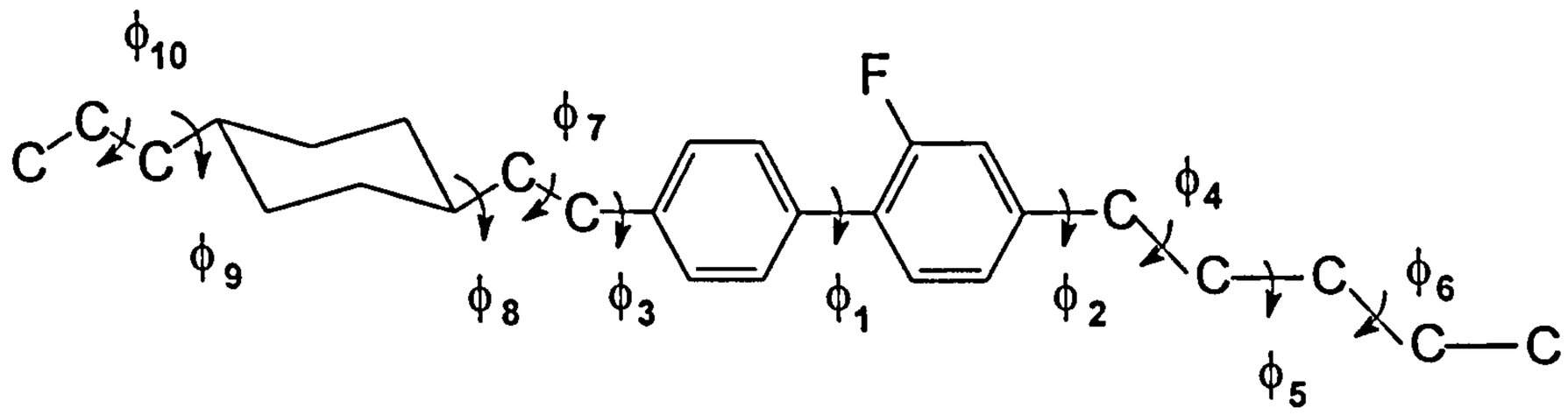

No.	ϕ_2	ϕ_3	ϕ_4	ϕ_5	ϕ_7	ϕ_8	ϕ_9	S_{zz}	S_{xx}-S_{yy}	S_{xy}	S_{xz}	S_{yz}	P_{LC}	P_{iso}
1	90	270	0	0	0	67	293	0.734	-0.056	0.019	-0.077	-0.212	0.028	0.014
16	90	90	0	0	0	67	293	0.763	-0.026	0.007	0.050	-0.013	0.023	0.014
17	270	90	0	0	0	180	67	0.741	-0.013	-0.028	-0.043	0.180	0.007	0.004
19	90	270	0	112	0	293	67	0.743	0.044	0.020	-0.160	-0.109	0.007	0.004
64	90	90	0	0	0	67	180	0.760	-0.014	-0.003	-0.009	-0.051	0.005	0.004
65	90	270	-112	0	0	293	67	0.567	0.046	0.076	-0.118	-0.184	0.002	0.004

Table 10. Selected conformations of I52 and their probabilities and orientational order parameters. The conformers are labelled according to their probabilities. In all conformers the value of ϕ_1 is 40°, and ϕ_{11} and ϕ_{12} are 0°.

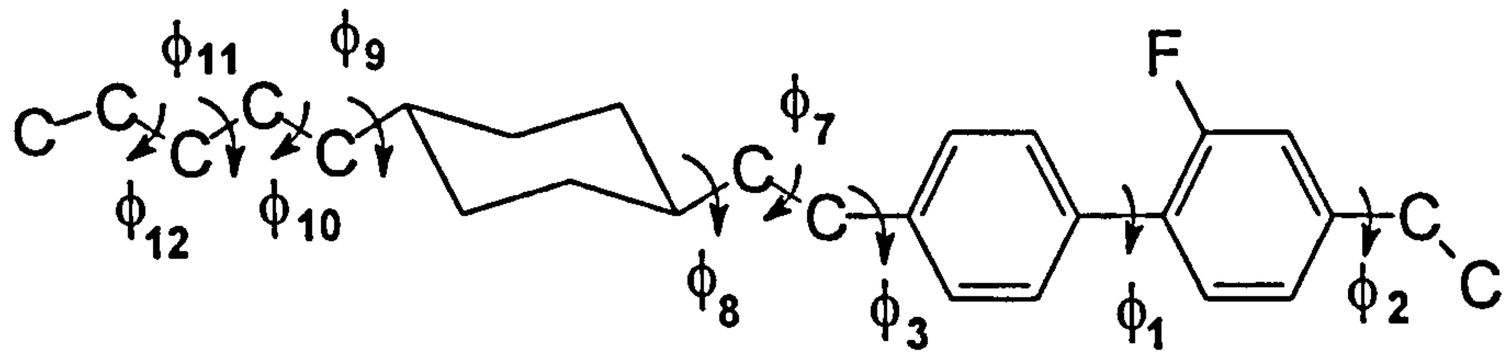

No.	ϕ_2	ϕ_3	ϕ_7	ϕ_8	ϕ_9	ϕ_{10}	ϕ_{11}	S_{zz}	S_{xx}-S_{yy}	S_{xy}	S_{xz}	S_{yz}	P_{LC}	P_{iso}
1	90	270	0	67	293	0	0	0.711	-0.051	0.033	-0.101	-0.217	0.027	0.014
16	90	90	0	67	293	0	0	0.733	-0.029	0.024	0.081	0.121	0.023	0.014
17	270	90	0	180	67	0	0	0.718	0.014	-0.039	-0.077	0.174	0.007	0.004
23	90	270	0	293	67	0	-112	0.740	0.028	0.015	-0.060	-0.122	0.006	0.004
65	90	270	0	293	67	-112	0	0.539	0.112	0.055	-0.099	-0.189	0.002	0.004

The overall conclusion from this work is that it has been shown that it is possible to study the conformation of large molecules in the liquid phase through the combination of ^{13}C-{^{1}H} NMR, VASS and the AP method. The pathway to the successful determination of the probability density for liquid crystals has been laid out and could be applied to other molecules which contain one or more F atoms.

6.6 References

[1] L.Rajnikant, D.Watkin, *Acta.Cryst.*, **C51**, 1452, (1995)

[2] D.W.Young, P.Tollin, H.H.Sutherland, *Acta.Cryst.*, **B24**, 161, (1968)

[3] B.Aldrige, G.De Luca, M.Edgar, S.Edgar, J.W.Emsley, M.I.C.Furby, M.Webster, *Liq.Cryst.*, **24**, 569, (1998)

[4] M.Edgar personal communication

[5] G.Celebre, G.De Luca, M.Longeri, D.Catalano, M.Lumetti, J.W.Emsley, *Mol.Phys.*, **85**,221, (1995)

[6] W.Caminati, D.Damiani, G.Corbelli, B.Velino, C.W.Bock, *Mol.Phys.*, **74**, 885, (1991)

[7] J.W.Emsley, G.De Luca, G.Celebre, M.Longeri, *Liq.Cryst.*, **20**, 569, (1996)

[8] S.J.Clark, C.J.Adam, D.J.Cleaver, J.Crain, *Liq.Cryst.*, **22**, 477, (1997)

[9] W.Haase, H.Paulus, *Mol.Cryst.Liq.Cryst.*, **100**, 111, (1983)

[10] M.R.Wilson, M.P.Allen, *Liq.Cryst.*, **12**, 157, (1992)

[11] A.J.Shaka, J.Keeler, *Prog.NMR.Spectrosc.*, **19**, 47, (1987)

[12] K.V.Schenker, D.Suter, A.Pines, *J.Mag.Reson.*, **73**, 99, (1987)

[13] D.Sandström, M.H.Levitt, *J.Am.Chem.Soc.*, **118**, 6966, (1996)

[14] D.Nanz, M.Ernst, M.Hong, M.A.Ziegeweid, K.Schmidt-Rohr, A.Pines, *J.Mag.Reson.* **A113**, 169, (1995)

[15] C.J.Turner in "Encyclopedia of NMR" (D.M.Grant and R.K.Harris, Eds.) Wiley, Chichester (1996). Heteronuclear Assignment Techniques, p 2335.

[16] J.W.Emsley, G.R.Luckhurst, C.P.Stockley, *Proc.Roy.Soc.London Ser A.* **381**, 117, (1982)

[17] P.J.Flory. Statistical Mechanics of Chain Models. Interscience, New York. (1996)

[18] G.Celebre, G.De Luca, M.Longeri, D.Catalano, C.A.Veracini, J.W.Emsley, *J.Chem.Soc. Faraday Trans.*, **87**, 2623, (1991)

Appendix A. - Input Files

A general description of the input files for the conformational analysis program LISTER are given below. No blank lines should exist in either file. The Molecule.data file contains experimental data and starting parameters for the calculation of the order parameters and conformational distribution of the molecule of interest. The Molecule.in file contains all structural information such as geometry and all axes of rotation. LISTER was designed initially to run interactively, however, the answers to the questions posed by LISTER can be stored in a batch file, an example of which is given in A.3. To execute LISTER to use this batch file, type the command in A.4.

A.1 Parameters File - Molecule.data

```
(1)     TITLE                                   FORMAT (a20)
```

Title Character String

```
(2)     ii                                      FORMAT (i2)
```

The number atoms including dummy atoms in the molecule or fragment of interest

```
(3)     ff.f,i,                                 FORMAT (f10.0,i1)
        ff.f,i,                                 FORMAT (f10.0,i1)
        ff.f,i,                                 FORMAT (f10.0,i1)
        ff.f,i,                                 FORMAT (f10.0,i1)
```

The function describing the form of the potential barrier for rotation used here is

$$V\phi_n = V_1\cos\phi_n + V_2\cos2\phi_n + V_3\cos3\phi_n + V_4\cos4\phi_n$$

The initial parameters for the fourier series are provided, with a flag to indicate whether the parameter should be allowed to vary in the calculation.

ff.f,i, V_1 for ϕ_n, vary=1 fix=0
ff.f,i, V_2 for ϕ_n, vary=1 fix=0
ff.f,i, V_3 for ϕ_n, vary=1 fix=0
ff.f,i, V_4 for ϕ_n, vary=1 fix=0

This list is repeated for each rotor, where V_n are in units of kJ mol^{-1}.

```
(4)     i,                                      FORMAT (i1)
```

Number of types of atoms present, including dummy atoms. The use of dummy

atoms is explained under part (8).

```
ff.f,ff.f,                                    FORMAT (2f10.0)
```

Lennard-Jones terms for each atom type. In normal operation both values are set to zero.

ff.f,ff.f, A / Å, E / kJ mol^{-1}

```
(5)     Observed Dipolar Couplings            FORMAT (a20)
```

Title Character String, indicating start of Dipolar Coupling list

```
A,B,C,D,                                      FORMAT (2i2,f10.0,i1)
```

A = Atom i

B = Atom j

C = dipolar coupling D_{ij} / Hz

D = weighting factor 1/0 indicating whether the coupling should be included are data in the calculation. Poorly resolved couplings are usually weighted as 0, and simply used for comparison with the calculated value.

```
0,0,0.0,0                                     FORMAT (2i2,f10.0,i1)
```

Line required to finish the list of D_{ij}.

```
(6a)    i,                                    FORMAT (i1)
```

Number of classes of rigid fragments within the molecule or fragment.

```
(6b)    i,                                    FORMAT (i1)
```

Number of rigid fragments in total within the molecule or fragment.

```
(6c)    A,B,                                  FORMAT (2i1)
```

For each fragment:

A Relates the fragment in the list to a fragment class.

B = 0/1 Fragment type ; unixial = 0, biaxial=1

```
(7)     f.f, f.f, f.f, i, i                   FORMAT (3f10.0,2i1)
```

ε_{ZZ}, ε_{XX}-ε_{YY}, ε_{XZ}, weighting ε_{ZZ} 1/0, weighting ε_{XX}-ε_{YY} 1/0

Local Epsilon values for each fragment type, in units of RT, plus flag indicating whether the parameter should be allowed to vary or not during the calculation.

(8) Fragment definitions FORMAT (a20)

Title - For each fragment, number 2 - total number of fragment.

2 atoms used to define symmetry axes. Unixial fragment only require 1 axis definition, the local z direction. Biaxial fragment require 3 axis definitions, in the local x,y and z directions. Given that some fragments such as benzene rings are planar, we need to define a 'dummy' atom orthogonal to the ring plane.

(8a) iz, jz FORMAT (2i2)
ix, jx FORMAT (2i2)
iy, jy FORMAT (2i2)

Fragment m / biaxial Z-direction

Fragment m / biaxial X-direction

Fragment m / biaxial Y-direction

(8b) iz, jz FORMAT (2i2)

Fragment n / uniaxial Z-direction

(9) 1,0,0,0, FORMAT (4i1)

Include one of these lines for each fragment type. This is really redundant now, with the introduction of biaxiality.

(10) Interacting Spins FORMAT (a20)

Title, Indicating start of list of atomic interactions affecting the Lennard-Jones potential.

i,j, FORMAT (2i1)

i and j are a pair of nuclei who are involved in a changing potential throughout molecular internal motion.

0,0, FORMAT (2i1)

Line required to finish the list of interacting spins.

(13a) averaging parameters FORMAT (a20)

Title, Indicating a list of dipolar couplings that are averaged over internal molecular motion. allows the reduction in the number of conformers to be sampled.

```
(13b)    A,                                          FORMAT (i2)
```

Number of sets of averaged couplings

```
(13c)    B,                                          FORMAT (i2)
```

For each set of averaged couplings in A, the number of couplings to be averaged

```
(13d)    i,j,                                        FORMAT (2i2)
```

For each set given by A and the number of couplings to be averaged in that set given by B include an atomic pair which define a D_{ij}.

```
(14)     0,                                          FORMAT (i1)
```

Flag for program execution type (0=iterative, 1=non iterative)

A.2 Molecular Structure File - molecule.in

```
(1)      24                                          FORMAT (i2)
```

Number of atoms including dummy atoms

```
(2)  0 0 0    0.0000     0.0000     0.0000     0.0000 00        FORMAT (3i2,4f10.4,i2)
     1 0 2    0.0        0.0        0.75      61.608   0        FORMAT (3i2,4f10.4,i2)
     2 1 2  120.0        0.0        1.4       61.608   0        FORMAT (3i2,4f10.4,i2)
     3 2 2 -120.0        0.0        1.4       61.608   0        FORMAT (3i2,4f10.4,i2)
     4 3 3  120.0        0.0        1.35     230.601   1        FORMAT (3i2,4f10.4,i2)
    14 3 1  120.0        0.0        1.075      0.0     0        FORMAT (3i2,4f10.4,i2)
    23 1 4    0.0       90.0        1.0        0.0     0        FORMAT (3i2,4f10.4,i2)
```

FORMAT (3i2,4f10.4,i2) = FORMAT (A,B,C,D,E,F,G,H)

Connectivity table for the molecule in question.

A (i2) Atom number

B (i2) Atom to which A has its position defined from.

C (i2) Atom type - related to Lennard Jones potential

D (f10.4) Bond Angle beween A and B and B' (where B' is the atom to which B had its postion defined from). The sign of the bond angle defines the bond direction.

E (f10.4) Bond Angle out of the XZ plane - try to avoid using this.

F (f10.4) Distance A-B, usually a bond length / Å

G (f10.4) Gyromagetic ratio

H (i2) Flag indicating D can change according to motion about ϕ_1.

- Note - The first atom in your molecule should be attatched to atom 0

```
(3)      0                              FORMAT (i1)
```

Atom number which is defined as the origin.

```
(4a)     A,B,C,                         FORMAT (3f10.0)
```

For each rotor, include the following definition.

A = Beginning step / °

B = Ending Step / °

C = Step Size / °. For steps of 0°, use 360°.

```
(4b)     7 1                            FORMAT (2i2)
```

Two atoms which define a rotation axis within the molecule or fragment.

```
(4c)     1                              FORMAT (i2)
         2                              FORMAT (i2)
         0                              FORMAT (i2)
```

List of atoms to be rotated about axis defined in (4b). Atom 0 indicates end of list.

Repeat similar list (4) for each rotor.

```
(5)      1,H                            FORMAT (i1,a2)
         2,C
         3,F
         4,x
         0,x
```

Associate atom type to an atomic symbol. This associaton is used to create .pdb data files for RASMOL, the molecular drawing package.

A.3 Initialisation - lister.ini

This is the general form of the initialisation file which tells LISTER which input files to use and which output files to write.

```
Molecule.data
Results.out
Molecule.in
Geometry.output
Molecule.pdb
```

Molecule.data - A.1 / B.1

Results.out - C.1

Molecule.in - A.2 / B.2

Geometry.output - C.2

Molecule.pdb

A.4 Execution - exe

```
#!/bin/csh
lister
chmod og+rx *
```

This simple UNIX shell script executes LISTER and once this has finished changes the file permissions of all files in the same directory so that they are readable via the World Wide Web, through the use of a suitable browser.

Appendix B. Examples of Input Files

The examples given below are the input files used for the calculations of the conformational distribution of the liquid crystal I35.

B.1 I35.data

```
I35
38
0.0,0,
-2.5,0,
0.0,0,
5.472,0,
0.0,0,
0.0,0,
0.0,0,
0.0,0,
0.0,0,
0.0,0,
0.0,0,
0.0,0,
0.0,0,
-2.5,0,
0.0,0,
0.0,0,
0.0,0,
0.0,0,
-2.5,0,
0.0,0,
0.0,0,
0.0,0,
0.0,0,
-2.5,0,
0.0,0,
0.0,0,
0.0,0,
0.0,0,
-2.5,0,
0.0,0,
0.0,0,
0.0,0,
0.0,0,
-2.5,0,
0.0,0,
0.0,0,
0.0,0,
0.0,0,
5,
2.42, 0.03,
3.55, 0.07,
2.94, 0.061,
0.0,0.0,
3.55, 0.07,
 dipolar couplings
 1,13,  705.4  ,1
 2,13, 1502.1  ,1
 3,13, -922.7  ,1
 4,13, -135.8  ,1
 5,13,   45.5  ,1
 6,13,  179.9  ,0
 7,13,    1.0  ,0
 8,13, -216.5  ,1
```

```
 9,13,  -139.9  ,1
10,13,  -105.1  ,1
11,13,  -139.9  ,1
12,13,  -216.5  ,1
13,15,  -102.0  ,1
13,20,   -42.0  ,0
13,25,   -73.5  ,1
13,26,   -51.5  ,1
13,27,   -33.5  ,1
13,28,   -23.0  ,1
13,29,   -38.5  ,1
13,30,   -26.0  ,1
13,31,   -21.5  ,1
13,32,   -21.5  ,1
13,33,   -13.5  ,1
13,34,   -13.5  ,1
13,35,   -12.5  ,1
13,36,    -1.0  ,0
13,37,    -7.0  ,1
13,38,    -6.0  ,1
00,00,     0.0  ,0
3,
18,
1,1,
1,1,
2,0,
3,0,
3,0,
3,0,
3,0,
3,0,
3,0,
3,0,
3,0,
3,0,
3,0,
3,0,
3,0,
3,0,
3,0,
0.7392, 1.6337, 0.0, 1, 1
-0.1283, 0.00, 0.0, 1, 0
0.8112, 0.00, 0.0, 1, 0
Fragment Definitions
 7,10,
 8,12,
 7,24,
 2,13,
15,25,
25,26,
26,27,
27,28,
29,20,
30,29,
31,30,
32,30,
33,31,
34,32,
35,33,
```

```
35,34,
36,35,
37,36,
38,37,
1,0,0,0,
1,0,0,0,
1,0,0,0,
interacting spins
2,8,
2,12,
2,18,
2,22,
6,8,
6,12,
6,18,
6,22,
8,13,
8,17,
12,13,
12,17,
13,18,
13,22,
17,18,
17,22,
0,0,
averaging parameters
4,
2,
2,
2,
2,
 8,13,
12,13,
 9,13,
11,13,
13,31,
13,32,
13,33,
13,34,
1,
```

B.2 I35.in

```
38
 0 0 0     0.0000     0.0000     0.0000     0.0000 00
 1 0 2     0.0        0.0        0.7457    61.608    0
 2 1 2   122.4021     0.0        1.3869    61.608    0
 3 2 2  -123.0297     0.0        1.3782    61.608    0
 4 3 2  -119.1023     0.0        1.3836    61.608    0
 6 1 2  -121.1391     0.0        1.3939    61.608    0
 5 6 2   121.8066     0.0        1.3839    61.608    0
 7 0 2   180.0        0.0        0.7457    61.608    0
 8 7 2  -120.7290     0.0        1.3881    61.608    0
 9 8 2   120.7378     0.0        1.3852    61.608    0
10 9 2   120.3870     0.0        1.3836    61.608    0
12 7 2   120.7290     0.0        1.3881    61.608    0
1112 2  -120.7378     0.0        1.3852    61.608    0
13 2 3   120.2025     0.0        1.35     230.601    0
```

```
14 3 1  118.9754     0.0        1.0739     0.0      0
15 4 5  119.7719     0.0        1.53      61.608    0
16 5 1 -119.8711     0.0        1.0748     0.0      0
17 6 1 -118.6108     0.0        1.0748     0.0      0
18 8 1 -119.6528     0.0        1.0746     0.0      0
19 9 1 -119.6598     0.0        1.0755     0.0      0
2010 5 -120.3958     0.0        1.53      61.608    0
2111 1  119.6598     0.0        1.0755     0.0      0
2212 1  119.6528     0.0        1.0746     0.0      0
23 1 4    0.0       90.0        1.0        0.0      0
24 7 4    0.0       90.0        1.0        0.0      0
2515 5 -120.0        0.0        1.53      61.608    0
2625 5  115.0        0.0        1.54      61.608    0
2726 5 -115.0        0.0        1.54      61.608    0
2827 5  115.0        0.0        1.54      61.608    0
2920 5  120.0        0.0        1.53      61.608    0
3029 5 -115.0        0.0        1.54      61.608    0
3130 5  125.265     54.735      1.54      61.608    0
3230 5  125.265    -54.735      1.54      61.608    0
3331 5 -115.265    -54.735      1.54      61.608    0
3432 5 -115.265     54.735      1.54      61.608    0
3534 5  115.0        0.0        1.54      61.608    0
3635 5 -115.0        0.0        1.54      61.608    0
3736 5  115.0        0.0        1.54      61.608    0
3837 5 -115.0        0.0        1.54      61.608    0
0
40,140,100,
 710
 8
 9
11
12
18
19
20
21
22
24
29
30
31
32
33
34
35
36
37
38
 0
90,270,180,
 415
25
26
27
28
 0
90,270,180,
1020
29
30
```

```
 31
 32
 33
 34
 35
 36
 37
 38
  0
-112,112,112,
1525
26
27
28
 0
-112,112,112,
2526
27
28
 0
-112,112,112,
2029
30
31
32
33
34
35
36
37
38
 0
67,293,113,
2930
31
32
33
34
35
36
37
38
 0
67,293,113,
3536
37
38
 0
1,H
2,C
3,F
4,x
5,C
0,x
```

Appendix C. The Output Files

There are 3 output files produced by the successful execution of LISTER.

C.1 Results.out

This file contains the final parameters found by minimising the difference between the observed and the calculated dipolar couplings, by varying the rotation potentails and the epsilon parameters. A list of all the explored conformations is included with their probabilities of existance in the liquid crystal and isotropic phases, and a sorted list of the top few conformers with their order parameters.

C.2 Geometry.output

This file contains the cartesian coordinates for a particular conformer. In normal running this is the final conformer calculated. However, molecule.in may be tailored so that single forms are only considered. This is useful once the minimum energy conformer is determined and the user wants to confirm the geometry. To do this a change is needed to the molecule.in file at the point Appendix A.2 section (4a). To confine this rotor to a fixed angle, define A,B and C as the same angle i.e. 90,90,90,. This will produce a fixed angle about the chosen rotor of 90° from the starting position.

C.3 Molecule.pdb

This file is a .pdb file that can be viewed by RASMOL, a molecular drawing package that can produce an image of the molecule. This again is very useful for looking at a particular conformer of interest. However, this file is much more useful for checking that the molecule has been correctly defined in the molecule.in file.

RASMOL is freeware software that is available for most platforms.

Appendix D. The Source Code - lister.f

This is the source code for the conformational analysis program, LISTER.

```
      PROGRAM lister

c*************************************************
c
c   Important parameters that may need to be changed
c   depending on molecule.
c
c
c   ndc is the most likely change, if it too big then the program
c   will be allocated less CPU time on the SUCS servers.
c
c   ndc=2000 - no.confs (influences greatly program speed and swap space)
c   (6 substitutions)
c
c   these are suitable for most cases, but may require changing for
c   for each experiment.
c
c   ntopfew=200 - printing the top 'ntopfew' probability conformers
c   rkelvin=300.0d0 - Temparature at which experiments are carried out (RT).
c   nop=40 - no. atoms
c   nta=10 - no. atom types
c   nft=18 - no. fragments
c   mdec=406 - no. couplings (45 * 10 spins) (300 sufficient for 24 spins)
c     I have written a small program to calculate this number (mdec.f)
c   ndec=18 - no. of variables (epsilons and potentials)
c   ngv=5 - no. of groups of averaged dipolar couplings
c   (can do a simple search and replace on above parameters)
c
c   nr=8 - no. rotors(requires additional code for nr>3 -(easy to add)
c   +
c   requires 6 code changes
c   search for *rotchange* to see where code needs adding
c
c*************************************************
c   Potential barrier energy, V(phi), is in kJ/mol it is divided
c   by RT within the program
c   Epsilons are in units of RT. Multilply by approx 2.5 for kJ/mol
c*************************************************************************

C*************************************************************************
C     CALCULATION OF A ROTATIONAL POTENTIAL SURFACE BY CALCULATION OF
C     DIPOLAR COUPLINGS AND MINIMISATION OF THE DIFFERENCE BETWEEN THESE
C     AND THE EXPERIMENTALLY OBSERVED COUPLINGS
C              THE MINIMISATION ROUTINE E04FCF IS USED TO ADJUST THE
C              EPSION VALUES AND WEIGHTING FACTORS TO MINIMISE
C              FDC(CALC)-DC(OBS)σ**2.
C
C     VARIABLE & PARAMETER NAME DEFINITIONS:
C
C     NS       = NO. INTERACTING SPINS
C     NFRAG    = NO. FRAGMENTS IN FLEXIBLE MOLECULE
C     NCON     = NO. CONFORMATIONS
C     DCOBS    = OBSERVED EXPERIMENTAL DIPOLAR COUPLINGS
C     DCAVE    = AVERAGED CALCULATED DIPOLAR COUPLINGS
C     DELTADC = DIFFERENCE BETWEEN CALC. & OBSERVED DIPOLAR COUP.
C     FX, FY, FZ = X, Y & Z COORD. FOR FRAG. LOCAL AXES
C     XCOS, YCOS, ZCOS = COS TERMS IN THE CALC. OF TOTAL EPSILON TERMS
C     C1, C2, C3, C4    = TERMS IN THE CALC. OF DIPOLAR COUPLINGS
C     SZZ, SDXY, SXY, SXZ, SYZ = ORDER PARAMETERS ( SDXY=SXX-SYY )
C     EP20, EP22 = EPSILON VALUES 2,0 & 2,2
C     PROB     = FRACTIONAL PROBABILITY OF CONFORMATIONS
C     SX, SY, SZ = X, Y, Z COORD. OF SPINS
C     GAMMA    = GAMMA VALUE ( K ) OF EACH SPIN
C     IA, JA   = VALUES TO CARRY AVERAGED DIPOLAR COUPLING INFO. TO SUBR
C     NG       = NO. GROUPS OF DC'S THAT ARE AVERAGED IN EACH CONF.
C     NIG      = NO. COUPLINGS IN EACH GROUP
C     NDEC, MDEC = NO. VARIABLES & NO COUPLINGS FOR MINIMISATION ROUTINE
```

```
C     X = ARRAY CONTAINING VARIABLES FOR ITERATION IE. EPS & PROBS
C     ETA     = SPECIFIES ACCURACY OF MINIMISATION
C     XTOL    = SPECIFIES ACCURACY OF X IN MINIMISATION
C     FSUMSQ  = VALUE OF SUM OF SQUARES
C     STEPMX  = ESTIMATE OF DISTANCE BETWEEN SOLUTION & STARTING POINT
C     IFAIL   = FLAG TO SHOW ERRORS IN NAG ROUTINE
C     IPRINT  = FLAG TO SET OFF PRINT ROUTINE
C     nopCAL  = 400*N ; nop NO. CALCULATIONS
C     N, M    = NO. VARIABLES & NO COUPLINGS FOR MINIMISATION ROUTINE
C     NF      = NO. PASSES THROUGH LSQFUN
C     NITER   = NO. ITERATIONS
C     FVEC    = VALUE OF RESIDUALS AFTER MINIMISATION
C     S       = SINGULAR VALUES AT END OF MINIMISATION
C     G       = GRADIENT OF SUM OF SQUARES
C     V, FJAC = ARRAYS IN E04FCF
C     LV, LJ  = ARRAY DIMENSIONS
C     IW, W   = WORKSPACE ARRAYS IN E04FCF
C     LIW, LW = WORK SPACE ARRAY LENGTHS
C     X02AJF  = MACHINE PRECISION
C     LSQFUN, LSQGRD, LSQMON = SUBROUTINES
C*********************************************************************
      IMPLICIT real*8 (A-H,O-Z)

      PARAMETER (nop=40, npl1=NOP-1, nta=10)
      PARAMETER (NDEC=18, mdec=406, LIW=1, LV=NDEC, LJ=MDEC)
      PARAMETER (LW=6*NDEC+MDEC*NDEC+2*MDEC+NDEC*(NDEC-1)/2)
      PARAMETER (NIN=20, NOUT=21, nr=8, ndc=2000, nft=18)
      parameter (nftref=(nft-1)*3)
      parameter (ngv=5)
      parameter (plow=0.01d0)

C     SCALARS IN COMMON:
      INTEGER NCON, NFRAG, NTFRAG, NG
      real*8 vp

C     ARRAYS IN COMMON:
      real*8 xcos(ndc,nftref), ycos(ndc,nftref), zcos(ndc,nftref),
     *     CEPDIAG(NDC,3,3), sinb(ndc,nftref), cosg(ndc,nftref),
     *     sing(ndc,nftref) ,DCOBS(npl1,nop), DCAVE(npl1,nop),
     *     C1(NDC,npl1,nop) ,C2(NDC,npl1,nop), C3(NDC,npl1,nop),
     *     C4(NDC,npl1,nop) ,SZZ(NDC), SDXY(NDC), SXY(NDC),
     *     SXZ(NDC), SYZ(NDC) ,PLC(NDC), PISO(NDC), CEPSN(NDC,3,3),
     *     DELTADC(npl1,nop), REPUL(NDC),vpot(nr,4),smatrix(7),
     *     cj(mdec),deltapc
      INTEGER IA(ngv,9), JA(ngv,9), NIG(ngv), KIND(NFT), biax(nft),
     *        REL2(NFT), WF(npl1,nop), FLAG(NFT), flag2(nft), VAR(NFT),
     *        REL(NFT), REL1(NFT), zzwei(nft), dxywei(nft),vvpot(nr,4)
      character*1 symbol(nta)

C     LOCAL SCALARS:
      real*8 ETA, FSUMSQ, STEPMX, XTOL
      INTEGER IFAIL, IPRINT, M, nopCAL, N, NF, NITER, NAT

C     LOCAL ARRAYS:
      real*8 FJAC(MDEC,NDEC), FVEC(MDEC), G(NDEC), S(NDEC),
     *     WORK(NDEC), V(LV,NDEC), W(LW), X(NDEC), EPZZ(NFT),
     *     EPDXY(NFT), epxz(nft),
     *     P(NDEC,NDEC), ATA(NTA), ATE(NTA)
      INTEGER IW(LIW), fa1(nftref), fa2(nftref), iswf(nop-1,nop)

c     arrays from subroutine coordinates
      real*8 gamma(nop),rots(ndc,nr),rot(nr),dclarge,plarge
      character*20 out,data
      logical nbool

      INTRINSIC SQRT, ACOS

C     EXTERNAL FUNCTIONS:
      real*8  X02AJF
      EXTERNAL X02AJF

C     EXTERNAL SUBROUTINES:
      EXTERNAL E04FCF, E04YCF, LSQFUN, LSQGRD, LSQMON
```

```
common/block1/nfrag,ntfrag
common/block1a/wf,flag,var,rel,rel1,rel2,flag2,vvpot
COMMON/BLOCK2/DCAVE
common/block3/XCOS, YCOS, ZCOS, SINB, COSG, SING, biax
common/block3a/KIND,zzwei, dxywei
COMMON/BLOCK4/C1, C2, C3, C4
COMMON/BLOCK5/NG, NIG, IA, JA
COMMON/BLOCK6/SZZ, SDXY, SXY, SXZ, SYZ, smatrix
COMMON/BLOCK7/DELTADC, PLC, PISO, CEPSN, CEPDIAG
common/block9/DCOBS
common/block9a/np, NCON
common/block10/REPUL
COMMON/BLOCK10a/EPZZ, EPDXY,vpot
common/block11/rots
common/block12/fa1,fa2,ata,ate
common/block13/dclarge
common/block14/symbol
```

```
c*********************************************************************
c**The beginning of the program
c*********************************************************************

c*********************************************************************
c** Reading lister.ini file containing
C** file names for inout and output files.
c*********************************************************************
      open(69,file='lister.ini',status='old')


c*********************************************************************
c** Reading data file "molecule.data" containing parameters
c** such as potential terms epsilons dij
c*********************************************************************
      read (69,'(a)') data
      read (69,'(a)') out
      open(20,file=data,status='old')
      open(21,file=out,status='unknown')

      READ (nin,'(A40)') TITLE
      WRITE (NOUT,'(A40)') TITLE


c*********************************************************************
c** Wobble term introduced for bond relaxation - curve modelled
c** on 4 term fourier series. If this file is not present LISTER
C** defaults the parameters to 0.
c*********************************************************************
       inquire(file='wobble',exist=nbool)
       if (nbool) then
          open(14,file="wobble",status='unknown')
          read(14,*) f0,f1,f2,f3,f4
          close(14)
       else
         f0=0.0d0
         f1=0.0d0
         f2=0.0d0
         f3=0.0d0
         f4=0.0d0
       end if
       write(nout,*)'Wobble terms included',f0,f1,f2,f3,f4


c*********************************************************************
c** Number of atoms in the molecule, including dummy atoms.
C** Dummy atoms are used to define the orthogonal axis to the XZ plane
c** in planar rigid biaxial fragments.
c*********************************************************************
      READ (nin,*) NP
      write (nout,*) 'num atoms = ',np

c*********************************************************************
c** V terms for fourier series modelling rotation potential.
c** currently set for the first 4 terms. Changing the form of the
c** potential requires coding changes. Units = kJ/mol.
```

```
c** A good suggestion here is to include the equation of choice in an input file
c**********************************************************************
      do nloop=1,nr
        do mloop=1,4
          read(nin,*) vp,nvv
          vpot(nloop,mloop) = vp
          vvpot(nloop,mloop) = nvv
          write(nout,*) 'V',mloop,'=',vp
        end do
      end do

c**********************************************************************
c**
c** Atoms types i.e. (C)=C (C)-C -(H) C=(O) (O)-C-O (F)-
c** These definations are important for repulsion calculations.
c** They are also related to their chemical symbols for the .pdb file.
c**********************************************************************
      READ(NIN,*) NAT
      write (nout,*) 'Number of atom types - ',nat
      WRITE(NOUT,*) 'ATOM TYPE    A-     E-'
      DO 110 I= 1, NAT
         READ(NIN,*) ATA(I), ATE(I)
         WRITE(NOUT,35) I, ATA(I), ATE(I)
 110  CONTINUE

c**********************************************************************
c** Input observed Dipolar couplings from analysis of NMR spectrum
c**********************************************************************
      READ(NIN,'(A)') LABEL
      call dccc(dcobs,wf,m)

c**********************************************************************
c** Define the rigid fragments of the molecule.
c** Unixial or biaxial and local epsilon values for ordering.
c**********************************************************************
      READ(NIN,*) NTFRAG
      WRITE(NOUT,10) 'NO. TYPES OF FRAGMENTS IN MOLECULE = ', NTFRAG
      READ(NIN,*) NFRAG
      WRITE(NOUT,10) 'NO. FRAGMENTS IN MOLECULE = ', NFRAG
      WRITE(NOUT,*) 'FRAGMENT 1 CONTAINS THE REFERENCE AXES.'

      do i=1, nfrag
         read(nin,*) kind(I), biax(i)
         write(nout,*) kind(i),biax(i)
      end do

c**********************************************************************
C** THE EPSILON VALUES FOR EACH FRAGMENT ARE READ IN
c** Ezz, Exx-Eyy and Exz. Weighting is only considered for Ezz and Exx-Eyy.
C** There may be a problem with Exz. Units = kJ/mol
c**********************************************************************
      do i=1, ntfrag
         read(nin,*) epzz(i), epdxy(i), epxz(i), zzwei(i), dxywei(i)
      end do


c**********************************************************************
C** The fragment axes are defined for each fragment, except fragment 1.
c** Note, only need 1 axis for unixial fragments, and 3 axes for biaxials.
c**********************************************************************
      READ(NIN,'(A)') LABEL
      icount = 0
      do i=2, nfrag
         if (biax(i).ne.1) then
            icount = icount + 1
            read(nin,*) fa1(icount), fa2(icount)
         else if (biax(i).eq.1) then
            do nloop=1,3
               icount = icount + 1
               read(nin,*) fa1(icount),fa2(icount)
            end do
         end if
      end do


c**********************************************************************
```

```
c** Start to output data to a file - molecule.out
c** Including results of fitting and final conformational distribution.
c*****************************************************************
      WRITE(NOUT,*)
      WRITE(NOUT,*) 'THE INITIAL VALUES FOR THE EPSILON VALUES ARE:'
      WRITE(NOUT,*)
      WRITE(NOUT,*) 'F. TYPE    EPZZ     EPXX-EPZZ   EPXZ'


c*****************************************************************
c** input values - entered into array for minimisation routine E04FCF
c*****************************************************************
      K= 0
      DO 155 I=1,NTFRAG
c*****************************************************************
c**  These parameters used to group uniaxial fragments into biaxial,
c**  so this is  really redundant now - input file requires :
C**  1,0,0,0, (var,rel,rel1,rel2). This only remains as it may be
c**  useful for making comparisons with the biaxial code.
c*****************************************************************
         READ (NIN,*) VAR(I), REL(I), REL1(I), REL2(I)

c*****************************************************************
c** the first if statement is the only one that is really used now
c** The epsilons are now inputed into an array that is call by the
c** iteration routine LSQFUN.
C** The epsilons are being imported into the array X() which is
c** requested by LSQFUN.
c*****************************************************************
         IF((VAR(I).EQ.1) .and. (rel(i).eq.0)) THEN
            if (zzwei(i).eq.1) then
               k=k+1
               x(k) = epzz(i)
            end if
            if (dxywei(i).eq.1) then
               if (epdxy(i).ne.0.0) then
                  k=k+1
                  x(k) = epdxy(i)
                  flag(i) = 1
               else
                  flag(i) = 0
               end if
            else
               if (epdxy(i).ne.0.0) then
                  flag(i) = 1
               else
                  flag(i) = 0
               end if
            end if
            if (epxz(i).ne.0.0) then
               k = k+1
               x(k) = epxz(i)
               flag2(i) = 1
            else
               flag2(i) = 0
            end if
         END IF


         WRITE(NOUT,35) I, EPZZ(I), EPDXY(I), epxz(i)
155   CONTINUE
c*****************************************************************
C** The V's are being imported into the array X() which is
c** requested by LSQFUN.
c*****************************************************************
      do nloop=1,nr
        do mloop=1,4
          if(vvpot(nloop,mloop).eq.1) then
            k=k+1
            x(k)=vpot(nloop,mloop)
          end if
        end do
      end do

c*****************************************************************
```

```
c**  no.of variables used in iteration : nndec
c*************************************************************************
      nndec = k

c*************************************************************************
c** Define interacting spins for repulsive term. Usually only need to
c** define a pair of atoms whose interatomic distance changes with
c** internal molecular motion and who are close enough to have a steric
c** or charge effect.
c*************************************************************************
      call iss(iswf,numints)


c*************************************************************************
c** Calculate cartesians from bond lengths and angles for each conformer
c*************************************************************************
      call coordinates(gamma,rots,rot,iswf,ndc)


      WRITE (NOUT,*) 'NO. CONFORMATIONS' , NCON


c*************************************************************************
C     AVERAGING:
C     SOME SYSTEMS GROUPS OF PROTONS ARE EQUIVALENT BECAUSE OF
C     INTERNAL ROTATIONS. GROUPS OF DIPOLAR COUPLINGS MUST BE
C     AVERAGED TO ALLOW FOR THIS. THE FOLLOWING SECTION DOES THIS.
c*************************************************************************
      WRITE(NOUT,*)
      WRITE(NOUT,*)'GROUPS OF COUPLINGS WHICH ARE AVERAGED :'
      READ (NIN,'(A)') LABEL
      READ(NIN,*) NG
      write (nout,*) ng

      IF (NG.ne.0) THEN
         do K= 1, NG
            READ(NIN,*) NIG(K)
         end do
         do K= 1, NG
            WRITE(NOUT,10) 'GROUP ',K
            do L= 1, NIG(K)
               READ(NIN,*) IA(K,L) ,JA(K,L)
               WRITE(NOUT,75) IA(K,L) ,JA(K,L)
            end do
         end do
      END IF



      N = nndec

c*************************************************************************
c** Writing to output file the variables that will be used in the calculation
c*************************************************************************
      write (nout,*)
      write (nout,*) 'Input Variables'
      WRITE(NOUT,80) (X(I),I=1,N)


c*************************************************************************
c** The first if statement is asking for the status of the flag which
c** determines whether the program will perform iterative calculation or not
c*************************************************************************
      read (nin,*) nflag
      close(20,status='keep')
      if (nflag.ne.1) then
c******** Chosen iterative routine *********
         IPRINT= 1
         nopCAL= 400*N
         ETA= 0.1d0
         XTOL= 1.0d-5
         STEPMX= 3.0d0
         IFAIL= -1
```

```
c*********************************************
c** E04FCF is the minimisation NAG routine
c** A description can be found at http://www.nag.ac.uk/......
c*********************************************
         CALL E04FCF (M, N, LSQFUN, LSQMON, IPRINT, nopCAL,
     *               ETA, XTOL, STEPMX, X, FSUMSQ, FVEC, FJAC,
     *               LJ, S, V, LV, NITER, NF, IW, LIW, W, LW,
     *               IFAIL)


         IF (IFAIL.NE.0) THEN
            WRITE(NOUT,85)' ERROR EXIT TYPE', IFAIL,'-SEE DOCUMENT'
         END IF

c*********************************************
c** RMS on the fit
c*********************************************
         IF (IFAIL.NE.1) THEN
            WRITE (NOUT,*)
            WRITE (NOUT,*)' ON EXIT, THE normalised SUM OF SQUARES IS'
            WRITE (NOUT,80) FSUMSQ

c*********************************************
c** This bit is associated with the normalisation of the Dij.
c** Normalisation may improve the efficieny of the minimisation routine.
c*********************************************
            unnormsumsq=0.0d0
            do i=1,np-1
             do j=i+1,np
              deltadc(i,j)=deltadc(i,j)*dclarge
               unnormsumsq=unnormsumsq+(deltadc(i,j)*deltadc(i,j))
              deltadc(i,j)=deltadc(i,j)/dclarge
             end do
            end do

c*****************************************
c** LISTER will print the results of statistical analysis
c** from the iterative process.
c*****************************************
            WRITE (NOUT,*)' ON EXIT, THE unnormalised SUM OF SQUARES IS'
            WRITE (NOUT,80) unnormsumsq
            WRITE (NOUT,*) ' AT THE POINT'
            WRITE (NOUT,80) (X(J),J=1,N)

            CALL LSQGRD(M,N,FVEC,FJAC,LJ,G)

            WRITE (NOUT,*)
            WRITE (NOUT,*) ' THE ESTIMATED GRADIENT IS'
            WRITE (NOUT,80) (G(J),J=1,N)
            WRITE (NOUT,*) ' (MACHINE DEPENDENT)'
            WRITE (NOUT,*)
            WRITE (NOUT,*) ' S VALUES'
            WRITE (NOUT,80) (S(J),J=1,N)
            WRITE (NOUT,*)
            WRITE (NOUT,*) ' V MATRIX'
            DO 310 I=1, N
               WRITE (NOUT,98) (V(I,J), J=1,N)
310         CONTINUE

            IFAIL=-1
            CALL E04YCF (-1,M,N,FSUMSQ,S,V,LV,cJ,WORK,IFAIL)
c*****************************************
c** A description of E04YCF can be found at http://www.nag.ac.uk/......
c*****************************************

            IF (IFAIL.NE.0) THEN
               WRITE(NOUT,85)' EXIT FROM ERROR ROUTINE: ERROR TYPE',
     *                       IFAIL,' '
            END IF

            IF ((IFAIL.NE.1) .AND. (IFAIL.NE.2)) THEN
               WRITE (NOUT,*)
               WRITE (NOUT,*)' VARIANCE-COVARIANCE MATRIX'
               do I=1, N
                  WRITE (NOUT,98) (V(I,J), J=1,N)
               end do
```

```
                WRITE (NOUT,*)
                WRITE (NOUT,*)' PARAMETER-CORRELATION MATRIX'
                do I=1, N
                   do J=1, N
                      P(I,J)= V(I,J)/(SQRT(V(I,I))*SQRT(V(J,J)))
                   end do
                end do
                do I=1, N
                   WRITE (NOUT,98) (P(I,J), J=1,N)
                end do

             END IF
          END IF

       else if (nflag.eq.1) then
c*********************************************
c** Non iterative form of the program. THe flag for this is found
c** at the bottom of the molecular parameters input file.
c*********************************************
          iflag = 1
          call lsqfun (iflag,m,n,x,fvec,iw,liw,w,lw)
       end if
****** end of iterative loop*************************


c*****************************************************
c** Now retrieve the epsilons and V's from the array x()
c*****************************************************
       L= 0
       DO 375 I= 1, NTFRAG
          IF ((VAR(I).EQ.1) .and. (rel(i).eq.0)) THEN

             if (zzwei(i).eq.1) then
                l=l+1
                epzz(i) = x(l)
             end if

             if (dxywei(i).eq.1) then
                if (flag(i).eq.1) then
                   l=l+1
                   epdxy(i) = x(l)
                else
                   epdxy(i) = 0.0d0
                end if
             else
                if (flag(i).eq.0) then
                   epdxy(i) = 0.0d0
                end if
             end if

             if (flag2(i).eq.1) then
                l=l+1
                epxz(i) = x(l)
             else
                epxz(i) = 0.0d0
             end if

          else IF ((VAR(I).Eq.0) .AND. (REL(I).EQ.2)) THEN
c*********************************************
c** redundant code if using proper biaxial notation
c*********************************************
             j=rel1(i)
             epzz(i) = epzz(j)

          else IF ((VAR(I).Eq.0) .AND. (REL(I).EQ.1)) THEN
c*********************************************
c** redundant code if using proper biaxial notation
c*********************************************
             J = REL1(I)
             K = REL2(I)
             EPZZ(I)= EPZZ(J)+EPZZ(K)
             EPZZ(I)=-EPZZ(I)
          END IF

 375   CONTINUE
```

```
c*****************************************************************
c** Writing final parameter values to the output file molecule.out
c*****************************************************************
      WRITE (NOUT,*)
      WRITE(NOUT,*) 'THE FINAL VALUES FOR THE EPSILON VALUES ARE: (RT)'
      WRITE(NOUT,*)
      WRITE(NOUT,*) 'F. TYPE    EPZZ     EPXX-EPZZ    EPXZ'
      do I=1,NTFRAG
         WRITE(NOUT,35) I, EPZZ(I), EPDXY(I), epxz(i)
      end do
      WRITE(NOUT,*)
      WRITE(NOUT,*) 'THE FINAL VALUES FOR THE POTENTIAL TERMS ARE: '
      write(nout,*) '(kJ/mol)'
      WRITE(NOUT,*)
      do nloop=1,nr
        do mloop=1,4
          if(vvpot(nloop,mloop).eq.1) then
            l=l+1
            vpot(nloop,mloop) = x(l)
          end if
          WRITE(NOUT,*) 'V',mloop,' bond ',nloop,' = ',vpot(nloop,mloop)
        end do
      end do
      WRITE(NOUT,*)
      WRITE(NOUT,*) ' I J      D(OBS)         D(CALC)       D(CA-OB)    %D'
      WRITE(NOUT,*)

      do I=1, np-1
         do J= I+1, np
            if (dcave(i,j).ne.0.0) then
c***normalisation of dij's**********************
               dcobs(i,j)=dcobs(i,j)*dclarge
               dcave(i,j)=dcave(i,j)*dclarge
               deltadc(i,j)=deltadc(i,j)*dclarge
c*****************************************************
               deltapc= ( 100.0d0 / dcave(i,j) ) * deltadc(i,j)
               WRITE(NOUT,90) I, J, DCOBS(I,J), DCAVE(I,J),
     *                        DELTADC(I,J), deltapc
            end if
         end do
      end do

c** Writing order parameter for every conformer to another output file.
c      open (25,file='order.conf',status='unknown')
c      WRITE(25,*) 'CON   SZZ       SDXY      SXY       SXZ       SYZ'
c      DO 390 I= 1, NCON
c         WRITE(25,95) I, SZZ(I), SDXY(I), SXY(I), SXZ(I), SYZ(I)
c 390  CONTINUE
c      close(25)

      WRITE(NOUT,*)
      write(nout,*) 'Final Order Parameters'
      write (nout,'(a3,7x,f10.6)') 'SZZ',smatrix(1)
      write (nout,'(a7,3x,f10.6)') 'SXX-SYY',smatrix(2)
      write (nout,'(a3,7x,f10.6)') 'SXY',smatrix(3)
      write (nout,'(a3,7x,f10.6)') 'SXZ',smatrix(4)
      write (nout,'(a3,7x,f10.6)') 'SYZ',smatrix(5)
      smatrix(6)=-0.5d0*(smatrix(1)-smatrix(2))
      smatrix(7)=-smatrix(1)-smatrix(6)
      write (nout,*) ' '
      write (nout,'(a3,7x,f10.6)') 'SXX',smatrix(6)
      write (nout,'(a3,7x,f10.6)') 'SYY',smatrix(7)
      WRITE(NOUT,*)
c*****************************************************
c* *rotchange* comment out 2 unwanted lines in output
c*****************************************************
      WRITE(NOUT,'(a4,4x,a4,
     *             4x,a4,
     *             4x,a4,
     *             4x,a4,
     *             4x,a4,
     *             4x,a4,
     *             4x,a4,
     *             4x,a4,
     *             4x,a4,
     *             2x,a5,4x,a6)')
```

```
     *              'conf','phi1',
     *              'phi2',
     *              'phi3',
     *              'phi4',
     *              'phi5',
     *              'phi6',
     *              'phi7',
     *              'phi8',
     *              'P(LC)','P(ISO)'
      WRITE(NOUT,*)

         plarge = 0.0d0
         do icount = 1,ncon
            if (plc(icount).gt.plarge) then
               plarge = plc(icount)
            end if
c*****************************************************
c*rotchange* comment out unwanted lines in output
c*****************************************************
               write(nout,37) icount,',',rots(icount,1),',',
     *                        rots(icount,2),',',
     *                        rots(icount,3),',',
     *                        rots(icount,4),',',
     *                        rots(icount,5),',',
     *                        rots(icount,6),',',
     *                        rots(icount,7),',',
     *                        rots(icount,8),',',
     *                        plc(icount),',',piso(icount)
         end do


c*************************************************************
c** This code extracts the most probable confomers and reports
c** the dihedral angles and order matrices for those particular conformers
c*************************************************************
c          write (nout,*)
c          write (nout,*)
c          write (nout,*)
c          write (nout,*) 'Most probable conformers '
c          write (nout,*) 'with their order matrices'
c          plarge = plarge/3.0d0
c          do icount = 1,ncon
c*************************************************************
c** The following if prevents printing of 0.0000 prob conformers
c** Normally remain commented out
c*************************************************************
c             if (plc(icount).gt.plarge) then
c                write(nout,37) icount,',',rots(icount,1),',',
c*****************************************************
c*rotchange* comment out unwanted lines in output
c*****************************************************
c     *                        rots(icount,2),',',
c     *                        rots(icount,3),',',
c     *                        rots(icount,4),',',
c     *                        rots(icount,5),',',
c     *                        rots(icount,6),',',
c     *                        rots(icount,7),',',
c     *                        rots(icount,8),',',
c     *                        plc(icount),',',piso(icount)
c             end if
c          end do
c          write (nout,*)
c
c          do icount = 1,ncon
c             if (plc(icount).gt.plarge) then
c                WRITE(NOUT,95) icount, SZZ(icount), SDXY(icount),
c     *                         SXY(icount), SXZ(icount), SYZ(icount)
c             end if
c          end do
c*************************************************************


c*********************************************************
c** Let's print the top X PLC
c*********************************************************
          call sorted
```

```
      close(21,status='keep')
      close(69,status='keep')

    5 FORMAT (I2)
   10 FORMAT (/1X,A,I2)
   18 FORMAT (1X,3F11.7,2X,I2,2X,I2,2X,F8.3)
   25 FORMAT (1X,A,F18.13)
   30 FORMAT (2F9.5)
   35 FORMAT ('   ',I3,3X,3F10.4)
c**************************************************
c*rotchange* comment out unwanted lines in output
c**************************************************
   37 FORMAT (i4,a1,
     *        F5.0,a1,
     *        F5.0,a1,
     *        f5.0,a1,
     *        f5.0,a1,
     *        f5.0,a1,
     *        f5.0,a1,
     *        f5.0,a1,
     *        f5.0,a1,
     *        F9.5,a1,f9.5)
   45 FORMAT (3F10.4)
   60 FORMAT (' D(',I2,',',I2,')',F12.4,I2)
   66 FORMAT (A,I4,A,F12.3)
   75 FORMAT (' D(',I2,',',I2,')')
   80 FORMAT (1X,F16.9)
   85 FORMAT (/1X,A,I3,A/)
   90 FORMAT (1X,2I2,2F13.4,2F13.4)
   95 FORMAT (1X,I5,5F10.5)
   98 FORMAT (1X,6E12.4)

      STOP
      END
c**************************************************
c** End of main program unit. Execution completed.
c** Start of subroutines.
c**************************************************

c**************************************************************
c**      Sort PLC's, highest first.
c**************************************************************
      SUBROUTINE sorted()

      parameter (ntopfew=200,ndc=2000,nout=21,nr=8)
      PARAMETER (nop=40, npl1=NOP-1, nta=10)
      implicit double precision (a-h,o-z)
      integer nconfcount(ndc),ntemp
      real*8  temp

C     ARRAYS IN COMMON:
      real*8 CEPDIAG(NDC,3,3), PLC(NDC), PISO(NDC), CEPSN(NDC,3,3),
     *       DELTADC(npl1,nop), SZZ(NDC), SDXY(NDC), SXY(NDC), SXZ(NDC),
     *       SYZ(NDC), rots(ndc,nr), smatrix(7)

      COMMON/BLOCK6/SZZ, SDXY, SXY, SXZ, SYZ,smatrix
      COMMON/BLOCK7/DELTADC, PLC, PISO, CEPSN, CEPDIAG
      common/block9a/np, NCON
      common/block11/rots

c** initialise array.
      do n=1,ncon
        nconfcount(n)=n
      end do

c** Bubble sort algorithm.
      do nloop=1,ncon
         do mloop=1,ncon-nloop
            if (plc(mloop).lt.plc(mloop+1)) THEN

               ntemp = nconfcount(mloop)
               nconfcount(mloop) = nconfcount(mloop+1)
```

```
                nconfcount(mloop+1) = ntemp

                temp = plc(mloop)
                plc(mloop) = plc(mloop+1)
                plc(mloop+1) = temp

                temp = piso(mloop)
                piso(mloop) = piso(mloop+1)
                piso(mloop+1) = temp

                temp = szz(mloop)
                szz(mloop) = szz(mloop+1)
                szz(mloop+1) = temp

                temp = sdxy(mloop)
                sdxy(mloop) = sdxy(mloop+1)
                sdxy(mloop+1) = temp

                temp = sxy(mloop)
                sxy(mloop) = sxy(mloop+1)
                sxy(mloop+1) = temp

                temp = sxz(mloop)
                sxz(mloop) = sxz(mloop+1)
                sxz(mloop+1) = temp

                temp = syz(mloop)
                syz(mloop) = syz(mloop+1)
                syz(mloop+1) = temp

                do nnnn=1,8
                  temp = rots(mloop,nnnn)
                  rots(mloop,nnnn) = rots((mloop+1),nnnn)
                  rots((mloop+1),nnnn) = temp
                end do
              end if
            end do
          end do

c**********************************
c** Now that the conformers have been sorted
c** Print out the top ntopfew to the output file.
c**********************************
          write  (nout,*)
          write  (nout,*)
c** *rotchange* comment out unwanted lines.
          write (nout,*) '    Conf',' phi1'
         *               ,' phi2'
         *               ,' phi3'
         *               ,' phi4'
         *               ,' phi5'
         *               ,' phi6'
         *               ,' phi7'
         *               ,' phi8'
         *               ,'   Plc','   Piso'
          do n=1,ntopfew
c** *rotchange* comment out unwanted lines.
            write(nout,'(2i5,8f5.0,2f10.5)') n,nconfcount(n)
         *                          ,rots(n,1)
         *                          ,rots(n,2)
         *                          ,rots(n,3)
         *                          ,rots(n,4)
         *                          ,rots(n,5)
         *                          ,rots(n,6)
         *                          ,rots(n,7)
         *                          ,rots(n,8)
         *                          ,plc(n)
         *                          ,piso(n)
          end do
          write (nout,*) '       conf','    szz','     sxx-syy',
         *               '       sxy','      sxz','       syz'
          do icount=1,ntopfew
            WRITE(NOUT,195) icount,nconfcount(icount),
         *                  SZZ(icount),
         *                  SDXY(icount),
         *                  SXY(icount),
```

```
     *                    SXZ(icount),
     *                    SYZ(icount)
      end do

 195  FORMAT (1X,2I5,5F10.5)

      end


c*************************************************************
c** subroutine called for reading the experimental Dij from
c** molecular parameters inout file.
c*************************************************************
      subroutine dccc(dcobs,wf,mcouplings)

      IMPLICIT real*8 (A-H,O-Z)

       parameter(nop=40,nin=20,nout=21)
       integer at1,at2,wf(nop-1,nop),mcouplings
       integer nat1,nat2,nweight
       real*8 dcobs(nop-1,nop),dc,dclarge

       common/block13/dclarge

c** Initialise arrays and variables.
       do n=1,nop-1
          do m=n+1,nop
            dcobs(n,m) = 0.0d0
            wf(n,m) = 0
          end do
       end do
       nat1=1
       nat2=1
       dclarge=0.0d0
       mcouplings=0

c** Read Dij's from parameter input file.
       read(nin,*) at1,at2,dc,nweight
       do while (at1.ne.0)
         if (nweight.eq.1)then
            mcouplings=mcouplings+1
         end if
         dcobs(at1,at2)=dc
         wf(at1,at2) = nweight

         write (nout,'(i3,a1,i3,a1,f10.4,a1,i1)')
     *     at1,',',at2,',',dcobs(at1,at2),',',wf(at1,at2)

         if (at1.gt.nat1) then
           nat1=at1
         end if
         if (at2.gt.nat2) then
           nat2=at2
         end if
         if (abs(dc).gt.dclarge) then
           dclarge=abs(dc)
         end if

         read(nin,*) at1,at2,dc,nweight
       end do

c*************************************************************
c** This loop normalises the Dij's if the line in the double
c** do loop below is not commented out. May as well leave it in.
c*************************************************************
      do n=1,nat1
         do m=n+1,nat2
           dcobs(n,m)= dcobs(n,m)/dclarge
         end do
       end do

      end
```

```
c*********************************************************************
c** Subroutine to set atoms which are involved in the repulsive term
c*********************************************************************
      subroutine iss(iswf,ncount)

      IMPLICIT real*8 (A-H,O-Z)

       parameter(nop=40,nin=20)
       integer at1,at2,iswf(nop-1,nop)
       character*80 label

       read(nin,'(a80)') label

c** Initialise array
       do n=1,nop-1
          do m=n+1,nop
            iswf(n,m) = 0
          end do
       end do

c** Read from parameters inout file.
        ncount=0
        read(nin,*) at1,at2
        do while (at1.ne.0)
          iswf(at1,at2)=1
          read(nin,*) at1,at2
          ncount=ncount+1
        end do

      end
```

```
      SUBROUTINE LSQFUN(IFLAG,M,N,XC,FVECC,IW,LIW,W,LW)
C*********************************************************************
C*                                                                   *
C*  THE PROGRAM TAKES THE EPSILON VALUES FOR EACH DIFFERENT FRAGMENT  *
C*  OF THE FLEXIBLE MOLECULE AND CALCULATES THE OVERAL EPSILON VALUES  *
C*  FOR EACH CONFORMATION. USING THESE, AND KNOWING THE COORD. OF EACH *
C*  CONFORMATION, THE PROGRAM CALCULATES THE ORDER PARAMETERS AND THUS *
C*  THE DIPOLAR COUPLINGS OF EACH CONFORMATION. THE DIPOLAR COUPLINGS  *
C*  ARE THEN AVERAGED OVER THE NUMBER OF CONFORMATIONS USING WEIGHTING *
C*  FACTORS IE. THE PROBABILITIES OF EACH CONFORMATION EXISTING.       *
C*                                                                   *
C*********************************************************************

      IMPLICIT real*8 (A-H,O-Z)

      PARAMETER (ndc=2000, nop=40, npl1=nop-1, nft=18)
      parameter (nftref=(nft-1)*3, NOUT=21, nr=8)
      parameter (rr=8.3144448d0,rkelvin=300.0d0,
     *           rkilo=1000.0d0,rt=rr*rkelvin/rkilo)
      PARAMETER (pi=3.1415926535897 93d0,RAD=180.0d0/pi,
     *           smallno=0.0000000001d0)

C     SCALAR ARGUMENTS      INTEGER IFLAG, LIW, LW, M, N

C     ARRAY ARGUMENTS
      real*8 FVECC(M), W(LW), XC(N),term(4)
c*    , rkelvin
      integer IW(LIW)

C     SCALARS IN COMMON
      INTEGER  NCON, NFRAG, NTFRAG
      real*8 SZZCON, DSCON, dclarge

C     ARRAYS IN COMMON
      real*8 DCOBS(npl1,nop), xcos(ndc,nftref), ycos(ndc,nftref),
     *     zcos(ndc,nftref), sinb(ndc,nftref), cosg(ndc,nftref),
     *     sing(ndc,nftref), SZZ(NDC), SDXY(NDC), SXY(NDC),
     *     SXZ(NDC), SYZ(NDC) , PLC(NDC), PISO(NDC),
     *     CEPSN(NDC,3,3), DELTADC(npl1,nop), DCAVE(npl1,nop),
     *     PROB(NDC), CEPDIAG(NDC,3,3), REPUL(NDC),vpot(nr,4),
```

```
*     smatrix(7), rots(ndc,nr)
      INTEGER KIND(NFT), biax(nft), WF(npl1,nop), FLAG(NFT),
     *        VAR(Nft), REL(NFT), REL1(NFT), REL2(NFT)
     *       ,zzwei(nft),dxywei(nft), flag2(nft),vvpot(nr,4)

C     LOCAL SCALARS
      real*8 DEPZZ, DDEPXY
      INTEGER I, J, K, L, nt

C     LOCAL ARRAYS
      real*8   FEPXX(nft), FEPYY(nft), FEPZZ(nft), EPSN(3,3),
     *       EPZZ(NFT), epxz(nft), EPDIAG(3,3), ROTN(3,3),
     *       UNORD(3,3), VPHI(NDC), ORD(3,3), ORDPAR(3,3),
     *       FEPXY(nft), FEPXZ(nft), FEPYZ(nft), EPDXY(NFT),
     *       EPDXYL(nft), EPXXL(nft), EPYYL(nft), EPZZL(nft),
     *       ORDINV(3,3), QZCON(NDC), QCON(NDC), ROTINV(3,3),
     *       epxzl(nft)


      common/block1/nfrag,ntfrag
      common/block1a/wf,flag,var,rel,rel1,rel2,flag2,vvpot
      COMMON/BLOCK2/DCAVE
      common/block3/XCOS, YCOS, ZCOS, SINB, COSG, SING, biax
      common/block3a/KIND,zzwei, dxywei
      COMMON/BLOCK6/SZZ, SDXY, SXY, SXZ, SYZ, smatrix
      COMMON/BLOCK8/PROB
      COMMON/BLOCK7/DELTADC, PLC, PISO, CEPSN, CEPDIAG
      COMMON/PARAM/ SZZCON, DSCON, ZCON
      common/block9/DCOBS
      common/block9a/np, NCON
      common/block10/REPUL
      COMMON/BLOCK10a/EPZZ, EPDXY,vpot
      common/block11/rots
      common/block13/dclarge


c*************************************************************
c** Extracting epsilons and V's from the array x() for use in calculations.
c*************************************************************
      L= 0
      DO 100 I= 1, NTFRAG
         IF ((VAR(I).EQ.1) .and. (rel(i).eq.0))THEN
if (zzwei(i).eq.1) then
   l=l+1
   epzz(i) = xc(l)
end if
if (dxywei(i).eq.1) then
   if (flag(i).eq.1) then
      l=l+1
      epdxy(i) = xc(l)
   else
      epdxy(i) = 0.0d0
   end if
else
   if (flag(i).eq.0) then
      epdxy(i) = 0.0d0
   end if
end if
if (flag2(i).eq.1) then
   l=l+1
   epxz(i) = xc(l)
else
   epxz(i) = 0.0d0
            end if
c** redundant pieces of code.
         else IF ((VAR(I).ne.1) .AND. (REL(I).EQ.2)) THEN
            j=rel1(i)
            epzz(i) = epzz(j)
         else IF ((VAR(I).NE.1) .AND. (REL(I).EQ.1)) THEN
            J = REL1(I)
            K = REL2(I)
            EPZZ(I)= -(EPZZ(J)+EPZZ(K))
c** end of redundant pieces of code.
         END IF
 100  CONTINUE
      do nloop=1,nr
```

```
          do mloop=1,4
            if(vvpot(nloop,mloop).eq.1) then
              l=l+1
              vpot(nloop,mloop) = xc(l)
            end if
          end do
        end do

c** For each fragment there are epsilons associated to it's type
        do I=1, NFRAG
           NT= KIND(I)
           EPZZL(I)= EPZZ(NT)
           EPDXYL(I)= EPDXY(NT)
           epxzl(i) = epxz(nt)
        end do

c** Separating Exx and Eyy from the Exx-Eyy parameter.

        do I=1, NFRAG
           if (ABS(EPDXYL(I)).LT.smallno) THEN
              EPXXL(I)= -0.5d0*EPZZL(I)
              EPYYL(I)= EPXXL(I)
           else
              EPXXL(I)=-0.5d0*(EPZZ(I)-EPDXYL(I))
              EPYYL(I)=EPXXL(I)-EPDXYL(I)
           end if
        end do


        QSUM= 0.0d0
        QZSUM= 0.0d0


         do i=1,ncon
           jcount=1
           DO 125 J=2, NFRAG
C** THE EPSILON VALUES FOR EACH FRAGMENT ARE NOW CALCULATED
C** WRT TO THE REFERENCE VALUES IN FRAGMENT 1

              if (biax(j).ne.1) then
C** If fragment is uniaxial
              FEPXX(J)
     *           = EPZZL(J)*(3.0d0*XCOS(I,Jcount)**2-1.0d0)/2.0d0

              FEPYY(J)
     *           = EPZZL(J)*(3.0d0*YCOS(I,Jcount)**2-1.0d0)/2.0d0

              FEPZZ(J)
     *           = EPZZL(J)*(3.0d0*ZCOS(I,Jcount)**2-1.0d0)/2.0d0

              FEPXY(J) = EPZZL(J)*SINB(I,Jcount)**2
     *           * SING(I,Jcount)*COSG(I,Jcount)
              FEPXY(J)= 3*FEPXY(J)/2

              FEPXZ(J) = EPZZL(J)*SINB(I,Jcount)*ZCOS(I,Jcount)
     *           *COSG(I,Jcount)
              FEPXZ(J)= 3*FEPXZ(J)/2

              FEPYZ(J) = EPZZL(J)*SINB(I,Jcount)*ZCOS(I,Jcount)
     *           *SING(I,Jcount)
              FEPYZ(J)= 3*FEPYZ(J)/2

              jcount = jcount + 1

            else if (biax(j).eq.1) then
C** If fragment is biaxial
              fepxx(j)
     *           = (epzzl(j)*(3.0d0*xcos(i,jcount)**2-1.0d0)/2.0d0)
     *           +   ((0.5d0*(epxxl(j) - epyyl(j))
     *           *   (xcos(i,jcount+1)**2 - xcos(i,jcount+2)**2)))

              fepyy(j)
     *           = (epzzl(j)*(3.0d0*ycos(i,jcount)**2-1.0d0)/2.0d0)
     *           +   ((0.5d0*(epxxl(j) - epyyl(j))
     *           *   (ycos(i,jcount+1)**2 - ycos(i,jcount+2)**2)))
```

```
            fepzz(j)
*              = (epzzl(j)*(3.0d0*zcos(i,jcount)**2-1.0d0)/2.0d0)
*              +   ((0.5d0*(epxxl(j) - epyyl(j))
*              *   (zcos(i,jcount+1)**2 - zcos(i,jcount+2)**2)))

            fepxy(j)
*              = epzzl(j)*(xcos(i,jcount)*ycos(i,jcount)
*              - 0.5d0*xcos(i,jcount+1)*ycos(i,jcount+1)
*              - 0.5d0*xcos(i,jcount+2)*ycos(i,jcount+2))
*              + (0.5d0*(epxxl(j)-epyyl(j))
*              * (xcos(i,jcount+1)*ycos(i,jcount+1)
*              - xcos(i,jcount+2)*ycos(i,jcount+2)))

            fepxz(j)
*              = epzzl(j)*(xcos(i,jcount)*zcos(i,jcount)
*              - 0.5d0*xcos(i,jcount+1)*zcos(i,jcount+1)
*              - 0.5d0*xcos(i,jcount+2)*zcos(i,jcount+2))
*              + (0.5d0*(epxxl(j)-epyyl(j))
*              * (xcos(i,jcount+1)*zcos(i,jcount+1)
*              - xcos(i,jcount+2)*zcos(i,jcount+2)))

               fepyz(j)
*                 = epzzl(j)*(ycos(i,jcount)*zcos(i,jcount)
*                 - 0.5d0*ycos(i,jcount+1)*zcos(i,jcount+1)
*                 - 0.5d0*ycos(i,jcount+2)*zcos(i,jcount+2))
*                 + (0.5d0*(epxxl(j)-epyyl(j))
*                 * (ycos(i,jcount+1)*zcos(i,jcount+1)
*                 - ycos(i,jcount+2)*zcos(i,jcount+2)))

               jcount = jcount + 3
            end if

 125     CONTINUE

c*****************************************************************
C        NOW WE CAN CALCULATE THE EPSILON VALUES FOR THE CONFORMATION
C        AS A WHOLE BY ADDING THE EPSILON VALUES FOR EACH FRAGMENT;
C        THEY ARE THEN PUT INTO A MATIX OF THE FORM EPSN(M,N) SO THAT
C        THE VALUES CAN BE FED INTO THE DIAGONALISATION ROUTINE
c*****************************************************************

c** initialise array
         DO 130 L= 1,3
            DO 130 J= 1,3
               EPSN(L,J)= 0.0d0
 130     CONTINUE

         EPSN(1,1) = EPXXL(1)
         EPSN(2,2) = EPYYL(1)
         EPSN(3,3) = EPZZL(1)
         epsn(1,3) = epxzl(1)
         IF (NFRAG.GT.1) THEN
            do J=2, NFRAG
               EPSN(1,1)= EPSN(1,1) + FEPXX(J)
               EPSN(2,2)= EPSN(2,2) + FEPYY(J)
               EPSN(3,3)= EPSN(3,3) + FEPZZ(J)
               EPSN(1,2)= EPSN(1,2) + FEPXY(J)
               EPSN(1,3)= EPSN(1,3) + FEPXZ(J)
               EPSN(2,3)= EPSN(2,3) + FEPYZ(J)
            end do
            EPSN(2,1)= EPSN(1,2)
            EPSN(3,1)= EPSN(1,3)
            EPSN(3,2)= EPSN(2,3)
         END IF

c** Changing very small numbers to zero.
         do L= 1,3
            do J= 1,3
               if (abs(epsn(1,j)).lt.smallno) then
                  EPSN(L,J)= 0.0d0
               end if
            end do
         end do

c** use for checks.
c          write (nout,*)
```

```
c          write (nout,*) 'Epsilon matrix for conformer - ',i
c          write (nout,'(3f10.6)') epsn(1,1),epsn(1,2),epsn(1,3)
c          write (nout,'(3f10.6)') epsn(2,1),epsn(2,2),epsn(2,3)
c          write (nout,'(3f10.6)') epsn(3,1),epsn(3,2),epsn(3,3)

          DO 136 L= 1,3
             DO 136 J= 1,3
                CEPSN(I,L,J)= EPSN(L,J)
 136      CONTINUE

c** Diagonalisation  routine matrices.f
          CALL DIAG(EPSN,EPDIAG,ROTN,ROTINV)

          DEPZZ= EPDIAG(3,3)
          E1= SQRT(2.0d0/3.0d0)
          DDEPXY= E1*(EPDIAG(1,1)-EPDIAG(2,2))

          DO 137 L= 1,3
             DO 137 J= 1,3
                CEPDIAG(I,L,J)= EPDIAG(L,J)
 137      CONTINUE

c** Order Calculation matrices.f
          CALL ORDER(DEPZZ,DDEPXY)

C** CALCULATE THE ORDER PARAMETERS WRT THE REFERENCE AXES
c** initialise array
c          DO 140 L= 1,3
c             DO 145 J= 1,3
c 145            ORD(L,J)= 0.0d0
c 140      CONTINUE
c** initialise array
          DO L= 1,3
             DO J= 1,3
                ORD(L,J)= 0.0d0
             end do
          end do

          SXXCON= -0.5d0*(SZZCON-DSCON)
          SYYCON= SXXCON-DSCON
          ORD(1,1)= SXXCON
          ORD(2,2)= SYYCON
          ORD(3,3)= SZZCON

c** Matrix multiplications matrices.f
          CALL MATMUL(ROTINV,ORD,ORDINV,3,3,3)
          CALL MATMUL(ORDINV,ROTN,UNORD,3,3,3)

C** NORMALISE THE ORDER PARAMETERS: DIVISION BY PARTITION FUNCTION
c          DO 150 L= 1,3
c             DO 155 J= 1,3
cc 155            ORDPAR(I,L,J)= UNORD(L,J)/ZCON
c 155            ORDPAR(L,J)= UNORD(L,J)/ZCON
c 150      CONTINUE
          DO L= 1,3
             DO J= 1,3
                ORDPAR(L,J)= UNORD(L,J)/ZCON
             end do
          end do

c** initialise array elements
          szz(i)=0.0d0
          sdxy(i)=0.0d0
          sxy(i)=0.0d0
          sxz(i)=0.0d0
          syz(i)=0.0d0

          SZZ(I)= ORDPAR(3,3)
          SDXY(I)= ORDPAR(1,1)-ORDPAR(2,2)
          SXY(I)= ORDPAR(1,2)
          SXZ(I)= ORDPAR(1,3)
          SYZ(I)= ORDPAR(2,3)
c          SZZ(I)= ORDPAR(I,3,3)
c          SDXY(I)= ORDPAR(I,1,1)-ORDPAR(I,2,2)
c          SXY(I)= ORDPAR(I,1,2)
c          SXZ(I)= ORDPAR(I,1,3)
```

```
c          SYZ(I)= ORDPAR(I,2,3)

c** Calculation of internal energy.
          do nl=1,4
            term(nl)=0.0d0
          end do
          do mloop=1,4
            do nloop=1,nr
              term(mloop)=term(mloop) +
     *                    ( vpot(nloop,mloop) *
     *                    (cos(dble(mloop)*(rots(i,nloop)/rad))))
            end do
          end do

          vphi(i) = 0.0d0
          do mloop=1,4
             vphi(i) = vphi(i) + term(mloop)
          end do
          vphi(i) = vphi(i)/rt
          vphi(i) = vphi(i) + repul(i)

          QCON(I)= EXP(-VPHI(I))
          QZCON(I)= QCON(I)*ZCON
          QSUM= QSUM + QCON(I)
          QZSUM= QZSUM + QZCON(I)

       end do

c** Calculate Piso and Plc
       DO 160 I = 1, NCON
          PROB(I)= QZCON(I)/QZSUM
          PISO(I)= QCON(I)/QSUM
          PLC(I)= PROB(I)
 160   CONTINUE

c** Calculate Dipolar Couplings according to the probabiltity of each conformer. PLC.
       CALL DCCALC(Np,NCON)

       K=0
       DO 165 I=1, Np-1
          DO 165 J= I+1, Np
             IF (WF(I,J).EQ.1) THEN
                DELTADC(I,J)= DCAVE(I,J)-DCOBS(I,J)
                K= K+1
                FVECC(K)= DELTADC(I,J)
             ELSE
                DELTADC(I,J) = 0.0d0
             END IF
 165   CONTINUE


  25   FORMAT (1X,A,F5.1)
  35   FORMAT ('    ',I3,3X,3E11.3)

       RETURN
       END
```

```
       SUBROUTINE DCCALC(np,NCON)
C*************************************************************
C THIS PROGRAM IS TO CALCULATE THE DIPOLAR COUPLINGS OF A
C A SYSTEM FROM THE CO-ORDINATES OF THE NUCLEI AND THE
C ORDER PARAMETERS  SZZ, SXX-SYY, SXY, SXZ, SYZ
C FIRSTLY : SET UP ARRAYS FOR CO-ORD. X(N), Y(N), Z(N), GAMMA(I)
C*************************************************************

       IMPLICIT real*8 (A-H,O-Z)

       PARAMETER (ndc=2000,nop=40,npl1=nop-1,ngv=5)
c***delete as soon as tested** ,NIN=20,NOUT=21)
```

```
      INTEGER NDC, nop, npl1, np, NCON
      real*8 dclarge

      real*8 SZZ(NDC), SDXY(NDC), SXY(NDC), SXZ(NDC),
     *       SYZ(NDC),smatrix(7)
     *      ,C1(NDC,npl1,nop), C2(NDC,npl1,nop), C3(NDC,npl1,nop)
     *      ,C4(NDC,npl1,nop), DCC(npl1,nop), DCAVE(npl1,nop),
     *       PROB(NDC)
      INTEGER  NG, NIG(ngv), IA(ngv,9), JA(ngv,9)

      COMMON/BLOCK2/DCAVE
      COMMON/BLOCK4/C1,C2,C3,C4
      COMMON/BLOCK5/NG,NIG,IA,JA
      COMMON/BLOCK6/SZZ,SDXY,SXY,SXZ,SYZ,smatrix
      COMMON/BLOCK8/PROB
      common/block13/dclarge

c** Initialise arrays
      do mmm=1,5
        smatrix(mmm)=0.0d0
      end do
      do I= 1, np-1
         do J= I+1, np
            DCAVE(I,J)= 0.0d0
         end do
      end do


      DO 250 N= 1, NCON
         DO 205 I= 1, np-1
             DO 200 J= I+1, np
C*************************************************************
C C1 IS K(I,J)/R**3 AND C2-C4 ARE X, Y & Z COS TERMS
C THESE ARE CALCULATED IN THE MAIN PROGRAM AS THEY DO NOT
C NEED TO BE RECALCULATED EVERY TIME THIS SUBROUTINE IS USE
C*************************************************************
C CALCULATION OF THE DIPOLAR COUPLINGS:
C THE CALCULATION IS BROKEN DOWN INTO SIMPLE STEPS AND
C VARIABLES SUM1-SUM5 USED TO STORE RUNNING TOTALS
C*************************************************************
                SUM1= SZZ(N)*(3*C4(N,I,J)**2-1)
                SUM2= C2(N,I,J)**2-C3(N,I,J)**2
                SUM2= SDXY(N)*SUM2
                SUM3= 4*SXY(N)*C2(N,I,J)*C3(N,I,J)
                SUM4= 4*SXZ(N)*C2(N,I,J)*C4(N,I,J)
                SUM5= 4*SYZ(N)*C3(N,I,J)*C4(N,I,J)
                SUM1= SUM1+SUM2+SUM3+SUM4+SUM5
                DCC(I,J)= -C1(N,I,J)*SUM1

c**include for Normalisation of Dij's
                dcc(i,j)=dcc(i,j)/dclarge
c**

 200         CONTINUE
 205      CONTINUE


C** AVERAGING:
          IF (NG.NE.0) THEN
             Do K= 1, NG
                ADC=0
                DO L= 1, NIG(K)
                I=IA(K,L)
                J=JA(K,L)
                ADC= ADC + DCC(I,J)
             end do
             GG= NIG(K)
             ADC= (1.0d0/GG)*ADC
             DO L= 1, NIG(K)
                I=IA(K,L)
                J=JA(K,L)
                DCC(I,J)=ADC
             end do
       end do
END IF
```

```
c** The Dij is the sum of the Dij for each conformer multiplied by
c** the probability of that conformer.
         do I=1, np-1
            do J= I+1, np
               DCAVE(I,J)= DCAVE(I,J)+(DCC(I,J)*PROB(N))
            end do
         end do
c** The same is true for the order parameters.
         smatrix(1) = smatrix(1) + (szz(n)*prob(n))
         smatrix(2) = smatrix(2) + (sdxy(n)*prob(n))
         smatrix(3) = smatrix(3) + (sxy(n)*prob(n))
         smatrix(4) = smatrix(4) + (sxz(n)*prob(n))
         smatrix(5) = smatrix(5) + (syz(n)*prob(n))
 250  CONTINUE

      RETURN
      END
```

```
      SUBROUTINE LSQMON(M,N,XC,FVECC,FJACC,LJC,S,IGRADE,
     *                  NITER,NF,IW,LIW,W,LW)

C**   MONITORING ROUTINE


C     PARAMETERS
      INTEGER    NDEC, MDEC, NOUT, NDC, nop, npl1
      PARAMETER  (NDEC=18, mdec=406, NOUT=21)
      PARAMETER (ndc=2000, nop=40, npl1=nop-1)

C     SCALAR ARGUMENTS
      INTEGER    IGRADE, LIW, LJC, LW, M, N,NF, NITER

C     ARRAY ARGUMENTS
      real*8 FJACC(LJC,NDEC), FVECC(MDEC), S(NDEC), W(LW),
     *       XC(NDEC)
      INTEGER    IW(LIW)

C     LOCAL SCALARS
      real*8       FSUMSQ, GTG

C     LOCAL ARRAYS
      real*8 G(NDEC)

C     SCALARS IN COMMON:
      INTEGER  NCON

C     ARRAYS IN COMMON:
      real*8 DCOBS(npl1,nop), DCAVE(npl1,nop),
     *     CEPDIAG(NDC,3,3),smatrix(7)
     *    ,SZZ(NDC), SDXY(NDC), SXY(NDC), SXZ(NDC), SYZ(NDC)
     *    ,PLC(NDC), PISO(NDC), CEPSN(NDC,3,3), DELTADC(npl1,nop)

C     EXTERNAL FUNCTIONS
      real*8       F06EAF
      EXTERNAL   F06EAF

C     EXTERNAL SUBROUTINES
      EXTERNAL   LSQGRD

      COMMON/BLOCK2/DCAVE
      COMMON/BLOCK6/SZZ, SDXY, SXY, SXZ, SYZ,smatrix
      COMMON/BLOCK7/DELTADC, PLC, PISO, CEPSN, CEPDIAG
      common/block9/DCOBS
      common/block9a/np, NCON

C     EXECUTABLE STATEMENTS

      FSUMSQ= F06EAF(M,FVECC,1,FVECC,1)
      CALL LSQGRD(M,N,FVECC,FJACC,LJC,G)
      GTG= F06EAF(N,G,1,G,1)
```

```
c*************************************************************
c** Prints out the state of the variables for every iteration.

c*************************************************************
      WRITE (NOUT,*)
      WRITE (NOUT,*)
      WRITE (NOUT,*)
     *  '    ITN     F EVALS         SUMSQ            GTG         GRADE'
      WRITE (NOUT,999) NITER, NF, FSUMSQ, GTG, IGRADE
      WRITE (NOUT,*)
      WRITE (NOUT,*)
     *  '         X                   G             SINGULAR VALUES'

      DO 20 J= 1, N
         WRITE (NOUT,998) XC(J), G(J), S(J)
   20 CONTINUE

c*************************************************
c* Leave these lines commented out to reduce the size of the outout.
c*************************************************
c*     print out Dij's for each iteration
c*************************************************
c       WRITE(NOUT,*)
c       WRITE(NOUT,*) ' I J     D(OBS)        D(CALC)        D(CA-OB)'
c       WRITE(NOUT,*)
c       DO 185 I=1, NS-1
c          DO 185 J= I+1, NS
c             WRITE(NOUT,99) I, J, DCOBS(I,J), DCAVE(I,J), DELTADC(I,J)
c 185  CONTINUE
c*************************************************
c*     print out Order parameters for each iteration
c*************************************************

c       WRITE(NOUT,*)
c       WRITE(NOUT,*) 'CON   SZZ        SDXY       SXY        SXZ        SYZ'
c       WRITE(NOUT,*)
c       DO 190 I=1, NCON
c          WRITE(NOUT,90) I, SZZ(I), SDXY(I), SXY(I), SXZ(I), SYZ(I)
c 190  CONTINUE
c*************************************************
c*     print out probabilities for each iteration
c*************************************************

c       WRITE(NOUT,*)
c       WRITE(NOUT,*) '  PHI   P(LC)   P(ISO)'
c       WRITE(NOUT,*)
c       PHI= 0.0 ,
c       DO 195 I=1, NCON
c          WRITE(NOUT,95) PHI, PLC(I), PISO(I)
c          PHI= PHI + PHIIN
c 195  CONTINUE

       RETURN

    5  FORMAT (/1X,A,I2)
   90  FORMAT (1X,I2,5F10.4)
   95  FORMAT (1X,F5.1,1X,2F7.3)
   99  FORMAT (1X,2I2,2F13.4,F13.4)
  999  FORMAT (1X,I4,6X,I5,6X,E13.3,5X,E12.3,4X,I3)
  998  FORMAT (1X,E16.4,7X,E13.3,7X,E13.3)
       END


       SUBROUTINE LSQGRD(M,N,FVECC,FJACC,LJC,G)
C** ROUTINE TO EVALUATE GRADIENT OF THE SUM OF SQUARES
c** Required by E04FCF

C      SCALAR ARGUMENTS
       INTEGER LJC, Mdec,ndec
```

```
      PARAMETER (mdec=406, NDEC=18)

C     ARRAY ARGUMENTS
      real*8 FJACC(LJC,NDEC), FVECC(MDEC), G(NDEC)

C     LOCAL SCALARS
      real*8 SUM
      INTEGER I, J

      do J= 1, N
         SUM= 0.0d0
         do I= 1, M
            SUM= SUM +FJACC(I,J)*FVECC(I)
         end do
         G(J)= SUM + SUM
      end do

      RETURN
      END
```

```
c*****************************************************
c** This routine begins the calculation of the
c** molecular geometry from bond lengths and
c** angles provided in the geometry input file.
c*****************************************************
      subroutine coordinates(gamma,rots,rot,
     *                       iswf,ndc)

      implicit double precision (a-h,o-z)

      parameter (pi=3.14159265358979 3d0, rads=180.0d0/pi)
      parameter (nop=40,nr=8)

      integer nsize,iswf(nop-1,nop),
     *        nattype(3,nop),rotatom(nr,nop)
      real*8 coord(5,nop),gamma(nop),
     *       rots(ndc,nr),rot(nr)

      CALL initialise(nop,coord,nattype,rads,nsize,
     *                gamma,rots,rot,rotatom,iswf,ndc)
      CALL write(nop,coord,nattype,nsize)

      END



c*****************************************************
c** Data file naming, and memory allocation
c*****************************************************
      SUBROUTINE initialise(nop,coord,nattype,rads,nsize,
     *                      gamma,rots,rot,rotatom,
     *                      iswf,ndc)


      implicit double precision (a-h,o-z)

      parameter(nr=8)

      character*20 data filename
      integer nop,nattype(3,nop),nsize,rotatom(nr,nop),
     *        iswf(nop-1,nop),nunit
      real*8 coord(5,nop),rads
     *       ,gamma(nop),rots(ndc,nr),rot(nr)


c** Opening the molecular geometry inout file.
      READ (69,'(a)'),data_filename
      nunit=10
      OPEN (nunit,FILE=data_filename,STATUS='OLD')

      read(nunit,*) nsize

      a1=0.0d0
```

```
      CALL position(nop,coord,nattype,rads,nsize,gamma,nunit,a1)
      CALL sort(nop,coord,nattype,nsize,gamma,nunit)
      CALL zrotate(coord,rads,nsize,rotatom,
     *             rots,rot,iswf,gamma,nattype,
     *             nunit,data_filename)

      CLOSE(nunit)

      END



c!*************************************************************
c!     Calculate new coordinates
c!*************************************************************
      SUBROUTINE position(nop,coord,nattype,rads,nsize,gamma,nunit,a1)

      implicit double precision (a-h,o-z)
      integer nop,nattype(3,nop),no,ntype,nunit,nv,nvib(100)
      real*8 coord(5,nop),rads,blength,ang,yang,angprev,yangprev,
     *       gamma(nop),gam,function,f0,f1,f2,f3,f4
      logical nbool

c**********************
c* include the vibration function in this subroutine
c* mark each atom in data.in file i.e. 1=vibrate 0=novibrate
c**********************
       inquire(file='wobble',exist=nbool)
       if (nbool) then
          open(14,file="wobble",status='unknown')
          read(14,*) f0,f1,f2,f3,f4
          close(14)
       else
          f0=0.0d0
          f1=0.0d0
          f2=0.0d0
          f3=0.0d0
          f4=0.0d0
       end if

c*********************************************
c** Reading geometry and atomic information.
c*********************************************
      READ (nunit,'(3i2,2f10.4,2f10.4,i3)')
     *                no,nconnect,ntype,ang,yang,blength,gam,nv
c** number
      nattype(1,1) = 0
c** type to
      nattype(2,1) = ntype
c** position
      nattype(3,1) = 0
c** x coord
      coord(1,1) = 0.0d0
c** y coord
      coord(2,1) = 0.0d0
c** z coord
      coord(3,1) = 0.0d0
c** angle in XZ
      coord(4,1) = ang
c** angle to Y
      coord(5,1) = yang
c** gamma value
      gamma(1) = gam
c** atom vib?
      nvib(1) = nv

      DO n=1,nsize
         READ (nunit,'(3i2,2f10.4,2f10.4,i3)')
     *             no,nconnect,ntype,ang,yang,blength,gam,nv
         ncount=1
         DO while (nattype(1,ncount).ne.nconnect)
            ncount = ncount + 1
         END DO
```

```
            gamma(n)=gam
            nvib(n)=nv
            nattype(3,n) = nattype(3,ncount) + 1
            npos = nattype(3,n)
            nattype(2,n) = ntype
            nattype(1,n) = no

c************************************
c**  if statement -
c**     This uses a fourier series to decide how
c**     a bond angle deviates from the starting position.
c**     Atoms affected by relaxation are marked with a '1'
c**     in 'molecule.data'.
c************************************
            if ( nvib(n).ne.0 ) then
               function = f0 +
     *                    f1*cos(a1/rads) +
     *                    f2*cos(2.0d0*a1/rads) +
     *                    f3*cos(3.0d0*a1/rads) +
     *                    f4*cos(4.0d0*a1/rads)
               if (nvib(n).eq.1) then
                 ang = ang + function
               else if (nvib(n).eq.-1) then
                 ang = ang - function
               end if

               if (nunit.eq.13) then
                 write(18,*) a1,',',ang
               end if
            end if

            ang = (ang + coord(4,ncount))
            angprev = ang
            yangprev = yang
            yang = yang + coord(5,ncount)

c******* Check whether npos is odd or even. This required a lot of thought
c******* into how the atoms were related to each other positionally.
            np = NINT(dble(npos)/2.0d0)
            np = np*2
            IF (npos.eq.np) THEN
               ang = ang + 180.0d0
            ELSE
               ang = ang + 0.0d0
            END IF

            IF (yang.ne.0.0) THEN
c********** coord in y axis
               coord(2,n) = coord(2,ncount) + sin(yang/rads)*blength
c*********** new bond length in the xz plane
               blength = cos(yang/rads)*blength
            ELSE
               coord(2,n) = coord(2,ncount)
            END IF
            coord(1,n) = coord(1,ncount) + sin(ang/rads)*blength
            coord(3,n) = coord(3,ncount) + cos(ang/rads)*blength
            coord(4,n) = angprev
            coord(5,n) = yangprev

         END DO
         END
```

```
c*************************************************************
c**      Rotate atoms defined in the inout file about the z axis
c*************************************************************
         SUBROUTINE zrotate(coord,rads,nsize,
     *                      rotatom,rots,rot,iswf,
     *                      gamma,nattype,
     *                      nunit,data_filename)

         implicit double precision (a-h,o-z)
```

```
      parameter(nop=40,nta=10,ndc=2000,nr=8,smallno=0.0001d0,
     *          nft=18,rr=8.3144448d0,rkelvin=300.0d0,
     *          rkilo=1000.0d0,rt=rr*rkelvin/rkilo,nftref=(nft-1)*3)

c** Arrays and variables only required for geometry
      character*20 data_filename
      integer nunit,bond,nattype(3,nop)
      integer rotatom(nr,nop),rota,rotb
      integer nrot_a(nr),nrot_b(nr),nnrot
      real*8 coord(5,nop),rads,rot(nr),rots(ndc,nr),rotang
      real*8 rotstart(nr),rotend(nr)
c*  rkelvin

c** Arrays and variables only required for conformational calculations
      real*8 c1(ndc,nop-1,nop), c2(ndc,nop-1,nop)
      real*8 c3(ndc,nop-1,nop), c4(ndc,nop-1,nop)
      real*8 xcos(ndc,nftref),ycos(ndc,nftref),zcos(ndc,nftref)
      real*8 sinb(ndc,nftref),sing(ndc,nftref),cosg(ndc,nftref)
      real*8 xi(nop),yi(nop),zi(nop),xl(2),yl(2),zl(2)
      real*8 repul(ndc),dx(nop-1,nop),dy(nop-1,nop),dz(nop-1,nop)
      real*8 r(nop-1,nop),a(nop-1,nop),e(nop-1,nop)
      real*8 aa(nop),ea(nop),ATA(NTA),ATE(NTA)
      real*8 gamma(nop), lr,lr1,ldy,ldx,ldz
      integer iswf(nop-1,nop),at(nop), matomtype
      integer biax(nft),fa1(nftref),fa2(nftref)
      logical nbool
      character*1 chemsymb,symbol(nta)

      common/block1/nfrag,ntfrag
      common/block3/XCOS, YCOS, ZCOS, SINB, COSG, SING, biax
      COMMON/BLOCK4/C1, C2, C3, C4
      common/block9a/np, NCON
      common/block10/REPUL
      common/block12/fa1,fa2,ata,ate
      common/block14/symbol



      do nloop=1,nr
        read (nunit,*) rotst,roten,rotang
        rotstart(nloop)=rotst
        rotend(nloop)=roten
        rot(nloop) = rotang
        read (nunit,'(2i2)') rota,rotb
        nrot_a(nloop) = rota
        nrot_b(nloop) = rotb

        read (nunit,*) nnrot
        num=0
        do while (nnrot.ne.0)
           num = num + 1
           rotatom(nloop,num) = nnrot
           rotatom(nloop,num+1)=0
           read (nunit,*) nnrot
        end do
      end do


c****************** Read in here atom types corresponding
c****************** to numbers for pdb file
       read (nunit,*) matomtype,chemsymb
       num=0
 do while (matomtype.ne.0)
   num=num+1
   symbol(num)=chemsymb
   read (nunit,*) matomtype,chemsymb
 end do

do n=1,ndc
  do m=1,3
    rots(n,m)=0.0d0
  end do
end do

do i = 1, np
   at(i) = nattype(2,i)
```

```
      end do

      DO 120 I= 1, NP
         MARK= AT(I)
         AA(I)= ATA(MARK)
         EA(I)= ATE(MARK)
 120  CONTINUE

      ncon=0
       inquire(file='wobble',exist=nbool)
       if (nbool) then
         open(18,file="frag.gnu",status="unknown")
       end if


c*rotchange* Comment out lines if reducing no. of rotors.
      do a8=rotstart(8),rotend(8),rot(8)
      do a7=rotstart(7),rotend(7),rot(7)
      do a6=rotstart(6),rotend(6),rot(6)
      do a5=rotstart(5),rotend(5),rot(5)
      do a4=rotstart(4),rotend(4),rot(4)
      do a3=rotstart(3),rotend(3),rot(3)
        do a2=rotstart(2),rotend(2),rot(2)
          do a1=rotstart(1),rotend(1),rot(1)

          nunit=13
          open(nunit,file=data_filename,status='old')
          read(nunit,*) nsize
          CALL position(nop,coord,nattype,rads,nsize,gamma,nunit,a1)
          CALL sort(nop,coord,nattype,nsize,gamma,nunit)

c*rotchange* There is 1 find_bod for each rotor.
            bond=8
            call find_bond(bond,coord,nop,nrot_a,nrot_b,rotatom,
     *                     rads,a8)

            bond=7
            call find_bond(bond,coord,nop,nrot_a,nrot_b,rotatom,
     *                     rads,a7)

          bond=6
          call find_bond(bond,coord,nop,nrot_a,nrot_b,rotatom,
     *                     rads,a6)

          bond=5
          call find_bond(bond,coord,nop,nrot_a,nrot_b,rotatom,
     *                     rads,a5)

          bond=4
          call find_bond(bond,coord,nop,nrot_a,nrot_b,rotatom,
     *                     rads,a4)

          bond=3
          call find_bond(bond,coord,nop,nrot_a,nrot_b,rotatom,
     *                     rads,a3)

          bond=2
          call find_bond(bond,coord,nop,nrot_a,nrot_b,rotatom,
     *                     rads,a2)

          bond=1
            call find_bond(bond,coord,nop,nrot_a,nrot_b,rotatom,
     *                     rads,a1)

            ncon=ncon+1
            n=ncon
    c*rotchange*
            rots(ncon,8)=a8
            rots(ncon,7)=a7
            rots(ncon,6)=a6
            rots(ncon,5)=a5
            rots(ncon,4)=a4
            rots(ncon,3)=a3
            rots(ncon,2)=a2
            rots(ncon,1)=a1
```

```
            do naa=1,np
               xi(naa) = coord(1,naa)
               yi(naa) = coord(2,naa)
               zi(naa) = coord(3,naa)
               if (abs(xi(naa)).lt.smallno) then
                  xi(naa) = 0.0d0
               end if
               if (abs(yi(naa)).lt.smallno) then
                  yi(naa) = 0.0d0
               end if
               if (abs(zi(naa)).lt.smallno) then
                  zi(naa) = 0.0d0
               end if
             end do

c*************************************************************************
c       Leonard Jones potential
c       j.phys.chem 99(32),1995,12239
c*************************************************************************
            REPUL(N) = 0.0d0
            DO 230 I= 1, NP-1
               DO 230 J= I+1, NP
                  DX(I,J)= XI(I) - XI(J)
                  DY(I,J)= YI(I) - YI(J)
                  DZ(I,J)= ZI(I) - ZI(J)
                  R(I,J)= SQRT(DX(I,J)**2 + DY(I,J)**2 + DZ(I,J)**2)
                  A(I,J)= AA(I) + AA(J)
                  E(I,J)= SQRT( EA(I) * EA(J) )
                  SUM1 = (A(I,J)/R(I,J))**12
                  SUM2 = (A(I,J)/R(I,J))**6
                  SUM3 = (SUM1 - SUM2) * E(I,J)
                  REPUL(N) = REPUL(N) + ( SUM3 * iswf(i,j) )
 230        CONTINUE
            REPUL(N)= REPUL(N)/(RT*rkilo)
c            WRITE(*,*) 'CONFORMATION',N,': potential=',REPUL(N)
c*************************************************************************


            IF(NFRAG.EQ.1) THEN
               PRINT*,'THE MOLECULE IS RIGID'
            ELSE
            jcount=0
            DO 260 J=2, NFRAG
               if (biax(j).ne.1) THEN
                  jcount = jcount + 1
                  I=FA1(Jcount)
                  XL(1) = XI(I)
                  YL(1) = YI(I)
                  ZL(1) = ZI(I)
                  I=FA2(Jcount)
                  XL(2) = XI(I)
                  YL(2) = YI(I)
                  ZL(2) = ZI(I)

                  LDX= XL(2) - XL(1)
                  LDY= YL(2) - YL(1)
                  LDZ= ZL(2) - ZL(1)
                  LR= SQRT(LDX**2 + LDY**2 + LDZ**2)

                  XCOS(N,Jcount)= LDX/LR
                  YCOS(N,Jcount)= LDY/LR
                  ZCOS(N,Jcount)= LDZ/LR

                  LR1= SQRT(LDX**2 + LDY**2)

c                 IF LR1 IS ZERO THEN WE CANNOT CAL. THE FOLLLOWING COZ THIS
C                 INVOVES DIVIDING BY LR1. THE PHYSICAL RESULT OF LR1 BEING
C                 ZERO IS THAT BETA IS ZERO AND THESE THREE CAN BE SET ZERO.
                  IF (LR1.EQ.0.0) THEN
                     COSG(N,Jcount)= 0.0d0
                     SING(N,Jcount)= 0.0d0
                     SINB(N,Jcount)= 0.0d0
                  ELSE
                     COSG(N,Jcount)= LDX/LR1
                     SING(N,Jcount)= LDY/LR1
                     SINB(N,Jcount)= LR1/LR
```

```
      END IF

   else if (biax(j).eq.1) then
      do ncount=1,3
         jcount = jcount + 1
         I=FA1(Jcount)
         XL(1) = XI(I)
         YL(1) = YI(I)
         ZL(1) = ZI(I)
         I=FA2(Jcount)
         XL(2) = XI(I)
         YL(2) = YI(I)
         ZL(2) = ZI(I)

         LDX= XL(2) - XL(1)
         LDY= YL(2) - YL(1)
         LDZ= ZL(2) - ZL(1)
         LR= SQRT(LDX**2 + LDY**2 + LDZ**2)

                  XCOS(N,Jcount)= LDX/LR
                  YCOS(N,Jcount)= LDY/LR
                  ZCOS(N,Jcount)= LDZ/LR

               end do
            end if

260            CONTINUE
         END IF


         do i = 1,np-1
           do j = i+1,np
              C1(N,i,J)= ( gamma(I)*gamma(J) / R(I,J)**3 )
              C2(N,i,J)= ( DX(I,J)/R(I,J) )
              C3(N,i,J)= ( DY(I,J)/R(I,J) )
              C4(N,I,J)= ( DZ(I,J)/R(I,J) )
           end do
         end do

   close(nunit)
c*rotchange* There is 1 do loop for each rotor.
          end do
        end do
      end do
      end do
      end do
      end do
      end do
      end do
      end do
      close(18)

  66  FORMAT (A,I4,A,F12.3)

      END



c*******************************************************
C**  Determine the rotations
c*******************************************************
      subroutine find_bond(bond,coord,nop,nrot_a,nrot_b,
     *                     rotatom,rads,arot)

      implicit double precision (a-h,o-z)

      parameter(nr=8,smallno=0.000001d0)

      integer bond,nop
      integer rotatom(nr,nop),nrot_a(nr),nrot_b(nr)
      real*8 ax,ay,az,bx,by,bz,blen,blenyz,x,y,z,x1,y1,z1
      real*8 siny,sinx,rads,arot,coord(5,nop)
```

```
      ncount = nrot_a(bond)
      ax = coord(1,ncount)
      ay = coord(2,ncount)
      az = coord(3,ncount)

      ncount = nrot_b(bond)
      bx = coord(1,ncount)
      by = coord(2,ncount)
      bz = coord(3,ncount)

      dx=bx-ax
      dy=by-ay
      dz=bz-az

c** total length of the bond we are rotating about
      blen = sqrt ( dx**2 + dy**2 + dz**2 )

c** new apparent bond length in the yz plane
      blenyz = sqrt ( dy**2 + dz**2 )

c** angle of the bond to the z axis in the yz plane ie. rot about x
      IF (abs(dy).gt.smallno) THEN
         sinx = dy/blenyz
         if (dz.gt.0.0d0) then
           sinx = asin(sinx)
         else
           sinx = -asin(sinx)
         end if
      ELSE
         sinx = 0.0d0
      END IF

c** angle of the bond to the z axis in the xz plane ie. rot about y
      IF (abs(dx).gt.smallno) THEN
         siny = dx/blen
         if (dz.gt.0.0d0) then
           siny = asin(siny)
         else
           siny = -asin(siny)
         end if
      ELSE
         siny = 0.0d0
      END IF


      num=1
      m=bond

      zzang=arot

      DO while (rotatom(m,num).ne.0)

c** a at the origin
          x = coord(1,rotatom(m,num)) - ax
          y = coord(2,rotatom(m,num)) - ay
          z = coord(3,rotatom(m,num)) - az

c** Rotate atom about the x axis to line up along the z axis
          x1 = x
          y1 = (y * cos(sinx)) + (z * (-sin(sinx)))
          z1 = (y * sin(sinx)) + (z * cos(sinx))

c** Rotate atom about the y axis to lie in the yz plane
          x = (x1 * cos(siny)) + (z1 * (-sin(siny)))
          y = y1
          z = (x1 * sin(siny)) + (z1 * cos(siny))

c** Actual rotation about the z axis by stated angle in the data file
          x1 = (x * cos(-zzang/rads)) +
     *           (y * (-sin(-zzang/rads)))
          y1 = (x * sin(-zzang/rads)) +
     *           (y * cos(-zzang/rads))
          z1 = z

c** Rotate back about the y axis to lie in 3D space
          x = (x1 * cos(-siny)) + (z1 * (-sin(-siny)))
```

```
            y = y1
            z = (x1 * sin(-siny)) + (z1 * cos(-siny))

c** Rotate back about the x axis out of the z axis into the yz plane
            x1 = x
            y1 = (y * cos(-sinx)) + (z * (-sin(-sinx)))
            z1 = (y * sin(-sinx)) + (z * cos(-sinx))

c** New rotated coordinates translated back to previous
            coord(1,rotatom(m,num)) = x1 + ax
            coord(2,rotatom(m,num)) = y1 + ay
            coord(3,rotatom(m,num)) = z1 + az

            num=num+1
         END DO

         END
```

```
c**********************************************************************
c**       Write the output
c**********************************************************************
      SUBROUTINE write(nop,coord,nattype,nsize)

      parameter(nta=10)

      implicit double precision (a-h,o-z)

      integer nattype(3,nop),nsize
      real*8 coord(5,nop)
      character*20 out_filename,pdb_filename
      character*1 chemsymb,symbol(nta)

      common/block14/symbol

c** Writing cartesian coordinates to output file defined by lister.ini
      READ (69,'(a)'),out_filename
      OPEN (11,FILE=out_filename,STATUS='unknown')
       DO n=1,nsize
          WRITE (11,'(3f18.14,i3)') coord(1,n),coord(2,n),coord(3,n),
     *                               nattype(1,n)
       END DO
       CLOSE(11)


c** Writing cartesian coordinates to .pdb file defined by lister.ini
      READ (69,'(a)'),pdb_filename
      open (13,file=pdb_filename,status='unknown')
      do n=1,nsize
         do m=1,3
           coord(m,n)=coord(m,n)*1
         end do
         chemsymb=symbol(nattype(2,n))
         if (chemsymb.ne.'x') then
           write (13,'(a4,6x,i2,a2,15x,3f8.2)')
     *               'ATOM',nattype(1,n),chemsymb,
     *               (10*coord(1,n)),(10*coord(2,n)),(10*coord(3,n))
         end if
       end do
      close(13)

      END


      SUBROUTINE DIAG(A,B,C,W)
C**********************************************************************
C** THIS SUBROUTINE DIAGONALISES THE real*8 SYMMETIC MATRIX A OF SIZE
C** 3 X 3. B IS THE DIAGONAL MATRIX AND C IS THE CARTESIAN ROTATION
C** MARTIX RELATING THE TWO COORDINATE FRAMES. B HAS THE LARGEST
C** ELEMENT IN THE (3,3) POSITION AND THE ELEMENTS (1,1) AND (2,2)
C** SUCH THAT THEIR DIFFERENCE IS POSITIVE. W IS THE INVERSE OF C.
C**********************************************************************

      IMPLICIT real*8 (A-H,O-Z)
```

```
      DIMENSION A(3,3),B(3,3),C(3,3),R(3),V(3,3),E(3),W(3,3)
      data imed, ismall /2*1/

      IA= 3
      N= IA
      IV= IA
      IFAIL= 0

      CALL F02ABF(A,IA,N,R,V,IV,E,IFAIL)
c*************************************************************
c** //F02ABF// calculates all the eigenvalues and eigenvectors of a
c** real symmetric matrix (A).
c** http://www.nag.co.uk:80/1/numeric/FLOLCH/mk16/F/F02AB
c*************************************************************
      IF(IFAIL.EQ.1) then
        write (6,15)
        stop
      else
      DO 5 J=1, 3
         DO 5 I=1, 3
         B(I,J)= 0.0d0
 5    CONTINUE
      BIG=R(1)
      IBIG= 1
      DO 20 I=2,3
         IF(BIG.lt.R(I)) then
           BIG= R(I)
           IBIG= I
         end if
20    CONTINUE
      B(3,3)= BIG

      IF(IBIG.EQ.1) then
        if (r(2).lt.r(3)) then
          imed=3
          ismall=2
        else
          imed=2
          ismall=3
        end if
      end if

      IF(IBIG.EQ.2) then
        IF(R(3).lt.R(1)) then
            IMED=1
            ISMALL= 3
        else
            IMED= 3
            ISMALL= 1
        end if
      end if

      IF(IBIG.EQ.3) then
        IF(R(1).lt.R(2)) then
            IMED=2
            ISMALL= 1
        else
            IMED= 1
            ISMALL= 2
        end if


        B(1,1)= R(IMED)
        B(2,2)= R(ISMALL)
        DO 100 I=1,3
           W(I,1)= V(I,IMED)
           W(I,2)= V(I,ISMALL)
           W(I,3)= V(I,IBIG)
 100    CONTINUE
c*************************************************************
C** THE ARRAY W CONTAINS THE EIGENVECTORS OF THE MATRIX A. HOWEVER
C** THIS IS THE INVERSE OF THE COORDINATE TRANSFORMATION C.
c*************************************************************
        DO J=1,3
          DO I=1,3
```

```
            C(I,J)= W(J,I)
          end do
        end do
      end if

  15  FORMAT (//' FAILURE IN THE SUBROUTINE DIAG IN THE CALL OF F02ABF'
     */'PROGRAM TERMINATED.')
      END




      SUBROUTINE ORDER(A,B)
C*************************************************************
C** THIS SUBROUTINE CALCULATES THE ORDER PARAMETERS, UNNORMALIZED,
C** FOR THE NON-CYLINDRICALLY SYMMETRIC POTENTIAL WITH COEFFICIENTS
C** EPZZ(=A) AND DELEP(=B)(=E1*(EXX-EYY)).
C*************************************************************

      IMPLICIT real*8 (A-H,O-Z)

      parameter(liw=102,lw=800)

      integer lw, iw(liw), liw, ifail
      real*8 fun1,fun2,fun3,liml,limu,eps,acc,ans,error,w(lw),pi

      EXTERNAL FUN1, FUN2, FUN3
      COMMON/INTER/ EPZZ, DELEP
      COMMON/PARAM/ SZZCON, DSCON, ZCON

C*************************************************************
C** SZZCON IS THE UNNORMALIZED SZZ ORDER PARAMETER FOR THIS
C** CONFIGURATION DEFINED BY THE VALUE OF EPZZ AND DELEP. DSCON IS
C** SXX-SYY AND ZCON IS THE PARTITION FUNCTION.
C*************************************************************

      PI= 3.141592654d0
      EPZZ= A
      DELEP= B
      LIMU= PI
      LIML= 0.0d0
      EPS= 1.0d-04
      ACC= 0.0d0
      IFAIL= 1

      CALL D01AJF(FUN1,LIML,LIMU,EPS,ACC,ANS,ERROR,W,LW,
     *            IW,LIW,IFAIL)
C*************************************************************
C** D01AJF is a general-purpose integrator which calculates an
C** approximation to the integral of a function f(x) over a finite
C** interval [a,b]
C** see http://www.nag.co.uk:80/1/numeric/FLOLCH/mk17/D/D01AJ
C*************************************************************


      IF(IFAIL.NE.0) then
        write (2,610)
        write (2,297) ifail,error
      end if
      ZCON= 2.0d0*PI*ANS
      EPS= 1.0d-04
      ACC= 0.0d0

C************************
C** CALCULATE SZZ
C************************
      IFAIL= 1

      CALL D01AJF(FUN2,LIML,LIMU,EPS,ACC,ANS,ERROR,W,LW,
     *            IW,LIW,IFAIL)

      IF(IFAIL.NE.0) then
        WRITE(2,620)
```

```
        WRITE(2,297) IFAIL, ERROR
      end if
      SZZCON= 2.0d0*PI*ANS
      EPS= 1.0d-04
      ACC= 0.0d0

c************************
C** CALCULATE SXX-SYY
c************************
      IFAIL= 1

      CALL D01AJF(FUN3,LIML,LIMU,EPS,ACC,ANS,ERROR,W,LW,
     *            IW,LIW,IFAIL)

      IF(IFAIL.NE.0) then
        WRITE(2,630)
        WRITE(2,297) IFAIL, ERROR
      end if
      DSCON= 2.0d0*SQRT(6.0d0)*PI*ANS


 297  FORMAT(' IFAIL=',I3,'   ERROR IN INTEGRATION=',E12.5)
 610  FORMAT(//' ERROR IN INTEGRATING FUN1 IN D01AGF'//)
 620  FORMAT(//' ERROR IN INTEGRATING FUN2 IN D01AGF'//)
 630  FORMAT(//' ERROR IN INTEGRATING FUN3 IN D01AGF'//)

      RETURN
      END



      real*8 FUNCTION D202(BETA)
c*************************************************************
C** CALCULATES D202 SMAlL WIGNER MATRIX FOR ANGLE BETA (RADIANS).
c*************************************************************
      IMPLICIT real*8 (A-H,O-Z)

      CONST= SQRT(6.0d0)/4.0d0
      SINB= SIN(BETA)
      D202= CONST*SINB*SINB

      RETURN
      END



      real*8 FUNCTION D200(BETA)
c*************************************************************
C** CALCULATES D200 SMALL WIGNER MATRIX FOR ANGLE BETA (RADIANS).
C** D200 IS THE SAME AS P2
c*************************************************************
      IMPLICIT real*8 (A-H,O-Z)

      COSB= COS(BETA)
      D200= 1.5d0*COSb*COSB-0.5d0

      RETURN
      END



      real*8 FUNCTION FUN1(X)
c*************************************************************
C** THIS FUNCTION IS FOR CALCULATING THE PARTITION FUNCTION.
c*************************************************************
      IMPLICIT real*8 (A-H,O-Z)
      real*8 x
      COMMON/INTER/ EPZZ, DELEP

      X1= EPZZ*D200(X)
```

```
      X2= EXP(X1)
      X3= DELEP*D202(X)
      IFAIL= 0
      X4= S18AEF(X3,IFAIL)
      IF(IFAIL.EQ.1) then
        write (6,20)
      end if
c*****************************************************************
C** S18AEF IS A NAG ROUTINE TO CALCULATE THE ZEROTH ORDER MODIFIED
C** BESSEL FUNCTION
c** http://www.nag.co.uk:80/1/numeric/FLOLCH/mk17/S/S18AE
c*****************************************************************
      FUN1= X4*X2*SIN(X)
      RETURN

   10 WRITE(6,20)
   20 FORMAT(//' ERROR IN FUN1 IN CALCULATING BESSEL FUNCTION'//)

      STOP
      END



      real*8 FUNCTION FUN2(X)
c*****************************************************************
C** THIS FUNCTION IS USED TO EVALUATE THE AVERAGE OF D200(SZZ)
c*****************************************************************
      IMPLICIT real*8 (A-H,O-Z)
      COMMON/INTER/ EPZZ, DELEP

      X1= D200(X)
      X2= EXP(EPZZ*X1)
      X3= DELEP*D202(X)
      IFAIL= 0
      X4= S18AEF(X3,IFAIL)
      IF(IFAIL.EQ.1) then
         write  (2,20)
      end if
      FUN2= X1*X4*X2*SIN(X)
      RETURN

   10 WRITE(10,20)
   20 FORMAT(//' ERROR IN FUN2 IN CALCULATING BESSEL FUNCTION'//)

      STOP
      END



      real*8 FUNCTION FUN3(X)
c*****************************************************************
C** THIS FUNCTION IS USED TO EVALUATE THE AVERAGE OF BIG D202 WHICH
C** IS RELATED TO SXX-SYY
c*****************************************************************
      IMPLICIT real*8 (A-H,O-Z)
      COMMON/INTER/ EPZZ, DELEP

      X1= EPZZ*D200(X)
      X2= EXP(X1)
      X3= D202(X)
      X4= DELEP*X3
      IFAIL= 0
      X5= S18AFF(X4,IFAIL)
      IF(IFAIL.EQ.1) GO TO 10
c*****************************************************************
C** S18AFF IS A NAG ROUTINE TO CALCULATE THE FIRST ORDER MODIFIED
C** BESSEL FUNCTION
c** http://www.nag.co.uk:80/1/numeric/FLOLCH/mk17/S/S18AF
c*****************************************************************
      FUN3= X3*X5*X2*SIN(X)
```

```
      RETURN

   10 WRITE(10,20)
   20 FORMAT(//' ERROR IN FUN3 IN CALCULATING BESSEL FUNCTION'//)

      STOP
      END



      SUBROUTINE MATMUL(A,B,C,L,M,N)
C*********************************************************************
C** SUBROUTINE TO MULTIPLY TOGETHER TWO MATRICES, A AND B, AND OUTPUT
C** THE RESULT IN C.
C** A IS L ROWS BY M COLUMNS, B IS M BY N AND C IS L BY N.
C*********************************************************************

      IMPLICIT real*8 (A-H,O-Z)
      DIMENSION A(3,3), B(3,3), C(3,3)

      DO I= 1,L
        DO J= 1,N
          C(I,J)= 0.0d0
          DO K= 1,M
            C(I,J)= C(I,J)+A(I,K)*B(K,J)
          end do
        end do
      end do

      RETURN
      END


C*********************************************************************
C** //E04FCF// is a comprehensive algorithm for finding an
c** unconstrained minimum of a sum of squares of m nonlinear
c** functions in n variables (m >= n). No derivatives are required.
c** The routine is intended for functions which have continuous first
c** and second derivatives (although it will usually work even if the
c** derivatives have occasional discontinuities).
c** http://www.nag.co.uk:80/0/numeric/FLOLCH/mk17/E/E04FC/OLS
C*********************************************************************

C*********************************************************************
c** //E04YCF// returns estimates of elements of the
c** variance-covariance matrix of the estimated regression
c** coefficients for a nonlinear least squares problem. The estimates
c** are derived from the Jacobian of the function f(x) at the
c** solution.http://www.nag.co.uk:80/1/numeric/FLOLCH/mk17/E/E04YC
C*********************************************************************
C!*********************************************************
C!      Sort records into atom number order, Bubble sort
C!*********************************************************
      SUBROUTINE sort(nop,coord,nattype,nsize,gamma,nunit)

      implicit double precision (a-h,o-z)
integer nop,itemp,nattype(3,nop)
real*8 rtemp,coord(5,nop)
real*8 gamma(nop),gamtemp
integer nunit

DO nloop=1,nsize
   DO mloop=1,nsize-nloop
      IF (nattype(1,mloop).gt.nattype(1,mloop+1)) THEN

         gamtemp = gamma(mloop)
         gamma(mloop) = gamma(mloop+1)
         gamma(mloop+1) = gamtemp
         do ncount = 1,3
            itemp = nattype(ncount,mloop)
            nattype(ncount,mloop) = nattype(ncount,mloop+1)
```

```
                  nattype(ncount,mloop+1) = itemp
               end do
               do ncount2 = 1,5
                  rtemp = coord(ncount2,mloop)
                  coord(ncount2,mloop) = coord(ncount2,mloop+1)
                  coord(ncount2,mloop+1) = rtemp
               end do

            END IF
         END DO
      END DO

C**   The default origin is atom 0, use this to make another atom
C**   the origin.
      read(nunit,*) ncentre
      x=coord(1,ncentre)
      y=coord(2,ncentre)
      z=coord(3,ncentre)
      do n=1,nsize
          coord(1,n)=coord(1,n)-x
          coord(2,n)=coord(2,n)-y
          coord(3,n)=coord(3,n)-z
      end do


      END
```

Appendix E. cat

This simple program calculates the bond angle defined by three atomic positions. This is particularly useful when attempting to relate cartesians coordinates, obtained from SPIROFORM, back to bond length and angles data required by LISTER.

E.1 source code - cat.f

```
      program cat
c**  to read input in xyz coords and calculate the bond lengths and
c**  angles between the atoms.
c**  Useful for translating spiroform optimised geometries into
c**  optimised bond lengths and angles.

        parameter (pi=3.1415926535893d0,rad=180.0d0/pi)
        parameter (smallno=0.00000001)

        real*8 xx,yy,zz,carry(12,3),x(3),y(3),z(3)
        real*8 vec1(3),vec2(3),dot
        integer natoms

        print *,'**    CAT    (c)M.I.C.Furby 1996    **'
        print *
        print *,'Mmmmm, something smells good"'
        print *,'It`s me!    I love this aftershave!"'

        open(10,file='coord',status='old')
        print *
        print *
        read(10,*) natoms

        do n=1,natoms
          read(10,*) xx,yy,zz
          carry(n,1) = xx
          carry(n,2) = yy
          carry(n,3) = zz
          write (*,'(i3,3f8.4)') n,xx,yy,zz
        end do

c**************
c  calculate bond lengths
c******************
        print *
        print *
        print *,'**** Bond Lengths ****'
        read(10,*) n1,n2
        do while(n1.ne.0)
          dx=carry(n1,1)-carry(n2,1)
          dy=carry(n1,2)-carry(n2,2)
          dz=carry(n1,3)-carry(n2,3)
          blen = sqrt ( dx**2 + dy**2 + dz**2 )
          write (*,'(2i3,f10.6)') n1,n2,blen
          read(10,*) n1,n2
        end do

c**************
c  calculate bond angles
c******************
        print *
        print *
        print *,'**** Bond Angles ****'
        read(10,*) n1,n2,n3
        do while(n1.ne.0)
          print *,n1,n2,n3
          x(1)=carry(n1,1)
```

```
y(1)=carry(n1,2)
z(1)=carry(n1,3)
x(2)=carry(n2,1)
y(2)=carry(n2,2)
z(2)=carry(n2,3)
x(3)=carry(n3,1)
y(3)=carry(n3,2)
z(3)=carry(n3,3)

do m=1,3
  if ((x(m)**2).lt.smallno) then
    x(m)=0.0d0
  end if
  if ((y(m)**2).lt.smallno) then
    y(m)=0.0d0
  end if
  if ((z(m)**2).lt.smallno) then
    z(m)=0.0d0
  end if
end do

vec1(1)=x(1)-x(2)
vec1(2)=y(1)-y(2)
vec1(3)=z(1)-z(2)
vec2(1)=x(3)-x(2)
vec2(2)=y(3)-y(2)
vec2(3)=z(3)-z(2)

call getdot(vec1,vec2,dot)
dot12=dot
call getdot(vec1,vec1,dot)
vlen1 = sqrt(dot)
call getdot(vec2,vec2,dot)
vlen2 = sqrt(dot)

phi=dot12/(vlen1*vlen2)
phi=acos(phi)
phi=phi*rad
write (*,'(f10.6)') phi
read(10,*) n1,n2,n3
end do

close(10)
end



subroutine getdot(vec1,vec2,dot)

real*8 vec1(3),vec2(3),dot

dot=0.0d0
do i =1,3
   dot=vec1(i)*vec2(i) + dot
end do

end
```

E.2 Input file - coord

```
(2a)  3,                                          FORMAT(i)
```

Number of atomic coordinates

```
(2b)   0.0, 0.0, -1.4,                            FORMAT(3f10.0)
       1.21243557, 0.0, -0.7,                     FORMAT(3f10.0)
       1.21243557, 0.0,  0.7,                     FORMAT(3f10.0)
```

Cartesian coordinates for each atom x,y,z.

```
(2c)   1,2,                                   FORMAT(2i)
       2,3,                                   FORMAT(2i)
       0,0,                                   FORMAT(2i)
```

Calculate the bondlength between the two atoms i,j,. Finish list with 0,0,.

```
(2d)   1,2,3,                                 FORMAT(2i)
       0,0,0,                                 FORMAT(2i)
```

Calculate the bond angle where 1 and 2 define the first bond and 2 and 3 define the second bond. Finish the list with 0,0,0,.